Individual Somatotopy of Primary Sensorimotor Cortex Revealed by Intermodal Matching of MEG, PET, and MRI

Henrik Walter*†, Rumyana Kristeva‡, Uwe Knorr*, Gottfried Schlaug*, Yanxiong Huang*, Helmuth Steinmetz*, Bruno Nebeling§, Hans Herzog@, and Rüdiger J. Seitz*

Summary: A method for comparing estimated magnetoencephalographic (MEG) dipole localizations with regional cerebral blood flow (rCBF) activation areas is presented. This approach utilizes individual intermodal matching of MEG data, of rCBF measurements with [^{15}O]-butanol and positron emission tomography (PET), and of anatomical information obtained from magnetic resonance (MR) images. The MEG data and the rCBF measurements were recorded in a healthy subject during right-sided simple voluntary movements of the foot, thumb, index finger, and mouth. High resolution 3D-FLASH MR images of the brain consisting of 128 contiguous sagittal slices of 1.17-mm thickness were used. MEG/MR integration was performed by superimposing the 3D head coordinate system constructed during the MEG measurement onto the MR image data using identical anatomical landmarks as references. PET/MR integration was achieved by a phantom-validated iterative front-to-back-projection algorithm resulting in one integrated MEG/PET/MR image. The estimated dipole locations followed the somatotopic organisation of the task-specific rCBF increases as evident from PET, although they did not match point-to-point. Our results demonstrate that intermodal matching of MEG, PET and MR data provides a tool for relating estimated neuromagnetic field locations to task-specific rCBF changes in individual subjects. Our method offers the perspective of refined dipole modelling.

Key words: Movement-related neuromagnetic fields; Movement evoked field I; Regional cerebral blood flow; Brain mapping; Motor activity.

Introduction

The dipole localization procedure in magnetoencephalography (MEG) is usually based on two assumptions: first, the underlying neuronal activity can be modelled as an equivalent magnetic dipole producing the measured neuromagnetic field and, second, the head is supposed to be spherically symmetic. Although these assumptions are somewhat simplistic and for dipole localization the inverse problem has no unique solution, reasonable dipole locations have been obtained for different neurophysiological activation paradigms (Hari and Lounasmaa 1989).

The most direct approach to validate the calculated dipole locations is a comparison with intracortical recordings, a method restricted only to selected patients undergoing brain surgery (Sutherling et al. 1988). A more common validation method used in healthy subjects utilizes the structural information of magnetic resonance (MR) imaging in order to project the estimated dipole locations onto cortical regions. Another approach for validation can be provided by positron emission tomography (PET). The regional cerebral blood flow (rCBF) and the metabolic rate of glucose can be measured with PET. These variables are coupled in a quantitative manner to synaptic activity in neuronal populations as has been demonstrated with autoradiography (Kuschinski et al. 1981; Yarowski et al. 1983). The digitized integration of functional and anatomical information using PET and MR images is a well established method to localize task-specific rCBF increases to brain structures for groups of subjects and in individuals (Seitz et al. 1990; Steinmetz et al. 1992).

In the present study we used intra-individual intermodal matching of MEG, PET and MR image data for

*Department of Neurology Heinrich-Heine-University Düsseldorf.
†Seminar B for Philosophy, Technical University of Braunschweig.
‡Institute for Experimental Audiology, University of Münster.
§Institute of Nuclear Chemistry, Research Center Jülich, Germany.
@Institute of Medicine, Research Center Jülich, Germany.
Accepted for publication: July 30, 1992.
The work was supported by the SFB 194 and the Klinische Forschergruppe "Biomagnetismus and Biosignalanalyse" of the Deutsche Forschungsgemeinschaft. The expert technical assistance of Dipl. Ing. S. Hampson, Dipl. Ing. B. Ross, Ms. H. Deitermann, E. Theelen und C. Tarras during the experiments is gratefully acknowledged. The authors thank Professor H.-J. Freund for continuous support in conducting this study.
Correspondence and reprint requests should be addressed to Dr. Rüdiger J. Seitz, Department of Neurology, Heinrich-Heine-University Düsseldorf, Moorenstraße 5, 4000 Düsseldorf 1, FRGermany.

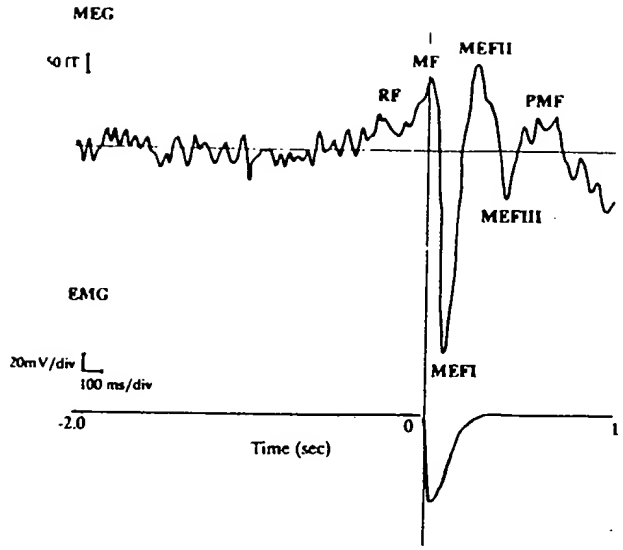

Figure 1. Upper trace: A representative MEG curve during right index finger movement recorded from a lateral position over the left scalp in relation to the EMG trigger (lower trace). The six different neuromagnetic field components are indicated on the MEG curve: readiness field (RF) starting approx. 500 msec prior to the movement, motor field (MF) (during movement onset), three different movement-evoked fields (MEFs: MEFI, MEFII and MEFIII) and a postmovement field (PMF).

validation of estimated dipole localizations. The functional data were obtained during simple unilateral movements. The task-specific activations in PET images were compared with the fitted dipoles to movement evoked field I (MEFI; figure 1). The MEFI is the largest and most stable neuromagnetic field component of movement related activity which has a somatotopic organisation (Kristeva et al. 1991). The results are discussed as a tool for validation of the commonly used dipole localization procedure.

Methods

A healthy 30-year-old, right-handed man (Annett 1967; Steingrüber 1971) volunteered in this study that was approved by the Ethics committee of the University of Düsseldorf and performed adhering to the Declaration of human rights of Helsinki 1975. Written informed consent was obtained prior to the study.

MEG recordings

Neuromagnetic fields (bandpass 0.1 - 50 Hz) were recorded from the left scalp using a 37-channel first-order gradiometer system (BTI San Diego, Ca.) while the subject performed voluntary flexions of the right foot, right thumb, right index finger, or mouth (contractions of the right cheek). A typical "Bereitschaftspotential" paradigm was used. Movement onset was detected from the rectified surface electromyogramm, recorded over the active muscles. A three-dimensional head coordinate system was created with a 3-D digitizer by use of three anatomical landmarks: left and right preauricular points and nasion. The position of the sensors were stored with respect to this coordinate system during each measurement. Averaged waveforms of movement related activity were produced from a minimum of 100 repetitions of each movement after thorough rejection of artifact contaminated trials (figure 1). The analysis time was set at two seconds before and one second after movement onset. The first 500 msec of this epoch served as a baseline. A single moving dipole model was applied for source analysis of the neuromagnetic field pattern corresponding to MEFI having mean latencies for the four different conditions as follows: foot movement - 115 ms, thumb movement - 91 ms, index finger - 97 ms and mouth movement - 89 ms. The parameters of the fitted dipoles were estimated as mean values from a 10 msec window around the peak value of MEFI component, which included the highest goodness of fit, the highest correlation and (with exception of the foot) the peak of the root mean square value of the field strength.

PET scanning

The subject was comfortably placed on the bed of the PET camera with his eyes covered and his head positioned in an individually moulded headholder. After hardening of the epoxy resin (PANDOX, PANDURO HARZCHEMIE GmbH, Köln, FRG), the headholder fits the subject's head only in the moulded position thus preventing head movements. A plastic catheter was placed into the right brachial vein for tracer administration, a further plastic catheter placed into the left brachial artery under local anaesthesia allowed recording of the arterial tracer concentration and the $PaCO_2$. There was no noise and no speech in the examination room. Scans were performed during rest and during repetitive movements of the right index finger, right thumb, right foot, and right mouth (cheek contractions). The subject was highly routined to perform the movements with a frequency of one Hz. Only the thumb abduction was a novel task.

The rCBF was measured with intravenous bolus injection of about 50 mCi [^{15}O]-butanol (Berridge et al. 1990, 1991) which is a freely diffusible tracer (Herscovitch et al. 1987). The count rates in the brain were recorded in list mode for 180 s using the SCANDITRONIX PC4096-

15WB PET camera (Rota Kops et al. 1990). Simultaneously, the arterial tracer concentration was recorded with a sampling rate of 1 Hz using an automated blood sampling device (Eriksson et al. 1988). PET image reconstruction employed the back projection algorithm with a Hanning filter of 6 mm and measured attenuation correction by use of a transmission scan. The resolution of the reconstructed images was 9 mm (FWHM) in plane and 7 to 8 mm (FWHM) in axial direction. For a medial image of the 15 recorded PET image slices the input function of the [^{15}O-butanol] was fitted providing an estimate of the delay and dispersion of the arterial tracer bolus, the blood-brain distribution coefficient, and the global cerebral blood flow. The rCBF was calculated pixel-by-pixel using a single scan of integrated 40 seconds (Herscovitch et al. 1983) and the fitted delay, dispersion, and blood-brain distribution coefficient.

For demonstration of the task-induced rCBF changes the PET image in rest was subtracted pixel-by-pixel from the PET images recorded during movement. In the subtraction images, regions of interest (ROIs) were drawn automatically at a 30%-isocontour of the maximal rCBF increase using a MIPRON workstation (KONTRON, Eching, FRG). This isocontour level provided the best estimate of signal size as demonstrated in a phantom study. Thereafter, a gamma-distribution was fitted to the maximal value and the spatial extent of each ROI using maximum likelihood estimations. For statistical evaluation, a critical value was calculated for a probability of error of 0.01 for both distributions. Since both distributions are given predominantly by noise, only ROIs with values in both gamma distributions higher than the critical values were accepted as significant. Taking the resolution and matrix of the PET images into consideration, this corresponded to a p-value <0.0005. The mean rCBF reference values were obtained by superimposing the ROIs onto the PET image recorded at rest. The ROIs were characterized spatially by theirs centers of gravity.

MR imaging

High-resolution MR scans were obtained with a 1.5 T Magnetom (SIEMENS, Erlangen, FRG) using the high-resolution 3D-FLASH-sequence. This sequence produced 128 contiguous sagittal MR images of 1.17 mm thickness with a 256 x 256 matrix covering the entire head. Two liver oil capsules marked the preauricular points of the subject's head.

MEG/MR matching

Reference landmarks were the preauricular points marked before MR imaging by liver oil capsules and the nasion identified anatomically. Individual dipole locations were determined by calculating the x, y and z voxel coordinates corresponding to the x, y and z coordinates of the three-dimensional head coordinate system of the neuromagnetic field recordings.

PET/MR matching

The matching algorithm of individual PET and MR image data has been validated in a phantom study (Steinmetz et al. 1992). In short, PET and MR data were aligned by iterative matching in three orthogonal planes of front-to-back projections of the outermost scalp contours in the PET and MR images. The distances of the two contours were minimized by least squares fitting resulting in optimal 2-D transformation parameters for each of the three projections. The remaining misfits of the outer contours in the three orthogonal planes (XY, XZ, YZ) and the average in-plane misalignment were in the range of 2.2 to 2.3 mm roughly corresponding to one PET pixel. By applying this algorithm to the MR images in which the MEG dipoles had been localized, integrated MEG/PET/MR images were created.

Results

The estimated dipole locations of the MEFI for those four different movement conditions are consistent with the somatotopic organization of the sensorimotor cortex, the dipole location for the foot being most medial, then followed by the dipole location for the thumb, index finger and most lateral for the mouth (figure 2).

The PET images revealed task-specific rCBF increases (67%) in the depth of the left central sulcus induced by the index and thumb movements. While the activation zone of the index flexion extended into the sensory hand area, the thumb abduction induced a more rostral activation zone in the precentral gyrus (figure 2a, b). Furthermore, the thumb movement also activated the left supplementary motor area (53% rCBF increase). The foot flexion resulted in an activation of 56% along the upper limb of the precentral gyrus (figure 2d). The right-sided mouth movement was associated with bilateral activation sites (67% left, 51% right) in the lower part of the precentral gyrus (figure 2c).

Table I summarizes the quantified differences in location of the estimated dipoles compared to the centers of gravity of the activation areas in PET. They ranged from 2.0 to 17.0 mm.

Discussion

Task-specific rCBF changes could be localized accurately to anatomical structures in individual subjects after spatial alignment of PET and MR images (Steinmetz et al. 1992). The cortical activation maps created by this

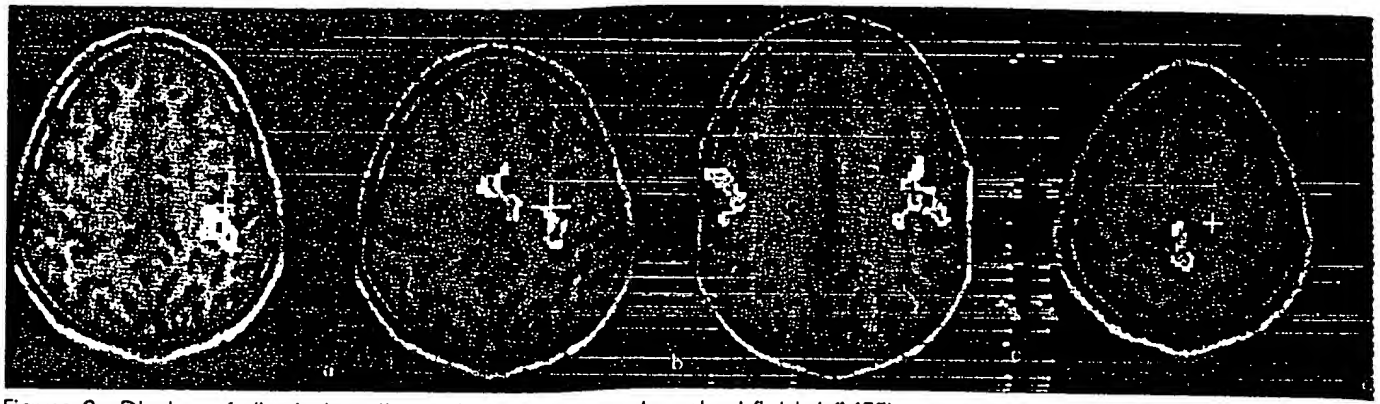

Figure 2. Display of dipole locations of the movement evoked fields I (MEFI, crosses) and task-specific rCBF increase (pseudocolor scale) induced by right-sided voluntary movements in integrated MEG/PET/MR images. The exact axi dipole locations are given in Table I. a) Index finger flexion with activation in the depth of the left central sulcus and th adjacent sensory hand area. b) Thumb abduction with activation of the left hand area in the depth of the central sulcu In this slice there was a further activation field corresponding to the supplementary motor area. c) Right-sided cheek le contraction (mouth movement) with bilateral activations along the central sulcus. d) Foot flexion with activation at th upper medial limb of the central gyrus. Right in the image corresponds to left in the subject.

Table I. Spatial relation of dipole locations and task-specific rCBF increases induced by unilateral movements in integrate MEG/PET/MR images.

Movement	Dipole coordinates*			Centers of gravity* of task-specific rCBF changes			Differences		
	x(mm)	y(mm)	z(mm)	x(mm)	y(mm)	z(mm)	x(mm)	y(mm)	z(mm)
Foot	141.0	158.0	210.5	124.3	173.4	204.0	+16.7	-15.4	+6.5
Thumb	157.0	146.0	192.0	158.8	159.8	191.0	-1.8	-13.8	+1.0
Index Finger	169.0	153.0	206.0	164.6	167.6	191.0	+4.4	-14.6	+15.0
Mouth	170.0	144.0	186.0	173.9	148.9	178.0	-3.9	-4.9	+8.0
	MEG reference coorinates*								
Nasion	127.0	46.0	76.5						
Right preauricular	191.0	143.0	66.5						
Left preauricular	59.0	143.0	63.5						

*Coordinate system: x = coronal, 0 = left; y = sagittal, 0 = frontal; z = axial, 0 = caudal.

approach allowed a far more detailed functional-structural analysis than inter-subject averaging techniques using brain atlases (Steinmetz and Seitz 1991). Thus, for the validation of dipole locations, the individual PET/MR alignment was used. The estimated dipole locations were roughly in correspondence with the activation sites apparent by the rCBF measurements with PET. Although the intermodal comparisons could be expressed in quantitative terms, the following problems have to be taken into consideration:

1. The most commonly used approach to enhance signal detection in subtraction images of PET activation studies is inter-subject averaging (Fox et al. 1988). In our approach of individual signal identification, we were able to demonstrate subject-specific and performance-related maximal activations. However, small areas of rCBF changes or minor rCBF increases may have remained undetected. The latter might explain the non-consistent activation of the supplementary motor. However, one could speculate that the high programming effort of this novel task activated the supplementary motor area to a

maximal extent substantiating earlier findings by Roland et al. (1980).

2. The MEFI reflects the activity at a specified period averaged over a number of sequentially performed single movements. The rCBF measurements, however, represent the neuronal activity integrated over 40 s during which a certain movement had to be performed repetitively. As a consequence, the pacing of the movements during the PET studies was 1 Hz to ensure a measurable rCBF response, whereas the pacing for recording the Bereitschaftspotential was one movement every 8-15 s. These technical constraints bore out slightly different activation paradigms.

3. Some inaccuracies due to the use of anatomical landmarks are inevitable in MEG/MR matching. A realistic head shape model might be more reliable for intermodal matching, since MR/PET matching is achieved by surface alignment.

Despite these limitations, intra-individual intermodal matching of MEG, PET and MR data appears as a promising validation tool for the results from the dipole localization procedure. Also, it provides the perspective of refined dipole modelling.

References

Annett, M. The binomial distribution of right, mixed and left handedness. Q J Exp Psychol, 1967, 19: 327-333.

Berridge, M.S., Cassidy, E.H., Terris, A.H. A routine, automated synthesis of oxygen-15-labeled butanol for positron tomography. J Nucl Med, 1990, 31: 1727-1731.

Berridge, M.S., Adler, L.P., Nelson, D., Cassidy, E.H., Muzic, R.F., Bednarczyk, E.M., Miraldi, F. Measurement of human cerebral blood flow with [^{15}O]butanol and positron emission tomography. J Cereb Blood Flow Metab, 1991, 11: 707-715.

Eriksson, L., Bohm, C., Kesselberg, M., Holte, S. An automated blood sampling system used in positron emission tomography. Nucl Sci Appl, 1988, 3: 133-143.

Fox, P.T., Mintun, M.A., Reiman, E.M., Raichle, M.E. Enhanced detection of focal brain responses using intersubject averaging and change-distribution analysis of subtracted PET images. J Cereb Blood Flow Metab, 1988, 8: 642-653.

Hari, R. and Lounasmaa, O.V. Recording and interpretation of cerebral magnetic fields. Science, 1989, 244: 432-436.

Herscovitch, P., Markham, J., Raichle, M.E. Brain blood flow measured with intravenous $H_2^{15}O$. I. Theory and error analysis. J Nucl Med, 1983, 24: 782-789.

Herscovitch, P., Raichle, M.E., Kilbourn, M.R., Welch, M.J. Positron emission tomographic measurement of cerebral blood flow and permeability-surface area product of water using [^{15}O]water and [^{11}C]butanol. J Cereb Blood Flow Metab, 1987, 7: 527-542.

Kristeva, R., Cheyne, D. and Deecke, L. Neuromagnetic fields accompanying unilateral and bilateral voluntary movements: topography and analysis of cortical sources., Electroenceph. clin. Neurophysiol, 1991, 81: 284-298.

Kuschinky, W., Suda, S., Sokoloff, L. Local cerebral glucose utilization and blood flow during metabolic acidosis. Am J Physiol, 1981, 241: H772-H777.

Roland, P.E., Larsen, B., Lassen, N.A., Skinhoj, E. Supplementary motor area and other cortical areas in organization of voluntary movements in man. J Neurophysiol, 1980, 43: 118-136.

Rota Kops, E., Herzog, H., Schmid, A., Holte, S., Feinendegen, L.E. Performance characteristics of an eight-ring whole body PET scanner. J Comp Ass Tomogr, 1990, 14: 437-445.

Seitz, R.J., Bohm, C., Greitz, T., Roland, P.E., Eriksson, L., Blomqvist, G., Rosenqvist, G., Nordell, B. Accuracy and precision of the computerized brain atlas programme for localization and quantification in positron emission tomography. J Cereb Blood Flow Metab, 1990, 10: 443-457.

Steingrüber, H.J. Zur Messung der Händigkeit. Z Exp Angew Psychol 1971, 18: 337-357.

Steinmetz, H., Seitz, R.J. Functional anatomy of language processing: neuroimaging and the problem of individual variability. Neuropsychologia, 1991, 29: 1149-1161.

Steinmetz, H., Huang, Y., Seitz, R.J., Knorr, U., Herzog, H., Hackländer, T., Kahn, T., Freund, H-J. Individual integration of positron emission tomography and high-resolution magnetic resonance imaging. J Cereb Blood Flow Metab, 1992, 12: 919-926.

Sutherling, W.W., Crandall, P.H., Cahan, L.D., Barth, D.S. The magnetic field of epileptic spikes agrees with intracranial localizations in complex partial epilepsy. Neurology 1988, 38: 778-786.

Yarowsky, P., Kadekaro, M., Sokoloff, L. Frequency-dependent activation of glucose utilization in the superior cervical ganglion by electrical stimulation of cervical sympathetic trunk. Proc Natl Acad Sci, 1983, 80: 4179-4183.

Biomagnetism: Clinical aspects. M. Hoke et al. editors.

Application of multichannel systems in magnetocardiography

W. Moshage[1], S. Achenbach[1], S. Schneider[2], K. Göhl[1], K. Abraham-Fuchs[2], R. Graumann[2] and K. Bachmann[1]

[1]Medical Clinic II (Cardiology) and Policlinic, University of Erlangen-Nürnberg; and [2]Siemens Medical Engineering Group, Erlangen, Germany

Introduction and history

In 1963, Baule and McFee achieved the first registration of the human magnetocardiogram [1]. The introduction of SQUIDs by Cohen et al. [2] was the technical prerequisite for the first practical applications of the biomagnetic method. Since then, MCG recordings have been performed with systems comprised of one to a few channels at several centers throughout the world [3–8]. Basic work by Fenici and others led to clinically significant applications, e.g. in the three-dimensional localization of cardiac rhythm disorders, in risk stratification of patients prone to arrhythmias, and in the follow-up of heart transplantation.

The main drawback of the method was the need for sequential repositioning of the sensors over the patient's chest. This required very long recording times and impaired localization accuracy. Thus, efforts were put into the development of multichannel systems, which means systems permitting the coherent registration of the MCG without repositioning of the sensors. Next to the reduction of recording times to just a few minutes, multichannel technology permits the registration of transient events such as singular VES, of hemodynamically effective arrhythmias, and even of polymorphic VT.

Present state of multichannel magnetocardiography

In February 1988, the first large-scale multichannel system (KRENIKON®) was ready for clinical application in cardiology and neurology in Erlangen, Germany [9]. The system was comprised of 31, later of 37, first-order gradiometers arranged in a planar array of 19 cm diameter. Measurements were performed in a magnetically shielded room. The positive experiences gained with this system led to the installation of a similar biomagnetic system in the hospital of Erlangen University in July 1990. Invasive electrophysiological studies as programmed endocardial stimulation and registration of the endocardial ECG can be conducted during the MCG investigation, multiplane fluoroscopy can be performed right outside the shielded room, and MRI is available in immediate proximity to the Biomagnetic Center Erlangen. Up to May 1991, more than 50 healthy volunteers and over 120 patients with ventricular hypertrophy, conduction disturbances, accessory path-

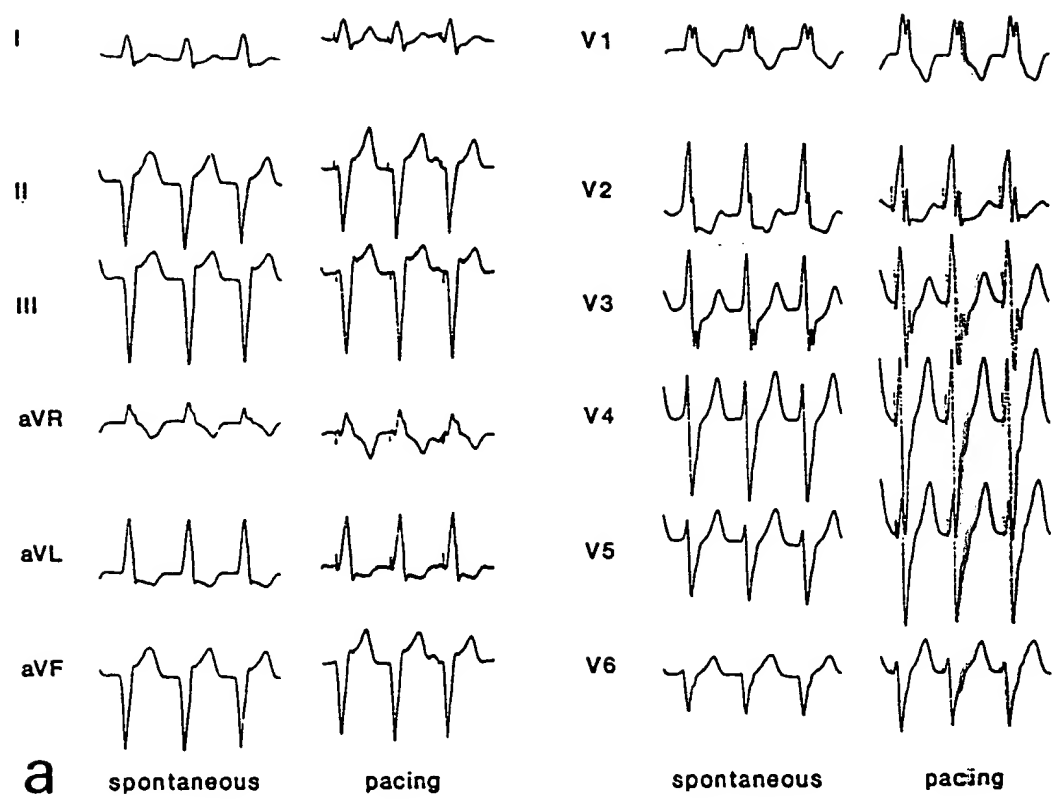

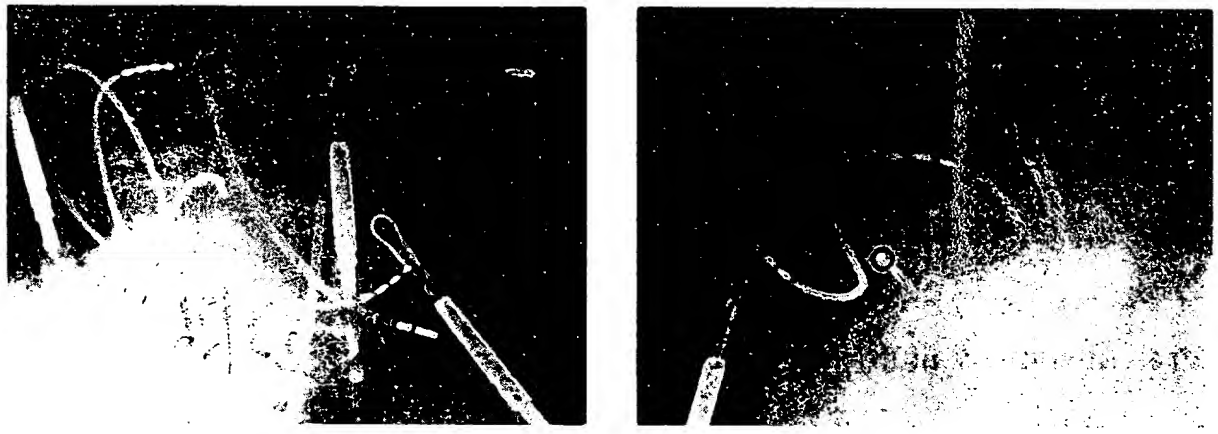

Fig. 1. Comparison of the localization results of incessant VT by invasive pace-mapping (a) and multichannel MCG (b) in a patient with a diaphragmal aneurysm after posterior myocardial infarction. Both methods show the exit-point of VT to be situated in the left ventricle at the septal margin of the aneurysm. a) Localization result of the pace-mapping investigation: Stimulation at the electrode marked with a circle (lower left in a.p. and lower right in lateral projection) showed the same QRS morphology as spontaneous VT in all 12 standard ECG leads (upper). b) Biomagnetic localization result: Registration of the VT (upper). Eight out of 37 recorded MCG channels, three ECG leads, and the respiration channel are shown. Localization results marked in the corresponding frontal (lower left) and axial MR images (lower right).

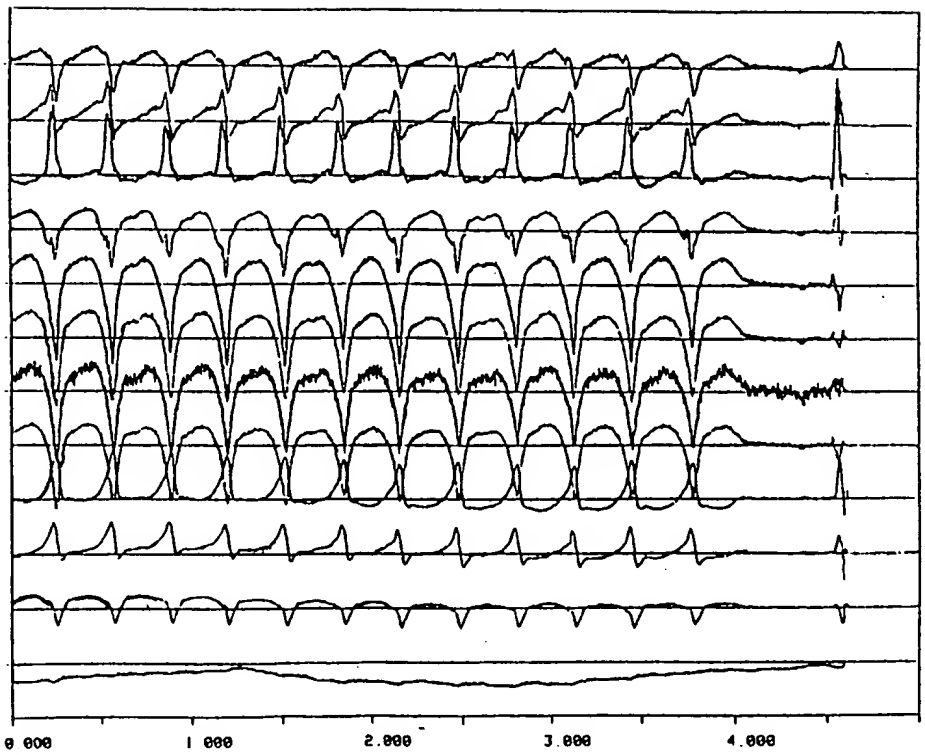

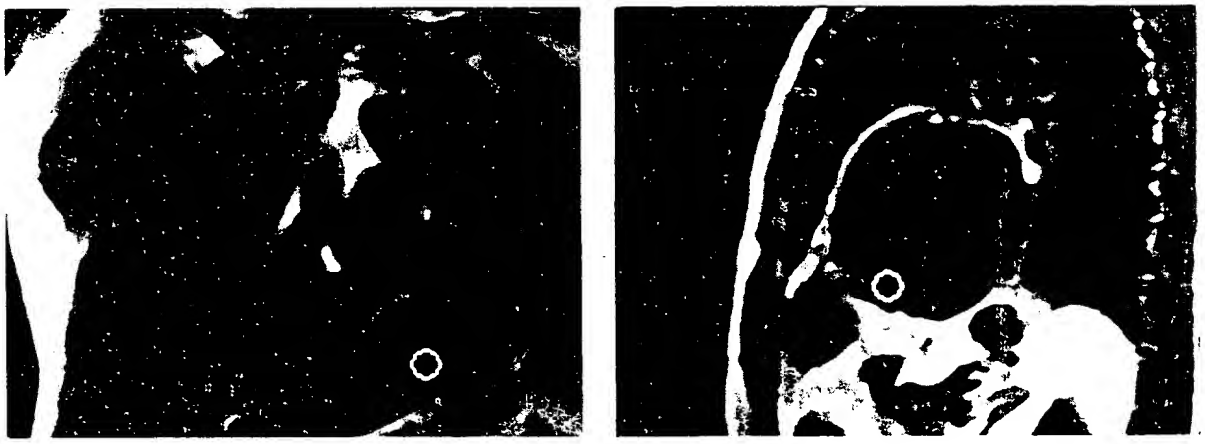

Fig. 1. Continued.

ways, exercise-induced ischaemia, spontaneous PVC, ventricular and supraventricular tachycardia, after heart transplantation or with various other cardiac diseases have been investigated with the KRENIKON® system. The recording times ranged from 30 s (for VT) to 15 min. Phantom studies, programmed endocardial stimulation in volunteers and comparative electrophysiological mapping investigations served for the evaluation of the method and confirmed the high spatial accuracy of multichannel magnetocardiographic localization in combination with MR imaging.

In this way, we could demonstrate in 18 patients with left ventricular hypertrophy documented by echocardiography and magnetic resonance imaging that quantification of hypertrophy is possible in MCG. The correlation coefficient between a "magnetic index" calculated from MCG maps and the degree of hypertrophy expressed by the combined wall thickness of the interventricular septum and posterior wall of the left ventricle was found to be $r = 0.79$, while the Sokolow-index derived from surface ECG correlated only poorly with echocardiography ($r = 0.20$) [10].

In 14 patients with WPW (Wolff-Parkinson-White) syndrome the position of the accessory conduction pathway was determined noninvasively by multichannel MCG. As a control for the localization, an invasive electrophysiological examination was performed in seven, and additional blood pool scintigraphy in five patients. Even though methodological problems in the compatibility of MCG and electrophysiological mapping restrict the value of the investigation of spatial differences between these two methods, the spatial differences were less than 20 mm in all patients investigated. Slight topographical differences result from the fact that the electrophysiological examination determines the atrial insertion of the accessory conduction pathway in the state of orthodromic reciprocal tachycardia, whereas MCG localizes the early ventricular depolarization via the accessory bundle. Patients with two or more accessory pathways still are a problem in MCG localization. A possibility to correctly interpret and localize MCG recordings of these patients may be the reconstruction of current density distributions (see below), which are not restricted to the reconstruction of a single source.

While accessory bundles in WPW-Syndrome could be investigated using systems comprised of one to a few channels, the coherent registration of transient events such as single premature ventricular complexes (PVC) and of hemodynamically effective ventricular tachycardias (VT) were possible only after the development of multichannel systems. So far, we have recorded the MCG of 12 patients with PVC using the KRENIKON® system. After correction for superimposed repolarization activity [11], the site of origin of the arrhythmias could be localized from the magnetic field distribution after the onset of the ectopic beat. In seven cases, the localization results could be confirmed with endocardial catheter mapping or agreed with ischemic lesions [12].

In order to directly verify the localization accuracy of multichannel MCG in combination with MRI, we have developed a nonmagnetic, MR-compatible pacing catheter [13]. With this catheter it is possible to induce PVC at an exactly known site within the heart. The position of the catheter tip can be documented in MRI to obtain a topographical reference point. So far, this catheter has been used in five volunteers to induce PVC during registration of the MCG at an exactly known site within the heart. In the investigation of these five cases, a mean localization error of 7 mm along the x-axis, 6 mm along the y-axis, and 3 mm along the z-axis with a mean three-dimensional error of 11 mm was found.

The localization of the arrhythmigenic tissue in patients with VT is of highest clinical relevance. So far, we have investigated four patients with induced or spontaneous VT both by multichannel MCG and invasive mapping and found good

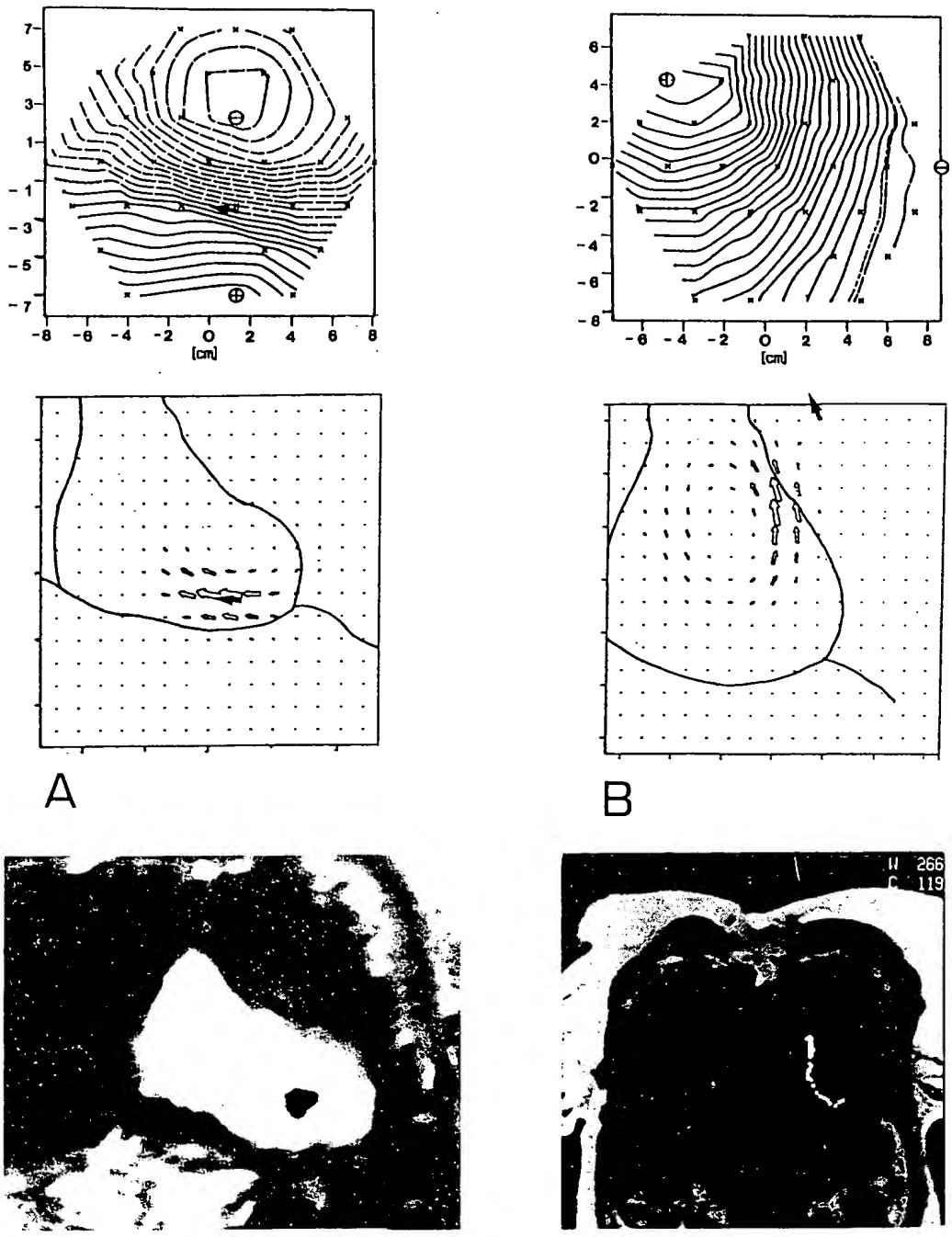

Fig. 2. Comparison of single current dipole (SCD) localization and reconstruction of the current density distribution in two patients; A: SCD localization and current density reconstruction in a volunteer with induced PVC. Magnetic field map recorded during stimulation and SCD localization (left). Reconstructed current density distribution (white arrows) compared to SCD localization (black arrow, lower left). The localization results of both methods lie right next to the position of the catheter tip as documented in MRI (right); and B: patient with incessant VT. Magnetic field distribution at the onset of averaged VT beats (left). The reconstructed current density distribution is concentrated in the right ventricular outflow tract (RVOT) while the SCD result is outside the heart contours (lower left). By pace mapping, the origin of VT was determined to be in the RVOT in good agreement with current density reconstruction (lower right).

agreement of the two methods in all cases (see Fig. 1). Due to the extremely short necessary recording time of less than 30 s, VT with strong hemodynamic effects could be noninvasively localized with high spatial accuracy for the first time.

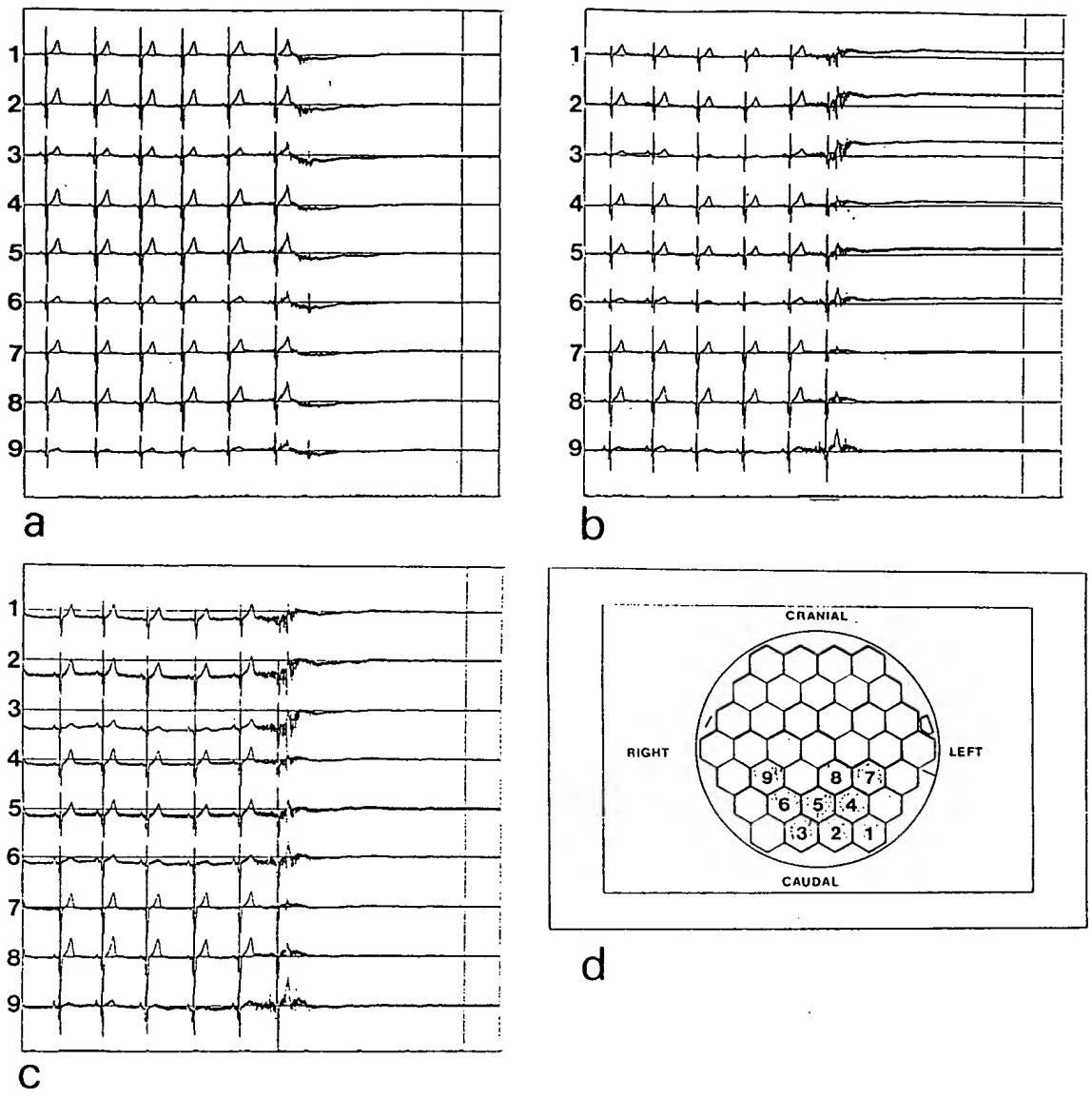

Fig. 3. Modulated DC recordings in a healthy volunteer. During registration of the MCG, the patient is moved out of the sensors' detection range. In this way, DC components of the MCG signal can be detected. However, measurements are strongly influenced by gastrointestinal (GI) activity: No DC-shift before and after removal of a healthy volunteer if the stomach is empty and GI activity is suppressed by medication (a). If the same procedure is repeated after a meal, a distinct baseline shift can be seen mainly in the sensor positions close to the abdomen (1–3). The baseline shift is reduced in channels 4–6 and can hardly be detected in the channels 7–9, which are farthest from the abdomen (baseline correction in the time interval after patient removal: (b), same recording with baseline correction in the time period before removal of the patient: (c)). The positions of the channels shown are marked in (d).

However, up to now it has only been possible to localize the earliest ventricular depolarization. This means that the localization results determine the exit-point of VT, while the area of slow conduction is not readily detectable so far.

Prospects

The possibilities of multichannel magnetocardiography in combination with MRI

permit a noninvasive localization of arrhythmogenic tissues with high spatial accuracy at recording times in the range of 30 s to a few minutes [12]. In the preliminary stages of operative treatment, invasive investigations may for the most part be replaced. If patients are considered for interventional catheter ablation, a previous MCG investigation may reduce the necessary investigation time [14]. Strategies to reduce inaccuracies in the localization of deep sources are currently investigated. The application of more advanced models than a single current dipole in the infinite halfspace are considered. A very promising development is the reconstruction of current density distributions applying lead fields reconstruction, which has recently become available for our clinical trials [15]. This method has proven to yield very good results if several areas of myocardium are active at the same time, as in VT (see Fig. 2) or WPW syndrome with one or more accessory pathways. Current density reconstruction can enable biomagnetic localization in these cases, which can hardly be described by the model of a single dipole in the infinite homogeneous halfspace. In the investigation of focal activities, current density reconstruction confirmed the results obtained by dipole localization (see Fig. 2). However, current density reconstructions tend to be of rather limited spatial resolution; mainly concerning the depth of the sources. Continuing work started by Cohen in 1975 [16], we have found modulated DC recording of the MCG to be feasible in a clinical setting if performed after extremely careful preparation of the patient. The DC measurements are influenced most by disturbing gastrointestinal activity (see Fig. 3) This method may turn out to be of clinical significance in the noninvasive detection of biological injury currents. In this way, it would b possible to determine whether ST-segment changes are primary and caused by abnormal repolarization or whether they are of a secondary nature and due to baseline shifts caused by ischemic injury currents. The encouraging results of preliminary investigations regarding risk stratification of patients prone to sudden cardiac death [8] or transplant rejection [17] have to be verified with sufficiently large patient groups and prospective multicenter studies to prove the predictive power of magnetocardiography in these fields.

References

1. Baule G and McFee R (1963) Am Heart J 66: 95–96.
2. Cohen D, Edelsack EA and Zimmermann JE (1970) Appl Phys Lett 16: 278–280.
3. Erné SN (1985) Med Biol Eng Comput 23: 1447–1450.
4. Fenici RR and Melillo G (1990) In: Williamson SJ, Hoke M, Stroink G and Kotani M (eds) Advances in biomagnetism, Plenum Press, New York, pp 409–415.
5. Katila T, Mariewski R, Maekijaervi M, Nenonen J and Siltanen P (1987) Phys Med Biol 32: 125–131.
6. Mori H and Nakaya Y (1988) CV World Report 1: 78–86.
7. Schmitz L, Brockmeier K, Trahms L and Erné SN (1990) In: Williamson SJ, Hoke M, Stroink G and Kotani M (eds) Advances in biomagnetism, Plenum Press, New York, pp 453–456.
8. Stroink G, McAulay CE, ten Voorde B, Montagne T and Horacek BM (1986) In: 8th Conf Eng Med Biol Soc, p 445.

9. Schneider S, Hoenig E, Reichenberger H, Abraham-Fuchs K, Moshage W, Oppelt A, Stefan H, Weikl A and Wirth A (1990) Radiology 176: 825–830.
10. Moshage W, Weikl A, Abraham-Fuchs K, Schneider S, Göhl K, Feistel H, Bachmann K and Wolf F (1990) Herz/Kreislauf 22: 245–249.
11. Achenbach S, Moshage W, Weikl A, Härer W, Abraham-Fuchs K, Göhl K and Bachmann K (1990) Biomed Technik 35 (3): 160–161.
12. Moshage W, Achenbach S, Göhl K, Weikl A, Abraham-Fuchs K, Schneider S and Bachmann K (1991) Radiology 180: 685–692.
13. Moshage W, Achenbach S, Bolz A, Weikl A, Wegener P, Bachmann K and Schaldach M (1990) Biomed Technik 35 (3): 162–163.
14. Oeff M, Erné SN, Jericzek H, Hennig L, Dulce M and Schröder R (1991) Magnetocardiographic guiding of catheter ablation of accessory pathways. XIII Congress of the European Society of Cardiology, Amsterdam.
15. Graumann R, Abraham-Fuchs K, Moshage W and Schneider S (1992) Reconstruction of current densities with anatomical constraints, this volume.
16. Cohen D and Kaufman L (1975) Circ Res 36: 414–424.
17. Schmitz L (1990) Clinical application of biomagnetism in heart transplantation. Symposium on the occasion of the Opening of the Biomagnetic Center Erlangen.

Psychophysiology, 32 (1995), 511-525. Cambridge University Press. Printed in the USA.

FOR DISTINGUISHED EARLY CAREER CONTRIBUTION TO PSYCHOPHYSIOLOGY: AWARD ADDRESS, 1994

Words and sentences: Event-related brain potential measures

CYMA VAN PETTEN
Department of Psychology, University of Arizona, Tucson, USA

Abstract

Interactions between sentences and the individual words that comprise them are reviewed in studies using the event-related brain potential (ERP). Results suggest that, for ambiguous words preceded by a biasing sentence context, context is used at an early stage to constrain the relevant sense of a word rather than select among multiple active senses. A study comparing associative single-word context and sentence-level context also suggests that sentence context influences the earliest stage of semantic analysis, but that the ability to use sentence context effectively is more demanding of working memory than the ability to use single-word contexts. Another indication that sentence context has a dramatic effect on single-word processing was the observation that high- and low-frequency words elicit different ERPs at the beginnings of sentences but that this effect is suppressed by a meaningful sentence context.

Descriptors: Event-related potential, N400, Semantic context, Sentence processing, Word frequency, Ambiguity

Language is marked by part-whole relationships at many levels: letters or phonemes make up words, words make up sentences, and sentences make up discourse. Some basic questions in psycholinguistics concern how these part-whole relationships map onto the human system for processing language. Research over the last century has suggested that neither comprehension nor production proceed in a strictly serial fashion from the simplest to the most complex units. Instead, both introspection and empirical measures demonstrate a multitude of context effects wherein higher-level units apparently influence the perception, production, or speed of analyzing lower units. In production, such context effects include the coarticulation of adjacent phonemes, so that the pronunciation of any given consonant or vowel will depend on the preceding and following phonemes. In speech perception, the same acoustic signal can be perceived as different phonemes depending on the speaker and his or her rate of speech; listeners normally adjust for these sources of variability by integrating information across more than one phoneme (for review, see Handel, 1989). For these context effects in speech perception and production, the relevant units seem to be phonemes and syllables. Other context effects can only be explained by granting that whole words are an important unit. In the auditory modality, a well-studied phenomenon is the phoneme restoration effect, wherein listeners claim to hear all of a word although one phoneme has been replaced with a cough or white noise (Warren, 1970). Analogous context effects occur for the orthographic pattern of written words. A character such as A might be reported as an "H" in "THE," but as an "A" in "CAT." Even for stimuli consisting of well-formed letters, word superiority effects indicate that whole words can be easier to perceive than isolated letters (Cattell, 1885, 1886; cited and discussed in Henderson, 1982).

The studies reviewed here investigate context effects that involve meaning and that operate at the level of interactions between sentences and words. Semantic context effects have stimulated a great deal of research, beginning with reports in the 1960s and 1970s that words which form a congruous completion to a sentence fragment are more likely to be identified with brief exposure durations and receive faster responses in a vari-

This paper is based on an address presented upon receipt of the Award for Distinguished Early Career Contribution to Psychophysiology at the 34th annual meeting of the Society for Psychophysiological Research, Atlanta, GA, October 1994.

The work described here was supported by a grant to Marta Kutas from the National Institute for Child Health and Human Development (HD22614), and to Cyma Van Petten from the National Institute for Neural Disorders and Stroke (NS30825). I was also supported by a graduate fellowship from the National Science Foundation during part of the time the work was conducted.

I am indebted to Marta Kutas for her mentorship and continuing collaboration. Some of the studies reviewed received major contributions from Jill Weckerly and Robert Kluender and could not have been completed without the technical expertise of Ronald Ohst and Jonathan Hansen. The comments of John Cacioppo, Melinda Clark, Marta Kutas, and Ava Senkfor on an earlier draft of this paper are appreciated.

Address reprint requests to: Cyma Van Petten, Department of Psychology, University of Arizona, Tucson AZ, 85721, USA.

ety of tasks than incongruous completions (e.g., Fischler & Bloom, 1979; Tulving, Mandler, & Baumal, 1964). Although event-related potentials (ERPs) came into widespread use at about the same time that language comprehension became (again) a respectable research topic, initial attempts to apply ERPs to the study of language processing were discouraging (e.g., see the conclusions of Donchin, McCarthy & Kutas, 1977; Galambos, Benson, Smith, Schulman-Galambos, & Osier, 1975). In contrast, research over the last 15 years has demonstrated that ERPs are a useful tool for the study of language processing. A great deal of our current confidence that ERPs elicited by linguistic stimuli are informative can be credited to a simple change in research strategy: investigators turned away from the requirement that the stimuli used to elicit ERPs in different conditions be physically identical; instead, they formed averaged ERPs from sets of stimuli that were physically diverse but conceptually similar. This research strategy led Kutas and Hillyard (1980a) to compare words that did and did not fit with an established semantic context. Their report that semantic context influenced a late negative component of the ERP, the N400, instilled new optimism that the ERP methodology could provide online, unobtrusive measures of language processing (for reviews of some of the many studies in the last 15 years, see Kutas & Van Petten, 1988, 1994).

The studies reviewed here focus on contextual interactions between sentences and the individual words that comprise them. Our intuition suggests that individual words can have vague, broad, or ambiguous meanings and that these are sharpened by our sense of what the speaker or writer is trying to convey. But the paradox remains that individual words are used to arrive at a sentence meaning, and yet overall sentence meaning determines the meaning of individual words. Views range from those of Schank (1978), who wrote "Analysis proceeds in a top-down predictive manner. Understanding is expectation based. It is only when the expectations are useless or wrong that bottom-up processing begins" (p. 94), to Kintsch and Mross (1985), who wrote "What readers say they expect at a certain place in a certain text has no effect on sense activation, or in other words, there are no top-down effects of thematic context on the sense activation phase of word identification" (p. 346). In recent years, the dominant view has more closely resembled that expressed by Kintsch and Mross (1985): the early phases of semantic analysis are insensitive to sentence or discourse context. For instance, one influential model supposes that word- and sentence-level analyses take place in distinct modular components of the language-processing system and that communication between them occurs in only one direction: from word to sentence (Fodor, 1983; Forster, 1979, 1981; Garrett, 1990). There may be stages of visual word recognition that precede any semantic analysis, as suggested by recent intracranial ERP recordings (McCarthy, Nobre, Bentin, & Spencer, 1995; Nobre & McCarthy, 1995; Nobre, Allison, & McCarthy, 1994), but the studies reviewed here suggest that sentence context modifies and permeates many aspects of the processing of single words.

Sentence Constraints on Ambiguous Words

My first sentence study used a paradigm considered to be definitive for isolating lexical from sentence-level semantics. Most English words have many subtly different senses, which may or may not be highlighted in different contexts, but a few are considered "ambiguous" because they possess at least two meanings that are unrelated to one another. Although we are not usually aware of the irrelevant meanings of homographic or homophonic words, Conrad (1974) was the first to reason that activation of these senses might be detected in a semantic priming paradigm. She presented auditory sentences ending with a homophonous word, followed by a word printed in colored ink. Color-naming times were slower for words related to either sense of the homophone than for completely unrelated words. The interpretation of this Stroop interference was that both meanings of the homophone were active enough to prime their semantic associates and make it more difficult to suppress those associates in favor of their ink colors. Conrad's observation was replicated (Oden & Spira, 1983) and followed by many studies using lexical decision or pronunciation latencies to measure priming of relevant and irrelevant associates of homographic or homophonous words that had been disambiguated by a sentence context (Blutner & Sommer, 1988; Kintsch & Mross, 1985; Onifer & Swinney, 1981; Seidenberg, Tanenhaus, Lieman, & Bienkowski, 1982; Swinney, 1979; Till, Mross, & Kintsch, 1988; also see review by Simpson, 1994). These studies manipulated the temporal interval between the ambiguous and probe words and found that a short interval yielded priming for both relevant and irrelevant associates, whereas a long interval yielded priming for only the contextually relevant target. These investigators thus converged on a two-stage model of semantic processing: (a) single words quickly and automatically activate all of their possible meanings, which in turn activate the meanings of their lexical associates; but (b) a slower-acting sentence processor selects the relevant meaning of each word and allows the irrelevant activations to fade. Onifer and Swinney (1981) described this model most succinctly:

> By this hypothesis, when an ambiguity (or any word) is encountered, all of its senses or meanings are at least momentarily made available to the comprehension device. ...Lexical access is viewed as being an isolable subprocess in the comprehension routine, one that operates in a bottom-up fashion based entirely on the (acoustic/phonetic) form of the word. The effects of contextual constraints are seen to operate on the accessed candidates in a subsequent, independent process. (p. 227)

A more recent (and still a minority) view argues that a sentence context of appropriate strength and nature can constrain initial meaning access (Kellas, Paul, Martin, & Simpson, 1991; Paul, Kellas, Martin, & Clark, 1992; Simpson & Kreuger, 1991; Tabossi, 1988; Tabossi & Zardon, 1993). Nonetheless, many textbooks offer lexical ambiguity research as a premier example of the failure of sentence processing to influence the initial stages of semantic analysis (Carroll, 1994; Garrett, 1990).

The claim that there are two discrete stages of semantic analysis is well suited to an evaluation with ERPs because these offer a continuous record of brain activity beginning at stimulus onset. We constructed a set of 120 sentences ending with homographs, together with an equal number ending in nonhomographic words (Van Petten & Kutas, 1987a). Each homograph sentence was followed by one of three types of probe words—contextually relevant, contextually irrelevant, or unrelated, as shown in Table 1. The sentences biased the less common, subordinant, sense of each homograph so that the contextually relevant probe word was related to the subordinant meaning. The sentences were presented visually, one word at a time, with a duration of 200 ms per word. The probe words were presented immediately at the offset of the final sentence word (200 ms stimulus onset asynchrony [SOA]) or 500 ms later (700 ms SOA) in separate groups of subjects.

Table 1. *Examples of the Lexical Ambiguity Stimuli*[a]

	Contextually relevant	Contextually irrelevant	Unrelated
Homograph sentences, subordinant			
He was not used to hard labor and soon began to tire.	sleep	wheel	rifle
The protestors wanted to shut down the nuclear power plant.	factory	green	mouth
When the judge entered the courtroom the audience all rose.	stood	flower	fashion
Homograph sentences, dominant			
The old car had a flat tire.	wheel	sleep	rifle
While she was away her next door neighbor fed the cats and watered the house plants.	factories	green	mouth
The florist gave his wife a single red rose.	flower	stood	fashion
Nonhomograph sentences			
His uncle wanted to know why he hadn't settled down and gotten married.	single	–	trade
She let the phone ring six times but there was no answer.	question	–	room

[a]The first ambiguity experiment described in the text (Van Petten & Kutas, 1987a) used sentences biasing the subordinant meaning of homographs. The second experiment (unpublished) used sentences biasing the dominant meaning. Both used an equal number of sentences ending with unambiguous words.

We first verified that the stimulus set was adequate by recording pronunciation latencies to the probe words. The behavioral data in the short SOA condition replicated the "multiple access" phenomenon in showing faster reaction times (RTs) for both relevant and irrelevant probe words versus the unrelated probes. At the longer SOA, irrelevant probes were responded to as slowly as unrelated words. The ERP version of the experiment was nearly identical to the reaction time version, except that we eliminated the naming task to avoid artifacts from muscle activity and tongue movements. To ensure that subjects read the probe words, we presented a single letter 1.5 s later and asked them to indicate whether or not the letter was in the probe word. This task delays any binary decisions until well beyond the probe word so that N400 latencies can be measured without the complication of overlapping decision-related P300s (see Kutas & Hillyard, 1989).

The ERP results are shown in Figure 1. With a long SOA (700 ms), the ERPs elicited by the sentence-final and probe words can be distinguished clearly from each other. There were no differences among the ERPs elicited by the sentence-final words, so the long SOA condition did not suggest that any special processing was accorded to the homographs as compared with the unambiguous final words. ERPs to the probe words did vary according to their semantic relationship to the sentence-final word. The unrelated probe words elicited larger N400s than contextually relevant probes following both homograph and nonhomograph sentences. The contextually irrelevant probes also elicited large N400s, which were indistinguishable from unrelated probes. The N400 differences had typical onset and peak latencies for words in pairs, beginning about 300 ms after stimulus onset and peaking at about 500 ms poststimulus. Even the two-stage model of semantic processing would predict this pattern of results, but the long SOA data indicate that if our subjects had a delayed realization that the irrelevant probe was related to the homograph, it was not reflected in the N400.

The ERPs recorded in the short SOA condition are different in waveshape from those observed with a longer SOA. At minimum, the ERPs elicited by the sentence-final and probe words are subject to temporal overlap and superimposition, but it is also possible that the waveform reflects a cognitive process not present in the long SOA condition, that is, processing two words at the same time. In either case, the influence of semantic relationship for the nonhomograph conditions was similar to that observed at the longer SOA: a monophasic negative difference between related and unrelated probes beginning at 300 ms poststimulus. In the homograph conditions, the difference between contextually relevant and completely unrelated

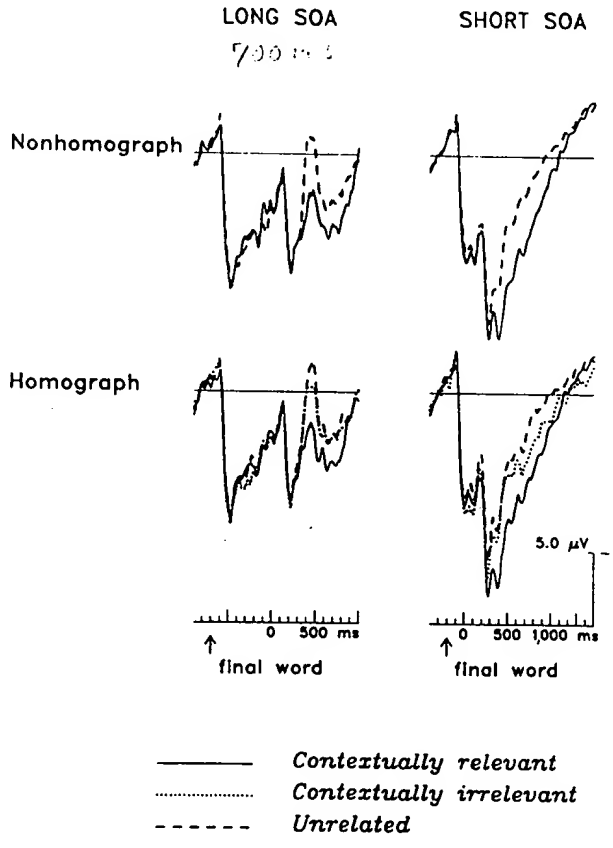

Figure 1. Grand average ERPs from site Cz. Fifteen subjects were in the long SOA group, and 18 were in the short SOA group. Time 0 marks the onset of probe words following sentences that end with homographic or nonhomographic words. Onset of the sentence-final words is marked by the arrow (data from Van Petten & Kutas, 1987a).

probes was much like the semantic context effect in the nonhomograph conditions.

As in the RT data, the short temporal interval yielded a difference between the contextually irrelevant and unrelated probes that was not observed with a long SOA. Beginning at about 500 ms after the probe word's onset, the ERPs elicited by the irrelevant probes are distinct from those to the unrelated words. However, this difference began well after the basic N400 semantic context effect. Both the unrelated and irrelevant probe ERPs diverge from the related ERP at about 300 ms poststimulus and are initially indistinguishable. It is only around 500 ms poststimulus that the response to irrelevant probes begins to resemble that of the contextually relevant probes. These results demonstrate that irrelevant probes are subject to a semantic context effect under this set of conditions but that priming for these words lags behind that for contextually relevant words. Even the delayed ERP context effect was, however, earlier than the RTs recorded in the behavioral portion of this study.

The results of this ambiguity study are not compatible with the "multiple-access" theory that all meanings of a word are activated simultaneously regardless of sentence context. The RT and ERP measures were both sensitive to the temporal interval between homograph and probe word: neither showed a priming effect for irrelevant probes at the long SOA, and both showed context effects at the short SOA. The ERP data, however, provided a more detailed picture of the time course of the context effects for relevant and irrelevant probes at the short SOA. Although both occurred early enough to affect overt behavior, the shorter onset latency for relevant probe words indicated an early influence of sentence context. The multiple access model predicted that, indeed, there are two temporally ordered phases of semantic analysis and two corresponding phases of context effect, but that sentential context influences only the late phase. The ERP latencies yielded the opposite pattern of results in suggesting that the meaning of a sentence constrained the earliest observable effect of semantic analysis.

But what accounts for the delayed N400 effect elicited by irrelevant probe words? The logic of the ambiguity paradigm is that the probe words serve as a tool for evaluating how subjects interpreted the preceding ambiguous word: if the probe word shows a priming effect, it can only be due to the prior interpretation of the ambiguous word. This logic can be challenged, however; perhaps the actual presentation of an irrelevant probe word activates the otherwise dormant meaning of the homograph. It may be counterintuitive to imagine that a probe word presented later could influence the meaning of the homograph. But all we need to assume is that analyzing a word's meaning is not instantaneous but rather a process that unfolds over time. Other experimental results have shown that reaction time and accuracy to respond to one word can be influenced by presenting a related word a short time later (Dark, 1988; Den Heyer, Briand, & Dannenbring, 1988; Kiger & Glass, 1983; Peterson & Simpson, 1989; Van Petten & Kutas, 1991b). This phenomenon has been called "backward" or "retroactive" priming, but we prefer to think of it as "mutual" priming. If two words are presented in close temporal conjunction, their processing is likely to overlap in time, and both words may benefit from this overlap if they are related. In the classic ambiguity paradigm, the preceding sentence context may provide an effective and constraining source of context for one reading of the ambiguous word. But while processing of the ambiguity is incomplete, the alternate meaning and its associated probe word can also form a related pair. The observed lag between the two ERP context effects may thus reflect the temporal lag between the presentation of the prior sentence context and the subsequent probe word context. The mutual priming account suggests that multiple access to both meanings of ambiguous words does occur but that it is an artifact of the laboratory paradigm rather than the natural state of affairs for words in context.

We performed a second experiment to test a possible alternative to the mutual priming account (Van Petten & Kutas, 1987b). As an alternative to the strong multiple access or selective access models, one can take an intermediate position that semantic activation is determined by an interplay between sentence context and the frequency of an ambiguous word's meaning (Kellas et al., 1991; Simpson, 1981; Simpson & Burgess, 1985). Most ambiguous words have a dominant and a subordinant sense when presented in isolation. Because the contextually irrelevant probes in the first experiment were related to the more dominant meaning, it is possible that the long-latency ERP context reflected a delayed, but obligatory, activation of this more common meaning. To test this possibility, we constructed a new set of sentences with the same homographic words, but now biasing the opposite, dominant, meaning of each homograph as shown in Table 1. If the late N400 context effect for irrelevant probes reflected obligatory access to a homograph's dominant meaning, then relating the irrelevant probes to the subordinant meaning should eliminate this effect. Alternatively, if the longer-latency ERP context effect were due to mutual priming between the homographs and irrelevant probe words, then the dominance manipulation should have no impact.

The general methodology for the second ambiguity experiment was much like the first; 18 subjects participated in the 200 ms SOA version and 21 in the 700 ms SOA version. The ERPs were visually similar to those observed in the first experiment. As seen in Figure 2, there was little difference between the irrelevant and unrelated probes when these were separated by 700 ms. With a short SOA, the ERP elicited by irrelevant probes was initially indistinguishable from that elicited by the unrelated words but became more similar to relevant probe ERP later in the epoch. However, the delayed context effect only approached statistical significance ($p = .065$) when evaluated by the same measurement and statistical procedures as used in the first experiment. The statistical pattern of results was otherwise identical to the first experiment in showing that the prior sentence context influenced the earliest phase of the N400. But because the second study was designed to evaluate the presence or absence of the delayed context effect for irrelevant probes, the outcome was not fully satisfactory.

The ambivalent outcome of the second experiment may have been due to a methodological flaw in the stimulus construction. In the first experiment, the sentences provided a strong bias for the interpretation of the homographic final words but were only moderately predictive of the identity of the final word. Predictability was measured in an offline cloze probability test wherein pilot subjects were given the sentences without the final words and asked to fill in "the best completion" of each sentence; an average of 55% of the subjects chose the desired homographs. Given the sentence frames biasing the dominant meanings, the same homographs were much more predictable (mean cloze probability of 80%). If the ERP subjects were in fact predicting the sentence-final homographs before their actual appearance, the functional interval between the homographs and probe words would have been longer than the nominal SOA of 200 ms.

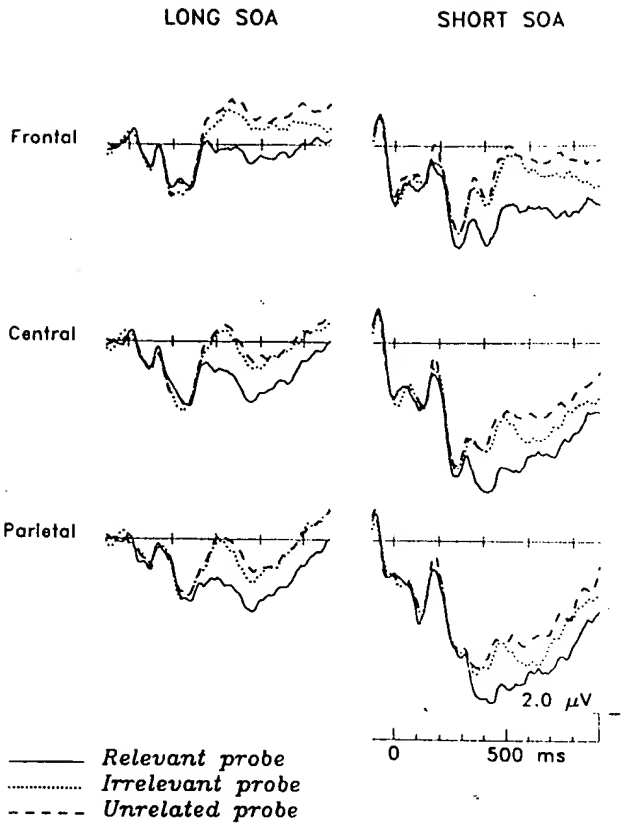

Figure 2. Grand average ERPs from Fz, Cz, and Pz. Eighteen subjects were in the long SOA group, and 21 were in the short SOA group. Time 0 marks the onset of probe words following sentences that end with homographic words (Van Petten & Kutas, 1987b).

Because the late context effect for irrelevant probes is only apparent when they are presented in close temporal proximity to the homographs, advance prediction of the homographs may have reduced the amount of temporal overlap in processing the homograph and probe words and weakened the late context effect.

The results of the two ambiguity experiments are in accord in indicating that the initial semantic processing of ambiguous words is guided by sentence context. This conclusion is inconsistent with the notion that there is a discrete stage of single-word semantic analysis independent of sentence context. Subsequent experiments, described below, explored other aspects of the interactions between single words and the sentences they comprise.

Influence of Sentence Context on Intermediate Words.

The initial experiments of Kutas and Hillyard (1980a, 1980b, 1980c, 1982) described the N400 effect as a difference between semantically congruent and anomalous sentence terminations. The terminal word congruity effect is robust and has been used as a tool to investigate differences between populations: monolinguals versus bilinguals (Ardal, Donald, Meuter, Muldrew, & Luce, 1990), children versus adults (Holcomb, Coffey, & Neville, 1992), young versus elderly adults (Gunter, Jackson, & Mulder, 1992; Woodward, Ford, & Hammett, 1993), deaf versus hearing individuals (Neville, Mills, & Lawson, 1992), language-impaired versus normal children (Neville, Coffey, Holcomb, & Tallal, 1993), and schizophrenic versus control subjects (Adams, Faux, Nestor, & Shenton, 1993; Andrews et al., 1993; Mitchell, Andrews, Catts, Ward, & McConaghy, 1991). The N400 semantic congruity effect has also been used to make comparisons among informational modalities (written, spoken and signed language, pictures, environmental sounds: Connolly & Phillips, 1994; Connolly, Philips, Stewart, & Brake, 1992; Connolly, Stewart, & Phillips, 1990; Holcomb & Neville, 1991; Ganis, Kutas, & Sereno, in press; Kutas, Neville, & Holcomb, 1987; Kutas & Van Petten, 1990; Neville, 1991; Nigam, Hoffman, & Simons, 1992; Van Petten & Rheinfelder, 1995) and to explore some aspects of syntactic processing (Garnsey, Tanenhaus, & Chapman, 1989). Despite the utility of the experimental effect, detecting semantically anomalous sentence endings is unlikely to be a core factor in natural language processing. Shortly after their initial description of the N400, Kutas and Hillyard quickly demonstrated that it is not restricted to final words, nor does it depend on semantic incongruity. In the middle of sentences, incongruous words also elicit a much larger N400 than congruous words (Kutas & Hillyard, 1983). More importantly, the amplitude of the N400 elicited by congruous final words is a graded function of their predictability from the sentence context (Kutas & Hillyard, 1984; Kutas, Lindamood, & Hillyard, 1984). These results are more in line with the view that linguistic incongruities, errors, or violations are likely to be epiphenomenal and reducible to more fundamental properties of language and cognition, at least some of which can be studied with the ERP methodology (see Kutas & Kluender, 1994).

It was with this view in mind that we examined the ERPs elicited by congruous intermediate words as a function of their ordinal position in sentences. Simple ordinal position is also unlikely to be a core factor in language processing. But for sentences outside of discourse context, the reader can have no knowledge of the content of any given sentence at its outset and thus must build a mental representation only as the sentence progresses. We thus predicted that words occurring early in sentences would elicit larger N400s than words that could benefit from more context because they occurred later. This prediction was confirmed; for the sentence materials initially examined, the amplitude of the N400 declined as a nearly linear function of each word's position in its sentence (Kutas, Van Petten, & Besson, 1988; Van Petten & Kutas, 1990). The linearity of the function may be an artifact of averaging across syntactically heterogenous sentences. Clause boundaries often mark semantic shifts so that a more fine-grained analysis with structurally and semantically homogenous sentences might reveal scallops in the N400/word position function corresponding to these boundaries.

Our first reports of the word position effect examined normal semantically congruous sentences. Subsequent experiments were designed to verify that the N400 amplitude decrement was indeed due to sentence context and not to some other factor such as a neural refractory period for the N400, similar to that described for the auditory N1 (Davis, Mast, Yoshie, & Zerlin, 1966). We also wanted to differentiate the possible contributions of a sentence's semantic and structural (syntactic) aspects. Finally, the initial experiment examined only the ERPs elicited by open class or content words (nouns, verbs, adjectives, -ly adjectives), whereas the next experiment in the series also examined the influence of word position on closed class or function

Table 2. *Examples of the Congruent, Syntactic, and Random Sentences*[a]

Congruent	The tenants were evicted when they did not pay the last two months rent.
	Most new drugs are tested on white lab rats.
	She played the drums in a rock and roll band.
Syntactic	He ran the half white car even though he couldn't name the raise.
	In the wet levels fathers were smoking by congress.
	He prepared at the back hand to pair up his robbers.
Random	To prided the bury she room she of peanut the had china.
	She which had jazz anchor a she to straight couldn't gun.
	Be place prefer the was city it and sure be perfume.

[a]One hundred sentences of each type were used in Van Petten and Kutas (1991a).

words (articles, prepositions, pronouns, etc).[1] The initial word-position finding was extended by using sentence materials like those shown in Table 2 (Van Petten & Kutas, 1991a). The *congruous* sentences were like those used in previous experiments. The *syntactic* sentences were constructed by taking a different set of normal sentences and replacing each open class word with one of the same form class (e.g., nouns for nouns, adjectives for adjectives, etc.) to leave a legal but meaningless English sentence.[2] *Random* "sentences" were constructed by starting with another set of normal sentences, replacing the open class words, and rearranging word order to create illegal and meaningless word strings.

The electroencephalographic (EEG) data from this experiment were initially averaged into 1-s ERP epochs beginning 100 ms before the onset of each word, contingent on sentence type and the position of the word in its sentence. These averages suggested that the prestimulus baselines for the various conditions were not equivalent; some of the differences between conditions appeared to begin at stimulus onset. Averages over a longer epoch with a pre-sentence baseline revealed that, in addition to the relatively short latency ERPs elicited by each word, there were slow potential differences between the three sentence types. In particular, Figure 3A shows that the random word strings were marked by a slow positive shift, which began at about the third word and increased in amplitude as the random strings progressed. Because the random strings were syntactically incoherent throughout, this slow positive potential may be similar to the recently reported "P600" response to occasional syntactic errors in otherwise normal sentences (Osterhout & Holcomb, 1992, 1993; Hagoort, Brown, & Groothusen, 1993). Because we were interested in evaluating the sensitivity of more phasic potentials to the experimental manipulations, we used a digital filter to separate higher-frequency components, such as the N400, from the slow positive potential. Figure 3B shows that N400 differences among the conditions could be observed after filtering out the slow potential.

For open class words, only the congruous condition yielded a decline in N400 amplitude as the sentences progressed; syntactic and random words elicited N400s of equivalent amplitude throughout the sentences (Van Petten & Kutas, 1991a). This result indicated that the word position effect is due to semantic aspects of sentence comprehension rather than some nonspecific effect of reading sequential words. We have observed the word position effect in every set of congruous sentences examined to date but have failed to find it in experiments in which subjects read connected text, as seen in Figure 4. We attribute this to the fact that readers do not start from scratch when processing sentences in coherent text but apply general discourse concepts derived from the preceding sentences and paragraphs. The absence of a word position effect in text suggests that the semantic factors driving N400 amplitude do not observe sentence boundaries but instead reflect the reader's conceptual representation of the material being read. This conclusion has been confirmed in a recent study by St. George, Mannes, and Hoffman (1994). The stimuli in their study consisted of deliberately vague paragraphs that are difficult to comprehend unless the reader is provided with an informative title beforehand, like those used by Bransford and Johnson (1972).[3] The amplitude of the N400 elicited by all the paragraph words was substantially smaller when subjects were allowed to read the informative title first.

[1]Linguists have traditionally divided words into "major" and "minor" classes, but the division has been labeled in different ways, reflecting a variety of ideas as to exactly what the distinction is and where it should be drawn (see Caplan, 1987; Garnsey, 1985). The major class is usually held to consist of nouns, verbs, most adjectives, and the *-ly* adverbs. An inclusive definition of the minor class consists of some 500 words in English, including auxiliary verbs (*was*), articles (*the*), complementizers (*which*), conjunctions (*or*), other sentence connectors (*thus*), interrogatives (*who*), verb particles (*not*), prepositions (*of*), pronouns, and some adjectives and adverbs (*much*, *often*, *very*). One dichotomy is "open versus closed class," which stresses the idea that new nouns and verbs are added to a living language on an almost daily basis, whereas the closed class does not readily admit new members. For example, the past few decades have seen attempts to add a new gender-neutral pronoun to English, but our continued use of "he or she" bears witness to the "closed-ness" of the "closed class." A different dichotomy—"content versus function"—stresses the idea that content words carry most of the semantic information in a sentence, whereas the function of "function" words is to create syntactic structure. Both contrasts are intuitive, but neither allow a true dichotomy. The open/closed contrast is based on historical language change, which occurs continuously. The content/function contrast is also more of a continuum than a sharp boundary. Generic content words such as *do*, *go*, and *stuff* convey little more semantic information than function words such as *beneath*, *toward*, and *often*. Moreover, the syntactic properties of content words, such as whether or not a verb can take a direct object, also play a major role in creating syntactic structure.

[2]Transitive verbs were replaced with other transitive verbs, and intransitive with intransitive. In addition, only *-ly* adverbs were replaced; quantifiers such as *some* and *many* were not replaced in constructing the syntactic sentences. Our dichotomous assignment of words to the open or closed class followed a similar principle of assigning words of ambiguous class to the closed class category.

[3]The stimuli in the study by St. George, Mannes, and Hoffman (1994) were full paragraphs, but analogous stimuli can consist of single sentences: "*parachute*; The haystack was important because the cloth had ripped."

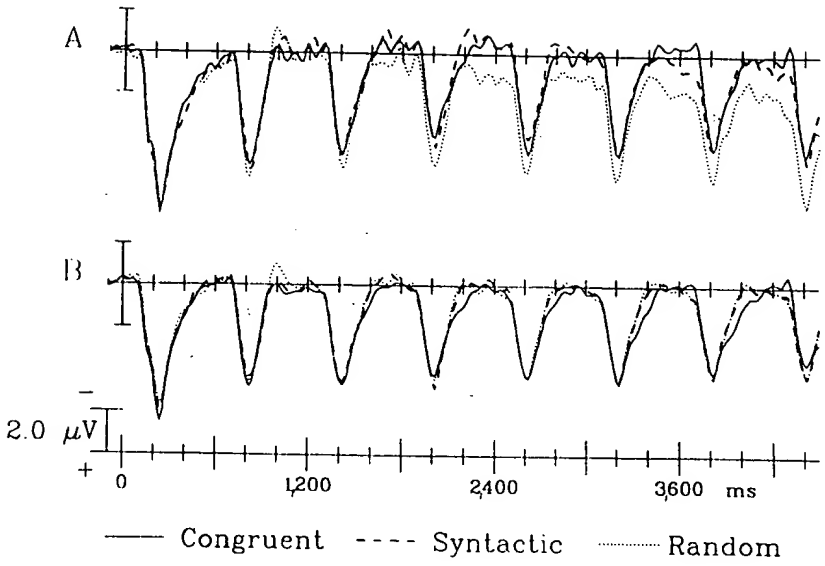

Figure 3. (A) Grand average ERPs from C3 for the first seven words of each sentence type, unfiltered. (B) The same data after applying a digital hipass filter to the EEG before averaging (Van Petten & Kutas, 1991a).

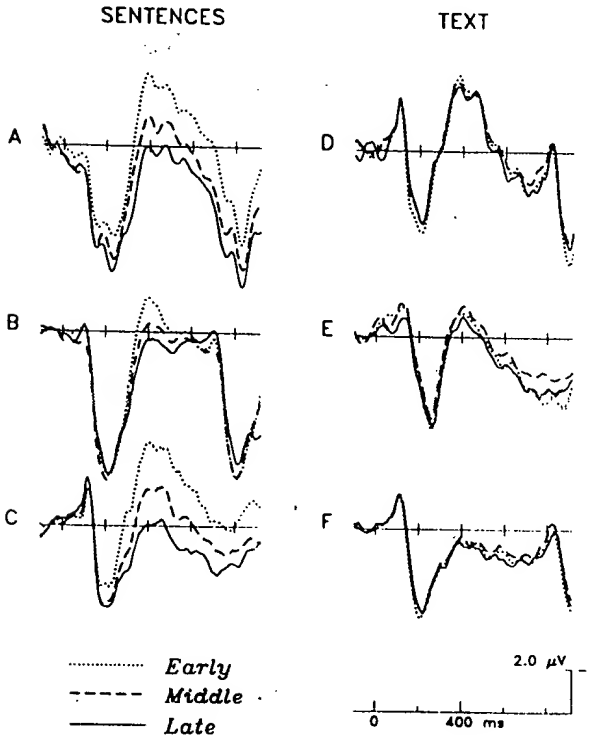

Figure 4. Grand average ERPs elicited by open class words according to position within congruous sentences, excluding initial and final words. Experiments A–C used isolated sentences; Experiments D–F used connected text. The numerical positions of *early*, *middle*, and *late* vary somewhat across experiments but correspond roughly to positions 2–3, 4–6, and 7+. Scalp site Cz. Data are from (A) Van Petten (1993), (B) Van Petten and Kutas (1991a), and (C) Van Petten and Kutas (1990). (D) Data are from unpublished observations from Kutas, Bates, Kluender, Van Petten, Clark, and Blesch (1988). The subjects were 15 adult monolingual English speakers reading children's stories in English. (E) Data are from unpublished observations from the experiment described in Van Petten, Kutas, Kluender, Mitchiner, and McIsaac (1991). The subjects were 16 adult monolingual English speakers reading nonfiction texts drawn from the *Reader's Digest*. (F) Data are from unpublished observations from Kutas et al. (1988). The subjects were 30 Spanish/English bilingual adults reading children's stories in Spanish.

Neither the syntactic nor random conditions yielded a word position effect for N400 amplitude. Moreover, the overall N400s elicited by open class words in these two conditions were indistinguishable, as seen in the left side of Figure 5. Given the dramatic subjective differences between the syntactic and random word strings, this latter finding may seem counterintuitive. But our hypothesis that N400 amplitude reflects the degree of contextual constraint would predict this result. At best, syntactic structure can indicate that the next open class word must be of a particular form class. This is a very weak constraint; knowing that an upcoming word should be a noun leaves a broad range of possibilities. In many cases, syntactic constraints on open class words are not even this strong; an article predicts a upcoming noun, but the noun might be preceded by one or more adjectives or adverbs. The weakness of syntactic as compared with semantic constraint is supported by the existing literature using behavioral measures (Tyler & Marslen-Wilson, 1986; Tyler & Wessels, 1983; Wright & Garrett, 1984). In contrast, syntactic constraints on closed class words might be stronger and more specific. For example, given the regularities of English, one might predict that *the* would follow *from*: prepositions are followed by noun phrases, most noun phrases begin with articles, and there are only a few articles in the English language (for comparisons of the predictability of open and closed class words, see Aborn, Rubenstein, & Sterling, 1959; Gough, 1983; Smith-Burke & Gingrich, 1979). Accordingly, we did observe N400 amplitude differences among the three sentence types for closed class words. The N400 elicited by closed class words is small overall, perhaps due to their high frequency of usage and predictability. But the right column of Figure 5 shows that a small amplitude negativity in the latency range of 300–400 ms was modulated by sentence context; the syntactic condition fell midway between the congruent and random conditions. This "closed class N400" had the same scalp distribution as that elicited by open class words; its shorter apparent duration is due to overlap with a later negative wave (the "N400–700") discussed below. However, the closed class N400 was not influenced by word position, suggesting that sentence constraints on closed class words operate locally rather than building up across the course of a sentence (for other reports of N400s elicited by closed

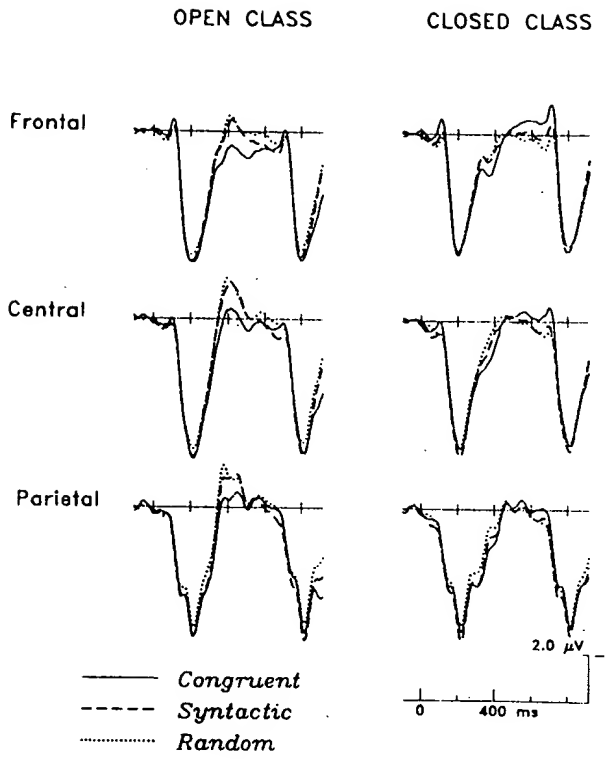

Figure 5. Grand average ERPs from Fz, Cz, and Pz recorded from 38 subjects (data from Van Petten & Kutas, 1991a). The amplitude and duration of the N400 difference is smaller than that observed in other experiments due to the application of a digital high-pass filter with a cutoff of 1 Hz. The text explains the motivation for applying this filter.

class words, see King & Kutas, in press; Kluender & Kutas, 1993b).

Differences between the ERPs elicited by open and closed class words have been reported in a number of studies (Kutas & Hillyard, 1983; Neville et al., 1992). Neville et al. described the differences as consisting of a larger N400 for open class words, a larger frontally distributed N280 for closed class words, and a slow frontally distributed negative wave dubbed the N400–700, which is also larger for closed than for open class words. Such ERP differences are potentially of great interest for two reasons. On the one hand, closed class words typically make different contributions to sentence structure than do open class words, such as introducing new sentence constituents. For instance, the word *that* in "The boy that the dog bit is feeling fine," introduces a relative clause. It is thus possible that one or more of the observed ERP differences reflect the utilization of the cues that closed class words offer for parsing a sentence. On the other hand, a variety of other processing distinctions have been attributed to the two vocabulary classes, some of which are independent of the differential roles they may play in sentences. Among these are that (a) production and comprehension of closed class words are more severely impaired in aphasia due to frontal lobe damage (Kean, 1985; Rosenberg, Zurif, Brownell, Garrett, & Bradley, 1985), (b) frequency of usage influences reaction time to open but not closed class words (Bradley, 1983), (c) divided visual field presentation produces different patterns of asymmetry for the two classes (Bradley & Garrett, 1983), (d) closed class words are less subject to speech errors (Garrett, 1982), and (e) closed class words are acquired later in childhood (Gleitman, Gleitman, Landau, & Wanner, 1989). However, some of these claims have been challenged on empirical grounds, and others have been attributed to factors that are correlated but not intrinsic to the open/closed distinction, such as the tendency for closed class words to be high in frequency of usage, short in length, and lacking in phonological stress (Bates & Wulfeck, 1989; Besner, 1988; Bock, 1989; Chiarello & Nuding, 1987; Dell, 1990; Gordon & Caramazza, 1985; Kean, 1979; Kolk & Blomert, 1985; Petocz & Oliphant, 1988; Shapiro & Jensen, 1986).

The observed ERP differences between open and closed class words in sentences may thus be related to (a) their differing syntactic roles, (b) intrinsic differences between the open and closed class vocabulary per se, and/or (c) other factors that are influential in processing both open and closed class words but that tend to be correlated with class membership. I have already suggested that the smaller N400 elicited by closed than open class words in sentences may be due to their higher frequency and greater predictability (see also Garnsey, 1985; Kluender & Kutas, 1993b). Recent work by King and Kutas (1995) has suggested that the N280 may be sensitive to word frequency and length rather than vocabulary class per se (but see Neville et al., 1992).

The contrast among congruent, syntactic, and random sentence types may shed some light on the functional significance of the N400–700 component. Figure 6A contrasts the ERPs elicited by open and closed class words in congruent sentences and illustrates the typical result of a larger N400–700 elicited by

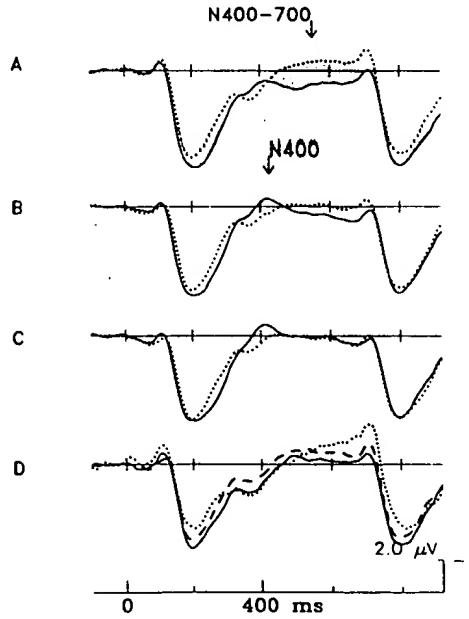

Figure 6. Intermediate sentence words. Rows A–C show the ERPs elicited by open (solid line) versus closed (dotted line) at Fz. In congruent sentences (A), these are distinguished by a slow late negative potential dubbed the N400–700. This potential is small in syntactically structured but semantically anomalous sentences (B) and absent in random word strings (C). Row D shows that the N400–700 develops over the course of congruent sentences: the solid line indicates closed class words occurring in the third and fourth sentence positions; the dashed line represents the fifth and sixth sentence positions; and the dotted line represents the ninth and tenth positions (data from Van Petten & Kutas, 1991a).

closed class words (this is also apparent in Figure 5). The N400-700 proved sensitive to overall sentence condition: Figure 6B shows that closed class words in syntactic sentences also elicited an N400-700, and Figure 6C shows that the same words in random sentences did not. These results indicate that the component is tied to some aspect of sentence processing rather than vocabulary class per se, but the larger amplitude in congruent than in syntactic sentences also suggests that the N400-700 is sensitive to more than purely syntactic factors. Finally, Figure 6D shows that the N400-700 develops over the course of congruous sentences, becoming larger with increasing word position. This pattern of results is consistent with the hypothesis that the N400-700 is a member of the contingent negative variation (CNV) family of potentials (Hillyard, 1973; McCallum & Papakostopoulos, 1973; Walter, Cooper, Aldridge, McCallum, & Winter, 1964) and that its amplitude reflects a subject's degree of anticipation while waiting for the next word to appear when sentences are presented in a word-by-word format. Closed class words are particularly likely to elicit anticipatory processes because they are fixated for short periods of time in natural reading, but our typical presentation format includes a uniform interval between words. Closed class words also tend to occur at the beginnings of phrases but signal that more informative open class words are coming (see King & Kutas, in press). The larger amplitude N400-700 in congruous sentences might thus be attributed to subjects' more active involvement in reading these as compared with meaningless word strings. These speculations about the identity of the N400-700 and CNVs elicited in nonlinguistic paradigms might be tested by varying the interval between successive words, and by comparing the scalp distributions of slow negative potentials elicited during sentences versus nonlinguistic strings of stimuli.

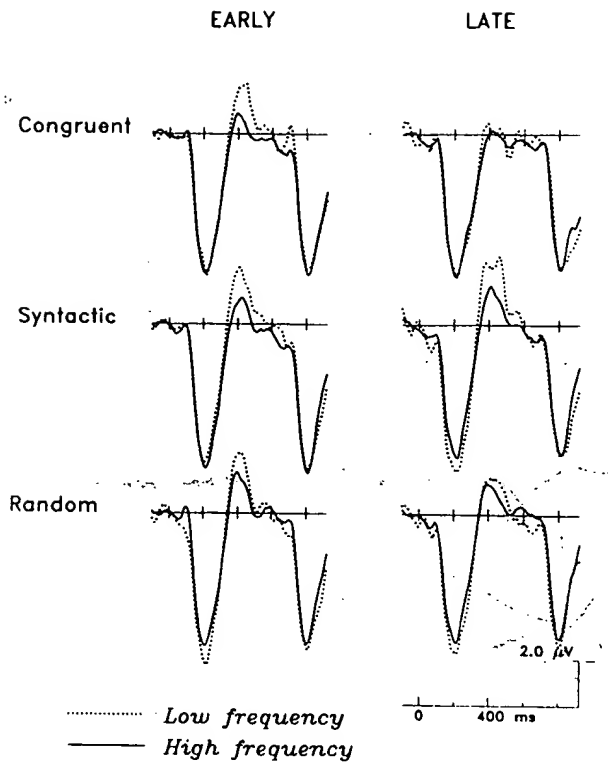

Figure 7. Grand average ERPs elicited by open class words at Cz in three sentence types. *Early* and *late* refer to approximately the first and second halves of the sentences, excluding the initial and final words. *High frequency* is defined as 30/million or higher when summed across all regularly inflected forms in the Francis and Kucera (1982) corpus; *low frequency* is 29/million or lower (Van Petten & Kutas, 1991a).

Sentence Context and Word Frequency

The experiments reviewed above indicate that the decline of N400 amplitude across a congruent sentence can be taken as an index of sentence-level semantic context. We have used this word position effect as a vehicle to examine the relationship between sentential context and lexical variables. One such lexical variable is *word frequency*. The normative frequency with which single words occur in the language is calculated by examining many samples of written or spoken discourse and scoring the number of occurrences of each word (see Francis & Kucera, 1982). As such, frequency is a purely lexical characteristic. In nearly all laboratory tasks using isolated words, subjects require longer exposure durations or more time to respond to rare than to common words (e.g., Rubinstein, Garfield, & Millikan, 1970; Solomon & Howes, 1951). The ubiquity of word frequency effects has led many theorists to give this factor a prominent place in models of word recognition (Becker, 1980; Bradley & Forster, 1987; Marslen-Wilson, 1987; Morton, 1969; Norris, 1986; Sharkey & Sharkey, 1992). The role of both frequency and semantic context has received different treatment across models, so that both additive and interactive effects of the two factors have been predicted (for reviews, see Van Petten & Kutas, 1990, 1991b). In several models, the underlying mechanisms for both frequency and context effects are closely tied to the demands of particular laboratory tasks such as pronunciation and lexical decision. Different information can be gleaned by examining dependent measures that can be collected without imposing a task in addition to language comprehension. Both eye movements and ERPs are elicited spontaneously as subjects read so that these methods do not depend on the imposition of a secondary task.[4] Both of these unobtrusive measures show word frequency effects. Gaze durations are longer for low- than for high-frequency words (see Rayner & Sereno, 1994). In lists of single words, larger N400s are elicited by low-frequency words (Rugg, 1990; Smith & Halgren, 1987).

We have used ERPs to examine the relationship between word frequency and sentence context. In the study including congruent, syntactic, and random sentence types, low-frequency words occurring near the beginning of all three sentence types elicited larger N400s than high-frequency words, as seen in Figure 7 (Van Petten & Kutas, 1991a). As the sentences progressed, the N400 frequency effect in congruent sentences was eliminated, but in the conditions without semantic context, low-frequency words continued to elicit larger N400s. Similar interactions between the word position effect (a measure of sentential semantic context) and the lexical variable of word frequency have been observed in several other experiments (Van Petten & Kutas, 1990; Van Petten, unpublished observations). Figures 8 and 9 show

[4]Of course, eye movements are detrimental to standard ERP recording procedures due to the associated electrooculographic artifacts. In all of the studies reviewed here, spontaneous eye movements were discouraged by presenting sentences one word at a time for brief durations, and trials contaminated by EOG artifacts were excluded from the averaged ERPs.

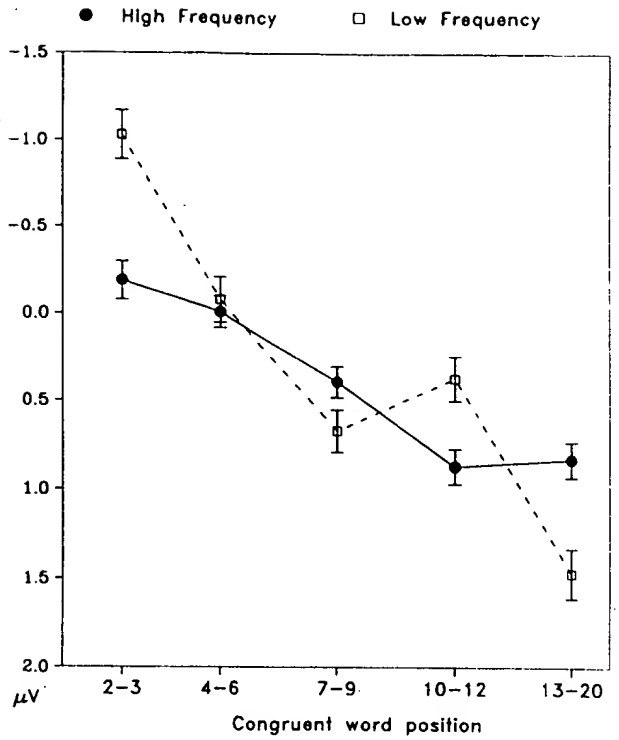

Figure 8. Mean voltage within the peak latency range of the N400 (300–500 ms poststimulus onset) for open class words in congruent sentences relative to a 100-ms prestimulus baseline. Examples of the sentences are shown in Table 3; the critical word pairs shown there were also excluded. The amplitude measure is averaged across all electrode sites (Van Petten, 1993).

that the word frequency effect is eliminated fairly early in meaningful sentences but persists throughout semantically anomalous sentences. Figure 8 also shows that the interaction between word position and frequency cannot be attributed to a "floor effect" in N400 amplitude. Although the word frequency effect was eliminated by about the fifth word of congruent sentences, N400 amplitude continued to decline with increasing word position. This pattern of results indicates that, although word frequency is a lexical variable, the human language-processing system does not always respect the boundary between lexical and sentential processing. These data thus conflict with hierarchical models of language processing that stipulate a purely "bottom-up" relationship between words and sentences. They do not, however, rule out the possibility that there may be several "word frequency effects," some of which are contingent on the use of particular behavioral tasks and are not reflected in N400 amplitude (see Balota & Chumbley, 1984, 1985; Van Petten 1991b).

Lexical Versus Sentential Semantic Context

Semantic context manipulations do not require sentence materials; reports of the impact of semantic context in pairs or lists of words number in the hundreds (see Balota, 1990; DeGroot, 1990). Shortly after Kutas and Hillyard (1980a) described the N400 in sentence contexts, other investigators reported similar N400 effects with word pairs or lists (Bentin, McCarthy, & Wood, 1985; Harbin, Marsh, & Harvey, 1984; Rugg, 1985). However, explaining how both single-word and sentence contexts can both yield "priming" effects has been a nagging problem in psycholinguistics. The most frequently cited explanation for lexical context effects is "spreading activation," a mechanism that allows the processing of one word to strengthen temporarily the long-term memory representation for another word due to structural links between associated items (Collins & Loftus, 1975). Whether or not spreading activation is a viable mechanism for lexical context effects, it clearly cannot account for sentential context effects. Because the number of congruent sentences is infinite in any natural language, there can be no preexisting links between every particular sentence and all the single words it may contain. Many investigators who have considered both varieties of context effect have opted for different underlying mechanisms. One view is that lexical context may exert at least some of its influence through a fast and automatic mechanism such as spreading activation within the mental lexicon, whereas sentential context acts via a slower, more strategic mechanism that is part of an entirely different "level" of the language-processing system (Fodor, 1983; Forster, 1981; Seidenberg et al., 1982; Till et al., 1988). This view is closely associated with those described in the lexical ambiguity section in proposing two discrete stages of semantic analysis, either of which can lead to differential processing (or priming) of subsequent words. One clear prediction from this model is that a sentence-level context effect should have a slower onset than a lexical-associative context effect.

A prediction about the time course of context effects is one well suited to a test by the ERP methodology. Sentences such as those shown in Table 3 were used to contrast the two vari-

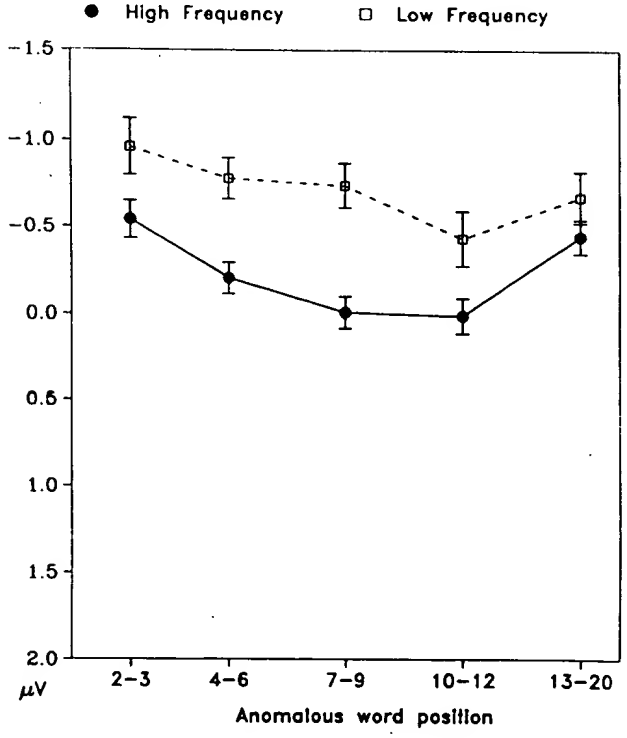

Figure 9. Mean voltage within the peak latency range of the N400 (300–500 ms poststimulus onset) for open class words in semantically anomalous sentences relative to a 100-ms prestimulus baseline. Examples of the sentences are shown in Table 3; the critical word pairs shown there were also excluded. The amplitude measure is averaged across all electrode sites (Van Petten, 1993).

Table 3. *Examples of the Stimuli Used to Compare Lexical and Sentence-Level Context*[a]

Congruent associated	When the *moon* is full it is hard to see many *stars* or the Milky Way.
	There were advantages to living in a *city* but Martha moved to a small *town* for the peace and quiet.
Congruent unassociated	When the *insurance* investigators found out that he'd been drinking they *refused* to pay the claim.
	The biologist went to the desert every *week* to collect a particular *species* of lizard that he hoped to study.
Anomalous associated	When the *moon* is rusted it is available to buy many *stars* or the Santa Ana.
	There was jewelry to drumming in a *city* but Martha turned to a gray *town* for the lizard and scones.
Anomalous unassociated	When the *insurance* supplies explained that he'd been complaining they *refused* to speak the keys.
	The shirt went to the gun every *week* to keep a good *species* of fumes that it hired to see.

[a]One hundred twenty sentences of each type were used in Van Petten (1993). Across conditions, the critical words (italicized) were matched for length, frequency, and position in the sentences. The experiment was conducted in two sessions so that subjects saw each critical word pair only once in each session.

eties of context (Van Petten, 1993). Each sentence contains a critical pair of words. In the *congruent-associated* condition, the two critical words are embedded in a meaningful sentence but are also related to each other independent of the sentence context. As compared with the first word of the pair, the second can thus benefit from a greater general sentence context and from its lexical-associative relationship to the first word. In the *anomalous-associated* condition, the same word pairs were embedded in syntactically legal but semantically anomalous sentences. In this condition, the second critical word can benefit only from the preceding lexical associate. In the *congruent-unassociated* condition, the critical words are only related via the general sentence context. The ERP elicited by the second critical word should differ from that of the first critical word only as a consequence of sentential context; the difference between the critical words in this condition is, in fact, a subset of the more general word position effect described earlier. Finally, the *anomalous-unassociated* condition is a control in which we expected no N400 amplitude difference between the first and second words of the critical pairs. Figure 10 shows that the results were as expected in that three of the four conditions resulted in a decrement of N400 amplitude from the first to second critical words. The latency data were, however, of greater interest for testing the hypothesis that the sentential context effect would be delayed relative to the lexical one. The onset latencies of the effects in the congruent-unassociated and anomalous-associated conditions were indistinguishable. Like the ambiguity study, these results provide no evidence for a strictly lexical stage of semantic analysis that precedes sentence integration.

The data did, however,[5] reveal an interesting difference between lexical and sentential contexts. Essentially every subject showed an N400 amplitude difference between associated and unassociated word pairs, but there was substantial individual variability in the amplitude of the sentential context effect.[5] Post hoc analyses showed that the amplitude of a subject's sentential context effect was correlated with performance in the behavioral task assigned during this experiment (Van Petten, 1993). Although an overt behavioral task is not necessary to observe semantic context effects in the ERP, including one is useful for encouraging subjects to stay alert and engaged in their primary task of reading for comprehension. The criteria I have used in selecting a task for sentence studies are that the task (a) not introduce decision-related P300s during the ERP epochs of greatest interest and (b) not draw attention away from comprehension of the sentences.[6] In this experiment, a single word appeared 1.5 s after each sentence, and subjects decided whether or not the word had been a part of the preceding sentence. Half of the probe words occurred in the preceding sentence and half

[5]The sentential context effect was defined as a subset of the more general word position effect: a decline in N400 amplitude from the first to second member of the critical pairs in the congruent unassociated condition. The slope of the more general word position effect across all congruent sentences also varied among subjects; those with a large sentential context effect also had steeper slopes in the function relating word position and N400 amplitude.

[6]A number of studies have reported that the typical N400 effects are reduced when subjects attend to stimuli other than the eliciting ones (see Bentin, Kutas, & Hillyard, 1995; Gunter, Jackson, Kutas, Mulder, & Buijink, 1994; McCarthy & Nobre, 1993; Otten, Rugg, & Doyle, 1993).

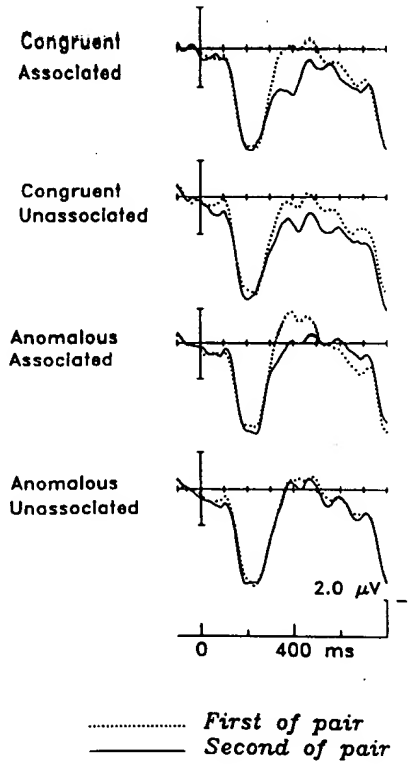

Figure 10. Grand average ERPs from 28 subjects at scalp site Cz (Van Petten, 1993).

did not; the words forming the critical pairs were never used as probe words. The amplitude of a subject's sentential context effect was correlated with his or her performance in this probe recognition task, particularly performance for closed class targets that had lower overall recognition levels ($R^2 = .40$). The top half of Figure 11 shows this correlation: the behavioral performance of each subject is plotted against the amplitude of the sentential context effect, where this is defined as the amplitude of the N400 elicited by the first word of the congruent-unassociated critical pairs minus the second word of these pairs. By contrast, the amplitude of the purely lexical context effect observed in the anomalous-associated condition was not related to performance in the probe recognition task, as shown in the bottom half of Figure 11.

Because the probe recognition task concerns only the immediately preceding sentence, it draws primarily on working memory. Many aspects of sentence comprehension—syntactic parsing, linking pronouns to their antecedents, and thematic role assignment—place clear demands on working memory. Other investigators have noted that working memory capacity is strongly correlated with language comprehension across a variety of tasks (for review, see Carpenter, Miyake, & Just, 1994). The relationship between the N400 measure of sentence comprehension and performance in a working memory task is thus a plausible one. In contrast, holding only a single related word in memory is sufficient to elicit a lexical context effect, and this is unlikely to place severe demands on working memory. In the study described here, working memory ability was defined by performance in the probe recognition task and linked with the sentential context effect in a post hoc analysis. In a follow-up study using the same sentence materials presented at a faster rate, we administered a more established measure of verbal working memory capacity before the experiment (the "reading span" test of Daneman and Carpenter, 1980). The subjects with low reading spans also performed more poorly on the probe recognition test than those with higher reading spans, suggesting that the two measures tap the same cognitive ability. The ERP results confirmed those of the first experiment in showing that the low-span readers lacked sentence-level context effects for intermediate words, although the amplitude of the lexical context effect was equivalent across reading span groups (Van Petten, Weckerly, McIsaac, & Kutas, in preparation).

The traditional model tested in the contrast between lexical and sentential context effects had two main tenets: (a) that sentence-level semantic analysis occurs only after analysis of the meanings of each individual word and (b) that each stage could exert an independent effect on the processing of subsequent words. The failure to observe a latency difference between the lexical and sentential context effects was inconsistent with the idea that the two sources of context are applied in serial order. The overall similarity between the lexical and sentential context effects suggests little difference in the timing or manner in which different sources of context are applied (see also Kutas, 1993). Instead, the differential relationship between measures of working memory capacity and the two context effects suggests that it may be more fruitful to think about how different sources of context are derived. Experimenters often define *context* as whatever stimuli are presented prior to a target item, but of course it is only the subject's mental representation of these stimuli that can influence his or her subsequent processing. The important difference between lexical and sentential contexts may be in the degree and nature of the effort required to compile the context

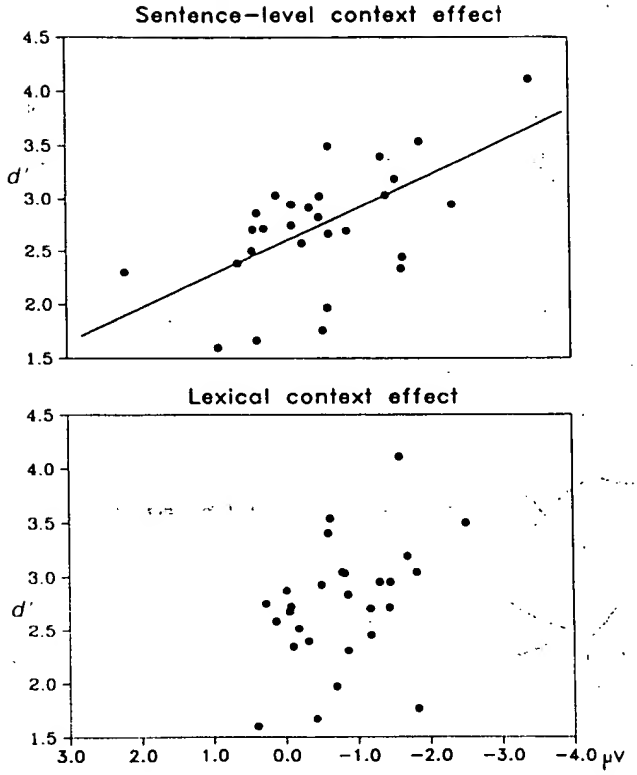

Figure 11. The top panel illustrates the relationship between behavioral performance in the working memory task embedded within the experiment. The y-axis represents performance summarized by *d'*. This measure combines accuracy for targets that occurred in the preceding sentence (correct response of "yes/present") and targets that did not occur in the preceding sentence (correct response of "no/absent"). The *d'* was calculated by considering correct responses to "present" probes as hits and incorrect responses to "absent" probes as false alarms. The x-axis represents the difference in the amplitude of the N400s elicited by the first and second members of the critical pairs in the congruent-unassociated condition (mean voltage 300–500 ms poststimulus onset, collapsed across all electrode sites). Negative amplitudes thus reflect larger context effects. Each data point represents one subject, and the regression line reflects the statistical relationship between performance and the ERP context effect. The bottom panel illustrates the lack of relationship between behavioral performance and our measure of the lexical context effect, the amplitude difference of the N400s elicited by the first and second members of anomalous-associated pairs. The regression analysis of the date in the bottom panel did not yield a significant correlation (data from Van Petten, 1993).

into a single concept, which can then facilitate the processing of upcoming words. The study of individuals supposed to have high or low working memory capacity is one avenue for quantifying the degree of effort involved in sentence comprehension. But because working memory is in danger of becoming a synonym for whatever computations and short-term storage are required to perform any task, controlled variation in stimulus materials is another avenue for understanding the nature and number of the processes involved in language comprehension. By analogy, single-unit physiologists working with nonhuman primates have dissociated cortical regions concerned with the short-term storage of spatial location versus object identity (Wilson, O'Scalaidhe, & Goldman-Rakic, 1993). It will be of some interest to determine whether or not all linguistic tasks and mate-

rials draw on a single pool of working memory resources; ERP researchers have just begun to approach this issue (see King & Kutas, in press; Kluender & Kutas, 1993a, 1993b). This review has focused on the N400, but the multicomponent structure of the ERP, together with newer functional imaging techniques, will aid in this endeavor.

REFERENCES

Aborn, M., Rubinstein, H., & Sterling, T. D. (1959). Sources of contextual constraint upon words in sentences. *Journal of Experimental Psychology, 57*, 171-180.

Adams, J., Faux, S. F., Nestor, P. G., & Shenton, M. (1993). ERP abnormalities during semantic processing in schizophrenia. *Schizophrenia Research, 10*, 247-257.

Andrews, S., Shelley, A. M., Ward, P. B., Fox, A., Catts, S. V., & McConaghy, N. (1993). Event-related potential indexes of semantic processing in schizophrenia. *Biological Psychology, 34*, 443-450.

Ardal, S., Donald, M. W., Meuter, R., Muldrew, S., & Luce, M. (1990). Brain responses to semantic incongruity in bilinguals. *Brain and Language, 39*, 187-205.

Balota, D. A. (1990). The role of meaning in word recognition. In D. A. Balota, G. B. Flores d'Arcais, & K. Rayner (Eds.), *Comprehension processes in reading* (pp. 9-32). Hillsdale, NJ: Erlbaum.

Balota, D. A., & Chumbley, J. I. (1984). Are lexical decisions a good measure of lexical access? The role of word frequency in the neglected decision stage. *Journal of Experimental Psychology: Human Perception and Performance, 10*, 340-357.

Balota, D. A., & Chumbley, J. I. (1985). The locus of word-frequency effects in the pronunciation task: Lexical access and/or production? *Journal of Memory and Language, 24*, 89-106.

Bates, E., & Wulfeck, B. (1989). Crosslinguistic studies of aphasia. In B. MacWhinney & E. Bates (Eds.), *The cross-linguistic study of sentence processing* (pp. 328-371). Cambridge: Cambridge University Press.

Becker, C. A. (1980). Semantic context effects in visual word recognition: An analysis of semantic strategies. *Memory and Cognition, 8*, 493-512.

Bentin, S., Kutas, M., & Hillyard, S. A. (1995). Semantic processing and memory for attended and unattended words in dichotic listening: Behavioral and electrophysiological evidence. *Journal of Experimental Psychology: Human Perception and Performance, 21*, 54-67.

Bentin, S., McCarthy, G., & Wood, C. C. (1985). Event-related potentials associated with semantic priming. *Electroencephalography and Clinical Neurophysiology, 60*, 343-355.

Besner, D. (1988). Visual word identification: Special-purpose mechanisms for the identification of open and closed class items? *Bulletin of the Psychonomic Society, 26*, 91-93.

Blutner, R., & Sommer, R. (1988). Sentence processing and lexical access: the influence of the focus-identifying task. *Journal of Memory and Language, 27*, 359-367.

Bock, K. (1989). Closed class immanence in sentence production. *Cognition, 31*, 163-186.

Bradley, D. C. (1983). *Computational distinctions of vocabulary type*. Bloomington, IN: Indiana University Linguistics Club.

Bradley, D. C., & Forster, K. I. (1987). A reader's view of listening. *Cognition, 25*, 72-103.

Bradley, D. C., & Garrett, M. F. (1983). Hemispheric differences in the recognition of closed and open class words. *Neuropsychologia, 21*, 155-159.

Bransford, J. D., & Johnson, M. K. (1972). Contextual prerequisites for understanding: Some investigations of comprehension and recall. *Journal of Verbal Learning and Verbal Behavior, 11*, 717-726.

Caplan, D. (1987). *Neurolinguistics and linguistic aphasiology*. Cambridge: Cambridge University Press.

Carpenter, P. A., Miyake, A., & Just, M. A. (1994). Working memory constraints in comprehension: Evidence from individual differences, aphasia, and aging. In M. Gernsbacher (Ed.), *Handbook of psycholinguistics* (pp. 1075-1122). San Diego: Academic Press.

Carroll, D. W. (1994). *Psychology of language* (2nd ed.). Pacific Grove, CA: Brooks/Cole.

Chiarello, C., & Nuding, S. (1987). Visual field effects for processing content and function words. *Neuropsychologia, 25*, 539-548.

Collins, A., & Loftus, E. (1975). A spreading activation theory of semantic processing. *Psychological Review, 82*, 407-428.

Connolly, J. F., & Phillips, N. A. (1994). Event-related potential components reflect phonological and semantic processing of the terminal words of spoken sentences. *Journal of Cognitive Neuroscience, 6*, 256-266.

Connolly, J. F., Phillips, N. A., Stewart, S. H., & Brake, W. G. (1992). Event-related potential sensitivity to acoustic and semantic properties of terminal words in sentences. *Brain and Language, 43*, 1-18.

Connolly, J. F., Stewart, S. H., & Phillips, N. A. (1990). The effects of processing requirements on neurophysiological responses to spoken sentences. *Brain and Language, 39*, 302-318.

Conrad, C. (1974). Context effects in sentence comprehension: A study of the subjective lexicon. *Memory and Cognition, 2*, 130-138.

Daneman, M., & Carpenter, P. A. (1980). Individual differences in working memory and reading. *Journal of Verbal Learning and Verbal Behavior, 19*, 450-466.

Dark, V. J. (1988). Semantic priming, prime reportability, and retroactive priming are interdependent. *Memory and Cognition, 16*, 299-308.

Davis, H., Mast, T., Yoshie, N., & Zerlin, S. (1966). The slow response of the human cortex to auditory stimuli: Recovery process. *Electroencephalography and Clinical Neurophysiology, 21*, 105-113.

DeGroot, A. M. B. (1990). The locus of the associative-priming effect in the mental lexicon. In D. A. Balota, G. B. Flores d'Arcais, & K. Rayner (Eds.), *Comprehension processes in reading* (pp. 101-124). Hillsdale, NJ: Erlbaum.

Dell, G. S. (1990). Effects of frequency and vocabulary type on phonological speech errors. *Language and Cognitive Processes, 5*, 313-349.

Den Heyer, K., Briand, K., & Dannenbring, G. L. (1988). Retroactive semantic priming in a lexical decision task. *Quarterly Journal of Experimental Psychology, 40A*, 341-259.

Donchin, E., McCarthy, G., & Kutas, M. (1977). Electroencephalographic investigations of hemispheric specialization. In J. E. Desmedt (Ed.), *Progress in clinical neurophysiology: Vol. 3. Language and hemispheric specialization in man: Event-related potentials* (pp. 212-242). Basel: Karger.

Fischler, I., & Bloom, P. A. (1979). Automatic and attentional processes in the effects of sentence contexts on word recognition. *Journal of Verbal Learning and Verbal Behavior, 18*, 1-20.

Fodor, J. A. (1983). *The modularity of mind*. Cambridge, MA: MIT Press.

Forster, K. I. (1979). Levels of processing and the structure of the language processor. In R. J. Wales & E. Walker (Eds.), *Sentence processing: Psycholinguistic studies presented to Merrill Garrett* (pp. 27-85). Hillsdale, NJ: Erlbaum.

Forster, K. I. (1981). Priming and the effects of sentence and lexical contexts on naming time: Evidence for autonomous lexical processing. *Quarterly Journal of Experimental Psychology, 33A*, 465-495.

Francis, W. N., & Kucera, H. (1982). *Frequency analysis of English usage: Lexicon and grammar*. Boston: Houghton Mifflin.

Galambos, R., Benson, P., Smith, T. S., Schulman-Galambos, C., & Osier, H. (1975). On hemispheric differences in evoked potentials to speech stimuli. *Electroencephalography and Clinical Neurophysiology, 39*, 279-283.

Ganis, G., Kutas, M., & Sereno, M. (in press). The search for "common sense": An electrophysiological investigation of semantic analysis of words and pictures in sentences. *Journal of Cognitive Neuroscience*.

Garnsey, S. M. (1985). *Function words and content words: Reaction time and evoked potential measures of word recognition* (Cognitive Science Tech. Rep. No. URCS-29). Rochester, NY: University of Rochester.

Garnsey, S. M., Tanenhaus, M. K., & Chapman, R. M. (1989). Evoked potentials and the study of sentence comprehension. *Journal of Psycholinguistic Research, 18*, 51-60.

Garrett, M. F. (1982). Production of speech: Observations from normal and pathological language use. In A. Ellis (Ed.), *Normality and pathology in cognitive function* (pp. 19-76). London: Academic Press.

Garrett, M. F. (1990). Sentence processing. In D. N. Osherson & H. Lasnik (Eds.), *An invitation to cognitive science: Language* (pp. 133-176). Cambridge, MA: MIT Press.

Gleitman, L., Gleitman, H., Landau, B., & Wanner, E. (1989). Great

expectations. In A. M. Galaburda (Ed.), *From reading to neurons* (pp. 91-136). Cambridge, MA: MIT Press.
Gordon, B., & Caramazza, A. (1985). Lexical access and frequency sensitivity: Frequency saturation and open/closed class equivalence. *Cognition, 21*, 95-115.
Gough, P. B. (1983). Context, form, and interaction. In K. Rayner (Ed.), *Eye movements in reading: Perceptual and language processes* (pp. 203-211). New York: Academic Press.
Gunter, T. C., Jackson, J. L., Kutas, M., Mulder, G., & Buijink, B. M. (1994). Focusing on the N400: An exploration of selective attention during reading. *Psychophysiology, 31*, 347-358.
Gunter, T. C., Jackson, J. L., & Mulder, G. (1992). An electrophysiological study of semantic processing in young and middle-aged academics. *Psychophysiology, 29*, 38-54.
Hagoort, P., Brown, C., & Groothusen, J. (1993). The syntactic positive shift (SPS) as an ERP measure of syntactic processing. *Language and Cognitive Processes, 8*, 439-484.
Handel, S. (1989). *Listening. An introduction to the perception of auditory events*. Cambridge, MA: MIT Press.
Harbin, T. J., Marsh, G. R., & Harvey, M. T. (1984). Differences in the late components of the event-related potential due to age and to semantic and non-semantic tasks. *Electroencephalography and Clinical Neurophysiology, 59*, 489-496.
Henderson, L. (1982). *Orthography and word recognition in reading*. New York: Academic Press.
Hillyard, S. A. (1973). The CNV and human behavior: A review. *Electroencephalography and Clinical Neurophysiology, 33*(Suppl.), 161-171.
Holcomb, P. J., Coffey, S. A., & Neville, H. J. (1992). Visual and auditory sentence processing: A developmental analysis using event related brain potentials. *Developmental Neuropsychology, 8*, 203-241.
Holcomb, P. J., & Neville, H. J. (1991). Natural speech processing: An analysis using event-related brain potentials. *Psychobiology, 19*, 286-300.
Kean, M. L. (1979). Agrammatism: A phonological deficit? *Cognition, 7*, 69-84.
Kean, M. L. (Ed.). (1985). *Agrammatism*. New York: Academic Press.
Kellas, G., Paul, S. T., Martin, M., & Simpson, G. B. (1991). Contextual feature activation and meaning access. In G. B. Simpson (Ed.), *Understanding word and sentence* (pp. 47-72). Amsterdam: Elsevier.
Kiger, J. I., & Glass, A. L. (1983). The facilitation of lexical decisions by a prime occurring after the target. *Memory and Cognition, 11*, 356-365.
King, J. W., & Kutas, M. (1995). The lexical processing negativity: An ERP whose latency indexes lexical characteristics of words. *Psychophysiology, 32*(Suppl. 1), S45.
King, J. W., & Kutas, M. (in press). Who did what and when? Using word- and clause-level ERPs to monitor working memory usage in reading. *Journal of Cognitive Neuroscience*.
Kintsch, W., & Mross, E. F. (1985). Context effects in word identification. *Journal of Memory and Language, 24*, 336-349.
Kluender, R., & Kutas, M. (1993a). Bridging the gap: Evidence from ERPs on the processing of unbounded dependencies. *Journal of Cognitive Neuroscience, 5*, 196-214.
Kluender, R., & Kutas, M. (1993b). Subjacency as a processing phenomenon. *Language and Cognitive Processes, 8*, 573-633.
Kolk, H. H. J., & Blomert, L. (1985). On the Bradley hypothesis concerning agrammatism: The nonword interference effect. *Brain and Language, 26*, 94-105.
Kutas, M. (1993). In the company of other words: Electrophysiological evidence for single-word and sentence context effects. *Language and Cognitive Processes, 8*, 533-572.
Kutas, M., Bates, E., Kluender, R., Van Petten, C., Clark, V., & Blesch, F. (1988). [ERPs elicited during reading Spanish and English text in monolingual and bilingual subjects]. Unpublished raw data.
Kutas, M., & Hillyard, S. A. (1980a). Event-related brain potentials to semantically inappropriate and surprisingly large words. *Biological Psychology, 11*, 99-116.
Kutas, M., & Hillyard, S. A. (1980b). Reading senseless sentences: Brain potentials reflect semantic incongruity. *Science, 207*, 203-205.
Kutas, M., & Hillyard, S. A. (1980c). Reading between the lines: Event related brain potentials during natural sentence processing. *Brain and Language, 11*, 354-373.
Kutas, M., & Hillyard, S. A. (1982). The lateral distribution of event-related potentials during sentence processing. *Neuropsychologia, 20*, 579-590.
Kutas, M., & Hillyard, S. A. (1983). Event-related potentials to grammatical errors and semantic anomalies. *Memory and Cognition, 11*, 539-550.
Kutas, M., & Hillyard, S. A. (1984). Brain potentials during reading reflect word expectancy and semantic association. *Nature, 307*, 161-163.
Kutas, M., & Hillyard, S. A. (1989). An electrophysiological probe of incidental semantic association. *Journal of Cognitive Neuroscience, 1*, 38-49.
Kutas, M., & Kluender, R. (1994). What is who violating? A reconsideration of linguistic violations in light of event-related brain potentials. In H.-J. Heinze, T. F. Munte, & G. R. Mangun (Eds.), *Cognitive electrophysiology* (pp. 183-210). Boston: Birkhauser.
Kutas, M., Lindamood, T., & Hillyard, S. A. (1984). Word expectancy and event-related brain potentials during sentence processing. In S. Kornblum & J. Requin (Eds.), *Preparatory states and processes* (pp. 217-238). Hillsdale, NJ: Erlbaum.
Kutas, M., Neville, H. J., & Holcomb, P. J. (1987). A preliminary comparison of the N400 response to semantic anomalies during reading, listening, and signing. *Electroencephalography and Clinical Neurophysiology, 39*(Suppl.), 325-330.
Kutas, M., & Van Petten, C. (1988). Event-related brain potential studies of language. In P. K. Ackles, J. R. Jennings, & M. G. H. Coles (Eds.), *Advances in psychophysiology* (Vol. 3, pp. 139-187). Greenwich, CT: JAI Press.
Kutas, M., & Van Petten, C. (1990). Electrophysiological perspectives on comprehending written language. In P. M. Rossini & F. Mauguiere (Eds.), *New trends and advanced techniques in clinical neurophysiology* (*Electroencephalography and Clinical Neurophysiology*, Suppl. 41, pp. 155-167). Amsterdam: Elsevier.
Kutas, M., & Van Petten, C. (1994). Psycholinguistics electrified: Event-related brain potential investigations. In M. Gernsbacher (Ed.), *Handbook of psycholinguistics* (pp. 83-143). New York: Academic Press.
Kutas, M., Van Petten, C., & Besson, M. (1988). Event-related potential asymmetries during the reading of sentences. *Electroencephalography and Clinical Neurophysiology, 69*, 218-233.
Marslen-Wilson, W. D. (1987). Functional parallelism in spoken word recognition. *Cognition, 25*, 71-102.
McCallum, W. C., & Papakostopoulos, D. (1973). The CNV and reaction time in situations of increasing complexity. *Electroencephalography and Clinical Neurophysiology, 33*(Suppl.), 179-185.
McCarthy, G., & Nobre, A. C. (1993). Modulation of semantic processing by spatial selective attention. *Electroencephalography and Clinical Neurophysiology, 88*, 210-219.
McCarthy, G., Nobre, A. C., Bentin, S., & Spencer, D. D. (1995). Language-related field potentials in the anterior-medial temporal lobe: I. Intracranial distribution and neural generators. *Journal of Neuroscience, 15*, 1080-1089.
Mitchell, P. F., Andrews, S., Catts, S. V., Ward, P. V., & McConaghy, N. (1991). Active and passive attention in schizophrenia – An ERP study of information processing in a linguistic task. *Biological Psychology, 32*, 101-124.
Morton, J. (1969). The interaction of information in word recognition. *Psychological Review, 76*, 165-178.
Neville, H. J. (1991). Whence the specialization of the language hemisphere? In I. G. Mattingly & M. Studdert-Kennedy (Eds.), *Modularity and the motor theory of speech perception* (pp. 269-294). Hillsdale, NJ: Erlbaum.
Neville, H. J., Coffey, S. A., Holcomb, P. J., & Tallal, P. (1993). Neurobiology of sensory and language processing in language-impaired children. *Journal of Cognitive Neuroscience, 5*, 235-253.
Neville, H. J., Mills, D. L., & Lawson, D. (1992). Fractionating language: Different neural subsystems with different sensitive periods. *Cerebral Cortex, 2*, 244-258.
Nigam, A., Hoffman, J. E., & Simons, R. F. (1992). N400 to semantically anomalous pictures and words. *Journal of Cognitive Neuroscience, 4*, 15-22.
Nobre, A. C., Allison, T., & McCarthy, G. (1994). Word recognition in the human inferior temporal lobe. *Nature, 372*, 260-263.
Nobre, A. C., & McCarthy, G. (1995). Language-related field potentials in the anterior-medial temporal lobe II. Effects of word type and semantic priming. *Journal of Neuroscience, 15*, 1090-1098.
Norris, D. (1986). Word recognition: Context effects without priming. *Cognition, 22*, 93-136.

Oden, G. L., & Spira, J. L. (1983). Influence of context on the activation and selection of ambiguous word senses. *Quarterly Journal of Experimental Psychology, 35A*, 51-64.

Onifer, W., & Swinney, D. A. (1981). Accessing lexical ambiguities during sentence comprehension: Effects of frequency of meaning and contextual bias. *Memory and Cognition, 9*, 225-236.

Osterhout, L., & Holcomb, P. J. (1992). Event-related brain potentials elicited by syntactic anomaly. *Journal of Memory and Language, 31*, 785-806.

Osterhout, L., & Holcomb, P. J. (1993). Event-related potentials and syntactic anomaly: Evidence of anomaly detection during the perception of continuous speech. *Language and Cognitive Processes, 8*, 337-640.

Otten, L. J., Rugg, M. D., & Doyle, M. C. (1993). Modulation of event related potentials by word-repetition: The role of visual selective attention. *Psychophysiology, 30*, 559-571.

Paul, S. T., Kellas, G., Martin, M., & Clark, M. B. (1992). The influence of contextual features on the activation of ambiguous word meanings. *Journal of Experimental Psychology: Learning, Memory, and Cognition, 18*, 703-717.

Peterson, R. R., & Simpson, G. B. (1989). Effects of backward priming on word recognition in single word and sentence contexts. *Journal of Experimental Psychology: Learning, Memory, and Cognition, 15*, 1020-1032.

Petocz, A., & Oliphant, G. (1988). Closed-class words as first syllables do interfere with lexical decisions for nonwords: Implications for theories of agrammatism. *Brain and Language, 34*, 127-146.

Rayner, K., & Sereno, S. C. (1994). Eye movements in reading: Psycholinguistic studies. In M. Gernsbacher (Ed.), *Handbook of psycholinguistics* (pp. 57-81). New York: Academic Press.

Rosenberg, B., Zurif, E., Brownell, H., Garrett, M., & Bradley, D. (1985). Grammatical class effects in relation to normal and aphasic sentence processing. *Brain and Language, 26*, 287-303.

Rubinstein, H., Garfield, L., & Millikan, J. A. (1970). Homographic entries in the internal lexicon. *Journal of Verbal Learning and Verbal Behavior, 9*, 487-494.

Rugg, M. D. (1985). The effects of semantic priming and word repetition on event-related potentials. *Psychophysiology, 22*, 642-647.

Rugg, M. D. (1990). Event-related brain potentials dissociate repetition effects of high- and low-frequency words. *Memory and Cognition, 18*, 367-379.

Schank, R. C. (1978). Predictive understanding. In R. N. Campbell & P. T. Smith (Eds.), *Recent advances in the psychology of language—Formal and experimental approaches* (pp. 91-101). New York: Plenum.

Seidenberg, M. S., Tanenhaus, M. K., Leiman, J. M., & Bienkowski, M. (1982). Automatic access of the meanings of ambiguous words in context: Some limitations of knowledge-based processing. *Cognitive Psychology, 14*, 489-537.

Shapiro, L. P., & Jensen, L. R. (1986). Processing open and closed class-headed nonwords: Left hemisphere support for separate vocabularies. *Brain and Language, 28*, 318-327.

Sharkey, A. J., & Sharkey, N. O. (1992). Weak contextual constraints in text and word priming. *Journal of Memory and Language, 31*, 543-572.

Simpson, G. B. (1981). Meaning dominance and semantic context in the processing of lexical ambiguity. *Journal of Verbal Learning and Verbal Behavior, 20*, 120-136.

Simpson, G. B. (1994). Context and the processing of ambiguous words. In M. Gernsbacher (Ed.), *Handbook of psycholinguistics* (pp. 359-374). New York: Academic Press.

Simpson, G. B., & Burgess, C. (1985). Activation and selection processes in the recognition of ambiguous words. *Journal of Experimental Psychology: Human Perception and Performance, 11*, 28-39.

Simpson, G. B., & Kreuger, M. A. (1991). Selective access of homograph meanings in sentence context. *Journal of Memory and Language, 30*, 627-643.

Smith, M. E., & Halgren, E. (1987). Event-related potentials during lexical decision: Effects of repetition, word frequency, pronounceability, and concreteness. In R. Johnson, Jr., J. W. Rohrbaugh, & R. Parasuraman (Eds.), *Current trends in event-related potential research (Electroencephalography and Clinical Neurophysiology*, Suppl. 40, pp. 417-421). Amsterdam: Elsevier.

Smith-Burke, M., & Gingrich, P. S. (1979). The differential role of function words and lexical items in narrative and expository text. In M. Kamil & A. J. Moe (Eds.), *Reading research: Studies and applications* (pp. 45-48). Clemson, SC: National Reading Conference.

Solomon, R. L., & Howes, D. H. (1951). Word frequency, personal values, and visual duration thresholds. *Psychological Review, 58*, 256-270.

St. George, M., Mannes, S., & Hoffman, J. E. (1994). Global semantic expectancy and language comprehension. *Journal of Cognitive Neuroscience, 6*, 70-83.

Swinney, D. A. (1979). Lexical access during sentence comprehension: (Re)consideration of context effects. *Journal of Verbal Learning and Verbal Behavior, 18*, 645-659.

Tabossi, P. (1988). Accessing lexical ambiguity in different types of sentential contexts. *Journal of Memory and Language, 27*, 324-340.

Tabossi, P., & Zardon, F. (1993). Processing ambiguous words in context. *Journal of Memory and Language, 32*, 359-372.

Till, R. E., Mross, E. F., & Kintsch, W. (1988). Time course of priming for associate and inference words in a discourse context. *Memory and Cognition, 16*, 283-298.

Tulving, E., Mandler, G., & Baumal, R. (1964). Interaction of two sources of information in tachistoscopic word recognition. *Canadian Journal of Psychology, 18*, 62-71.

Tyler, L. K., & Marslen-Wilson, W. (1986). The effects of context on the recognition of polymorphemic words. *Journal of Memory and Language, 25*, 741-752.

Tyler, L. K., & Wessels, J. (1983). Quantifying contextual contributions to word-recognition processes. *Perception and Psychophysics, 34*, 409-420.

Van Petten, C. (1993). A comparison of lexical and sentence-level context effects and their temporal parameters. *Language and Cognitive Processes, 8*, 485-532.

Van Petten, C., & Kutas, M. (1987a). Ambiguous words in context: An event-related potential analysis of the time course of meaning activation. *Journal of Memory and Language, 26*, 188-208.

Van Petten, C., & Kutas, M. (1987b). [Ambiguous words in sentences biasing the dominant mening]. Unpublished raw data.

Van Petten, C., & Kutas, M. (1990). Interactions between sentence context and word frequency in event-related brain potentials. *Memory and Cognition, 18*, 380-393.

Van Petten, C., & Kutas, M. (1991a). Influences of semantic and syntactic context on open and closed class words. *Memory and Cognition, 19*, 95-112.

Van Petten, C., & Kutas, M. (1991b). Electrophysiological evidence for the flexibility of lexical processing. In G. Simpson (Ed.), *Word and sentence* (pp. 129-174). Amsterdam: Elsevier.

Van Petten, C., Kutas, M., Kluender, R., Mitchiner, M., & McIsaac, H. (1991). Fractionating the word repetition effect with event-related potentials. *Journal of Cognitive Neuroscience, 3*, 131-150.

Van Petten, C., & Rheinfelder, H. (1995). Conceptual relationships between spoken words and environmental sounds: Event-related brain potential measures. *Neuropsychologia, 33*, 485-508.

Walter, W. G., Cooper, R., Aldridge, V. J., McCallum, W. C., & Winter, A. L. (1964). Contingent negative variation: An electric sign of sensorimotor association and expectancy in the human brain. *Nature, 203*, 380-384.

Warren, R. M. (1970). Perceptual restoration of missing speech sounds. *Science, 167*, 392-393.

Wilson, F. A. W., O'Scalaidhe, S. P., & Goldman-Rakic, P. S. (1993). Dissociation of object and spatial processing domains in primate prefrontal cortex. *Science, 260*, 1955-1958.

Woodward, S. H., Ford, J. M., & Hammett, S. C. (1993). N4 to spoken sentences in young and older subjects. *Electroencephalography and Clinical Neurophysiology, 87*, 306-320.

Wright, B., & Garrett, M. (1984). Lexical decision in sentences: Effects of syntactic structure. *Memory and Cognition, 12*, 314-315.

(Received March 6, 1995; Accepted May 15, 1995)

Electroencephalography and clinical Neurophysiology, 87 (1993) 154–163

EEG 92149

Spatial sampling of head electrical fields: the geodesic sensor net

Don M. Tucker

Department of Psychology, University of Oregon, Eugene, OR 97403 (USA)

(Accepted for publication: 12 April 1993)

Summary In studying brain electrical activity from scalp sensors (electrodes), the optimal measurement would sample the potential field over the entire surface of the braincase, with a sufficient density to avoid spatial aliasing of the surface electrical fields. The geodesic sensor net organizes an array of sensors, each enclosed in a saline sponge, in a geodesic tension structure comprised of elastic threads. By fixing a sensor pedestal at each geodesic vertex, the geometry of the tension structure insures that the sensor array is distributed evenly across the the accessible head surface. Furthermore, the tension of the network is translated into compression that is divided equally among the sensor pedestals and directed along head-radial vectors. Various geodesic partitioning frequencies may be selected to provide an even surface distribution of the dense sensor arrays (e.g., 64, 128, or 256) that appear to be necessary to provide adequate spatial sampling of brain electrical events.

Key words: Brain electrical activity; Geodesic sensor net; Spatial sampling; Electrical field

In the rapidly developing approaches to neuroimaging, radiologic and magnetic resonance methods are providing visualizations of brain metabolism and blood flow with increasingly fine anatomical detail. However, the inherent time lag of metabolic and hemodynamic responses limits the temporal resolution of these measures of brain activity. Recordings of the brain's magnetic and electrical fields provide data with the temporal precision required to examine the dynamic operations of cortical networks.

Both electrical and magnetic recording methods are non-invasive, allowing the collection of the large normative samples that may be required for statistical hypothesis-testing with multivariate datasets. A major disadvantage of electromagnetic methods is the difficulty of localizing the source of the data in specific brain structures. Recent studies suggest that the spatial localization from electrical (EEG) data may be similar to that from magnetic (MEG) data. In both cases, the localization is limited by the number of measurement sites (as well as other factors such as noise; Cohen et al. 1990). Because the cost per channel for EEG is now around 1–5% of that for MEG, the most rapid advances in neuroimaging research may be made by improving the spatial sampling of head electrical fields with a dense sensor array.

Correspondence to: Dr. D.M. Tucker, Department of Psychology, University of Oregon, Eugene, OR 97403 (USA).

The convention for sensor placement for many years has been the international 10–20 system (Jasper 1958). In this approach, measurements between skull landmarks are divided into proportions, and sensors are placed at the proportional distances along the measurement lines. Although this venerable system has provided standardization of sites over the the major divisions of the skull, it provides proportional placements only along the measurement lines, rather than an even distribution across the 2-dimensional surface of the head. A systematic 2-D surface partitioning method is required for dense sensor arrays. In this paper, I describe the geodesic sensor net, a device that achieves an even distribution of an array of EEG sensors across the head surface.

Objectives for spatial sampling of head electrical fields

Although the low conductivity of the skull limits the spatial resolution of scalp recordings, studies of somatosensory event-related potentials (ERPs) have suggested that an intersensor distance of less than 3 cm is required to avoid spatial aliasing of the information available from scalp recordings (Gevins 1990; Spitzer et al. 1989). In time domain measurements, a sampling frequency substantially greater than the folding or Nyquist frequency is known to be necessary to avoid aliasing (Bendat and Piersol 1971). Sampling the spatial frequency of scalp potential fields with this preci-

sion would require many more sensors than are provided in conventional recordings. Even when additional measurement sites fail to provide unique information on surface fields, they provide unique noise estimates, thus improving the constraints on source localization algorithms.

In addition to achieving sufficient sensor density, it is important to sample the entire surface of the head. Because of volume conduction, each electrical source in brain tissue generates a dipole field that conducts throughout the head volume (Nunez 1981). For dipole modeling studies, an even and complete sampling of the potential field across the whole braincase surface would characterize a dipole's fields entirely (superimposed, of course, with the fields of all other generators). When the specific source distribution is not known, an even spatial distribution of sampling points across the braincase surface provides the optimal data set for decomposition and dipole localization algorithms.

Practical problems of a dense sensor array

Most of the inferior surface of the braincase cannot be accessed, of course, with non-invasive methods. An important exception is provided by nasopharyngeal electrodes (MacLean 1958) inserted through the nasal passage into the nasopharynx and rotated laterally to a position within 2 cm from the temporal pole. Sensors can be placed on the face and neck to assess the current that is volume conducted to the inferior surface. Although the distance from the braincase and the complexity of the current paths cause the source of these potentials to be uncertain, they nonetheless provide valuable information about the portion of the total electrical field directed toward the inferior braincase (Nunez 1981).

Given the limits imposed by skull anatomy, a dense sensor array is needed to distribute measurement sites across the accessible surface of the braincase. For each head there is a distance which when spanned between each sensor and its neighbors will distribute the array across the surface of the head (up to the inferior boundary such as formed by the canthomeatal line). Because computation of this distance and placement of each sensor individually is impractical, a device is required that approximates this distance for each subject.

An elastic device is the obvious choice. Points on the surface of a balloon, for example, expand and contract in equidistant fashion as the internal air pressure is varied. There have been many designs, such as shown in the International Patent art, for using elastic straps and caps for this purpose. Although workable in certain forms, elastic straps and caps present a number of practical problems. Straps apply pressure along a line of skin, effectively restricting blood supply to an area of the scalp. At first, the effect is not noticed, but after a few minutes it can become painful. In addition, both straps and caps are placed over the hair. Because the hair slides easily, it does not afford a good friction purchase. Therefore to hold elastic straps or caps on the head, chin or chest straps have been necessary. Such straps apply tension between the friction points on the chin or chest and the top of the head, such that the lines of tension of the overall apparatus are unevenly distributed across the head. Therefore, when the elastic device does not grip the head evenly, the effective tension of the overall structure is not apportioned adequately to distribute the sensor sites evenly across the head surface.

An additional issue that has become important in recent years is the infection risk introduced when the preparation of the sensor site requires that the scalp be abraided, such as with a blunt syringe needle. Although sterile procedures may be followed, many subjects are concerned with the risk of HIV infection. In addition, if each site of a dense sensor array receives even a minor abrasion, the cumulative injury may be unpleasant. Abrasion has been traditional in EEG practice to achieve low (3–5 kΩ) scalp sensor impedances. However, with the possible exception of recording high-frequency (brain-stem) ERPs, we have found that modern high input impedance amplifiers provide excellent recordings with sensor impedances in the 50 kΩ range. Therefore, a design goal is to achieve 50 kΩ impedances with no scalp abrasion and with minimal attention to individual sensors.

Electrodes with a saline electrolyte absorbed in a cotton or sponge covering can provide impedances in this range, and designs of this type have been available for many years. However, because these sensors rest on the hair, the saline is rapidly wicked away by the hair, causing the sensor to become dry and non-functional in a few minutes. A design is required that applies the electrolyte to the scalp and shields it from the hair.

The geodesic tension structure

A tension structure was designed for 2 purposes: (1) distributing the sensors uniformly across the head surface, and (2) holding the sensors against the head. If tension is distributed evenly across the surface of a sphere, such as occurs with a soap bubble, the surface tension is balanced by compression directed from all points on the surface toward the sphere center, such as compresses the air inside the soap bubble. If a single quantity of tension is exerted between all pairs of a network of sensors, the network will adjust the spatial location of each sensor until a single distance spans all pairs. For accurate control of this tension, it must be applied in direct lines between the sensor pairs, and

only along those lines. Each line is a geodesic, the shortest distance between two points on the surface of a sphere. More precisely, because simple tension lines must be straight rather than curved along the sphere surface, the geodesics form a network of triangles approximating the spherical surface.

Plato (400 B.C.E.) found that approximations to a sphere are approached most closely by the solid polygonal structures of the dodecahedron and icosohedron. More recently, Fuller (1969) found that by further partitioning the triangular subunits of these polygons into smaller triangles, and then allowing the angles at all vertices to relax in a balanced fashion, a close approximation to a sphere could be achieved by a structure comprised solely of straight lines. The straight lines provide the simplest vectors for the forces of either tension or compression.

In his search for elegant structural efficiency, Fuller (1969) reflected that all material stress could be resolved to the forces of tension and compression. The architectural geodesic dome optimally distributes the forces of compression caused by the action of gravity on the structure. Applied to the objective of a sensor positioning network, a geodesic tension structure distributes both the tension and the location of the vertices (where the sensors are placed) evenly across the surface of the head.

Design of a sensor positioning network

In the present design of the geodesic sensor net [1], the fundamental polygonal structure is the icosohedron, a solid comprised of 20 triangular faces. As shown in Fig. 1, somewhat more than half of the icosohedron is used to form a dome-shaped structure to cover the accessible surface of the braincase. The geodesic structure is thus configured to approximate the sphere that best fits the braincase, including the inferior as well as superior surfaces. An advantage of the geodesic design is that various vertex densities can be achieved simply by changing the frequency of partitioning of the major triangles of the icosohedron. Fig. 1 shows a vertex density that places 106 sensors within the network structure, leaving 22 channels of a 128-channel EEG for sensors on the face and neck. Fig. 1 outlines the positioning of the icosohedron and the partitioning of its major triangles for this 128-channel design. A lower geodesic frequency was used to create a 64-channel net.

[1] Commercial use and sale of this invention is protected by U.S. and foreign patents pending. Non-profit research use and non-profit clinical use are licensed for a nominal fee. Electrical Geodesics, Inc., P.O. Box 3628, Eugene, OR 97440, USA.

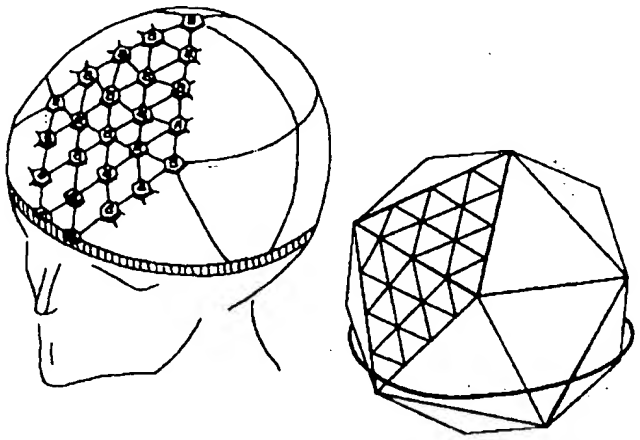

Fig. 1. General structure of the 128-channel geodesic sensor net. Sensor pedestals are shown populating two of the basic triangles of the icosohedron. In this configuration, 106 sensors are arrayed in the net, and 22 sensors are placed on the face and neck. For this configuration, the geodesic frequency, i.e., the number of divisions of each icosohedron triangle leg, is 4.

In the geodesic sensor net, elastic threads form the tension lines of the geometric network. At each vertex is an Ag/AgCl sponge sensor housed in a sensor pedestal (Fig. 2). The sensor pedestal is a plastic tube, flared at one end, with a plastic collar that forms an anchor point for the elastic tension lines. Each vertex (pedestal) receives 6 tension lines, except the major vertices of the icosohedron, which receive 5 (Fig. 3).

When the net is stretched over the head, the surface tension of the network is balanced by compression directed from each vertex toward the center of the spheroidal head. The compression serves to hold each sensor pedestal against the head, providing the major friction purchase required for mechanical stability. The

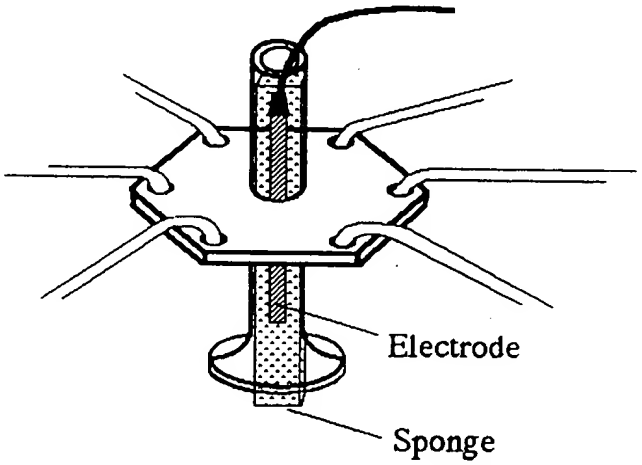

Fig. 2. Detail of the sensor pedestal. The sensor (electrode) is an Ag/AgCl pellet, adjoined on both sides by a sponge containing saline (KCl). The collar maintains the pedestal tube in a sphere-radial orientation, i.e., perpendicular to the surface tension of the network.

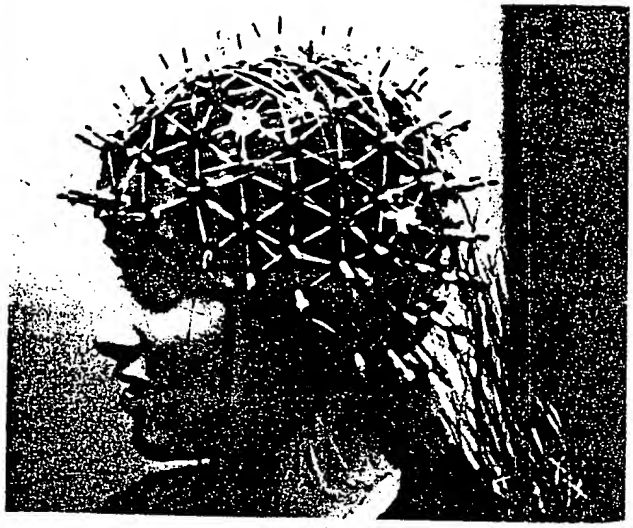

Fig. 3. Photograph of the 128-channel geodesic sensor net. The net is applied with the lower band placed across the brow ridge and along the canthomeatal line. Spatial 3-D digitizing of the location of the band pedestals and those at the major vertices of the icosohedron, plus the major skull landmarks, allow for precise spatial description, such as for registration with MRI.

organized tension network equates the pressure applied to each sensor pedestal. This effect helps to equate the sensor impedances throughout the network. Because the tension of the network is translated to compression that is divided across the many pedestal feet, there is little interference with scalp circulation, and the net can be worn for several hours in comfort.

Two features of the sensor pedestal proved critical to an effective net design: the collar and the flared foot. The collar links the sensor pedestal to the elastic network (Fig. 2). As described above, the organized tension network results in radial force vectors from each vertex toward the head center. But if the vertex shifts somewhat, such as from an abrupt head movement, a new force vector is applied from the new vertex location, and if this new vector is applied against a now tilted sensor, the structure collapses about the subject's head in an unattractive tangle of thread, wire, plastic parts, and wet sponges.

This problem was solved by adding a collar to the sensor pedestal, oriented in the plane of the tension network surface, causing any deviation of the pedestal from the sphere-radial orientation to be opposed by the balanced surface tension of the elastic network. This design feature is essential to keep the sensor pedestals upright, and to keep the tension network from shifting parallel to the head surface.

The sensor pedestal keeps the elastic tension network out of the subject's hair. Only the bottom or foot of the pedestal needs to enter into the hair. Achieving the desired positioning was facilitated by designing the sensor pedestals to insert their feet under the hair as the net is applied. The foot of the sensor pedestal is flared. As the net is applied, it is moved back and forth slightly, during which time the radial force on each sensor pedestal is slight but continuous, such that the flare on the pedestal foot not only parts but rakes and lifts up the hair strands it contacts, inserting itself below them. After a few movements, the foot rests directly on the scalp, overlying only those few hairs whose pores are directly below it. The protruding sponge is compressed against the scalp, shielded from evaporation by the flared pedestal foot, thus concentrating its limited saline electrolyte load on the goal of hydrating the underlying scalp.

Positioning with skull landmarks

An initial decision is whether the geodesic positioning network is to be adjusted for an even distribution of vertices (1) across the surface of a sphere or (2) across the surface of a typical head shape. If the tension of all elastic lines is equated, the vertices will position themselves in an equidistant array on the surface of a sphere. Because the human head varies in shape, usually smaller in the front than the back, an equidistant tension structure conforms to a head shape with differential tensions and differential distances. Because each vertex is drawn toward the center of the sphere, this conformation of the net vertices to a head's shape is along sphere-radial lines. In this configuration the net therefore computes a spherical projection of the head. Each sensor pedestal is placed on the site through which a ray of light would pass from the head center to the corresponding geodesic vertex on a sphere encompassing the head.

Although this spherical projection is an interesting feature of the mechanical structure, the important perspective for spatial sampling of head fields may not be volumetric in an idealized sense, i.e., sphere-radial, but a surface perspective, in which sampling error is best minimized by an even coverage of the actual, irregularly shaped, head surface. Therefore, the initial adjustment of the net has been made to achieve a somewhat more equal distribution of the sensors across the surface of a typically shaped human head than would be achieved by an exact spherical projection. An adjusted projection of the geodesic structure onto an average-sized model head is made, in which the surface areas of the basic triangles of the icosohedron are approximately equal. The tension lines of the net are then adjusted so that, once the net is aligned with the major skull landmarks, each pedestal is constrained to locate on the appropriate geodesic vertex. As the net is applied to a subject's head, the conformation is still mostly sphere-radial, but the conformation is now that

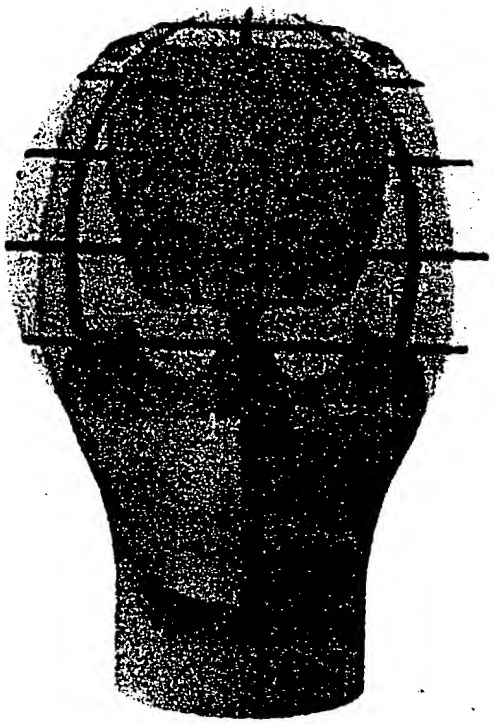

Figs. 4 and 5. Best-fit sphere (front and side views) selected by the net's geodesic partitioning of the braincase. The geodesic surface partitioning of the accessible upper surface may be adjusted to account for the extension of the geodesic pattern to the inferior braincase, such that the sphere is fit to an even sampling of the entire braincase surface.

of a geodesic tension structure that is generally head-shaped.

For relating the electrical measurements to brain anatomy, the positions of the sensors must be specified accurately. In our present procedures, the net is oriented such that the icosohedron is generally parallel to the canthomeatal line (CML), which extends from the external canthus to the external auditory meatus (ear canal). This line is extended to the back of the head, and an "adjusted inion" is marked where the line crosses the midline. An "adjusted vertex" is marked at the point equidistant from the nasion and the adjusted inion, centered between the ear canals. As the net is applied, the top vertex of the icosohedron (Fig. 1) is placed on the adjusted vertex mark. The headband is spread between the spread fingers of both hands, and the net is stretched over the head so that the pedestals closest to the top vertex are seated on the scalp first, followed by those progressively closer to the band. The technician visualizes the intended distribution throughout this placement, so that when the band is placed at its destination there is minimal adjustment required to the overall positioning. As each line of sensors is placed, small back-and-forth or circular movements of the net allow the flared pedestal feet to part and lift the hair and insert themselves against the scalp. The headband is placed across the brow ridge, stretched down along the CML, extending approximately to the adjusted inion. The major vertices of the icosohedron are inspected for general alignment and lateral symmetry. Each pedestal is then grasped and its foot scrubbed briskly against the scalp, insuring its fit under the hair and against the scalp.

To provide accurate location of the sensor sites, a 3-D digitizer may be used to measure skull landmarks, such as the nasion and periauricular points, and the glabella and inion, together with the location of each sensor foot. These coordinates may then be used to align the subject's electrical data with the MRI (magnetic resonance image).

Spherical models of the braincase

Although the primary goal of a geodesic partitioning network is to array electrode sensors to evenly sample brain potential fields, the geodesic sensor net provides an additional advantage: it optimally samples the shape of the accessible surface of the braincase. Electrical models that rely on spherical geometry, such as spherical splines (Perrin et al. 1989) or dipole models (Scherg 1989), produce results whose anatomical accuracy depends on the selection of a sphere that fits the shape, and thus the conductance characteristics, of the subject's braincase. Although Perrin et al. and Scherg have used arbitrary spheres, others have used least squares

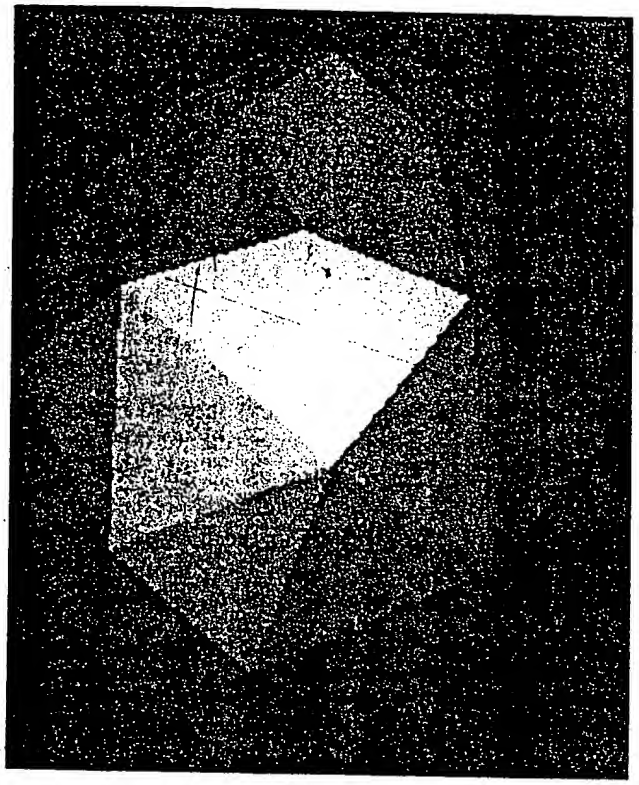

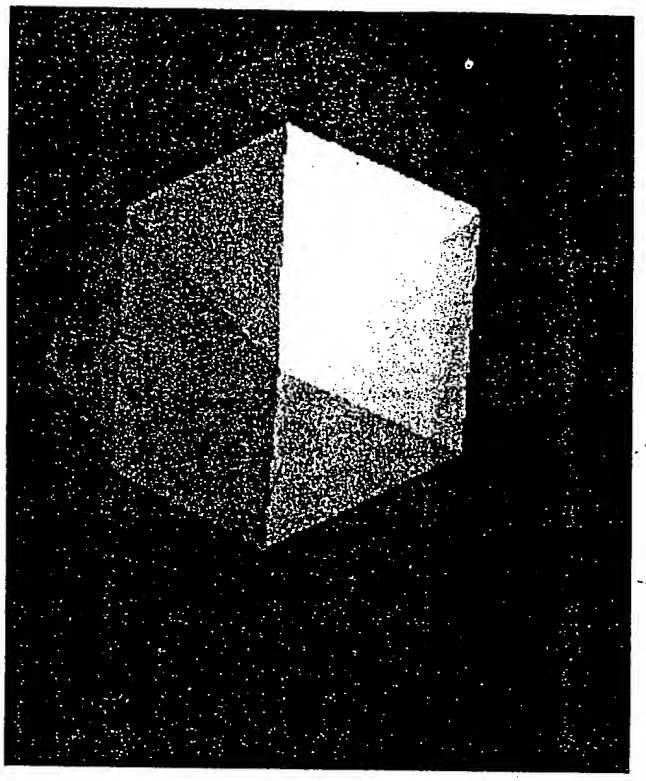

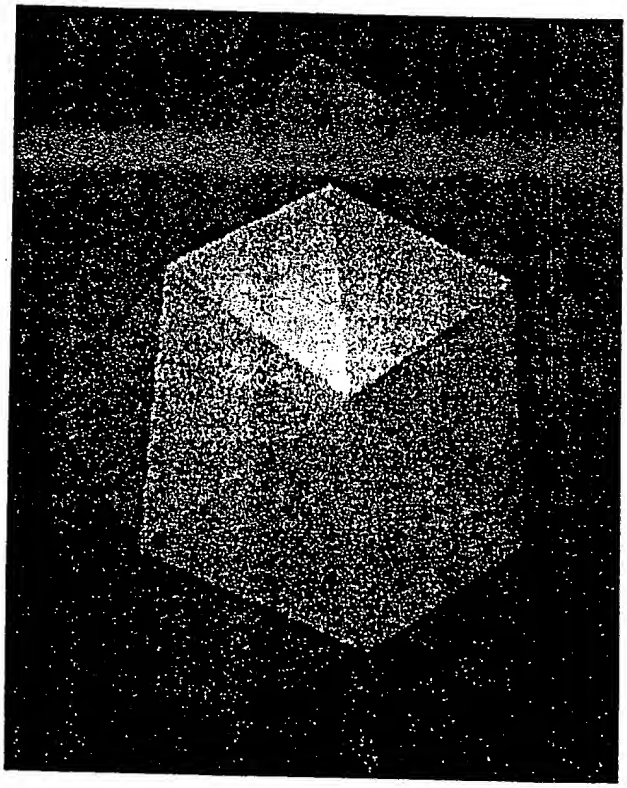

Figs. 6–8. 3-D digitization of sensor positions resulting from a 64-channel net placement for subjects 1–3. The 3-space (xyz) coordinates of the sensor-scalp junctions were digitized, then used as vertices of polygons to create a display object that shows the shape of the subject's head and the distribution of the sensors across the head surface. The nose is at the top in each figure.

methods to select the sphere that best fits the shape of the braincase (Lukenhoner et al. 1990). It can be seen that these methods are dependent on a representative sampling of the shape of the braincase; if the fit points are biased to certain regions of the braincase, the resulting sphere will be similarly biased. A geodesic partitioning method provides the optimal distribution of a sparse set of points across the irregular surface of the braincase.

The inferior surface of the braincase is, of course, inaccessible. However, the best-fit (least-squares) sphere selected from a geodesic partitioning of the accessible surface of the braincase can be adjusted to account for the points that would be obtained if the geodesic pattern were extended to the inferior surface. Worden et al. (in prep.) sampled the braincase of several skull models and found that a small (5%) superior (upward) displacement of the best-fit sphere computed from the geodesic points on the scalp provided an accurate adjustment for the entire surface of the braincase. Figs. 4 and 5 show a best-fit sphere, positioned according to the correction factor, superimposed on a graphic model of the head.

Three-dimensional scalp sensor positions

To illustrate the actual 3-D locations of sensors on individual subjects, a 64-channel geodesic sensor net

TABLE I

Intersensor distances. Measurements are in millimeters, computed as straight-line distances from nearest 5 or 6 vertices.

	Mean intersensor distance	Standard deviation
All net sensors		
Subject 1	38.1	3.6
Subject 2	38.2	3.7
Subject 3	37.8	3.6
Posterior region		
Subject 1	38.6	4.7
Subject 2	37.2	4.7
Subject 3	38.8	4.5
Anterior region		
Subject 1	37.9	2.0
Subject 2	39.1	2.3
Subject 3	37.0	2.2

was applied to 3 subjects, and the locations of the sensor-scalp contacts were measured in 3-space coordinates with an electromagnetic digitizer (Isotrack). Skull landmarks were also digitized, including the nasion, glabella, left and right external canthus, infraorbital points, left and right external auditory meatus (center of the opening in the plane of the head), mastoid bones (approximate center), vertex, and inion. The head circumferences for subjects 1–3 were 57, 58, and 54.5 cm. The nasion-inion distances were 35.5, 33.5, and 34 cm. To aid in visualizing the 3-space coordinates, the digitized points were interconnected into a surface with polygons, which were then shaded and imaged (Figs. 6–8) for each subject.

Examination of the spatial array of these vertices shows the nature of the spherical projection that results from the sphere-radial contraction of the vertices of the tension structure. The contraction is typically somewhat greater in the front of the head than in the back, resulting in closer spacing in the front. Subject 2's head was an exception to this generalization (Fig. 7). Because the present net tension is adjusted for a typical head-shape (rather than the equal tension of the geodesics on a sphere surface), the intersensor spacing is more uniform across most subjects' heads than would be the case for exact spherical projections.

From these sensor 3-space coordinate data for each subject, the intersensor distances, i.e., the straight-line distances to the neighboring vertices, were computed. Each vertex has 6 neighbors in the geodesic structure, except for the major vertices of the icosohedron which have 5 neighbors. Table I shows the means and standard deviations of the intersensor distances for the 3 subjects. The regularity of the intersensor distances is shown by the small standard deviations, which are only about twice the error of the electromagnetic digitizer (2 mm). When computed for the posterior 40% of the sensors, the standard deviations are somewhat higher than for the anterior 60%, reflecting the greater spread among vertices across the broad parietal region than across the more inferior posterior locations.

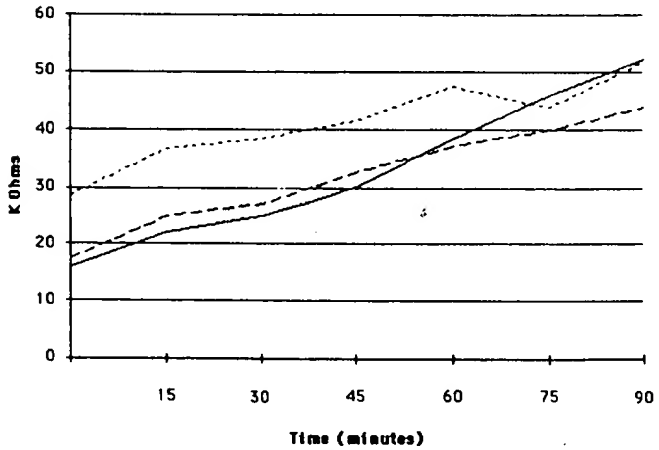

Fig. 9. Impedance changes over 90 min for 3 subjects. The initial impedance of 10–20 kΩ climbs over 90 min to 40–50 kΩ, still an adequate level for recording excellent EEGs with high input impedance (i.e., > 100 MΩ) amplifiers. Factors such as humidity, temperature and the nature of the subject's hair influence the stability of the impedance. Sealing the top of the pedestal tube, such as with silicone, limits the evaporation and decreases electrolyte evaporation.

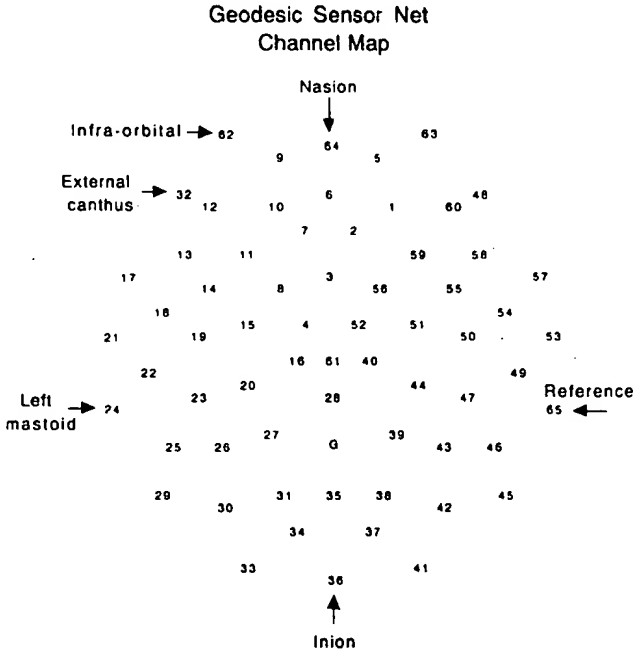

Fig. 10. Channel map for 64-channel geodesic sensor net. These are the locations of the data shown in Fig. 11.

Application and typical sensor impedances

Application of the 64-channel net is achieved easily within 0.5 h for most subjects, and for skilled technicians a 15 min application time is not unusual. By introducing computer-assisted impedance testing, additional improvements in speed and ease of application can be expected. For the first few minutes after application, the excess saline may wet the scalp and hair between the sensor pedestals. However, given the temperature of the scalp, these areas soon dry out, so that the only remaining wet areas are those beneath the sponges. With minimal individual attention, the initial impedances of the saline sponge sensors typically range from 10 to 40 kΩ.

With high input impedance amplifiers (i.e., > 100 MΩ), our experience shows that low noise EEG can be recorded with sensor impedances in the 50 kΩ range, even in an electrically noisy environment, such as in front of a computer monitor. The sensor impedance is limited, of course, by the sensor design, not by the geometric structure of the net. By abrading the scalp slightly and applying saline paste electrolyte under the sponge, impedances of 3–5 kΩ are easily achieved with the net. However, we find that, for our routine recordings, abrading the scalp to achieve low sensor impedances is unnecessary.

As the liquid saline evaporates from the sponges, the impedance of the sensor-to-scalp contact rises. Fig. 9 plots the average impedance of 64 sensors for 3 subjects at 15 min intervals. Low noise EEG is still obtained at the end of a 2 h recording session, when impedances may be in the 60–80 kΩ range. The rate of evaporation can be decreased by closing the top of

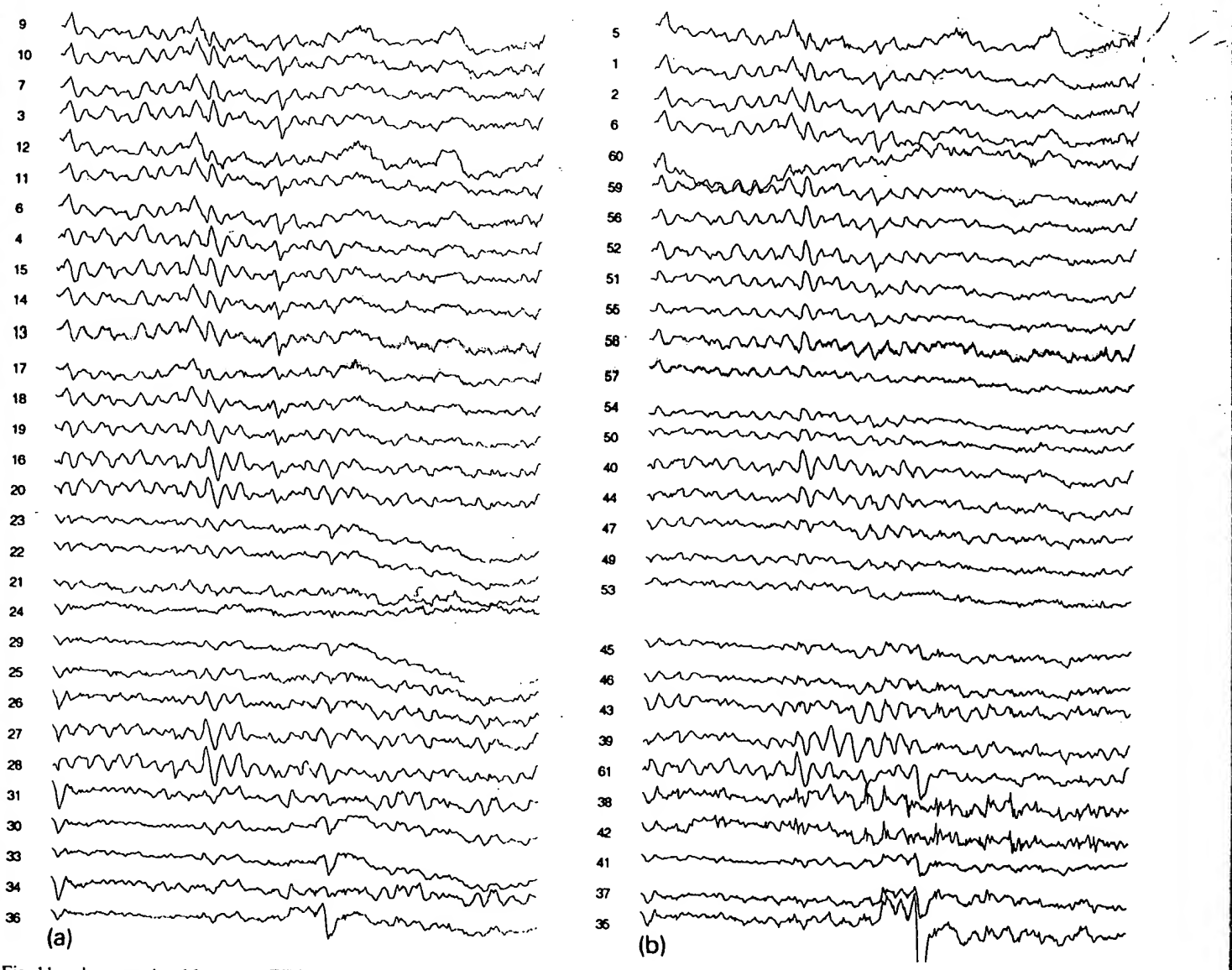

Fig. 11. a, b: example of 3 sec raw EEG recorded with the geodesic sensor net with right mastoid reference. Resting EEG from a normal subject. Bandpass: 0.1–50 Hz. a shows the left hemisphere sites and b shows those from the right hemisphere (see Fig. 10).

the sensor pedestal tube, although this precludes re-wetting. Through re-wetting once/h, i.e., applying a few drops of saline to each pedestal, impedances in the 10–40 kΩ range can be maintained indefinitely.

EEG data collection

The 64-channel net design has been used in our laboratory for over 1 year, for approximately 200 experimental sessions, with excellent results in EEG and ERP (event-related potential) studies (Compton et al. 1991; Curran et al. 1993; Chung et al. submitted). Geodesic sensor nets have been used in studies of 4- and 7-year-olds, and in pilot studies with 6- and 2-month-olds.

An example of raw EEG recorded with the net is given in Fig. 11. The reference is the right mastoid; channel locations are shown in Fig. 10. These 64-channel data are a randomly selected 3 sec epoch of the resting EEG of a subject selected at random from a recent experiment in the Oregon Brain Electrophysiology Laboratory. Each EEG channel is the differential voltage between the reference site and the index site. Because of volume conduction there are no "inactive" sites on the head or body. Therefore, the potential appearing at the right mastoid site comprises some fraction of each wave form in Fig. 11.

To show the potentials recorded at each site independent of the reference, and thus to illustrate the intersensor variability of the EEG in a 64-channel recording, these data were re-referenced to the average reference, the mean in the voltage at each sample point across all channels (Fig. 12). With 64-channel data, the average reference is virtually indistinguishable from the distance-weighted average reference,

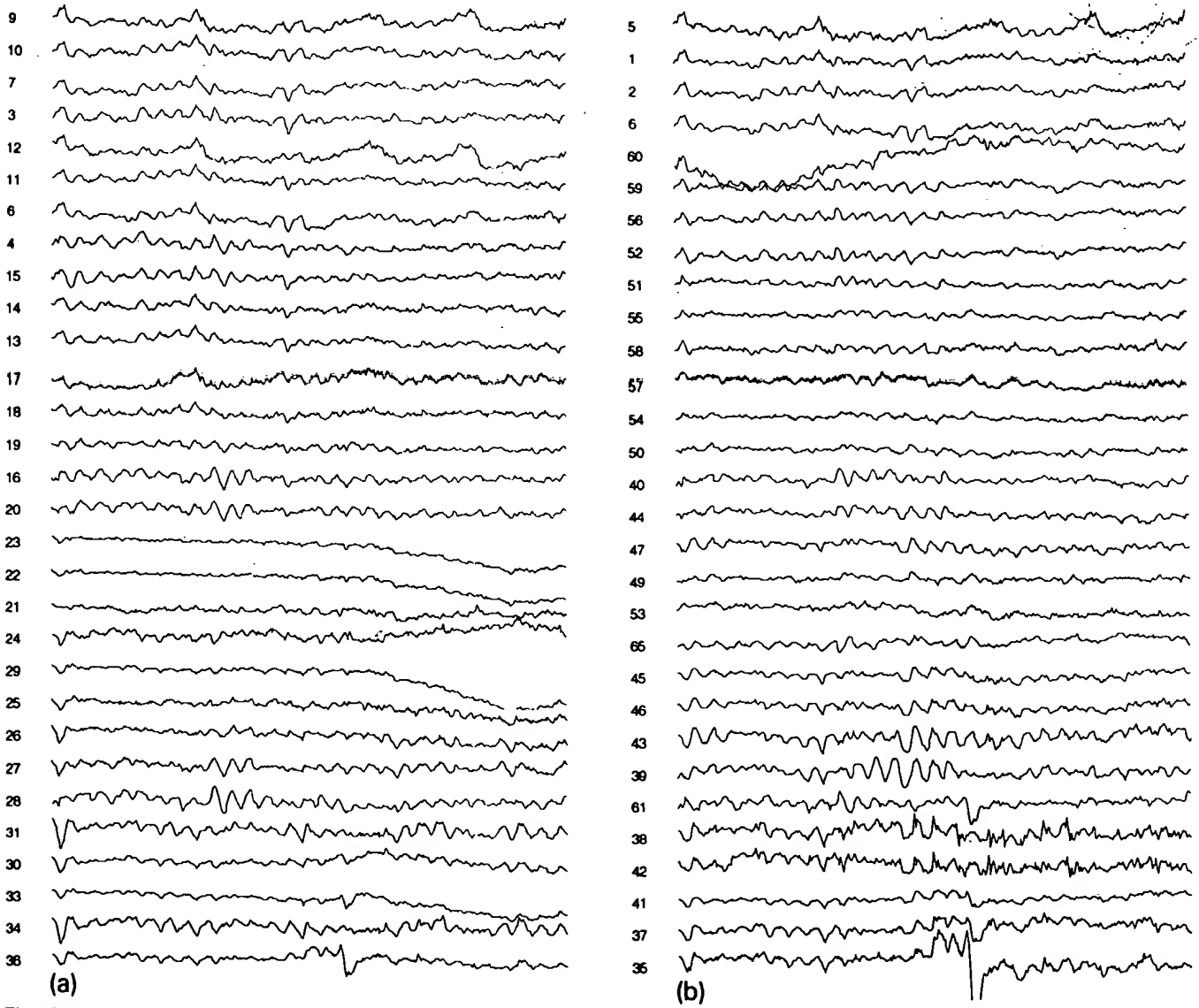

Fig. 12. a, b: data from Fig. 11 with average reference derivation. Each channel is re-computed as the differential voltage between that site and the mean of all channels. Plotted for the right mastoid site is zero minus the average of all channels.

although with fewer channels, the distance-weighting correction appears necessary (Curran et al. 1993). Channel 65 plots the inverse of the average reference. If the entire surface of the braincase, including the inaccessible inferior surface, were sampled evenly, this signal could be attributed to the right mastoid site itself (consider it as the right mastoid site recorded with 64 alternate reference sensors). However, given the incomplete surface sampling in this case, some unknown fraction of channel 65 represents the inverse of the potentials recorded at superior (scalp) locations that is not balanced by even sampling of fields at inferior sites.

It can be seen comparing Figs. 11 and 12 that greater intersensor variability is given by the reference-independent derivation. This variability suggests, in turn, that greater density of spatial sampling, e.g., 128 or 256 channels, will be necessary (Wikswo et al. 1993).

Several 128-channel net prototypes, such as shown in Fig. 3, have been constructed, and initial recordings are underway. These nets are mechanically stable and quite comfortable for several hours of wearing. They provide similar impedances as the 64-channel design. Our initial measurements suggest the 128-channel nets decrease the intersensor distance to about 28–30 mm (on an adult male head). Thus, even denser arrays may be required to achieve the 2 cm intersensor spacing that appears necessary to avoid spatial aliasing of scalp electrical fields (Spitzer et al. 1989; Gevins 1990; Wikswo et al. 1993). Systematic data are required to understand the intersensor distance necessary to avoid spatial aliasing in EEG scalp recordings. This data can only be provided through sampling with a sufficient density that spatial aliasing is eliminated.

With the development of volumetric dipole localization models using approximate inverse solutions, and finite element conductance models constrained by the anatomical information of the MRI (Wood 1992), powerful new methods for visualizing brain electrical activity may soon be available. The geodesic sensor net is a practical way to provide the new mathematical models with an adequate basis in measurement.

I thank Michael Murias and Daren Jackson for their assistance in developing net prototypes, Dave Caulton and Paul Compton for signal analysis software, and Matt Rubin and Eric Gorr for distance computation and imaging software.

References

Bendat, J.S. and Piersol, A.G. Random Data: Analysis and Measurement Procedures. John Wiley, New York, 1971.

Bertrand, O., Perrin, F. and Pernier, J. A theoretical justification of the average reference in topographic evoked potential studies. Electroenceph. clin. Neurophysiol., 1985, 62: 462–464.

Chung, G., Tucker, D.M., West, P., Potts, G. and Liotti, M. Emotional expectancy: brain electrical activity associated with mood-congruent cognitive bias. Submitted.

Cohen, D., Cuffin, B.N., Hunokuchi, K., Maniewski, R., Purcell, C., Cosgrove, G.R., Ives, J., Kennedy, J.G. and Schomer, D.L. MEG versus EEG loacalization test using implanted sources in the human brain. Ann. Neurol., 1990, 28: 811–817.

Compton, P., Grossenbacher, P., Posner, M.I. and Tucker, D.M. A cognitive-anatomical approach to attention in lexical access. J. Cogn. Neurosci., 1991, 3: 304–312.

Curran, T., Tucker, D.M., Kutas, M. and Posner, M.I. Topography of the N400: brain electrical activity reflecting semantic expectancy. Electroenceph. clin. Neurophysiol., 1993, 88: 188–209.

Fuller, R.B. Ideas and Integrities. Macmillan, New York, 1969.

Gevins, A. Distributed neuroelectric patterns of human neocortex during simple cognitive tasks. In: H.B.M. Uylings, C.G. Van Eden, J.P.C. De Bruin, M.A. Corner and M.G.P. Feenstra (Eds.), Progress in Brain Research, Vol. 85. Elsevier Science Publishers, Amsterdam, 1990.

Jasper, H.H. Appendix to report to Committee on Clinical Examination in EEG: the ten–twenty electrode system of the International Federation. Electroenceph. clin. Neurophysiol., 1958, 10: 371–375.

Lukenhoner, B., Pantev, C. and Hoke, M. Comparison between different methods to approximate an area of the human head by a sphere. In: F. Grandori, M. Hoke and G.L. Romani (Eds.), Auditory Evoked Magnetic Fields and Electric Potentials. Advances in Audiology, Vol. 6. Raven Press, New York, 1990: 103–118.

MacLean, P.D. Contrasting functions of limbic and neocortical systems of the brain and their relation to psychophysiological aspects of medicine. Am. J. Med., 1958, 25: 611–626.

Nunez, P.L. Electric Fields of the Brain: the Neurophysics of EEG. Oxford University Press, New York, 1981.

Perrin, F., Bertrand, O. and Pernier, J. Scalp current density mapping: value and estimation from potential data. Biomed. Eng., 1987, 34: 283–288.

Perrin, F., Pernier, J., Bertrand, D. and Echallier, J.F. Spherical splines for scalp potential and current density mapping. Electroenceph. clin. Neurophysiol., 1989, 72: 184–187.

Scherg, M. Fundamentals of dipole source analysis. In: F. Grandori and G.L. Romani (Eds.), Auditory Evoked Magnetic Fields and Potentials. Advances in Audiology. Raven Press, New York, 1989: 1–30.

Spitzer, A.R., Cohen, L.G., Fabrikant, J. and Hallett, M. A method for determining optimal interelectrode spacing for cerebral topographic mapping. Electroenceph. clin. Neurophysiol., 1989, 72: 355–361.

Tomberg, C., Noel, P., Ozaki, I. and Desmedt, J.E. Inadequacy of the average reference for the topographic mapping of focal enhancements of brain potentials. Electroenceph. clin. Neurophysiol., 1990, 77: 259–265.

Wikswo, J., Gevins, A. and Williamson, S. The future of the EEG and MEG. Electroenceph. clin. Neurophysiol., 1993, 87: 1–9.

Wood, C.C. Identification of currents in the human brain by noninvasive electrical and magnetic recordings. Paper presented to the International Neuropsychological Society, San Diego, February, 1992.

Worden, M., Tucker, D.M. and Jackson, D. Spatial sampling of head electrical fields: spherical generalization of the braincase. In prep.

Electroencephalography and clinical Neurophysiology, 81 (1991) 284–298

ADONIS 0924980X9100086R

ELMOCO 90594

Neuromagnetic fields accompanying unilateral and bilateral voluntary movements: topography and analysis of cortical sources

Rumyana Kristeva, Douglas Cheyne and Lüder Deecke

Neurological University Clinic, A-1090 Vienna (Austria)

(Accepted for publication: 2 October 1990)

Summary Movement-related magnetic fields (MRMFs) accompanying left and right unilateral and bilateral finger flexions were studied in 6 right-handed subjects. Six different MRMF components occurring prior to, and during both unilateral and bilateral movements are described: a slow pre-movement readiness field (RF, 1–0.5 sec prior to movement onset); a motor field (MF) starting shortly before EMG onset; 3 separate "movement-evoked" fields following EMG onset (MEFI at 100 msec; MEFII at 225 msec; and MEFIII at 320 msec); and a "post-movement" field (PMF) following the movement itself. The bilateral topography of the RF and MF for both unilateral and bilateral movements suggested bilateral generators for both conditions. Least-squares fitting of equivalent current dipole sources also indicated bilateral sources for MF prior to both unilateral and bilateral movements with significantly greater strength of contralateral sources in the case of unilateral movements. Differences in pre-movement field patterns for left versus right unilateral movements indicated possible cerebral dominance effects as well. A single current dipole in the contralateral sensorimotor cortex could account for the MEFI for unilateral movements and bilateral sensorimotor sources for bilateral movements. Other MRMF components following EMG onset indicated similar sources in sensorimotor cortex related to sensory feedback or internal monitoring of the movement. The results are discussed with respect to the possible generators active in sensorimotor cortex during unilateral and bilateral movement preparation and execution and their significance for the study of cortical organization of voluntary movement.

Key words: Magnetoencephalography; Motor cortex; Source localisation; Readiness field; Cerebral dominance; Reafference

It is known that various areas of the cerebal cortex play important roles in the preparation and performance of human voluntary movement and that the functional interaction of these areas differs for different types of movement. A means of monitoring the activation of motor cortical areas during various motor tasks can provide a better understanding of such functional organization. The various methodological approaches that have been used to study these processes include: (1) intra-cortical and surface recording from cortical motor areas (Arezzo and Vaughan 1980; Hashimoto et al. 1980; Tanji et al. 1987; Neshige et al. 1988), (2) single-unit recording from pyramidal tract neurones (PTNs; Fromm and Evarts 1982; Requin 1985), (3) scalp recording of cortical slow potentials and other movement-related potentials (MRPs; Kornhuber and Deecke 1965; Vaughan et al. 1968; Kutas and Donchin 1974; Shibasaki et al. 1980; Brunia 1988), and (4) in vivo measurements of regional cerebral blood flow (rCBF; Halsey et al. 1979; Roland 1985). The latter two techniques, MRPs and rCBF, have the advantage of allowing non-invasive measurement of motor behaviour in normal human subjects, but also have their respective limitations — MRPs having limited spatial resolution due to distortion of the scalp-recorded potentials by volume conduction effects, and rCBF methods being unable to separate temporal features of movement-related activity due to the need to sample over long time intervals.

The use of neuromagnetic or magnetoencephalographic (MEG) recording offers a new, non-invasive, approach towards the study of the movement-related brain activity which overcomes some of the difficulties in the interpretation of EEG records posed by problems of volume conduction. Because of the relative insensitivity of magnetic flux to the differing conductivities of the tissues of the head, MEG recording has proved to be a useful means of localizing the generators of event-related electrical activity of the brain with a high degree of accuracy (Williamson and Kaufman 1981; Romani and Rossini 1988). Initial studies of movement-related magnetic fields (MRMFs) related to voluntary movements (Deecke et al. 1982; Hari et al. 1983; Weinberg et al. 1983) indicated that slow magnetic field changes could be observed over the cortical motor areas prior to and during voluntary movements which resembled movement-locked EEG changes. More recent studies (Cheyne and Weinberg 1989; Cheyne et al. 1991) have

Correspondence to: Dr. Rumyana Kristeva, Neurological University Clinic, Lazarettgasse 14, A-1090 Vienna (Austria).

successfully combined neuromagnetic recording and dipole source analysis to identify motor cortex sources related to unilateral movements.

One of the key areas of interest in the study of human motor control is the functional organization of cortical areas during the preparation and performance of bilateral versus unilateral voluntary movement and, additionally, the role of cerebral dominance factors in this organization. In the present study, we describe the topographical distribution of the neuromagnetic fields over the cortical motor areas preceding and accompanying unilateral and bilateral finger movements in right-handed subjects and provide an analysis of the cortical sources active in sensorimotor areas during these tasks.

Methods

Subjects

The experiments were carried out on 6 right-handed subjects. All subjects had 100% dextrality after a modified Oldfield questionnaire (Oldfield 1971) and had previously participated in movement-related slow potential experiments.

Experimental procedure

MRMFs were investigated under the following 3 experimental conditions: (i) left-sided "pulse" movements (rapid flexion followed by extension) of the index finger of the left hand (LH); (ii) pulse movements of the right index finger (RH); and (iii) bilateral (simultaneous) pulse movements of both index fingers (BH). The subject lay on a non-magnetic bed in a magnetically shielded room (Vacuumschmelze, GmbH, Hanau) and was instructed to produce the above movements at his own pace irregularly, with intervals of about 8–15 sec between movements.

The voluntary movements were performed while the subject fixated on a target and while holding the breath 2–3 sec prior to the movement and at least 1 sec after the movement onset. However, the subjects were also instructed to perform brisk movements from complete muscular relaxation. Each subject was given several practice trials prior to the experiment until reaching a consistent EMG pattern. The 3 experimental conditions were pseudo-randomized during the experiment in blocks of 30 movements.

Recording

Neuromagnetic fields were recorded using two 7-channel second-order gradiometer systems (BTi, San Diego, Model 607) with a sensing coil diameter of 1.8 cm, coil spacing of 2.2 cm, and gradiometer baseline of 4.0 cm. Each 7-channel probe covered a curved area over the scalp of about 6 cm in diameter. In the first 3 subjects, MRMFs were recorded from 84 positions over a wide area of the scalp, including the anterior midline. For the subsequent subjects, a distribution of 42 positions over both sensorimotor areas was found to be adequate to record the field gradients observed in the first 3 subjects. The amplified signals (bandpass 0.1–50 Hz) were digitized at a rate of 100 samples/sec. The overall noise level was about 15 femtotesla/$Hz^{1/2}$ (at 1 Hz). Adaptive balancing of the gradiometer signals by 3 orthogonal noise channels was used to reduce further the environmental noise in the lower frequency range, and was found to produce a stable pre-movement baseline. Ninety trials were collected for each recording position of the dewar(s) for each of the experimental conditions. Each recording session lasted approximately 1–1.5 h and subjects performed no more than 2 sessions in 1 day. Extensive care was taken to eliminate artefacts due to eye movements and breathing movements of the head and body. This was achieved by fixating the head and upper body with vacuum casts and having the subjects fixate their gaze and hold their breath during the task. Additional records were made in 1 subject whose respiration was monitored through a short plastic tube with a thermistor placed at the end in order to ensure that breathing could be suppressed in this manner for the duration of the recording epoch. Recording positions were occasionally repeated in order to ex-

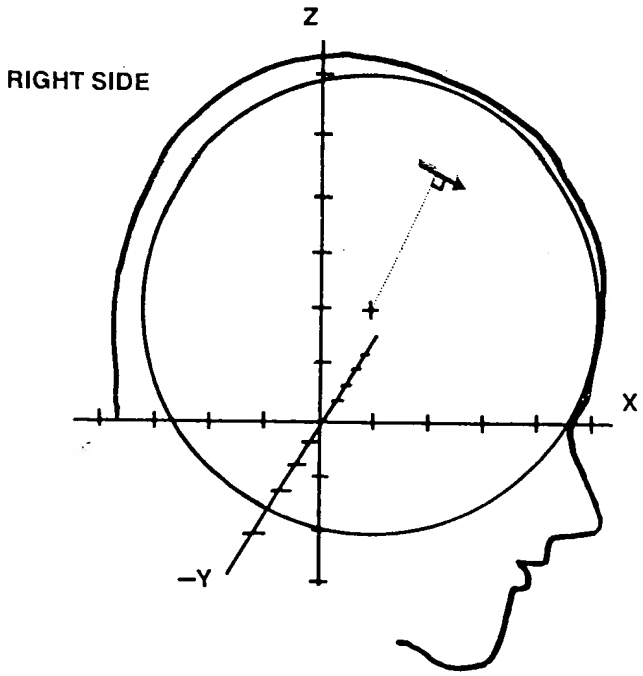

Fig. 1. Definition of the head coordinate system. The positive x axis passes through the nasion, the y axis through both pre-auricular points and the z axis passes through the top of the head, 2–3 cm posterior to C_z. Dipole source localization used a spherical model where theoretical sources were maintained orthogonal to their radii in a sphere fitted to the curvature of the head, as shown in the diagram.

amine the reproducibility of the data or if excessive movement artefacts occurred.

The EMG was recorded from Beckmann silver-silver chloride electrodes overlying the flexor digitorum communis muscles (pars indicis) of both forearms. The trigger pulse was generated by the onset of the rectified EMG burst from the active muscles.

For each subject a 3-dimensional head coordinate system was created on the basis of 3 anatomical landmarks (nasion and both pre-auricular points) and the position and orientation of the gradiometers were located in this coordinate system prior to each recording, using an electronic 3-dimensional probe positioning system (BTi, San Diego) with an accuracy of 2–3 mm. This head coordinate system (shown in Fig. 1) was defined as a horizontal axis passing through the left and right ear canals and an antero-posterior axis bisecting this line and passing through the nasion. The vertical axis projected up from the point of bisection towards the vertex of the head, so that the coronal (y-z) plane lay approximately parallel, and slightly posterior, to the precentral gyrus.

Data analysis

Averaging was done after off-line elimination of artefact-contaminated trials and visual correction of the alignment of the trigger to the very first onset of EMG activity. Trials without a clear and sharp onset of EMG activity were also excluded from the average. Analysis time was from 2.0 sec before to 0.5 sec after EMG onset, using the first 250 msec as baseline.

Iso-contour maps of field intensity for selected time intervals of 10 msec were produced by a 2-dimensional linear interpolation of an equidistant projection of the recording positions about the z-axis (assuming constant radius). These spatial maps were used for determining dipolar field patterns and to determine the time periods for source localization analysis for the different components identified in the wave forms.

The equivalent current dipole sources were defined as current dipoles oriented tangential to their radius in a sphere, defined to lie within the spherical portion of the head as shown in Fig. 1. The strength, position and orientation of one or more dipoles could be adjusted using a least-squares fitting algorithm which optimized the extent to which the field of the theoretical sources accounted for the variance of the observed data, expressed as a percentage or "goodness of fit" (g).

Results

(I) Peripheral measures

(i) Unilateral movements. With right-sided and left-sided movements, the EMG of the non-active side was not completely silent and showed a slight but delayed

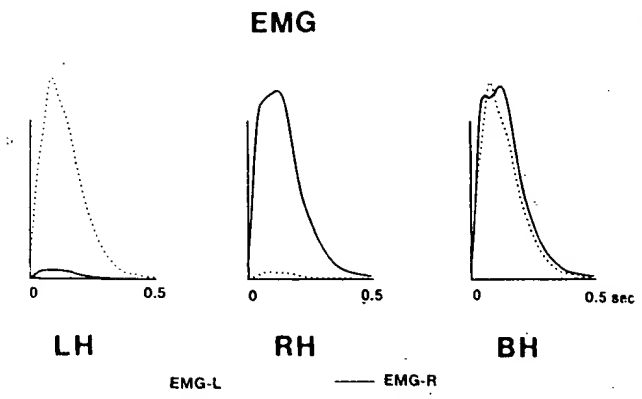

Fig. 2. The averaged rectified EMG from 6 experimental sessions shown in Fig. 4: LH (left index finger), RH (right index finger) and BH (both index fingers). Surface EMG overlying pars indicis of m. flexor digitorum longus of the left hand (dotted line) and from the right hand (solid line). Note the well pronounced mirror activity in conditions LH and RH.

mirror activity in all subjects studied (see Fig. 2). The delay of the mirror activity was approximately 30 msec on either side. This observed mirror EMG activity showed considerable inter-individual differences. However, intra-individual differences in the appearance of the mirror activity for different sessions was less pronounced. A common observation was that the mirror activity was more expressed when fatigue appeared during the experiment and when the vigilance of the subject became lower. The mirror activity appeared to express a non-conscious synkinesis of the homologous muscles as indicated by the subject's report after the experiment.

The peak activity in the EMG of the active side occurred approximately 50 msec after movement onset. The mean duration of the movement of the active side was approximately 400 msec.

(ii) Bilateral movements. In two of the subjects the maximal amplitudes of the EMG recorded from either arm were of equal size. In the other 4 right-handed subjects, the EMG on the right was of slightly larger amplitude than on the left. These amplitude differences were not significant. The synchronization error between the initiation of LH and RH EMG activity was approximately 10 msec with the right hand leading. The peak activity in the EMG was at approximately 50 msec after movement onset.

(II) Movement-related magnetic fields (MRMFs)

(i) Description and terminology of MRMF components. Six different movement-related magnetic fields were identified in the MEG wave forms (Fig. 3) as follows.

A slow magnetic field shift was observed starting 500–1000 msec prior to the movement onset, as measured from the very first onset of the rectified EMG burst, and was termed the readiness field (RF), corresponding to that described as *Bereitschaftsmagnetfeld*

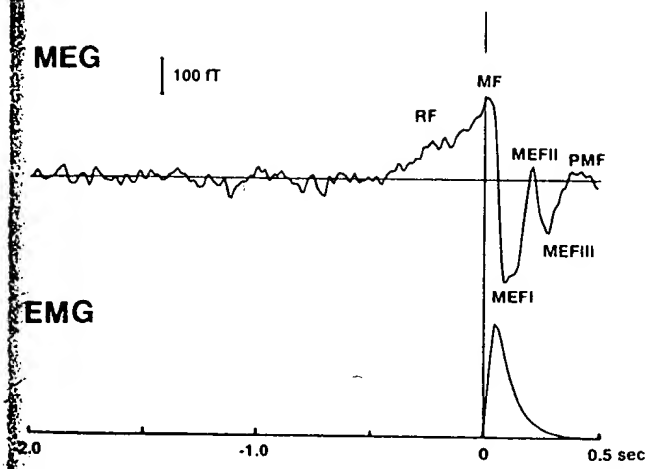

Fig. 3. Upper trace: representative MEG wave form from a lateral position over the left hemisphere of subject 4 showing the major MRMF components identified in the present study. RF: readiness field starting approximately 500–1000 msec prior to EMG onset (0 msec); MF: motor field reaching its peak after the movement onset. The peaks occurring during EMG onset are termed movement-evoked fields at the following post-EMG onset latencies: MEFI at 100 msec; MEFII at 225 msec and MEFIII at 320 msec. PMF: post-movement field at 440 msec after EMG onset. Upward deflection indicates magnetic flux directed out of the head. Lower trace: the rectified EMG used as a trigger showing the movement onset of the EMG burst (= 0 sec).

by Deecke et al. (1982) and Weinberg et al. (1983) or readiness field by Hari et al. (1983).

The neuromagnetic field between 50 msec prior to the movement onset to 30–50 msec after EMG onset showed a slight increase in amplitude and was labelled the motor field (MF). This component is similar to the "motor potential" described by Deecke et al. (1969, 1976) and the "N2" component described by Vaughan et al. (1968).

Deflections occurring after the onset of the rectified EMG activity were termed "movement-evoked fields" (MEFs) after the terminology used by Cheyne and Weinberg (1989), three of which could be discerned in the present study and were given the additional suffixes I, II, and III. These 3 components consisted of: MEFI at a latency of 100 msec after EMG onset (103 ± 5 msec for LH, 101 ± 7 msec for RH, and 103 ± 7 msec for BH); MEFII at a latency of 225 ± 13 msec (210 ± 14 msec for LH, 236 ± 24 msec for RH and 103 ± 6 msec for BH) and MEFIII at a latency of approximately 320 msec after EMG onset. An additional fourth component was observed following the movement itself (440 ± 10 msec after EMG onset) and was termed the post-movement field (PMF). The first 3 components, RF, MF and MEFI were observed in all of the subjects, whereas the later 3 components MEFII, MEFIII and PMF were present in only some of the subjects and appeared to vary with the consistency of the performance of the movement over different experimental sessions.

(ii) Topography of MRMFs. Fig. 4 shows a typical set of averaged MEG wave forms from 1 subject for each of the 3 experimental conditions studied. In this subject it can be seen that voluntary movements were preceded by slow magnetic field shifts as follows: over the left hemisphere the fields were outward going laterally and inward going medially with reversal over the left central sulcus; over the right hemisphere a similar field reversal occurred but with an outgoing field medially and ingoing field laterally. The slow magnetic fields were more symmetrical prior to the bilateral movements and asymmetrical prior to the unilateral movements, being stronger contralaterally. These slow magnetic fields started 0.5–1 sec prior to the onset of the rectified EMG burst and reached peak amplitudes of 200–300 femtotesla (fT) at a latency of 30–50 msec after EMG onset.

The pre-movement fields were followed by a larger field reversal (up to 600 fT in some subjects) at about 100 msec after EMG onset. In the case of unilateral movements, this reversal was observed only over the contralateral hemisphere, whereas in the case of bilateral movements, the field reversals at the same latency were observed over both hemispheres. The field direction of the component at 100 msec was opposite to the field direction of MF, as shown in Fig. 4.

The 3 components, RF, MF and MEFI, were identified in all the subjects studied. In Fig. 5, iso-contour maps of field intensity show the topography of the MF and MEFI in 1 subject for each of the experimental conditions. Note that, in these maps, an asymmetry of field strength can be seen when comparing the maxima over lateral locations to maxima over medial locations, suggesting some cancellation of fields of opposite direction which overlap at the vertex. This is particularly notable in the MF and MEFI for bilateral movements (Fig. 5, bottom row).

Fig. 6 shows iso-contour maps for the 5 components, MF, MEFI, MEFII, MEFIII and PMF which could be clearly identified in one of the subjects. MEFII was characterized by a pattern similar to that of the RF and MF but with a slightly rotated orientation over the central sulcus. For unilateral movements this pattern consisted of a reversal restricted to the contralateral hemisphere with a unidirectional field over the ipsilateral hemisphere and for bilateral movements it was symmetrical over the hemispheres. The MEFIII was characterized by a pattern similar to MEFI with a reversal over the contralateral hemisphere but with some additional ipsilateral activity. The PMF resembled to a great extent the RF but was of smaller amplitude. The topographies of the last 3 components (MEFII, MEFIII and PMF) were difficult to distinguish in all subjects, possibly due to variability in the physical parameters of the movement performed; particularly the movement duration varied across experimental sessions.

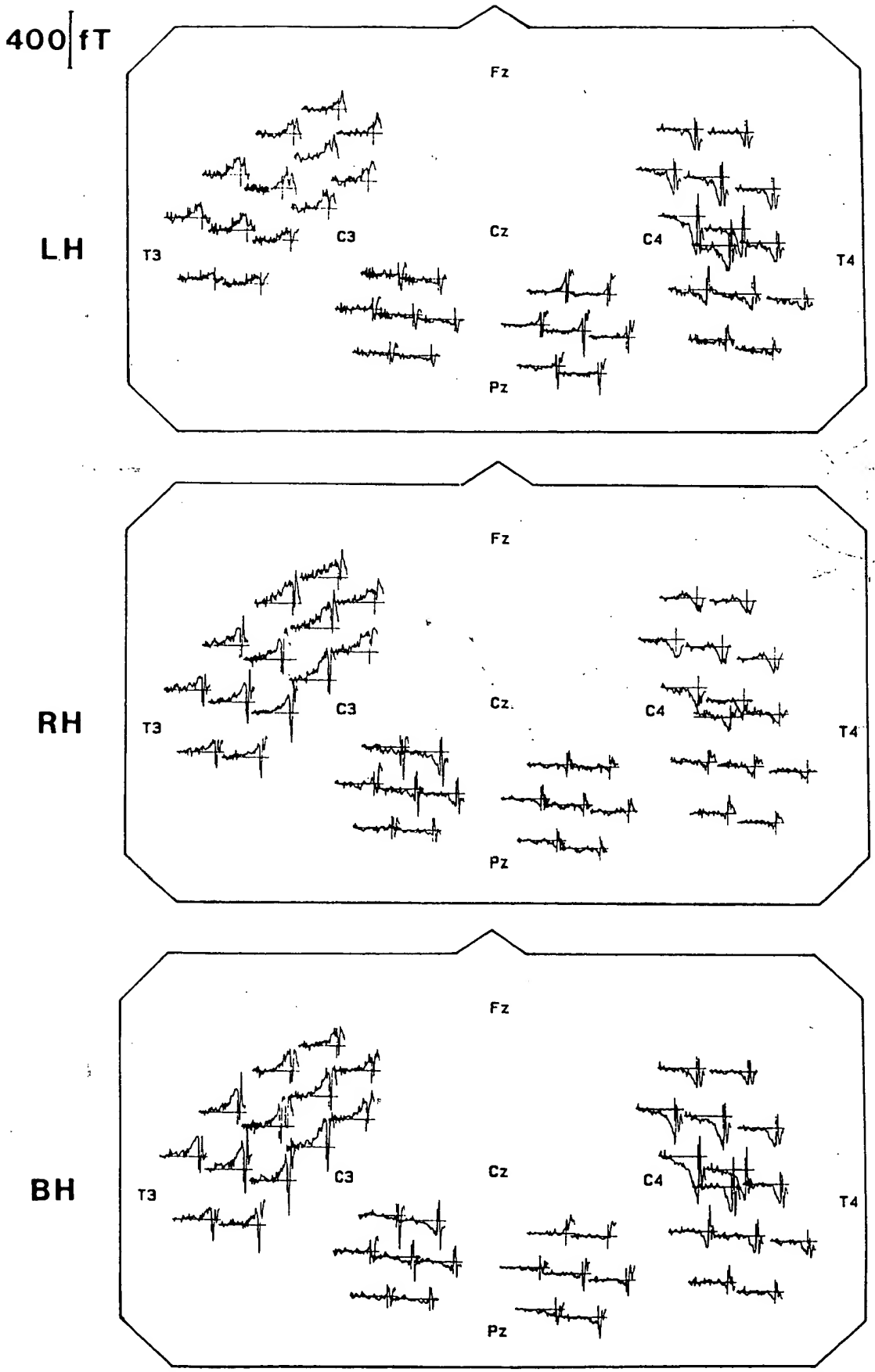

Fig. 4. Averaged wave forms from 1 subject showing the distribution of MRMFs over the surface of the scalp for unilateral left-sided (LH), right-sided (RH), and bilateral (BH) voluntary movements. Upward deflections = outgoing flux. Downward = ingoing flux. Averages of 9[illegible] movements for each condition, performed in randomized blocks of 30 movements. Note dipolar pattern over both hemispheres for conditions LH and RH with greater field strength contralaterally.

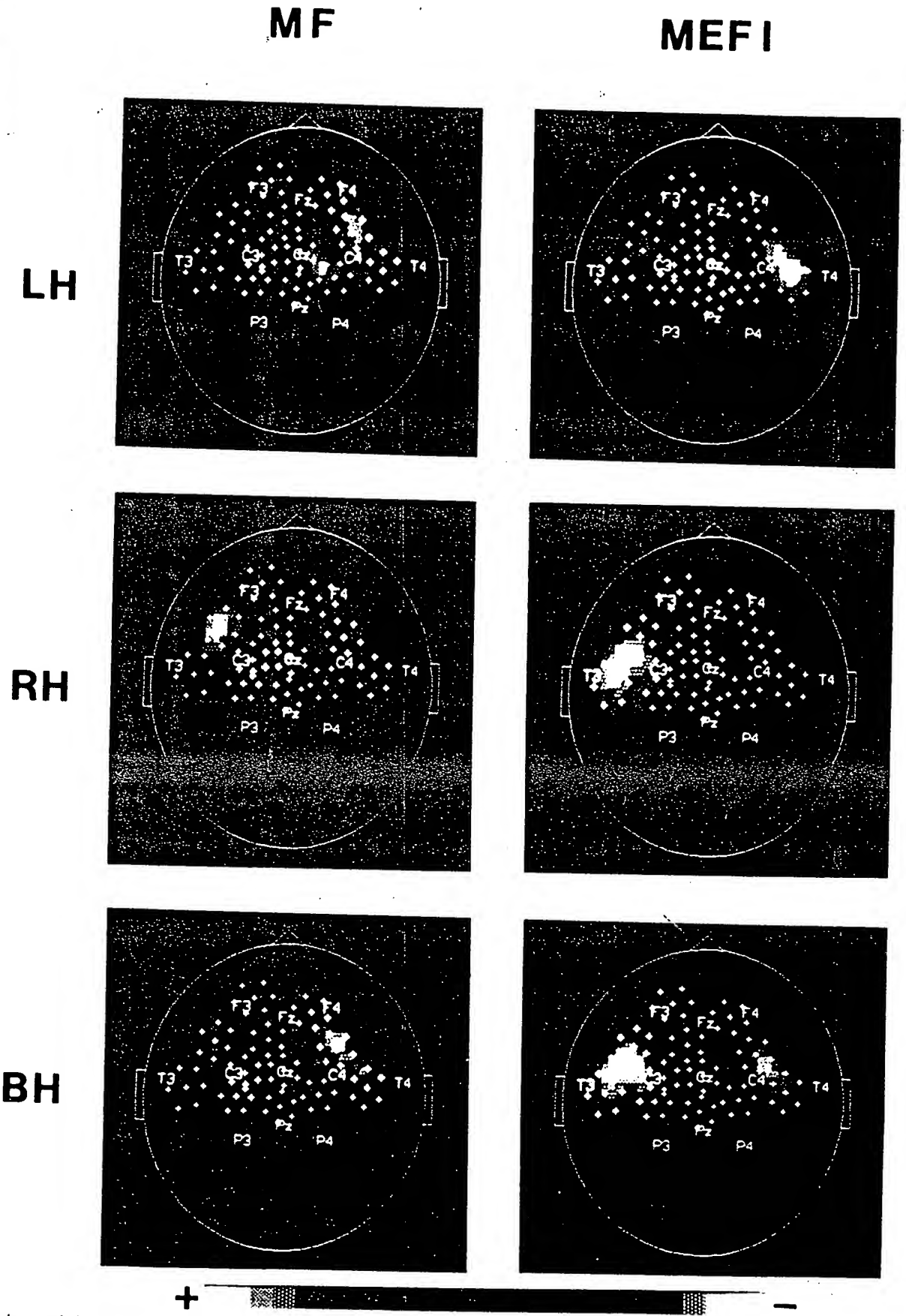

Fig. 5. Colour-coded iso-contour maps showing the movement-related neuromagnetic patterns in 1 subject for motor field (MF) and movement-evoked field I (MEFI). Blue shading indicates magnetic flux exiting the scalp and red shading indicates flux entering the scalp. All maps are individually scaled to their respective maximum values.

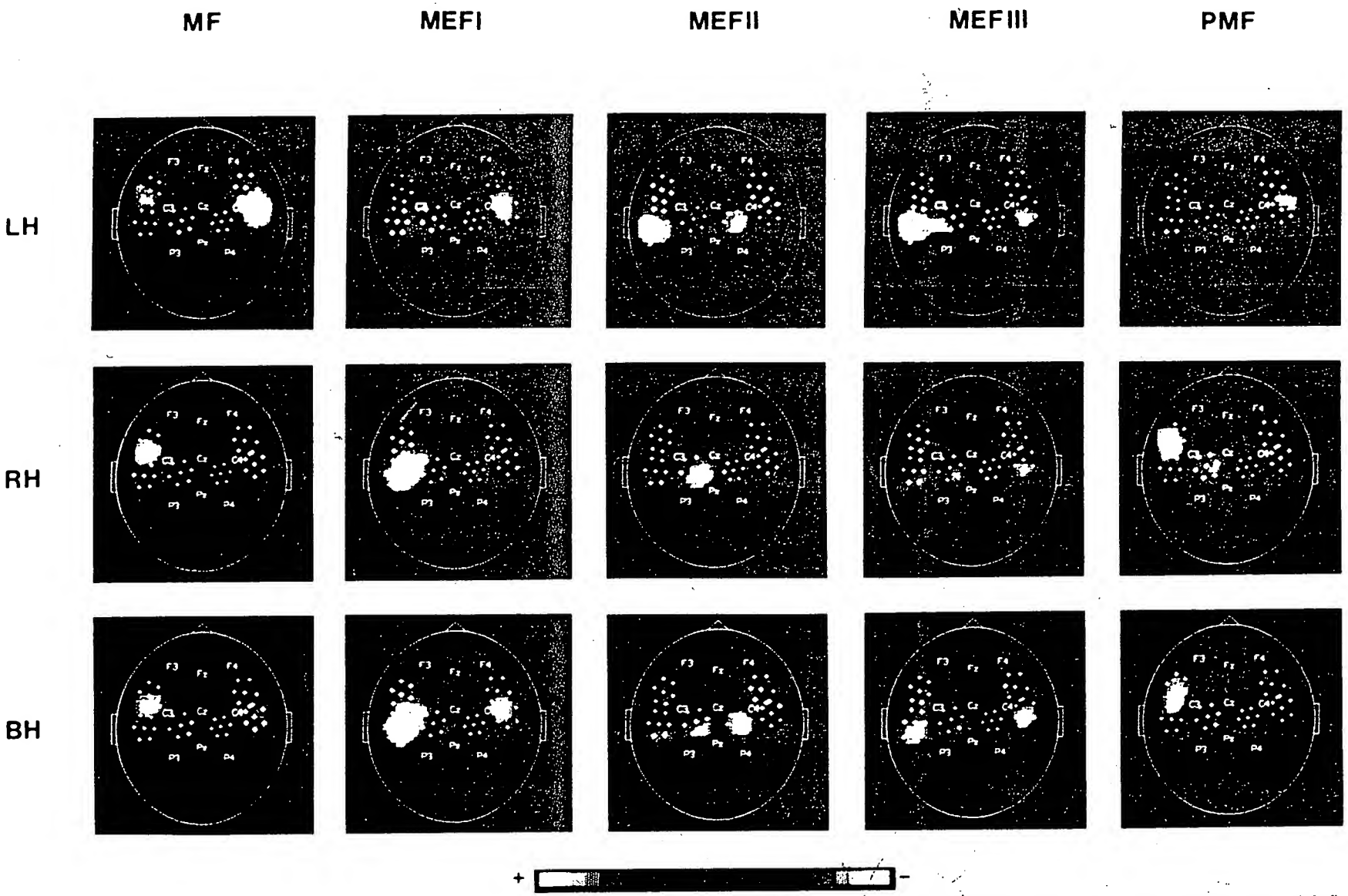

Fig. 6. Colour-coded iso-contour maps showing 5 of the identified movement-related neuromagnetic field patterns in 1 subject across conditions. RH = right finger movement; LH = left finger movement; BH = simultaneous bilateral finger movements; MF = motor field; MEF = movement evoked field; PMF = post-movement field. Blue shading indicates magnetic flux exiting the scalp and red shading indicates flux entering the scalp. Maps are individually scaled.

TABLE I

Parameters for least-squares fitted equivalent dipoles for the MF for the 3 experimental conditions, LH, RH and BH, in all subjects. Two current dipoles chosen to describe the field pattern over both hemispheres were fitted simultaneously (L = left hemisphere; R = right hemisphere). Q = dipole moment (current density in nA-m). The x, y, and z positions (in cm) of the dipoles are with respect to a right-handed coordinate system described in Fig. 1. Goodness of fit (g) is the percentage of variance accounted for by each theoretical source. The mean strength and position for each condition are also given.

Subject	Cond.	Left hand					Right hand					Both hands				
		Q	Position (cm)			g (%)	Q	Position (cm)			g (%)	Q	Position (cm)			g (%)
			x	y	z			x	y	z			x	y	z	
1	L	8.6	3.2	3.5	10.1		8.6	−0.6	3.8	9.3		9.9	−2.2	4.3	10.0	75
	R	11.1	0.8	−3.6	10.2	85	6.4	2.9	−3.8	10.8	75	8.9	1.7	−4.3	10.5	
2	L	5.9	0.1	4.6	9.0		8.3	3.5	5.2	11.1		6.7	4.0	4.9	11.2	91
	R	10.3	3.5	−4.2	11.1	90	7.0	4.1	−4.2	11.1	91	8.5	2.3	4.3	11.5	
3	L	10.5	−1.0	5.4	8.0		8.0	5.1	4.6	9.9		8.5	4.9	4.9	9.9	81
	R	11.4	0.0	−5.2	10.0	89	7.2	8.0	−5.7	8.4	74	7.3	1.3	−4.2	10.5	
4	L	7.2	3.9	2.8	9.5		8.8	3.9	3.8	10.2		6.1	3.3	4.4	10.2	
	R	9.6	3.8	−3.0	10.4	84	4.8	1.6	−4.0	9.3	81	9.1	3.8	−3.7	10.5	79
5	L	6.9	2.9	3.7	9.6		8.0	2.7	4.3	10.3		6.5	2.8	4.1	9.8	
	R	7.3	1.0	−4.3	9.9	90	6.2	−2.6	−4.0	8.2	90	6.8	1.4	−4.5	9.7	87
6	L	5.5	4.2	3.9	10.8		14.1	3.3	3.5	10.6		6.9	4.3	4.3	11.0	
	R	5.8	3.3	−4.9	10.7	87	5.6	0.1	−4.2	7.9	92	5.0	3.6	−5.2	11.0	88
Mean	L	7.4	2.2	4.0	9.5		9.3	3.0	4.2	10.2		7.4	2.8	4.5	10.3	
	R	9.2	2.1	−4.2	10.4		6.2	2.4	−4.3	9.5		7.6	2.4	−4.4	10.6	
S.D.	L	1.8	2.1	0.9	0.9		2.4	1.9	0.6	0.6		1.5	2.6	0.3	0.6	
	R	2.2	1.6	0.8	0.4		0.9	3.6	0.7	1.5		1.6	1.1	0.5	0.6	

Systematic differences in the MEFs between the 3 conditions studied cannot be described at this stage and are the object of further investigation. The MRMFs studied in these 6 subjects showed considerable inter-individual differences (for example, in 1 subject the RF pattern over the left hemisphere was rotated 90° with respect to all other subjects) but were relatively stable across recording sessions within individuals. No systematic relationship between the relative amplitudes of pre- and post-movement magnetic fields was found.

(iii) Dipole source analysis. Since field amplitudes measured over different locations over the scalp are dependent on the absolute distance of the sensing coils from the source, comparisons between movement conditions were made on the basis of the parameters of estimated sources which could be fitted to the observed data, taking into account the position and tilt of the gradiometers. Only dipole source locations which were physiologically feasible (i.e., located at a radius which would suggest a cortical location) were included in the comparisons.

For modelling the MRMFs preceding EMG onset, a 2-dipole model was chosen for both unilateral and bilateral movements, assuming equivalent sources in either hemisphere based on the bilaterality of the field topography, in which both sources were adjusted simultaneously by the fitting algorithm. Dipole source analysis yielded similar results for both the RF and MF, but with lower dipole strengths for the RF. Only the MF sources are described further here. The dipole locations for the MF component are shown in Table I. The locations for both left and right fitted dipoles were consistent across subjects for all the conditions studied (with the exception of condition RH in subject 3) and indicated current flow in the region of the sensorimotor cortex in the anterior direction. This was based both on the position of the sources within a digitized head outline within some subjects (i.e., the depth of the source relative to the scalp surface) and their location relative to international 10–20 system electrode locations (i.e., with reversal of field direction over positions C_3 or C_4, known to overlie the hand representation area of the primary motor cortex in the precentral gyrus). These locations were also comparable to those we have obtained in a previous study using the same coordinate system, in which source locations prior to movements of the digits were confirmed to be within these cortical areas by projecting the sources onto magnetic resonance images taken from the same subjects (Cheyne et al. 1991).

Paired t tests were performed for the mean dipole moments and indicated that, for unilateral movements, the contralateral MF source was significantly stronger ($P < 0.05$) of the order of 2–3 nA-m. This was true for both left- and right-sided unilateral movements. No significant differences in the dipole strength for bilateral movements between left and right hemispheres were found (mean dipole moments of 7.4 ± 1.5 nA-m and 7.6 ± 1.6 nA-m for left and right MF sources, respectively). It was also noted that the lateralization of

TABLE II

Parameters of the least-squares fitted dipoles for MEFI for the 3 conditions studied: LH, RH and BH across all subjects. For unilateral movements (LH and RH) a single equivalent dipole model was used and for bilateral movements (BH) a 2-dipole model was used. Dipole parameter definitions as in Table I.

Subject	Cond.	Left hand					Right hand					Both hands				
		Q	Position (cm)			g (%)	Q	Position (cm)			g (%)	Q	Position (cm)			g (%)
			x	y	z			x	y	z			x	y	z	
1	L	–	–	–	–		34.0	1.9	4.1	10.6	93	36.1	2.1	4.1	10.6	
	R	49.0	1.8	−4.0	10.9	96	–	–	–	–		42.2	2.4	−4.2	11.1	88
2	L	–	–	–	–		24.4	3.4	4.7	10.7	97	36.1	2.8	4.2	10.5	
	R	14.1	2.7	−4.9	9.2	93	–	–	–	–		19.8	3.4	−3.9	8.6	96
3	L	–	–	–	–		21.0	4.4	4.2	9.1	56	14.8	4.5	5.1	10.0	
	R	20.4	3.3	−4.7	10.1	94	–	–	–	–		23.1	3.8	−4.7	9.3	73
4	L	–	–	–	–		27.8	2.4	3.1	9.9	82	29.5	2.6	3.1	10.0	
	R	21.1	3.3	−3.2	10.1	74	–	–	–	–		27.2	3.3	−2.7	10.0	89
5	L	–	–	–	–		24.1	2.5	4.2	9.2	95	22.0	3.3	4.2	9.4	
	R	38.9	1.5	−3.8	8.1	88	–	–	–	–		20.6	1.4	−4.2	8.9	92
6	L	–	–	–	–		21.0	2.5	3.5	9.9	79	22.0	1.7	3.1	10.0	
	R	18.4	0.5	−2.9	10.2	94	–	–	–	–		18.0	0.2	−3.1	9.8	82
Mean	L	–	–	–	–		25.4	2.9	4.0	9.9		26.8	2.8	4.0	10.1	
	R	26.9	2.2	−3.9	9.8		–	–	–	–		25.2	2.4	−3.8	9.6	
S.D.	L	–	–	–	–		4.9	0.9	0.6	0.7		8.6	1.0	0.8	0.4	
	R	13.7	1.1	0.8	1.0		–	–	–	–		9.0	1.4	0.8	0.9	

dipole strength for RH was greater than for LH (3.1 compared to 1.8 nA-m), although this difference was not statistically significant.

A single equivalent dipole model was chosen for MEFI for right and left unilateral movements (LH and RH) since this field was primarily contralateral (although some additional flux was present over the ipsilateral hemisphere). These sources were fitted using only data recorded over the hemisphere contralateral to the movement (since inclusion of data from the ipsilateral hemisphere had only the effect of artificially increasing the residual variance for the modelled contralateral source, but not in changing its location). The results for the dipole parameters for MEFI are summarized in Table II. For the BH condition a 2-dipole model was used with sources located in both hemispheres. The sources fitted to MEFI were generally stronger in current density than the pre-movement sources but had locations which tended to be slightly posterior and deeper in comparison to the sources fitted to the MF and were directed posteriorly rather than anteriorly.

Fig. 7 shows the position of the fitted dipoles for the MF and MEFI for each of the experimental conditions in 1 subject as projections within the head coordinate system. For the MF 2 equivalent current dipole sources were fitted simultaneously to both sensorimotor cortices for each movement condition and their locations shown by filled or empty circles with the tail showing the principle direction of current flow to be in the anterior direction. The MEFI sources (filled and empty squares) tended to be posteriorly directed and are bilaterally represented only in condition BH. It was noted that only the MF source for unilateral movements (conditions RH and LH) differed in its location across conditions, appearing to have a greater depth when ipsilateral to the movement. Calculations of the relative depths of these sources (estimated from their radii within the head coordinate system) showed these ipsilateral MF sources to be 8–10 mm deeper in comparison to the location during contralateral or bilateral movement. For example, the mean radius of the left hemisphere MF source was similar for both bilateral and right-sided movements (11.87 ± 0.77 cm and 11.59 ± 0.85 cm, respectively) but less (10.75 ± 0.88 cm) for left-sided movements, although this difference did not reach statistical significance.

Discussion

(I) Magnetic fields preceding movement

Primary motor cortex activation preceding movement onset. In the present study slow magnetic field changes (readiness field, RF) were observed over the sensorimotor areas of both hemispheres prior to the onset of both unilateral and bilateral movements. The bilaterality of the RF suggests bilateral activation of the motor cortex beginning about 500 msec prior to EMG onset. This time period also corresponds to the change in slope of the pre-movement potential, termed contralateral preponderance of negativity by Deecke et al. (1969 1976), and negative slope, NS′ by Shibasaki et al. (1980). The RF, however, is not characterized by a change in slope,

but rather shows a linear increase in amplitude up to EMG onset, after which it increases slightly in slope for up to 50 msec (motor field, MF). This may indicate a slightly different interpretation of MI activation than that based on EEG studies, which suggests lateralization of the readiness potential due to onset of *only* the contralateral motor cortex around 500 msec pre-EMG onset, since the MEG data indicate that *both* motor cortices become active at this time, but with unequal intensities, which could produce the contralateral preponderance observed in the readiness potential. It must be noted however, that magnetic field changes were observed only up to 1 sec preceding EMG onset and do not bear on the changes observed in the EEG, which can precede movement onset by as much as 3 sec (cf., Kristeva et al. 1990).

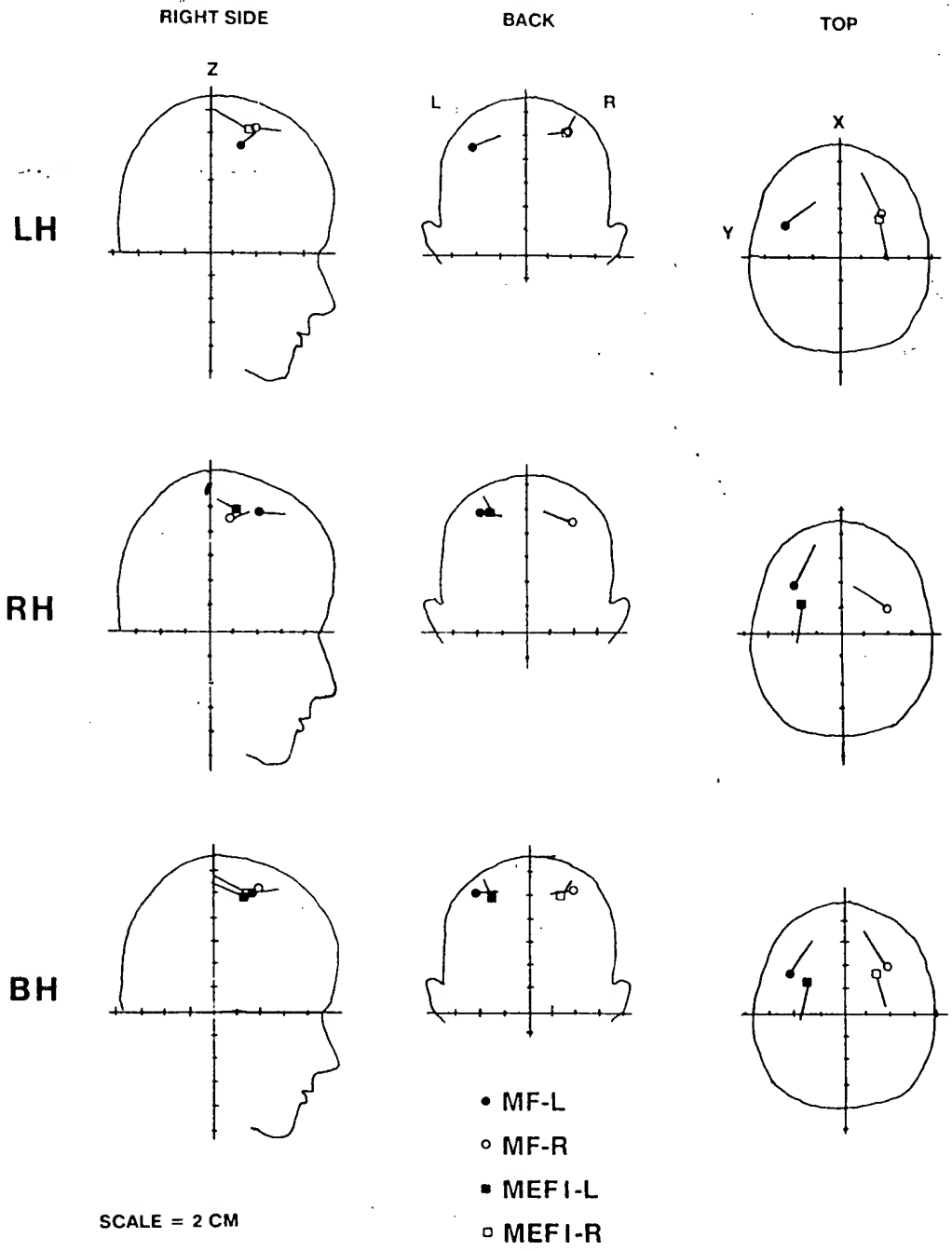

Fig. 7. Location of the fitted dipoles for the motor field (MF) over the left hemisphere (MF-L) and over the right hemisphere (MF-R) and for the movement-evoked field I (MEFI) (MEFI-L over the left hemisphere and MEFI-R over the right hemisphere) for 1 subject (S4) shown as projections in the head coordinate system described in Fig. 1. Dipole location is shown by circles (MF) or squares (MEFI) with a tail indicating the amount and direction of current flow within each plane of projection. Left: head viewed from right (x-z projection). Middle: head viewed from behind (z-y projection). Right: head viewed from above (x-y projection). Scale is 2 cm.

The present findings agree with the observation of bilateral magnetic fields prior to unilateral finger flexions reported by Deecke et al. (1982) and Cheyne and Weinberg (1989). One striking feature in the topography of these fields is the degree of asymmetry of the field maxima over either hemisphere such that the medial fields over the vertex were smaller in amplitude and reduced in their extent. This has been previously described (Cheyne et al. 1991) and was suggested to be a result of overlapping of fields of opposite direction over the central scalp, arising from generators of similar orientation in both hemispheres, even in the case of unilateral movements. The topography observed for bilateral movements in the present study tends to confirm this hypothesis, since the patterns for both unilateral and bilateral movements were similar, showing constricted field patterns over the vertex which varied a great deal from subject to subject: in some cases revealing relatively well separated and symmetrical reversals over the lateral aspect of the scalp, and in other cases indicating more medially positioned reversals with strong attenuation of the medially located maxima. However, it was possible to achieve dipole fits to similar cortical locations for these reversals, regardless of the degree of their asymmetry, if two bilateral dipoles were fitted simultaneously. These observations indicate that it is important to consider possible interactions of fields from multiple sources when interpreting movement-related field patterns recorded near the vertex, particularly if measurements are restricted to one hemisphere.

Dipole source analysis for the motor field MF (considered most likely to represent the final motor outflow of the pyramidal system prior to muscle contraction) was conducted using a hypothesis of bilaterally symmetrical generators located in both primary motor cortices (MI). With this model it was possible to explain a high degree of variance in the data as indicated by the high goodness of fit and stable dipole locations across subjects. Cheyne and Weinberg (1989) also located bilateral generators prior to unilateral index finger flexions but with inconsistent location of the ipsilateral source, indicating that differences in spatial sampling or signal-to-noise ratio, or in task performance might be critical for identification of ipsilateral sources. The current dipole sources in both hemispheres were of opposite orientation to that predicted from volume currents associated with surface negativity of the precentral gyrus, thought to be responsible for movement-preceding negativity at the scalp (cf., Deecke 1987; Neshige et al. 1988), consistent with the concept that magnetic fields at the scalp surface reflect primarily intracellular current (Hari et al. 1980). These sources may thus reflect synaptic activation within the superficial cortical layers of area 4 situated within the anterior bank of the central sulcus, producing intracellular currents in pyramidal cells oriented tangentially to the scalp surface (Cheyne and Weinberg 1989). Thus, MRMFs preceding voluntary movement seem primarily to reflect activation of the primary motor cortex MI, although it is not known to what extent co-activation of PTNs in post-central cortex, which are also known to be active prior to voluntary movements (Pieper et al. 1980; Fromm and Evarts 1982), may also contribute to these fields.

One of the main indications of the dipole source analysis was that ipsilateral activation of MI differed from that of contralateral activation prior to unilateral movements. This is based on the observation that, (1) the positions of the pre-movement sources were similar contralaterally for both unilateral and bilateral movements, but differed ipsilaterally for unilateral movement (being somewhat deeper), and (2) the strength (current density) for the contralateral source was significantly higher than that of the ipsilateral source for unilateral movements. Note that this difference not only reflects the stronger or weaker activation of the corresponding cortical area but also a difference in the nature of ipsilateral MI activation, as indicated by the change in source location. Dipole strength and position for a given hemisphere did not differ significantly depending upon whether the movement was performed unilaterally (contralateral) or bilaterally, indicating similar MI activation patterns in both cases, this being in agreement with reports of similar (contralateral) precentral PTN firing rates in monkeys for both unilateral and bilateral movements (Tanji et al. 1987). It has been previously speculated that variability in ipsilateral source location for unilateral movements may reflect less focal activation within the ipsilateral sensorimotor cortex (Cheyne 1988; Cheyne and Weinberg 1989). Since multiple dipoles or tangentially oriented dipole layers will tend to be "seen" as a single dipole with an over-estimation of depth by some number of millimeters due to dispersion of the field maxima (Okada 1985), the observation of somewhat deeper locations (8–10 mm) of the ipsilateral sources in the present study is consistent with an extended source in the tangential direction. This effect could be explained in 2 ways: either in terms of a less focal or multiple-source nature of inhibitory processes occurring in the ipsilateral motor cortex, or as due to less specific (less somatotopically organized) activation of the ipsilateral motor cortex over many repetitions of the movement (i.e., either widespread activation within a specific area or non-stationarity of a spatially restricted source over time). More detailed studies may be necessary to determine the exact nature of the ipsilateral generators prior to unilateral movements.

Bilateral organization of unilateral voluntary movement. The observed bilaterality of the pre-movement fields in the present study confirms the observations of Cheyne and Weinberg (1989) and supports the idea of bilateral generators for the pre-movement brain poten-

tials (*Bereitschaftspotential*) prior to unilateral movements, as initially proposed by Kornhuber and Deecke (1965; see also Kristeva et al. 1979). Intracortical recording of brain activity in non-human primates (Evarts 1966; Hashimoto et al. 1979; Tanji 1987) and epicortical recording in humans (Goldring and Ratcheson 1972; Neshige et al. 1988) have also shown bilateral generators in sensorimotor cortex prior to movement onset. This bilateral activation of the primary motor cortices prior to unilateral movement is interesting in many regards and indicates that both unilateral and bilateral movements may involve to some extent bilateral preparation in cerebral motor systems.

The above speculations are congruent with theories of inhibition of ipsilateral motor system activity during the preparation for unilateral movement, an idea proposed by Walshe as early as 1948, and supported by the observations of involuntary "mirror" movements which are known to occur during development of motor systems in childhood prior to full myelination of the cortico-spinal tract (Connoly and Stratton 1961) and which are also observed in adults during movement-related tasks (Cernacek 1961; Basmajian 1962; Hopf et al. 1974; Kristeva et al. 1979). Such organizational principles could explain the observation of ipsilateral magnetic fields prior to and during instructed unilateral voluntary movements. Although the presence of ipsilateral EMG activity was considered not to play a significant role in the occurrence of ipsilateral magnetic fields by Cheyne and Weinberg (1989), our observation of mirror activity in the EMG records of all subjects requires greater attention to this issue. One explanation for such mirror movement activity offered by Cernacek (1961) and by Basmajian (1962), is that mirror movements constitute a physiological phenomenon dependent upon decreased arousal or fatigue which results in insufficient pyramidal system inhibition of the ipsilateral musculature. In this regard, we also noted increased mirror activity towards the end of long recording sessions, suggesting that, when the subject gets tired he or she is unable to inhibit the finger which is not supposed to be moved. However, it is not yet possible to explain the nature of the observed non-linearity between the amplitude of the ipsilateral field (for unilateral movements) and the amount of registered mirror EMG activity within the context of the present study.

One alternative hypothesis for the occurrence of ipsilateral magnetic fields prior to movement involves the role of the non-crossed portion of the cortico-spinal tract (Brodal 1981) in the control of the ipsilateral musculature but, as found by Brinkman and Kuypers (1973) in split-brain rhesus monkeys, this ipsilateral control appeared strongest for axial and proximal musculature and weakest for individual finger movements, in agreement with Brodal's (1973) statement that the innervation of the distal musculature has contralateral origin. Since the present study involved only distal movements performed in a relatively isolated manner (and it can be assumed that postural changes would have been minimal since subjects were highly immobilized), this type of ipsilateral control may not have had a major influence.

One observation in the topographical analysis of pre-movement MRMFs was that for non-dominant left-sided movement they were more similar to those for bilateral movements than for dominant right-sided movements, indicating that cerebral dominance factors may also play a role in MI activational patterns. Thus, the LH pattern was more similar to the BH pattern than the RH pattern (e.g., comparing the MF for the 3 movement conditions as shown in Figs. 5 and 6). Lateralization of the dipole strengths also tended to be slightly greater for right finger movements compared to left, although these differences were not statistically significant. The issue of lateralization of movement-related activity for dominant and non-dominant sided movements is unclear although observed in a number of movement-related potential studies (Boschert and Deecke 1986; Uhl et al. 1988 for BP and Lang et al. 1990 for performance-related negativity). However, movement-related magnetic fields may provide a better estimate of lateralization of MI activity, independent of volume conduction effects.

Pre-motor and supplementary motor cortex activation. It is well known that in addition to primary motor cortex, both pre-motor and supplementary motor areas are active prior to, and play an important role in, voluntary movement. It is known from MRP data that the Bereitschaftspotential has its earliest onset and largest amplitude over the anterior midline and appears to arise from midline structures such as the SMA (Deecke and Kornhuber 1978; Kristeva and Deecke 1980; Deecke et al. 1985). This and evidence from other measures of brain activity (reviewed in Goldberg 1985) indicate bilateral activation of the supplementary motor area (SMA) prior to voluntary movement. The fact that very little magnetic field activity was observed over the frontal midline prior to unilateral or bilateral voluntary movements in the present study is at first puzzling. However, an explanation proposed by Cheyne (1988; see also Cheyne and Weinberg 1989) suggested that if both SMA cortices are active prior to movement onset, this would produce 2 equivalent current dipoles of opposing orientations within the mesial cortical surfaces of both hemispheres, resulting in overlapping fields of opposite direction over the midline. The opposing direction of these fields (which would be relatively weak due to the greater depth of sources within the interhemispheric fissure) would thus tend to cancel, making the observation of these generators difficult. (A recent observation in our laboratory of pre-movement MEG fields over the anterior midline in a patient having a unilateral

lesion of the SMA tends to confirm this hypothesis and will be reported elsewhere.)

The absence of magnetic fields which appear to arise from pre-motor areas is also not yet clear, since such areas may also be active prior to movement (Roland 1987) and, in particular, may encode aspects of unilaterality or bilaterality of movement execution (Tanji 1987; Tanji et al. 1987). At present, it can only be speculated that if such cortical sources were radial in orientation they may not be observed in the magnetic field records restricted to observation of tangentially oriented currents.

(II) Neuromagnetic fields during movement

In the present study, 4 components following the onset of electromyographic activity were observed. The first 3 formed a triphasic pattern which occurred during the movement itself and were labelled "movement-evoked fields" (MEFs) I, II and III. The first and largest event, MEFI, was observed in all subjects and its generator was localized slightly posterior and deeper to the contralateral generator of the RF and MF for unilateral movements, similar to the "movement-evoked field" described by Cheyne and Weinberg (1989). The generator of the MEFI could be described by an equivalent dipole of greater strength in comparison to the generator of MF and directed posteriorly, suggestive of current flow directed away from the posterior bank of the central sulcus. The location of this dipole suggests that it could reflect reafferent activity from the periphery to somatosensory areas (e.g., areas 3a and 3b) as suggested by Cheyne and Weinberg (1989), although these authors also provided evidence that precentral sources may remain active during this time period as well, in agreement with reported afferent input to motor cortex in monkeys during movement (Wiesendanger and Miles 1982).

It is important to note that, in the present study, the MEFI was observed *only* over the contralateral hemisphere for unilateral movements even though mirror EMG activity was observed during these movements. This could mean that the amount of reafferent input from the mirror motor activity was of insufficient strength to produce a clear movement-evoked response, consistent with the fact that mirror EMG activity did not involve observable movement of the ipsilateral fingers implying minimal input from muscle afferents. An alternative explanation is that this response reflects internal (e.g., cortico-cortical) monitoring of the movement which is expected or *intended* (subjects reported not to be consciously aware of the mirror movements) also resulting in less activation of the ipsilateral sensorimotor areas.

The MEFII which was observed at a latency of 225 msec after movement onset had a similar pattern to the RF and MF but a different orientation, suggesting activation of a neuronal population in precentral gyrus different from that for the MF, although significant dipole fits were not achieved. The third post-movement component, MEFIII, appeared at a post-EMG onset latency of approximately 320 msec and had a topography similar to that of the MEFI, suggesting new or continued reafferent input to the post-central gyrus. One hypothetical explanation of this observed sequence of MEF patterns could be as follows: (i) initial input to post-central gyrus (SI) from muscle afferents due to digit flexion, producing the large MEFI response, followed by (ii) additional precentral gyrus activation (motor command for finger extension?) which overlaps in time with the continued input to SI, producing the slightly more complex patterned MEFII, and (iii) renewed reafferent input to SI due to digit extension which produces MEFIII, with a similar topography to MEFI. Thus, the triphasic field pattern accompanying the present movement task probably reflects the complex input-output organization of the sensorimotor cortex related to control and monitoring of the movement in progress. In future studies, observed changes in these patterns accompanying changes in physical parameters of the movement (e.g., force, duration) as well as changes in motor performance or accuracy could provide useful information regarding the role of cortical control in the learning of motor skills. However, in should be noted that these later components (e.g., MEFII) probably reflect the simultaneous activation of neuronal populations in both pre- and post-central cortex and the use of more sophisticated dipole modelling procedures capable of separating temporally overlapping sources is indicated.

The fourth post-EMG onset component observed in the present motor task had an unclear relationship to the movement performed since it occurred at latencies following completion of the movement itself and was termed simply "post-movement field" (PMF). Its very similar topography to the RF, however, suggests similar activity in primary motor cortex although of lower intensity. This activity would appear to occur too late to constitute a type of "corollary discharge" to be used during the motor planning and execution phase (e.g., in order to monitor finger position), but rather, might play a more important role in learning the motor task in terms of updating representations within motor cortex or monitoring the resting finger position after completion of the movement task. The relationship between the occurrence of this field and changes in strategy or accuracy of movement performance also warrants further study.

The present study indicates that magnetic field recording of movement-related brain activity can be used to help elucidate many processes related to bilateral organization of voluntary movements previously studied

by means of movement-related brain potentials. Although the MEG technique provides much new information about generators within sensorimotor cortex, many limitations were also noted, including the need to combine data from different experimental sessions (since the entire scalp surface could not be mapped simultaneously) resulting in variation in both physical parameters of movement execution as well motivational and attentional factors and additionally, the inability to record significant MEG activity in the movement foreperiod related to early movement preparation. The future ability to combine multi-channel MEG recording with studies of movement-related potentials (particularly those employing reference-free or source analysis techniques) may provide the most powerful tool for the non-invasive study of cerebral organization of unilateral and bilateral voluntary movements.

The first author was supported by an IBRO/UNESCO Research Fellowship and the second author by an NSERC of Canada Postdoctoral Fellowship.

The authors wish to express their thanks to Gerald Lindinger, Dipl. Eng. for technical support and to Dr. Christoph Baumgartner for critical reading of the manuscript.

References

Arezzo, J. and Vaughan, H.G. Cortical sources and topography of the motor potential and the somatosensory evoked potential in the monkey. In: H.H. Kornhuber and L. Deecke (Eds.), Motivation, Motor and Sensory Processes of the Brain. Prog. Brain Res., Vol. 54. Elsevier, Amsterdam, 1980: 77–83.

Basmajian, J.V. Muscles Alive, their Functions Revealed by Electromyography. Williams and Wilkins, Baltimore, MD, 1962.

Boschert, J. and Deecke, L. Handedness, footedness, and finger and toe movement-related cerebral potentials. Hum. Neurobiol., 1986, 5: 235–243.

Brinkman, J. and Kuypers, H.G.J.M. Cerebral control of contralateral and ipsilateral arm, hand and finger movements in the split-brain rhesus monkey. Brain, 1973, 96: 653–674.

Brodal, A. Self-observations and neuro-anatomical considerations after a stroke. Brain, 1973, 96: 675–694.

Brodal, A. Neurological Anatomy in Relation to Clinical Medicine, 3rd edn. Oxford University Press, New York, 1981.

Brunia, C.H.M. Movement and stimulus preceding negativity. Biol. Psychol., 1988, 26: 165–178.

Cernacek, J. Contralateral motor irradiation — cerebral dominance: its changes in hemiparesis. Arch. Neurol., 1961, 4: 165–172.

Cheyne, D. Magnetic and electric field measurements of brain activity preceding voluntary movements: implications for supplementary motor area function. Unpublished doctoral dissertation. Simon Fraser University, Burnaby, Canada, 1988.

Cheyne, D. and Weinberg, H. Neuromagnetic fields accompanying unilateral finger movements: pre-movement and movement-evoked fields. Exp. Brain Res., 1989, 78: 604–612.

Cheyne, D., Kristeva, R. and Deecke, L. Homuncular organization of human motor cortex as indicated by neuromagnetic recordings. Neurosci. Lett., 1991, 122: 17–20.

Connoly, K. and Stratton, P. Developmental changes in associated movements. Dev. Med. Child Neurol., 1968, 10: 49–56.

Deecke, L. Bereitschaftspotential as an indicator of movement preparation in supplementary motor area and motor cortex. In: R. Porter (Ed.), Motor Areas of the Cerebral Cortex. Ciba Foundation Symposium 132. Wiley, Chichester, 1987: 231–250.

Deecke, L. and Kornhuber, H.H. An electrical sign of participation of the mesial "supplementary" motor cortex in human voluntary finger movements. Brain Res., 1978, 159: 473–476.

Deecke, L., Scheid, P. and Kornhuber, H.H. Distribution of readiness potential, pre-motion positivity, and motor potential of the human cerebral cortex preceding voluntary finger movements in humans. Exp. Brain Res., 1969, 7: 158–168.

Deecke, L., Grözinger, B. and Kornhuber, H.H. Voluntary finger movements in man: cerebral potentials and theory. Biol. Cybern., 1976, 23: 99–119.

Deecke, L., Weinberg, H. and Brickett, P. Magnetic fields of the human brain accompanying voluntary movements: Bereitschaftsmagnetfeld. Exp. Brain Res., 1982, 48: 144–148.

Deecke, L., Kornhuber, H.H., Lang, W., Lang, M. and Schreiber, H. Timing function of the frontal cortex in sequential motor and learning tasks. Hum. Neurobiol., 1985, 4: 143–154.

Evarts, E.V. Pyramidal tract activity associated with a conditioned hand movement in the monkey. J. Neurophysiol., 1966, 29: 1011–1027.

Fromm, C. and Evarts, E.V. Pyramidal tract neurons in somatosensory cortex: central peripheral inputs during voluntary movement. Brain Res., 1982, 238: 186–191.

Goldberg, G. Supplementary motor area structure and function: review and hypothesis. Behav. Brain Sci., 1985, 8: 567–616.

Goldring, S. and Ratcheson, R. Human motor cortex: sensory input data from single neuron recordings. Science, 1972, 175: 1493–1495.

Halsey, Jr., J.H., Blauenstein, U.W., Wilson, E.M. and Wills, E.H. Regional cerebral blood flow comparison of right and left hand movement. Neurology, 1979, 29: 21–28.

Hari, R., Aittoniemi, K., Järvinen, M.-L., Katila, T. and Varpula, T. Auditory evoked transient and sustained magnetic fields of the human brain. Exp. Brain Res., 1980, 40: 237–240.

Hari, R., Antervo, A., Katila, T., Poutanen, T., Seppänen, M., Tuomisto, T. and Varpula, T. Cerebral magnetic fields associated with voluntary limb movements. Nuova Cimento, 1983, 2D: 484–494.

Hashimoto, S., Gemba, H. and Sasaki, K. Premovement slow cortical potentials and required muscle force in self-paced hand movements in the monkey. Brain Res., 1980, 197: 415–423.

Hopf, N.S., Schlegel, N. and Lowitzsch, K. Irradiation of voluntary activity to the contralateral side in movements of normal subjects and patients with cerebral motor disturbances. Eur. Neurol., 1974, 12: 142–147.

Kornhuber, H.H. and Deecke, L. Hirnpotentialänderungen bei Willkürbewegungen und passiven Bewegungen des Menschen: Bereitschaftspotential und reafferente Potentiale. Pflügers Arch., 1965, 284: 1–17.

Kristeva, R. and Deecke, L. Cerebral potentials preceding right and left unilateral and bilateral finger movements in sinistrals. In: H.H. Kornhuber and L. Deecke (Eds.), Motivation, Motor and Sensory Processes of the Brain. Prog. Brain Res., Vol. 54. Elsevier, Amsterdam, 1980: 748–754.

Kristeva, R., Keller, E., Deecke, L. and Kornhuber, H.H. Cerebral potentials preceding unilateral and simultaneous bilateral finger movements. Electroenceph. clin. Neurophysiol., 1979, 47: 229–238.

Kristeva, R., Cheyne, D., Lang, W., Lindinger, G. and Deecke, L. Movement-related potentials accompanying unilateral and bilateral finger movements with different inertial loads. Electroenceph. clin. Neurophysiol., 1990, 75: 410–418.

Kutas, M. and Donchin, E. The effect of handedness, the responding hand, and response force on the contralateral dominance of the readiness potential. Science, 1974, 186: 545–548.

Lang, W., Obrig, H., Lindinger, G., Cheyne, D. and Deecke, L. Supplementary motor activation while tapping bimanually different rhythms in musicians. Exp. Brain Res., 1990, 79: 504–514.

Neshige, R., Lüders, H. and Shibasaki, H. Recording of movement-related potentials from scalp and cortex in man. Brain, 1988, 111: 719–736.

Okada, Y. Discrimination of localised and distributed current dipole sources and localised single and multiple sources. In: H. Weinberg, G. Stroink and T. Katila (Eds.), Biomagnetism: Applications and Theory. Pergamon Press, Toronto, 1985: 266–272.

Oldfield, R.C. The assessment and analysis of handedness. The Edingburgh inventory. Neuropsychologia, 1971, 9: 97–113.

Pieper, C.F., Goldring, S., Jenny, A.B. and McMahon, J.P. Comparative study of cerebral cortical potentials associated with voluntary movements in monkey and man. Electroenceph. clin. Neurophysiol., 1980, 48: 266–292.

Requin, J. Looking forward to moving soon: antefactum selective processes in motor control. In: M.I. Posner and O. Marin (Eds.), Attention and Performance XI. Erlbaum, Hillsdale, NJ, 1985: 147–167.

Roland, P.E. Cortical organization of voluntary behaviour in man. Hum. Neurobiol., 1985, 4: 155–167.

Romani, G.L. and Rossini, P. Neuromagnetic functional localization: principles, state of the art, and perspectives. Brain Topog., 1988, 1: 5–21.

Shibasaki, H., Barrett, G., Halliday, A.M. and Halliday, E. Scalp topography of movement-related cortical potentials. In: H.H. Kornhuber and L. Deecke (Eds.), Motivation, Motor and Sensory Processes of the Brain. Prog. Brain Res., Vol. 54. Elsevier, Amsterdam, 1980: 237–242.

Tanji, J. Neuronal activity in the primate non-primary cortex is different from that in the primary motor cortex. In: R. Porter (Ed.), Motor Areas of the Cerebral Cortex. Ciba Foundation Symposium 132. Wiley, Chichester, 1987: 142–146.

Tanji, J., Okano, K. and Sato, K.C. Relations of neurones in the non-primary motor cortex to bilateral hand movements. Nature, 1987, 327: 618–619.

Uhl, F., Lang, W., Lang, M., Kornhuber, A. and Deecke, L. Cortical slow potentials in verbal and spatial tasks — the effect of material, visual hemifield and performing hand. Neuropsychologia, 1988, 26: 769–775.

Vaughan, Jr., H.G., Costa, L.D. and Ritter, W. Topography of the human motor potential. Electroenceph. clin. Neurophysiol., 1968, 25: 1–10.

Weinberg, H., Brickett, P., Deecke, L. and Boschert, J. Slow magnetic fields of the brain preceding movements and speech. Nuovo Cimento, 1983, 2D: 495–504.

Wiesendanger, M. and Miles, T.S. Ascending pathway of low-threshold muscle afferents to the cerebral cortex and its possible role in motor control. Physiol. Rev., 1982, 62: 1234–1270.

Williamson, S.J. and Kaufmann, L. Magnetic fields of the cerebral cortex. In: S.N. Erne, H.D. Hahlbohm and H. Lübbig (Eds.), Biomagnetism. Walter de Gruyter, Berlin, 1981: 353–402.

ELSEVIER

Electroencephalography and clinical Neurophysiology 95 (1995) 323–334

ISSN 0924-980X

Movement-related potentials associated with bilateral simultaneous and unilateral movements recorded from human supplementary motor area

Akio Ikeda [a,*], Hans O. Lüders [b], Hiroshi Shibasaki [a], Thomas F. Collura [b], Richard C. Burgess [b], Harold H. Morris III [b], Toshiaki Hamano [b]

[a] *Department of Brain Pathophysiology, Kyoto University School of Medicine, Shogoin, Sakyo-Ku, Kyoto 606, Japan*
[b] *Department of Neurology, The Cleveland Clinic Foundation, 9500 Euclid Avenue, Cleveland, OH 44106, USA*

Accepted for publication: 22 April 1995

Abstract

To clarify the differences of movement-related potentials (MRPs) among ipsilateral, contralateral and simultaneous bilateral movements, MRPs with finger, thumb or foot movements were recorded from subdural electrodes chronically implanted on the supplementary motor area (SMA) in 3 patients, and also from the primary sensorimotor area in two of them being evaluated for epilepsy surgery. As a result: (1) SMA generated clear pre-movement potentials regardless of the type of movement. Its amplitude was almost identical between contralateral and bilateral movements except for the motor potential (MP). The pre-movement potentials associated with ipsilateral movements were relatively smaller than those with contralateral or bilateral movements. (2) The primary sensorimotor area generated clear pre-movement potentials in contralateral and bilateral movements with similar amplitude. With ipsilateral hand movements, however, only a small Bereitschaftspotential (BP) and no negative slope (NS') or MP was seen, and ipsilateral foot movements were not preceded by any BP. It is, therefore, most likely that, as far as the preparation for simple voluntary self-paced movement is concerned, the SMA plays an equally important role in unilateral and bilateral movements, whereas the primary sensorimotor area is involved predominantly in the preparation of contralateral movements.

Keywords: Bereitschaftspotential; Bilateral movements; Supplementary motor area

1. Introduction

The functional role of the supplementary motor area (SMA) in relation to the primary sensorimotor area is still debated. Namely, two hypotheses, i.e., "supramotor" and "supplementary" function have been proposed (Deecke et al., 1985; Goldberg, 1985; Wiesendanger, 1986; Wiesendanger et al., 1987). The "supplementary" function hypothesis speculates that the SMA and primary sensorimotor area are active in parallel with and complementary to each other in the programming, initiation and execution of the voluntary movements. This hypothesis was suggested when it was initially named so in humans (Penfield and Welch, 1951; Woolsey et al., 1952), and subsequently it has been supported not only by clinical observations but also by experimental animal studies (Penfield and Jasper, 1954; Laplane et al., 1977; Fox et al., 1985; Schell et al., 1986; Hyland et al., 1989; Alexander and Crutchler, 1990a,b; Crutchler and Alexander, 1990; Chen et al., 1991; Schmidt et al., 1992). The "supramotor" function hypothesis, on the other hand, speculates that the SMA initiates and regulates voluntary movements contributing to the generation of a new motor program and to the control of the execution of established movements (Eccles, 1982; Goldberg, 1985). This idea was supported by cerebral blood flow studies in human (Orgogozo and Larsen, 1979; Roland et al., 1980; Rao et al., 1993) and by experimental animal studies (Tanji and Kurata, 1982, 1985a,b; Tanji et al., 1987, 1988; Matsuzaka et al., 1992).

Damage to the SMA in humans initially produces reduced spontaneous speech, akinesia and slowness of repetitive or alternating movements of the upper limb contralateral to the SMA lesion (Penfield and Jasper, 1954; Laplane et al., 1977; Schell et al., 1986; Rostomily et al., 1991),

* Corresponding author. Tel.: +81-75-751-3603; Fax: +81-75-751-3202.

SSDI 0013-4694(95)00086-0

EEG 94105

but those symptoms recover in several weeks. Eventually, only slowness, mainly involving the opposite extremities, and difficulties in bimanual motor performances as well as in rapid alternating movements remained. Similar observations were also made on lesion studies in monkeys. Transient neglect of the contralateral arm and impairment of smooth movements (Brinkman, 1984), severe difficulty of sequential movements (Halsband, 1983), and deficits in bimanual coordination (Brinkman, 1981,1984) were observed. Therefore, it is certain that the SMA has a significant role in preparation and/or execution of bilateral movements (Porter, 1990), although the question as to whether the SMA is upstream of or parallel to the primary motor area still remains unsolved.

In previous studies of movement-related potentials (MRPs) in which cortical potentials were directly recorded from human SMA with subdural electrodes in patients during preparation for epilepsy surgery, it was demonstrated that bilateral SMAs generated pre-movement potentials (Bereitschaftspotential: BP by Deecke et al., 1969 and negative slope: NS' by Shibasaki et al., 1980), even preceding unilateral simple movements (Ikeda and Shibasaki, 1992; Ikeda et al., 1992). Furthermore, potentials recorded subdurally from the human SMA preceding single unilateral movements were as large as those with repetitive unilateral movements (Ikeda et al., 1993). These results led us to the hypothesis that the SMA might play an equally significant role in preparation for simple and "complex" movements, provided that the motor task was unilateral.

As has been mentioned above, it is apparent that an SMA lesion permanently affects bimanual maneuvers as well as unilateral sequential movements. However, our previous invasive MRP studies did not give any clue to the question as to whether the SMA generates pre-movement potentials more actively in bilateral movements than in unilateral ones. Comparison of MRPs of the SMA between bilateral and unilateral movements would shed light on the SMA function, especially regarding the hypothesis that the SMA plays a more significant role in bilateral than in unilateral movements. Thus the present study is aimed at complementing our previous results for understanding human SMA function.

2. Materials and methods

2.1. Subjects

The data were obtained from 3 patients with a diagnosis of medically intractable partial epilepsy. All patients were evaluated for epilepsy surgery using chronically implanted subdural electrode grids according to the Cleveland Clinic Epilepsy Surgery Protocol (Morris, 1992). Invasive recording and electrical stimulation of the cortex were done with chronically implanted subdural electrode strips or grids (Hahn and Lüders, 1987). Each electrode was made of stainless steel, 3 mm in diameter, and the center-to-center interelectrode distance was 1 cm. This technique can help to identify (1) the extent of the epileptogenic region, and (2) the function of the cortex around the epileptogenic region (Lueders et al., 1982; Lüders et al., 1987). Informed consent was obtained from all patients following the procedures approved by the Institutional Review Board at the Cleveland Clinic Foundation.

Patient 1 was a 19-year-old right-handed woman with medically intractable partial seizures of unknown etiology since the age of 11 years, consistent with supplementary motor seizures (Morris et al., 1988). Her neurological examination was unremarkable. Bimanual alternating and unilateral sequential movements of the hand or foot were also normal. An MRI of the brain was normal. PET scan demonstrated hypometabolism at the left fronto-central area. The intracarotid sodium amobarbital (Wada) test demonstrated speech and memory dominance in the right hemisphere. The Wechsler Adult Intelligence Scale (WAIS) full-scale IQ was 87. For presurgical evaluation of the seizures, the patient had initially one 1×11 and one 1×4 subdural electrode strip at the left mesial fronto-central area, one 1×11 at the right mesial fronto-central area, and two 1×11 and one 1×4 at the left lateral frontal area. Seven days afterwards, two more 1×11 subdural electrode strips were added on the right mesial to lateral fronto-central region in order to localize the seizure focus. The 3 strips placed on the mesial areas are illustrated in Fig. 1.

Patient 2 was a 48-year-old right-handed man with medically intractable partial seizures since the age of 27 years, which always started with a sudden vibration-like pain in the left third to fifth fingers. The etiology was unknown. His neurological examination demonstrated dysesthesia in the left third to fifth fingers, and absent deep tendon reflexes throughout. Postictally, the patient demonstrated a transient weakness of those 3 fingers, but not in the thumb. Bimanual alternating and unilateral sequential movements of the hand or thumb were normal. An MRI of the brain was normal. The Wada test demonstrated that the left hemisphere was dominant for speech and that memory function was represented by each hemisphere independently. For presurgical evaluation of the seizures, the patient had an 8×8 subdural electrode grid at the right lateral fronto-parietal area and two 1×11 subdural electrode strips at the right mesial fronto-central area, as shown in Fig. 1.

Patient 3 was a 33-year-old right-handed man with medically intractable partial seizures of unknown etiology since the age of 12 years. Supplementary motor seizures were suspected. His neurological examination was normal, and bimanual alternating and unilateral sequential movements of the hand or fingers were normal. An MRI of the brain was normal. A PET scan demonstrated patchy hypometabolic areas in the right hemisphere. The Wada test demonstrated speech and memory dominance in the right

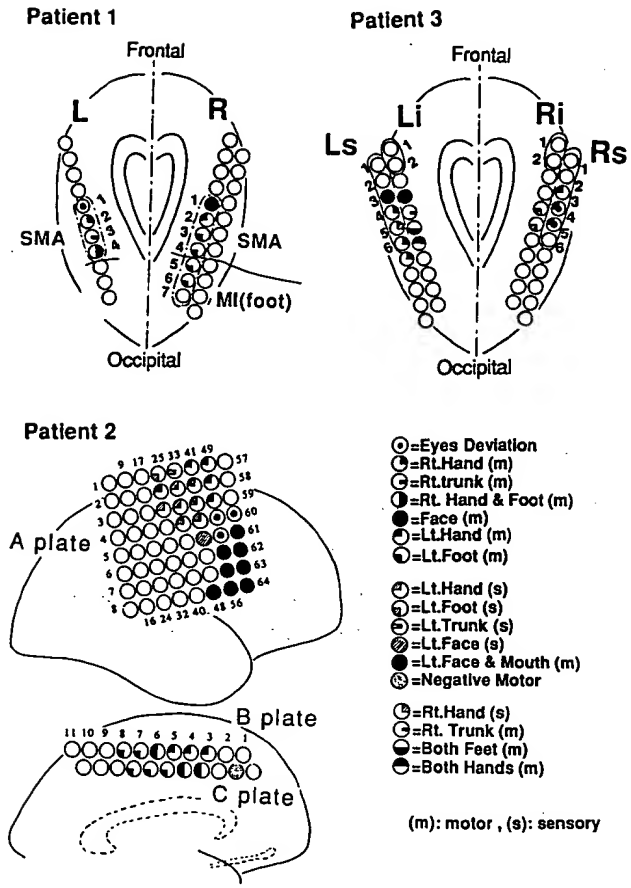

Fig. 1. Schematic representation of the placement of subdural electrode strips (patients 1, 2 and 3) and grid (patient 2). Each diagram shown was copied directly from the lateral view of an X-ray film and the sagittal views of MRI as described in Methods. The lines across the subdural electrode strips in patient 1 represent the location of the precentral sulcus. The site of the responses to electrical stimulation of each of the different implanted electrodes is indicated in the symbol in the figure. More details are given in the text.

and left hemispheres, respectively. WAIS full-scale IQ was 75. For surgical intervention of the seizures, the patient had a total of six 1 × 11 subdural electrode strips; two on each side of the bilateral mesial fronto-central areas, and one each at the left lateral frontal and parietal areas. The strips at the bilateral mesial fronto-central areas are illustrated in Fig. 1.

2.2. *Cortical stimulation and anatomical localization of the electrodes*

Each subdural electrode was individually stimulated to identify cortical function. Electrical currents were applied at progressively increasing intensity until (1) either movements or paresthesias were elicited, (2) after-discharges occurred, or (3) a maximum stimulus intensity of 15 mA was reached. Details of the stimulation methodology have been described elsewhere (Lüders et al., 1987; Lesser et al., 1992). It has been confirmed that the current spread to the adjacent or distant areas, which could lead to false positive findings, does not occur in this method (Lüders et al., 1987; Lesser et al., 1992; Nathan et al., 1993). Cortical regions at which stimulation elicited muscle contraction were identified as "positive motor area" (Lüders et al., 1985, 1988). The SMA was identified by its unique responses on the mesial surface as described by Penfield and Welch (1951), consisting of predominantly tonic positive motor responses of the upper as well as lower limb and of the trunk, neck and face, either unilaterally or bilaterally. Stimulation of some rostral parts of the SMA elicited negative motor responses affecting any part of the body.

The anatomical location of the subdural electrodes in the interhemispheric fissure was also assessed as follows, and it was taken into account when interpreting the functional mapping of the cortex by electrical stimulation as described above (Lim et al., 1994). A lateral view of the skull X-ray film, taken with subdural electrode grids or strips, was superimposed upon the sagittal view of the T1-weighted MRI image taken before surgery, using common landmarks (i.e., nasion and inion) by adjusting the size to each other.

2.3. *Movement paradigms*

Unilateral and bilateral voluntary movements of the foot were studied in patient 1, and those of the thumb and finger in patients 2 and 3. For unilateral foot movements in patient 1, the patient was laid in a supine position on a bed, and brisk extensions of an ankle joint, immediately followed by a return to the resting position by relaxing the dorsiflexed foot, were repeated at a self-paced rate of approximately once every 5 sec. This was done for the right and left foot movements separately, and for bilateral simultaneous movements.

For unilateral finger movements in patient 2, brisk voluntary abductions of the thumb at the metacarpophalangeal joint, immediately followed by a return to the resting position by relaxing the abducted thumb, were repeated at a self-paced rate of approximately once every 5 sec in a supine position. Like in the foot movements, the thumb movements as described above were executed unilaterally for each hand and bilaterally simultaneously. In patient 3, brisk voluntary extensions of the middle finger were employed for the movement and were also studied for unilateral and bilateral simultaneous movements.

The subject was told to keep quiet during each recording session and also asked to postpone the next task movement for several seconds if he accidentally moved prior to the task movement. Before recording sessions, the subject was given a training period until the examiner was satisfied that the subject consistently produced brisk movements preceded and followed by complete relaxation. One recording session typically lasted 5–6 min. The sessions of the left, right and bilateral movements were repeated in this order at least 3 times for each, with an intermission of a few minutes between sessions.

2.4. Recording of MRPs

Cortical recordings were done simultaneously from 66 to 86 subdural electrodes in each patient. All the recordings were performed in the Epilepsy Monitoring Unit concurrently with continuous video-EEG seizure monitoring (Burgess, 1992; Collura et al., 1992). For electromyogram (EMG) recording, a pair of cup electrodes were placed on the skin overlying the anterior tibial muscle for foot dorsiflexion (patient 1), abductor pollicis brevis muscle at the thenar eminence for thumb abduction (patient 2), and the extensor digitorum muscle in the forearm for middle finger extension (patient 3). All subdural electrodes were referenced to a scalp electrode over the left mastoid (TP7) in patient 1, one of the subdural electrodes over the lateral convexity in patient 2, and one subdural electrode over the mesial frontal area in patient 3. The reference subdural electrode did not elicit any symptom on stimulation and showed no ictal or interictal epileptiform discharges. All recorded potentials were led to two or three 32-channel EEG amplifiers (NEC San-ei BIOTOP) for amplification, filtering and simultaneous monitoring. Recording amplitude was set to 5 mV full-scale, 12 bits for the EEG, and 500 μV full-scale, 12 bits for the EMG. The low frequency filter (LFF) was set to 0.016 Hz for EEG recording and to 5 Hz for EMG recording. The high frequency filter (HFF) was set to 100 Hz for both EEG and EMG recordings. A 60 Hz notch filter was used in all channels. Signal monitoring with a non-fade graphic terminal at a sweep speed of 30 mm/sec was done throughout the examination. All of the above electrographic output signals were digitized by an analog-to-digital converter at a sampling rate of 200 Hz/channel, and stored on an HP9000/835 using 670 Mbyte disks for subsequent off-line analysis.

2.5. Data analysis

To average EEG signals time-locked to the onset of the movements of interest, computer programs adopting a concept originally described by Barrett et al. (1985) were developed. Visual inspection on an interactive graphics terminal permitted us to obtain essentially artifact-free epochs and allowed precise manual identification of the EMG onset of the trigger movements (Neshige et al., 1988; Ikeda et al., 1992, 1993). Movements which were not brisk enough to identify a clear EMG onset or movements associated with other recording artifacts were eliminated. Bilateral movements in which the difference of EMG onset between the two sides was more than 100 msec were also eliminated. Otherwise, a leading EMG onset of either side was taken as the fiducial point for averaging. A total of 123–163 epochs were selected for each trial. After confirming that two ensemble averaged EEGs of 61–81 epochs each were almost identical, a grand averaged EEG was finally made. All analysis epochs began 3000 msec before and ended 2000 msec after the time-locking fiducial EMG onset. Computer-assisted methods were used to measure time intervals and amplitudes, based on the calibration data obtained during data collection. The baseline was derived from the average of the segment from 3000 to 2500 msec before the trigger point for each channel. For the terminology of components of the subdurally recorded potentials in the present study, the conventional one used for the scalp-recorded MRPs was adopted except for the polarity; Bereitschaftspotential (BP) was defined as a slow, usually negative, shift which started about 1.5–2 sec before the EMG onset and gradually increased in amplitude (Kornhuber and Deecke, 1965). The steeper potential following the BP, starting about −300 msec to the EMG onset, was defined as negative shift (NS′) (Shibasaki et al., 1980; Barrett et al., 1986). The much steeper potential following the NS′, starting about −100 to −50 msec to the EMG onset, was defined as a motor potential (MP) (Deecke et al., 1969; Shibasaki et al., 1980).

3. Results

3.1. Cortical mapping (Fig. 1)

Cortical mapping of the mesial brain surface was based on the results of electrical stimulation and on the anatomical location of the electrodes. The results of electrical stimulation are illustrated in Fig. 1.

In patient 1, the nearly horizontal lines across the electrode strips indicate the location of the precentral sulcus. Stimulation at R5 elicited clonic movements at the left ankle, while stimulation at R2, R3 and R4 elicited tonic posturing with flexion of the right hip and knee and inversion of the right ankle at the same time. The precentral sulcus was located between R4 and R5. It was concluded, therefore, that the SMA was located at and anterior to R4, and the primary motor foot area was located at and posterior to R5. The anterior part of the SMA demonstrated positive motor responses in the arm and face. Antero-posterior somatotopy, as previously reported in the human SMA (Fried et al., 1991; Lim et al., 1994), was observed. In patient 2, stimulation of the right mesial fronto-central subdural electrodes elicited mainly positive motor responses as illustrated in Fig. 1. These motor responses were seen in the face, arm, trunk and bilateral feet. All these responses were typical SMA responses (Penfield and Welch, 1951) and also demonstrated somatotopy. Stimulation of the subdural grids at the right lateral convexity elicited a somatotopic representation of the primary sensorimotor cortex along the central sulcus. In patient 3, stimulation of bilateral subdural strip electrodes elicited a somatotopic representation in the SMA which was similar to that seen in the two other patients.

3.2. Movement-related potentials

Unilateral movements

Fig. 2a demonstrates MRPs associated with left foot movements recorded subdurally from the left and right mesial brain surfaces in *patient 1*. On the mesial surface contralateral to the movements (right hemisphere), a clearly defined positive BP started at about −2600 msec at both SMA foot areas (R3) and primary motor foot areas (R5). The BP at R3 gradually increased in amplitude until −60 msec (+55.5 μV), then it was followed by a slowly increasing negative deflection until +2000 msec. The positive BP at R5 was followed by a steeper negative deflection (NS′) at −400 msec, then turned into a much steeper negativity at −50 msec (MP). A clear transient negative activity started at +115 msec and peaked at +140 msec (reafferent potential: RAP by Kornhuber and Deecke, 1965). In the SMA ipsilateral to the movements (left SMA), a clearly defined positive BP started at about −2600 msec at L4 and L3, which was similar to that seen in the contralateral (right) SMA. The positive BP at L4 was stable in amplitude until the EMG onset (−28.8 μV), at which time a steeper positive deflection of 600 msec duration occurred. Otherwise no clear MP was seen, although a small negative shift was apparently seen at L3 and L2 from −400 msec to +2000 msec.

Fig. 2b demonstrates MRPs associated with the right foot movements recorded subdurally from the left and right mesial surface in *patient 1*. In the mesial surface ipsilateral to the movements (right hemisphere), a clearly defined positive BP started at about −1300 msec. It was seen at the SMA foot area (R3), but not at all at the primary motor foot area (R5). The BP at R3 gradually increased in amplitude and peaked at +65 msec (+36.1 μV), then it decreased in amplitude gradually over the following 2 sec. A clear negative transient activity started at +168 msec and peaked at +223 msec at R5. Otherwise no slow potentials were seen at R5 throughout. A smaller deflection which corresponded to the transient negative activity, as described above at R5, was also seen at R4. In the SMA contralateral to the movements (left SMA), a clearly defined positive BP started at about −2500 msec at L4 and L3. The overall distribution and wave forms of pre-and post-movement potentials at the left SMA (L4, L3 and L2) were almost identical between the left and right movements (Fig. 2a and 2b, respectively).

Fig. 3a demonstrates MRPs recorded from the right primary sensorimotor area and the right SMA in association with left thumb abduction in *patient 2*. At the primary sensorimotor area, a negative BP started at −2500 msec in the wider area along the central sulcus (A41, A45 and A49–51), and a steeper "negative" NS′ started at −500 msec in a more localized area (especially A43 and A41), at which electrical stimulation elicited either motor or sensory responses of the right hand. A positive NS′ was also seen at the hand sensory area (A35). At the right SMA, a BP started at −2200 msec at B3 and C4, and a clearly defined NS′ started at −500 msec mainly at the SMA hand area (B5, B4 and C6). MPs at the primary sensorimotor area and SMA were similar in amplitude (−51.1 μV at A43, and −57.1 μV at B5 at the EMG onset).

Fig. 3b demonstrates MRPs recorded from the right primary sensorimotor area and the right SMA in association with right thumb abduction in *patient 2*. At the primary sensorimotor area, a negative BP started at −2000 msec at a small number of electrodes (A50 and A41). No clear pre-movement potentials were seen at other electrodes (A43, A35, etc.) where the large BP, NS′ and MP were seen with the left thumb movements. Moreover, the BP was not followed by clear NS′ or MP. At the right SMA, on the contrary, a clearly defined, mostly negative BP/NS′ started at −2200 to −500 msec, mainly at the SMA hand area (B2–5, C3 and C4). The amplitude of BP and NS′ to right thumb movements was 50–60% of that elicited by left thumb movements (−24.0 μV and −40.7 μV, respectively, at B5 at −100 msec). MP elicited by right thumb movements starting at the EMG onset was ill defined as compared with left thumb movements.

In *patient 3*, in association with the right middle finger movements, a clear positive BP was seen at Rs4 (right SMA hand area). The BP started at about −1800 msec and gradually increased in amplitude until the EMG onset (+30.9 μV at Rs4). Small BP and NS′ were also seen at the adjacent electrodes (Rs3, Rs2, Rs5) as well as at the left SMA hand area (Ls4, Ls5). In association with left middle finger movements, pre-movement potentials were seen at the right and left SMA hand areas (Rs4, Ls4, Ls5). The wave form and amplitude of these potentials were similar to those elicited by right finger movements.

Bilateral movements

Fig. 2c demonstrates MRPs associated with simultaneous bilateral foot movements recorded subdurally from the left and right mesial brain surface in *patient 1*. In the right mesial area, the BPs at R3 (SMA foot area) and R5 (primary motor foot area) were almost identical to those with the left foot movements (Fig. 2a) in terms of wave form and amplitude. The post-movement potentials at R5 were also identical in bilateral and left foot movements (Fig. 2d). However, the MP at R3 (SMA foot area) started at −105 msec and became more positive with bilateral movements as compared with left foot movement. The MP peaked at +105 msec with an amplitude of +72.2 μV. Fig. 2d shows superimposed MRPs elicited by bilateral and left foot movements, demonstrating the similar BPs and significantly different MPs and post-movement potentials in the two movements.

In the left SMA, the pre-movement potentials with the bilateral foot movements were almost identical to those with either the left or right foot movements (Fig. 2c). However, the positive MP at L4, which started at the EMG

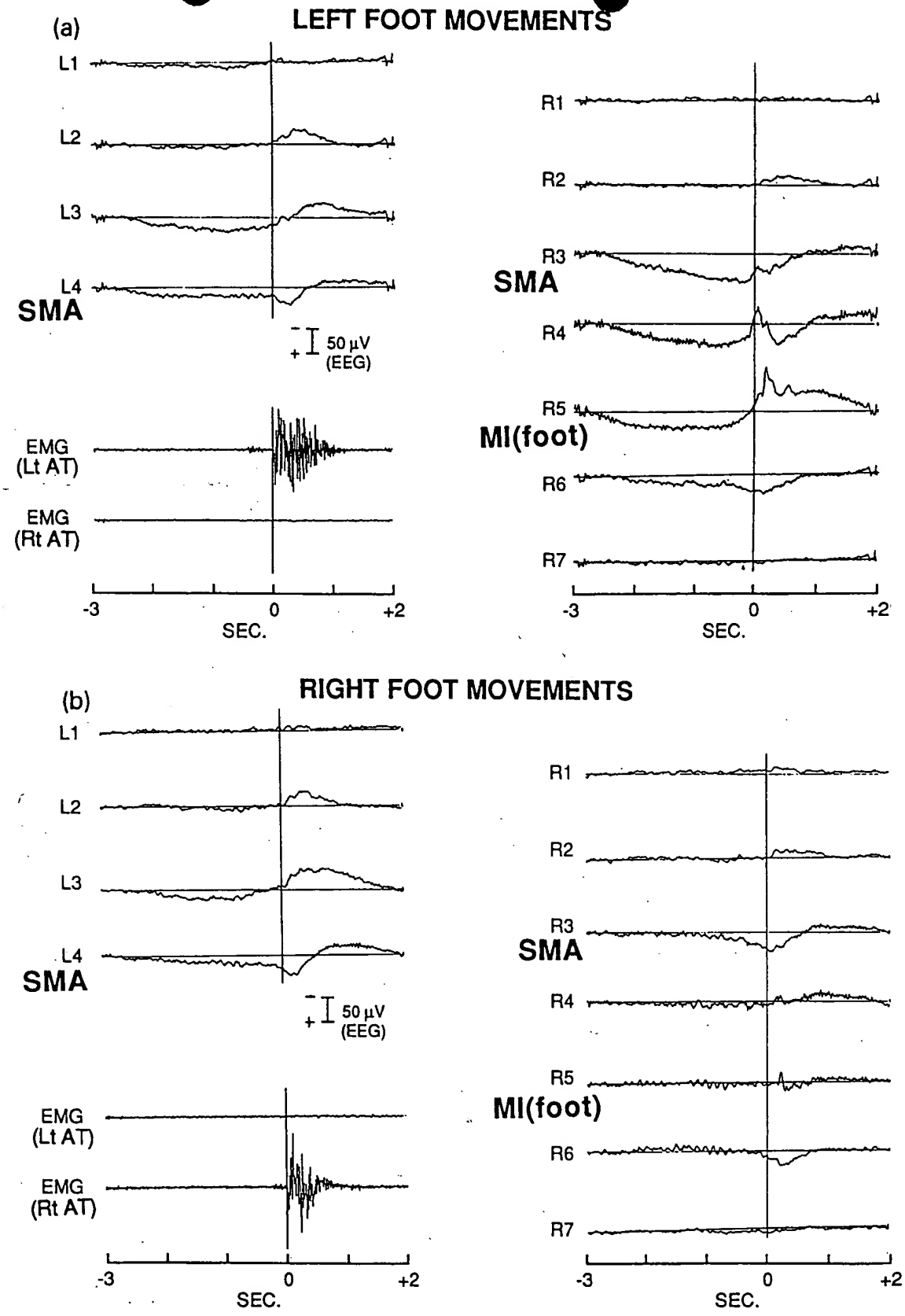

Fig. 2. Movement-related potentials (MRPs) recorded subdurally from both the left and right mesial brain surfaces in patient 1 in association with voluntary, self-paced, left (a), right (b) and bilateral simultaneous (c) foot dorsiflexions. Each electrode number corresponds to that in Fig. 1. Lt AT = left anterior tibial muscle; Rt AT = right anterior tibial muscle; SMA = supplementary motor area; MI = primary motor area.. a: average of 142 trials. b: average of 151 trials. c: average of 123 trials. d: superimposition of the averaged wave forms associated with the left foot (thin lines) and the bilateral foot (thick lines) movements.

onset, was larger (+55.5 μV at +110 msec) than that with the left (+28.8 μV at +110 msec) or the right (+38.8 μV at +110 msec) foot movements.

Fig. 3c demonstrates MRPs recorded from the right primary sensorimotor area and the right SMA in association with bilateral thumb abductions in *patient* 2. At the primary sensorimotor area, like in case of the left thumb movements (Fig. 3a), a negative BP started at −2500 msec at the primary hand sensorimotor area along the central sulcus (A41–43 and A49–51), and an NS′ started

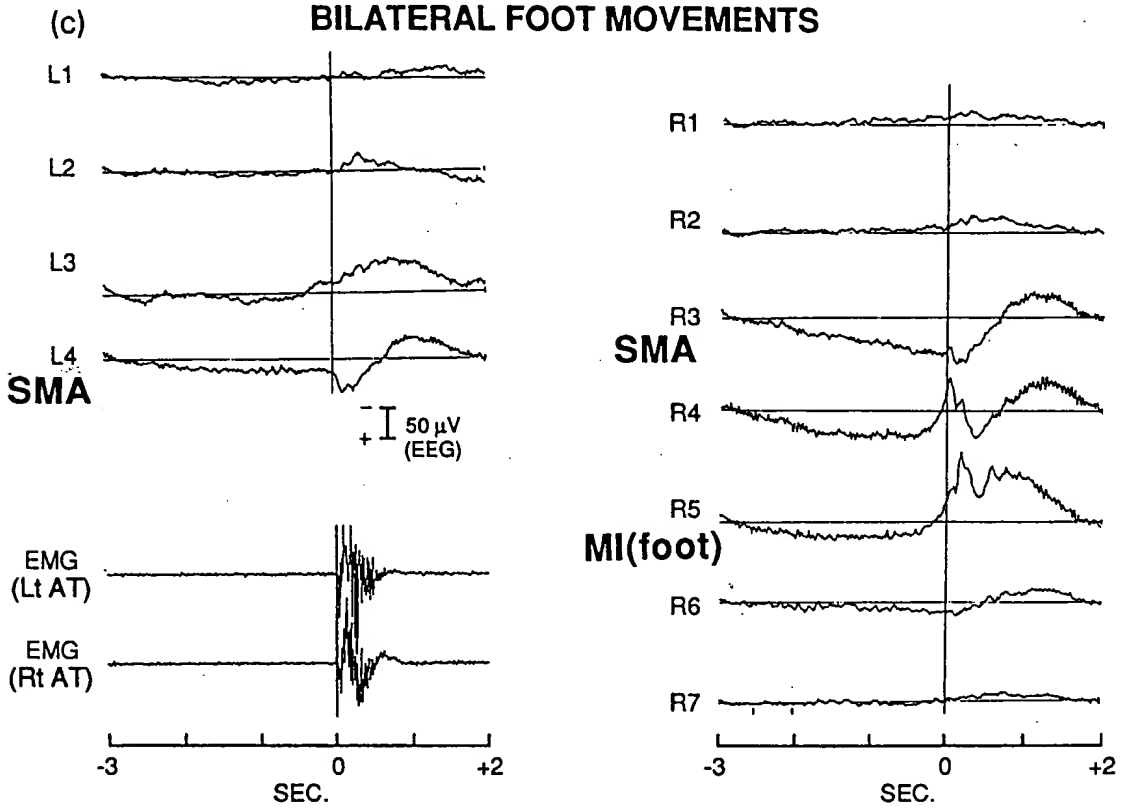

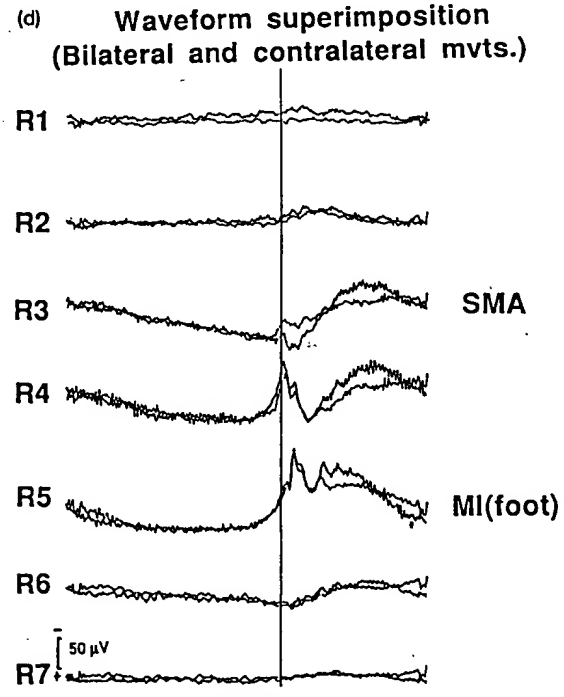

Fig. 2 (continued).

at −500 msec at a more localized area (A43 and A41). A positive NS′, as elicited also with left thumb movements, was present at the hand sensory area (A35). At the right SMA, as seen also with unilateral movements, a BP started at −2200 msec mainly at B3, and a clear NS′ started at −500 msec at the SMA hand area mainly at B5. The potentials at the primary sensorimotor area and at the SMA were similar in amplitude (−45.7 μV at A43, and −37.1 μV at B5 at the EMG onset). At B5, MP followed and peaked at +200 msec with an amplitude of −71.4 μV. It

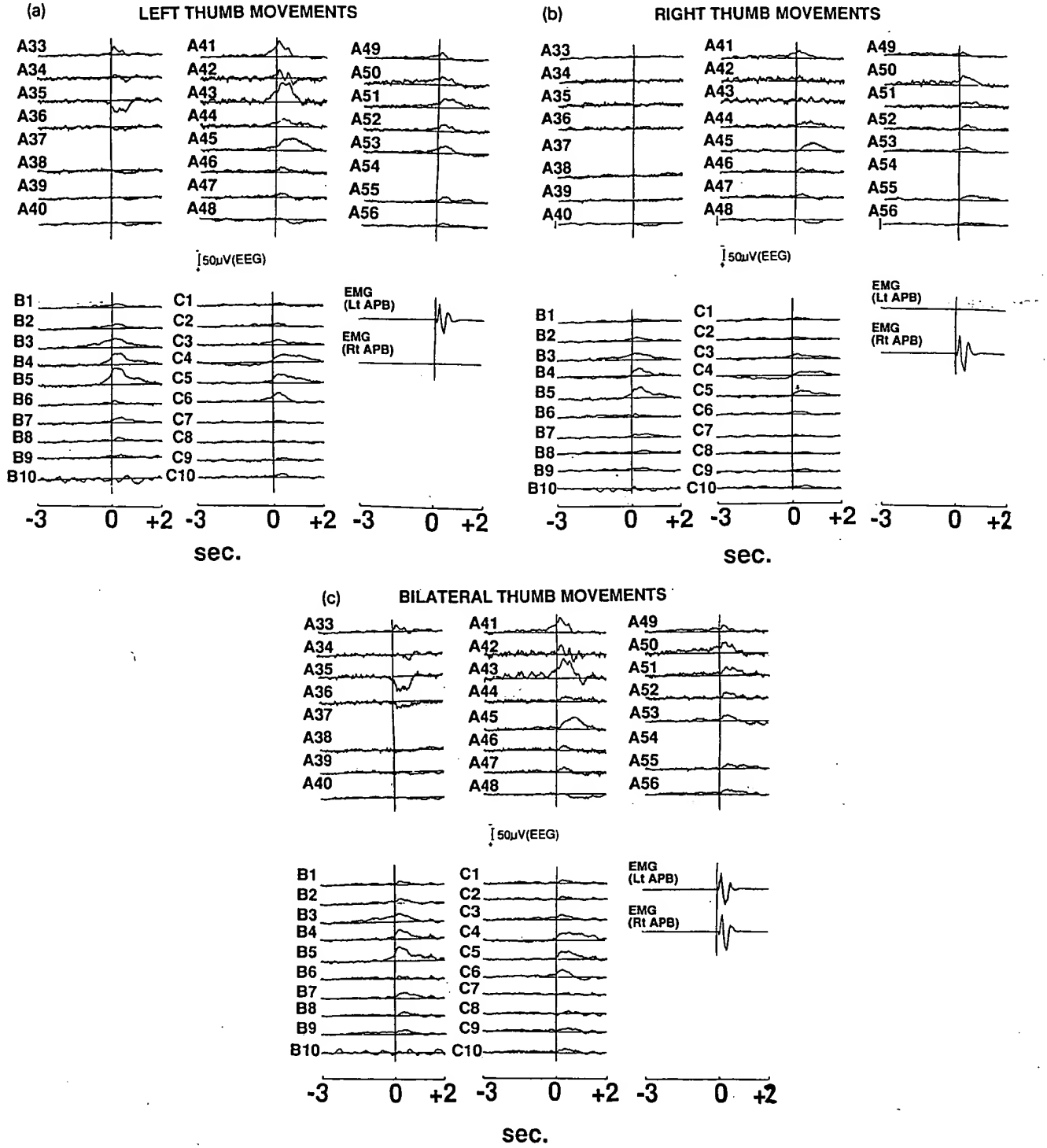

Fig. 3. MRPs subdurally recorded from the right primary hand sensorimotor area (upper panel: A33–A56) and the right SMA (lower panel: B1–10, C1–10) in patient 2 in association with voluntary, self-paced, left (a), right (b) and bilateral simultaneous (c) thumb abductions. Each electrode number corresponds to that in Fig. 1. Lt APB = left abductor pollicis brevis muscle; Rt APB = right abductor pollicis brevis muscle. a: average of 128 trials. b: average of 163 trials. c: average of 134 trials.

was larger than that elicited by the right thumb movements (−51.4 μV at B5), and similar to that elicited by left thumb movements (−80.0 μV at B5).

In *patient 3*, in association with bilateral finger movements, a clear positive BP was seen at Rs4 (right SMA hand area). The distribution, wave form and amplitude of pre- and post-movement potentials were similar in bilateral and unilateral movements (+28.1 μV and +30.9 μV with bilateral and left finger movements, respectively, at Rs4 at the EMG onset).

4. Discussion

The present study revealed mainly 2 findings about the SMA function for the initiation of voluntary movements, as compared with the primary sensorimotor area. (1) The SMA generated clear pre-movement potentials for either contralateral, ipsilateral or bilateral movements. BP and NS′ were almost identical for contralateral and bilateral movements, but MP was different between them. BP, NS′ and MP generated by ipsilateral movements were slightly smaller than those generated by contralateral or bilateral movements. (2) The primary sensorimotor cortex generated almost identical pre-movement potentials for contralateral and bilateral movements. However, it generated ill-defined pre-movement potentials for ipsilateral movements.

As regards the first finding, it is worthwhile noting that the amplitude of pre-movement potentials seen with bilateral movements was smaller than those expected from a simple summation of two potentials associated with ipsilateral and contralateral movements. In experimental studies of single unit recordings in monkeys, it was previously reported that a very small subgroup (4.3%, 5.4% and 11%) of SMA movement-related neurons was active before voluntary movements, exclusively for right, left, and bilateral movements, respectively ("exclusive neurons") (Tanji et al., 1987, 1988). This type of exclusive neuron was not seen in the primary motor area. In addition, Tanji et al. (1987) reported another population (38%) of SMA movement-related neurons which were active before all 3 types of movement (right, left and bilateral). Therefore, taking into account these experimental findings, the present results suggest that movement-related potentials, which are the expression of extracellular field potentials, are most likely to be predominantly a reflection of SMA neurons activated by all 3 types of movement with only a small contribution of the "exclusive neurons."

Regarding the components of pre-movement potentials seen in SMA, particularly in patient 1, it was shown that BP and NS′ at SMA elicited by contralateral and bilateral movements were almost identical, whereas the following MP at SMA had a larger deflection for bilateral movements. This finding is consistent with the recent scalp-recorded MRP study with unilateral and bilateral movements (Lang et al., 1991). This study demonstrated that, during actual motor execution, negative potentials at the vertex were present in bimanual complex motor sequences, but absent with simple unilateral motor sequences, whereas BP was seen in both situations. This finding suggests the possibility that SMA plays a more significant role during the actual execution of bilateral movements (represented as MP), rather than prior to the onset of the movements (represented as BP and NS′). They also reported that a significantly higher activity at the vertex during execution was seen during either unilateral or bilateral sequential movements rather than during single motor performance (Lang et al., 1988, 1989, 1990). It is also in good agreement with the result of cerebral blood flow study with complex finger movements (Shibasaki et al., 1993). It is thus suggested that the SMA may play a special role in the execution but not necessarily in the preparation of the so-called precise or skillful motor tasks.

With regard to the second finding, the pre-movement potentials with hand movements were recorded from the primary hand sensorimotor area in one patient (patient 2), and those with foot movements from the primary motor foot area in another patient (patient 1). Neshige et al. (1988), in similar recording circumstances to the present study, reported the presence of BP at the primary hand sensorimotor area with ipsilateral hand movements in 3 epilepsy patients. The ipsilateral BP was relatively small, and no NS′ and MP followed the BP in their studies. These findings are consistent with the results observed in patient 2 in the present study. Namely, with ipsilateral hand movement a small BP was seen from the primary hand sensorimotor area but no clear NS′ or MP developed. For ipsilateral foot movements, the authors previously reported the absence of any pre-movement potential at the primary motor foot area in 2 patients (Ikeda et al., 1992). Patient 1 in the present study confirmed these results. These findings suggest that the ipsilateral primary sensorimotor hand or foot area of the human brain plays an almost negligible role in the generation of pre-movement as well as post-movement potentials. Therefore, unlike the SMA, the amplitude of pre-movement potentials recorded in the primary sensorimotor area with bilateral movements was just like a simple summation of two potentials associated with ipsilateral and contralateral movements. This result is consistent with previous animal studies which showed that, contrary to SMA neurons, most movement-related neurons in the primary motor area were simply related to the activity of the contralateral muscles (Evarts, 1966; Matsunami and Hamada, 1981; Tanji et al., 1987, 1988).

Scalp-recorded MRPs with unilateral and bilateral movements were previously studied (Kristeva et al., 1979, 1990, 1991). They interpreted their results as suggesting active participation of bilateral sensorimotor areas for generating pre-movement potentials. However, with the methodology used in their studies it is still uncertain how much of the pre-movement potentials was generated in the SMA as opposed to the primary sensorimotor area.

Previously cerebral blood flow studies demonstrated that SMA was significantly more active during actual execution of unilateral motor sequences than during simple movements (Orgogozo and Larsen, 1979; Roland et al., 1980; Shibasaki et al., 1993). It certainly means that the SMA is more active in association with the so-called complex movements than the simple ones. However, it remains unclear as to whether the observed activity at the SMA is the cause or the consequence of the behavioral act, because those studies provide the information about the total changes in the cerebral blood flow or metabolism occurring from about 40 sec before the measurement (Wiesendanger, 1986). The same limitations, i.e., poor temporal resolution, are also applied to functional MRI studies which showed similar results (Rao et al., 1993). In contrast, field potential studies, like the present one, provide information with high temporal resolution, and complement blood flow studies. Therefore, we can conclude that both electrophysiological and cerebral blood flow studies suggest that during movement preparation the human SMA is similarly active in unilateral and bilateral movements, but that during the actual motor execution it becomes more active in bilateral than in unilateral movements.

In the present study, patients 1 and 3 had pre-movement potentials with positive polarity. Invasive animal studies demonstrated that the pre-movement potentials had a dipolar distribution with a negative pole at the surface and a positive pole in the deep gray matter. Therefore it most likely represents excitatory postsynaptic potentials (EPSPs) generated in the superficial parts of apical dendrites of cortical pyramidal neurons (Hashimoto et al., 1979). Previously the authors' group showed the positive pre-movement potentials recorded by subdural electrodes in some subjects, regardless of the type of movement (Ikeda et al., 1992, 1993, 1995). Therefore, as previously discussed (Ikeda et al., 1992), these positive potentials recorded by subdural electrodes could be explained by the orientation of the dipole; a dipolar generator in a sulcus would project out of the positive and negative potentials toward the opposite direction. In this case only the positive potentials could be recorded because of the limited placement of subdural electrodes.

Recent anatomical and physiological studies in monkeys demonstrated that the SMA is subdivided at least into rostral (pre-SMA or F6) and caudal parts (SMA-proper or F3) (Luppino et al., 1991, 1993; Matsuzaka et al., 1992), and that the two had independent functions. Since the SMA-proper in monkeys has a somatotopic organization, it is possible that MRPs demonstrated in the SMA in the present and previous studies (Ikeda et al., 1992, 1993) were generated from the SMA-proper also in man. However, it still remains unsolved whether human SMA could be subdivided into the SMA-proper and pre-SMA as seen in monkeys.

Finally, it is worthwhile considering several technical limitations when interpreting the results of subdural MRP studies and comparing them with other scalp-recorded MRP studies. Closely spaced subdural electrodes can only record field potentials which is a reflection of the activity of neurons covered by the subdural electrodes. No single unit activity can be detected. In addition, the subdural electrodes do not cover the whole brain surface. Therefore, only part of the SMA was explored in each patient, and the possibility that more active parts of SMA adjacent to the explored areas might have been missed, cannot be excluded. Comparative studies of cerebral blood flow with PET or functional MRI would be helpful to complement those results. In addition, the stainless steel electrodes used in these studies are not optimal to record the so-called DC brain potentials (Caspers, 1974). Although we opened the LFF down to 0.016 Hz for cortical recordings, the type of electrode used indicates that the actual LFF cut-off was most probably higher than that. Therefore, the present data may not completely be comparable to scalp-recorded DC potentials, recorded by silver-silver chloride electrodes. In spite of these limitations, subdural MRP studies have provided new insight into the generation of MRPs (Neshige et al., 1988; Sakamoto et al., 1991; Ikeda and Shibasaki, 1992; Ikeda et al., 1992, 1993, 1995), and certainly the comparison of potentials recorded from different cortical areas in the same patient should give reliable results.

Acknowledgements

The authors are grateful to the EEG technologists and the staffs in the Neurological Computing Section of Cleveland Clinic for their technical help.

This study was partly supported by Grant-in-Aid for Scientific Research on Priority Areas 06260225, New Program 06NP0101 and Scientific Research 06404031, and International Scientific Research Grant 07044258, all from the Japan Ministry of Education, Science and Culture for H.S.

References

Alexander, G.E. and Crutchler, M.D. (1990a) Preparation for movement: neural representations of internal direction in three motor areas of the monkey. J. Neurophysiol., 64: 133–150.

Alexander, G.E. and Crutchler, M.D. (1990b) Neural representations of the target (goal) of visually guided arm movements in three motor areas of the monkey. J. Neurophysiol., 64: 164–178.

Barrett, G., Shibasaki, H. and Neshige, R. (1985) A computer-assigned method for averaging movement-related cortical potentials with respect to EMG onset. Electroenceph. clin. Neurophysiol., 60: 276–281.

Barrett, G., Shibasaki, H. and Neshige, R. (1986) Cortical potentials preceding voluntary movement: evidence for three periods of preparation in man. Electroenceph. clin. Neurophysiol., 63: 327–339.

Brinkman, C. (1981) Lesions in supplementary motor area interfere with a monkey's performance of a bimanual coordination task. Neurosci. Lett., 27: 267–270.

Brinkman, C. (1984) Supplementary motor area of the monkey's cerebral cortex: short- and long-term deficits after unilateral ablation and the effects of subsequent callosal section. J. Neurosci., 4: 918–929.

Burgess, R.C. (1992) Design and integration of computer systems. In: H.O. Lüders (Ed.), Epilepsy Surgery. Raven Press, New York, pp. 291–296.

Caspers, H. (1974) DC potentials recorded directly from the cortex. In: A. Rémond (Ed.), Handbook of Elecroencephalography and Clinical Neurophysiology, Vol. 10, Part A. Elsevier, Amsterdam, pp. 7–11.

Chen, D.F., Hyland, B., Maier, V., Palmeri, A. and Wiesendanger, M. (1991) Comparison of neuronal activity in the supplementary motor area and in the primary motor cortex in monkeys. Somatosens. Motor Res., 8: 27–44.

Collura, T.F., Jacobs, E.C. and Burgess, R.C. (1992) Operations support and users interface of computer systems. In: H.O. Lüders (Ed.), Epilepsy Surgery. Raven Press, New York, pp. 297–305.

Crutchler, M.D. and Alexander, G.E. (1990) Movement-related neuronal activity selectively coding either direction or muscle pattern in three motor areas of the monkey. J. Neurophysiol., 64: 151–163.

Deecke, L., Scheid, P. and Kornhuber, H.H. (1969) Distribution of readiness potentials, pre-motion positivity and motor potentials of the human cerebral cortex preceding voluntary movements. Exp. Brain Res., 7: 158–168.

Deecke, L., Kornhuber, H.H., Lang, W. and Schreiber, H. (1985) Timing function of the frontal cortex in sequential motor and learning task. Hum. Neurobiol., 4: 143–154.

Eccles, J.C. (1982) The initiation of voluntary movements by supplementary motor area. Arch. Psychiat. Nervenkr., 231: 423–441.

Evarts, E.V. (1966) Pyramidal tract neuron activity associated with a conditioned hand movement in the monkeys. J. Neurophysiol., 29: 1011–1027.

Fox, P.T., Fox, J.M., Raichle, M.E. and Burde, R.M. (1985) The role of cerebral cortex in the generation of voluntary saccades: a positron emission tomographic study. J. Neurophysiol., 54: 348–369.

Fried, I., Katz, A., McCarthy, G., Sass, K.J., Williamson, P., Spencer, S.S. and Spenser, D.D. (1991) Functional organization of supplementary motor cortex studied by electrical stimulation. J. Neurosci., 11: 3655–3666.

Goldberg, G. (1985) Supplementary motor area structure and function; review and hypotheses. Behav. Brain Sci., 8: 567–616.

Hahn, J. and Lüders, H. (1987) Placement of subdural grid electrodes at the Cleveland Clinic. In: J. Engel, Jr. (Ed.), Surgical Treatment of the Epilepsies. Raven Press, New York, pp. 621–627.

Halsband, U. (1983) Higher disturbances of movements in *Macaca fascicularis* following discrete neocortical ablations. Neurosci. Lett., Suppl. 14: S154.

Hashimoto, S., Gemba, H. and Sasaki, K. (1979) Analysis of slow cortical potentials preceding self-paced hand movements in the monkeys. Exp. Neurol., 65: 218–229.

Hyland, B., Chen, D.F., Maier, V., Palmeri, A. and Wiesendanger, M. (1989) What is the role of the supplementary motor area in movement initiation? Progr. Brain Res., 80: 431–436.

Ikeda, A. and Shibasaki, H. (1992) Invasive recording of movement-related cortical potentials in human. J. Clin. Neurophysiol., 9: 509–520.

Ikeda, A., Lüders, H.O., Burgess, R.C. and Shibasaki, H. (1992) Movement-related potentials recorded from supplementary motor area and primary motor area: role of supplementary motor area in voluntary movements. Brain, 115: 1017–1043.

Ikeda, A., Lüders, H.O., Burgess, R.C. and Shibasaki, H. (1993) Movement-related potentials associated with single and repetitive movements recorded from human supplementary motor area. Electroenceph. clin. Neurophysiol., 89: 269–277.

Ikeda, A., Lüders, H.O., Burgess, R.C., Sakamoto, A., Klem, G.H., Morris, H.H. and Shibasaki, H. (1995) Generator locations of movement-related potentials with tongue protrusions and vocalizations: subdural recording in human. Electroenceph. clin. Neurophysiol., 96: 310–328.

Kornhuber, H.H. and Deecke, L. (1965) Hirnpotentialänderungen bei Willkürbewegungen und passiven Bewegungen des Menschen: Bereitschaftspotential und reafferente Potentiale. Pflügers Arch., 284: 1–17.

Kristeva, R., Keller, E., Deecke, L. and Kornhuber, H.H. (1979) Cerebral potentials preceding unilateral and simultaneous bilateral finger movements. Electroenceph. clin. Neurophysiol., 47: 229–238.

Kristeva, R., Cheyne, D., Lang, W., Lindinger, G. and Deecke, L. (1990) Movement-related potentials accompanying unilateral and bilateral finger movements with different inertial loads. Electroenceph. clin. Neurophysiol., 75: 410–418.

Kristeva, R., Cheyne, D. and Deecke, L. (1991) Neuromagnetic fields accompanying unilateral and bilateral voluntary movements: topography and analysis of cortical sources. Electroenceph. clin. Neurophysiol., 81: 284–298.

Lang, W., Lang, M., Uhl, F., Koska, Ch., Kornhuber, A. and Deecke, L. (1988) Negative cortical DC shifts preceding and accompanying simultaneous and sequential finger movements. Exp. Brain Res., 71: 579–587.

Lang, W., Zilch, O., Koska, Ch., Lindinger, G. and Deecke, L. (1989) Negative cortical DC shifts preceding and accompanying simple and complex sequential movements. Exp. Brain Res., 74: 99–104.

Lang, W., Obrig, H., Lindinger, G., Cheyne, D. and Deecke, L. (1990) Supplementary motor area activation while tapping bimanually different rhythms in musicians. Exp. Brain Res., 79: 506–514.

Lang, W., Cheyne, D., Kristeva, R., Lindinger, G. and Deecke, L. (1991) Functional localization of motor processes in the human cortex. In: C.H.M. Brunia, G. Mulder and M.N. Verbaten (Eds.), Event-Related Brain Research. Electroenceph. clin. Neurophysiol., Suppl. 42. Elsevier, Amsterdam, pp. 97–115.

Laplane, D., Talairach, J., Meininger, V., Bancaud, J. and Orgogozo, J.M. (1977) Clinical consequences of corticectomies involving the supplementary motor area in man. J. Neurol. Sci., 34: 301–314.

Lesser, R.P., Gordon, B., Fisher, R., Hart, J. and Uematsu, S. (1992) Subdural grid electrodes in surgery of epilepsy. In: H.O. Lüders (Ed.), Epilepsy Surgery. Raven Press, New York, pp. 399–408.

Lim, S.H., Dinner, D.S., Pillay, P., Lüders, H., Morris, H.H., Klem, G., Wyllie, E and Awad, I. (1994) Functional anatomy of the human supplementary sensorimotor area: results of extraoperative electrical stimulation. Electroenceph. clin. Neurophysiol., 91: 179–193.

Lueders, H., Hahn, J., Lesser, R.P., Dinner, D.S., Rothner, D. and Erenberg, G. (1982) Localization of epileptogenic spike foci: comparative study of closely spaced scalp electrodes, nasopharyngeal, sphenoidal, subdural, and depth electrodes. In: H. Akimoto, H. Kazamatsuri, M. Seino and A.A. Ward (Eds.), Advances in Epileptology. The 13th Epilepsy Int. Symp. Raven Press, New York, pp. 185–189.

Lüders, H., Lesser, R.P., Dinner, D.S., Hahn, J.F., Salanga, V. and Morris, H.H. (1985) The second sensory area in human: evoked potential and electrical stimulation studies. Ann. Neurol., 17: 177–184.

Lüders, H., Lesser, R.P., Dinner, D.S., Morris, H.H., Hahn, J.F., Friedman, L., Skipper, G., Wyllie, E. and Friedman, D. (1987) Commentary: Chronic intracranial recording and stimulation with subdural electrodes. In: J. Engel, Jr. (Ed.), Surgical Treatment of the Epilepsies. Raven Press, New York, pp. 297–321.

Lüders, H., Lesser, R.P., Dinner, D.S., Morris, H.H., Wyllie, E. and Godoy, J. (1988) Localization of cortical function: new information from extraoperative monitoring of patients with epilepsy. Epilepsia, 29 (Suppl.): S56–S65.

Luppino, G., Matteli, M., Camarda, R.M., Gallese, V. and Rizzolatti, G. (1991) Multiple representations of body movements in mesial area 6 and the adjacent cingulate cortex: an intracortical microstimulation study in the macaque monkey. J. Comp. Neurol., 311: 463–482.

Luppino, G., Matteli, M., Camarda, R. and Rizzolatti, G. (1993) Cortico-

cortical connections of area F3 (SMA-proper) and area F6 (pre-SMA) in the macaque monkey. J. Comp. Neurol., 338: 114–140.

Matsunami, K. and Hamada, I. (1981) Characteristics of the ipsilateral movement-related neuron in the motor cortex of the monkey. Brain Res., 204: 29–42.

Matsuzaka, Y., Aizawa, H. and Tanji, J. (1992) A motor area rostral to the supplementary motor area (presupplementary motor area) in the monkey: neuronal activity during a learned motor task. J. Neurophysiol., 68: 653–662.

Morris, H.H. (1992) Protocols for surgery of epilepsy in different centers. In: H.O. Lüders (Ed.), Epilepsy Surgery. Raven Press, New York, pp. 786–788.

Morris, H.H., Dinner, D.S., Lüders, H., Wyllie, E. and Kramer, R. (1988) Supplementary motor seizures: clinical and electroencephalographic findings. Neurology, 38: 1075–1082.

Nathan, S.S., Sinha, S.R., Gordon, B., Lesser, R.P. and Thakor, N.V. (1993) Determination of current density distributions generated by electrical stimulation of the human cerebral cortex. Electroenceph. clin. Neurophysiol., 86: 183–192.

Neshige, R., Lüders, H. and Shibasaki, H. (1988) Recording of movement-related potentials from scalp and cortex in man. Brain, 111: 719–736.

Orgogozo, J.M. and Larsen, B. (1979) Activation of the supplementary motor area during voluntary movements in man suggests it works as a supramotor area. Science, 206: 847–850.

Penfield, W. and Jasper, H. (1954) Functional localization in the cerebral cortex. In: Epilepsy and the Functional Anatomy of the Human Brain. Little, Brown and Co., Boston, MA, pp. 88–102.

Penfield, W. and Welch, K. (1951) The supplementary motor area of the cerebral cortex: a clinical and experimental study. Arch. Neurol. Psychiat., 66: 289–317.

Porter, R. (1990) The Kubelberg lecture. Brain mechanisms of voluntary motor commands. A review. Electroenceph. clin. Neurophysiol., 76: 282–293.

Rao, S.M., Binder, J.R., Bandettini, P.A., Hammeke, T.A., Yetkin, F.Z., Jesmanowicz, A., Lisk, L.M., Morris, G.L., Mueller, W.M., Estkowski, L.D., Wong, E.C., Haughton, V.M. and Hyde, J.S. (1993) Functional magnetic resonance imaging of complex human movements. Neurology, 43: 2311–2318.

Roland, P.E., Larsen, B., Lassen, N.A. and Skinhøj, E. (1980) Supplementary motor area and other cortical areas in organization of voluntary movements in man. J. Neurophysiol., 43: 118–136.

Rostomily, R.C., Berger, M.S., Ojemann, G.A. and Lettich, E. (1991) Postoperative deficits and functional recovery following removal of tumors involving the dominant hemisphere supplementary motor area. J. Neurosurg., 75: 62–68.

Sakamoto, A., Lüders, H. and Burgess, R. (1991) Intracranial recordings of movement-related potentials to voluntary saccades. J. Clin. Neurophysiol., 8: 223–233.

Schell, G., Hodge, C.J. and Cacayorin, E. (1986) Transient neurological deficit after therapeutic embolization of the arteries supplying the mesial wall of the hemisphere, including the supplementary motor area. Neurosurgery, 18: 353–356.

Schmidt, E.M., Porter, R. and McIntosh, J.S. (1992) The effects of cooling supplementary motor area and midline cerebral cortex on neuronal responses in area 4 of monkeys. Electroenceph. clin. Neurophysiol., 85: 61–71.

Shibasaki, H., Barrett, G., Halliday, E. and Halliday, A.M. (1980) Components of the movement-related cortical potentials and their scalp topography. Electroenceph. clin. Neurophysiol., 49: 213–226.

Shibasaki, H., Sadato, N., Lyshkow, H., Yonekura, Y., Honda, M., Nagamine, T., Suwazono, S., Magata, Y., Ikeda, A., Miyazaki, M., Fukuyama, H., Asato, R. and Konishi, J. (1993) Both primary motor cortex and supplementary motor area play an important role in complex finger movement. Brain, 116: 1387–1398.

Tanji, J. and Kurata, K. (1982) Comparison of movement-related activity in two cortical motor areas of primates. J. Neurophysiol., 48: 633–653.

Tanji, J. and Kurata, K. (1985a) Contrasting neuronal activity in supplementary and precentral motor cortex of monkeys. I. Responses to instructions determining motor responses to forthcoming signals of different modalities. J. Neurophysiol., 53: 129–141.

Tanji, J. and Kurata, K. (1985b) Contrasting neuronal activity in supplementary and precentral motor cortex of monkeys. II. Responses to movements triggering vs. nontriggering sensory signals. J. Neurophysiol., 53: 142–152.

Tanji, J., Okano, K. and Sato, K.C. (1987) Relation of neurons in the nonprimary motor cortex to bilateral hand movement. Nature, 327: 618–620.

Tanji, J., Okano, K. and Sato, K.C., (1988) Neuronal activity in cortical motor areas related to ipsilateral, contralataral, and bilateral digit movements of the monkeys. J. Neurophysiol., 60: 325–343.

Wiesendanger, M. (1986) Recent developments in studies of the supplementary motor area of primates. Rev. Physiol. Biochem. Pharmacol., 103: 1–59.

Wiesendanger, M., Hummelsheim, H., Bianchetti, M., Chen, D.F., Hyland, B., Maier, V. and Wiesendanger, R. (1987) Input and output organization of the supplementary motor area. In: R. Porter (Ed.), Motor Area of the Cerebral Cortex. Ciba Foundation Symposium 132. John Wiley and Sons, Chichester, pp. 40–53.

Woolsey, C.N., Settlage, P.H., Meyer, D.R., Spencer, W., Pinto-Hamuy, T.P. and Travis, A.M. (1952) Patterns of localization in precentral and "supplementary" motor areas and their relation to the concept of a premotor area. Res. Publ. Ass. Res. Nerv. Ment. Dis., 30: 238–264.

Neuroscience Letters, 122 (1991) 17–20
Elsevier Scientific Publishers Ireland Ltd.

NSL 07450

Homuncular organization of human motor cortex as indicated by neuromagnetic recordings

Douglas Cheyne, Rumyana Kristeva and Lüder Deecke

Neurological University Clinic, Vienna (Austria)

(Received 30 August 1990; Accepted 24 September 1990)

Key words: Magnetoencephalography; Motor cortex; Homunculus; Neuromagnetic source localization

Sources of neural activity identified using non-invasive measurements of cerebral magnetic fields (magnetoencephalography) were found to confirm the somatotopic organization of primary motor cortex for movements of different parts of the body in normal human subjects. Somatotopic maps produced with this technique showed slight differences to the 'classic' homunculus obtained from studies using direct cortical stimulation. These findings indicate that neuromagnetic recordings are capable of localizing cortical activity associated with voluntarily produced movements without the use of external stimulation and provide a new method for studying the functional organization of human motor cortex and its role in voluntary movement.

Early studies by Penfield and colleagues using electrical stimulation of the human brain [13, 14] indicated an orderly representation of movement for different parts of the body in the region of the contralateral precentral gyrus (primary motor cortex). These studies produced a somatotopic map for motor output which became known as the motor 'homunculus'. Although such somatotopic maps have been studied extensively in non-human primates using a variety of intracortical stimulation techniques [9–11], there remains considerable disagreement over both the fine structure of these maps, as well as the specific parameters of movement that are represented [10, 16]. Much of this disagreement stems from the problems posed by the artificial nature of movements which are evoked by electrical stimulation. Although some degree of somatotopy can be demonstrated using scalp-recorded EEG potentials [1], it has not been possible to demonstrate these somatotopic maps in detail using such non-invasive methods.

The recent development of neuromagnetic recordings (magnetoencephalography, MEG) provides a new non-invasive method for the localization of circumscribed regions of both normal and pathological activity in the human brain [6, 15]. Generators of the radial component of magnetic flux measured over the scalp, modelled as equivalent (vector sum) current dipoles lying tangential to the scalp surface, can be localized to specific regions of the cortex with accuracies of up to 1–2 mm [7]. Slow magnetic field changes have also been observed immediately prior to voluntary movements [4] and sources contributing to these shifts have been localized in the region of the primary motor cortex [2]. In the present study, we have studied slow MEG shifts preceding voluntary movements of different parts of the body and report here the first detailed mapping of the somatotopic organization of human motor cortex using these new methods.

Neuromagnetic data were recorded from 5 healthy, right-handed individuals. Subjects were positioned lying on a wooden bed inside a magnetically shielded room with their head stabilized by a vacuum cast. Magnetic fields (bandpass 0.1–50 Hz) were recorded over the left scalp using a 7-channel second-order gradiometer system (BTi San Diego, CA) while subjects performed voluntary (self-initiated) flexions of the right index finger (2nd digit), small finger (5th digit) and unilateral contractions of the lower right face. Adaptive balancing of the gradiometer signals was used to reduce environmental noise in the lower frequency range and provided a stable pre-movement baseline. Movement onset was detected from the rectified surface electromyogram (EMG) recorded over the active mucles. In addition, a 3-dimensional head coordinate system was measured for each subject using a 3-D digitizer and the position of the sensors with respect to this coordinate system stored during each measurement. Averaged waveforms of magnetic activity preceding and during EMG onset were produced from a

Correspondence: D. Cheyne, Department of Psychology, Simon Fraser University, Burnaby, B.C., Canada V5A 1S6.

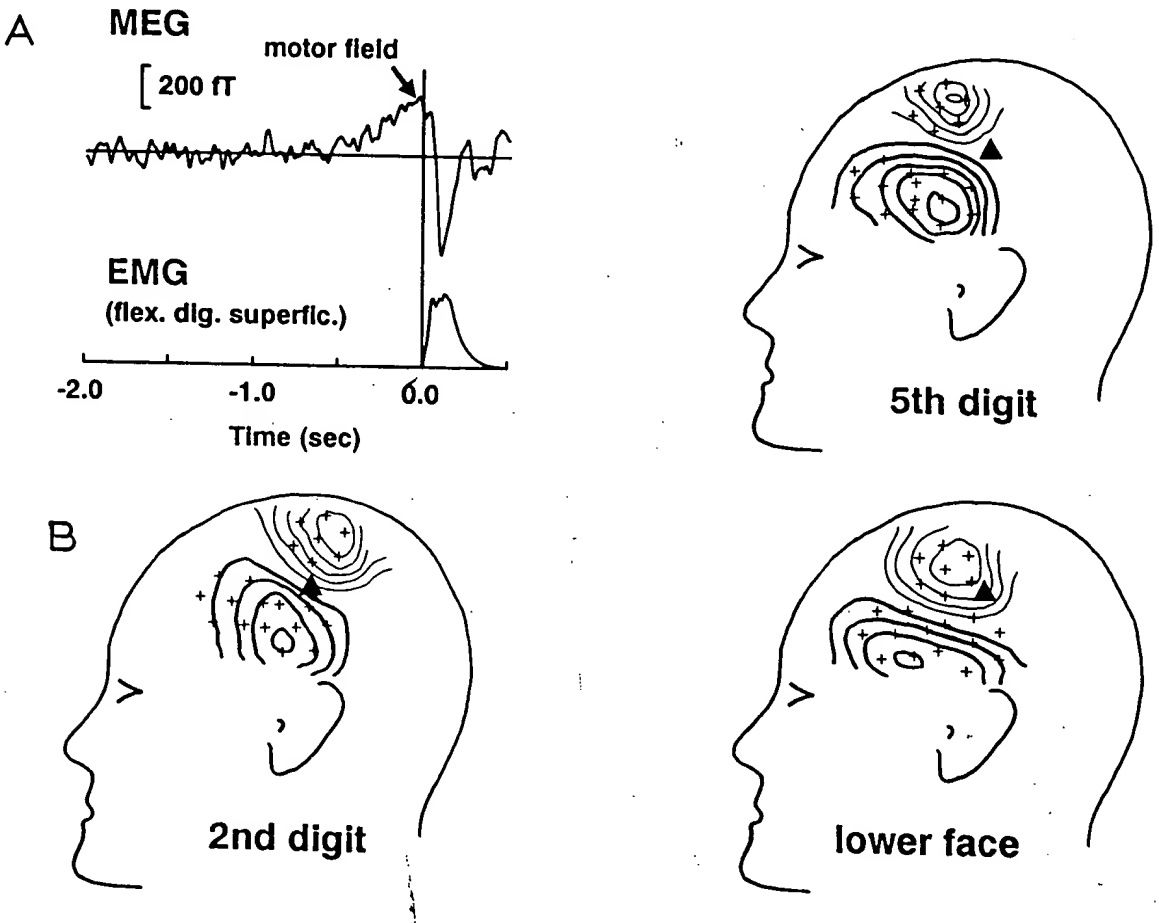

Fig. 1. A: MEG waveform (upper trace) during right index finger movement recorded from a lateral position over the left hemisphere shown in relation to onset of EMG activity (lower trace) recorded over the surface of the forearm. The motor field is indicated as peak of slow shift prior to EMG onset. B: topographic distribution of the motor field over the left hemisphere for movements of the 2nd, and 5th right digits and lower right face. Maps are equidistant projections centered over the electrode position C_3 (International 10–20 system) which roughly overlies the lateral portion of the precentral gyrus [8] and is indicated by the solid triangle in each map. Thick lines represent magnetic flux directed out of the scalp and thin lines flux directed into the scalp. Recording positions are indicated by small crosses. Contour steps are 30 fT.

minimum of 70 repetitions of each movement after rejection of artifact contaminated trials.

Voluntary movements were preceded by a slow magnetic field shift beginning about 500 ms prior to EMG onset and reaching peak amplitudes of 100-200 fT at, or immediately prior to EMG onset (Fig. 1A). This slow preparatory or 'readiness' field has been previously described [4] and is followed by a number of larger phasic shifts, possibly related to short-latency reafferent signals due to the movement itself [2]. The 10 ms interval representing the peak of the pre-movement shift ('motor field'), was chosen for further analysis as most likely representing the period of corticospinal outflow from primary motor cortex immediately prior to onset of muscle contraction, corresponding to the 'motor potential' observed in EEG recordings [5]. Fig. 1B illustrates the spatial distribution of the motor field for 3 different movement conditions, showing slightly different positions of the field maxima.

Source localization was achieved by fitting of the theoretical field produced by a tangential current dipole source to the observed data using a least-squares minimization procedure [2]. The adequacy of the dipole model was assessed by the amount of variance in the observed data accounted for by the resulting theoretical dipole source (goodness of fit), which was 90% or greater in all except 2 cases. Dipole orientations were anteriorly directed suggesting intracellular current flow directed away from the surface of the anterior bank of the central sulcus — consistent with extracellular currents of opposite direction (surface negativity) which are observed in electrical potential recordings.

Fig. 2 shows the averaged source locations for each of the 3 movement conditions in the vertical-lateral plane of the left hemisphere. The mean spatial separation between sources for movements of the 2nd and 5th digits was 2.12 ± 1.62 cm. This difference was statistically significant ($P < 0.05$, paired t-test) as was the separation

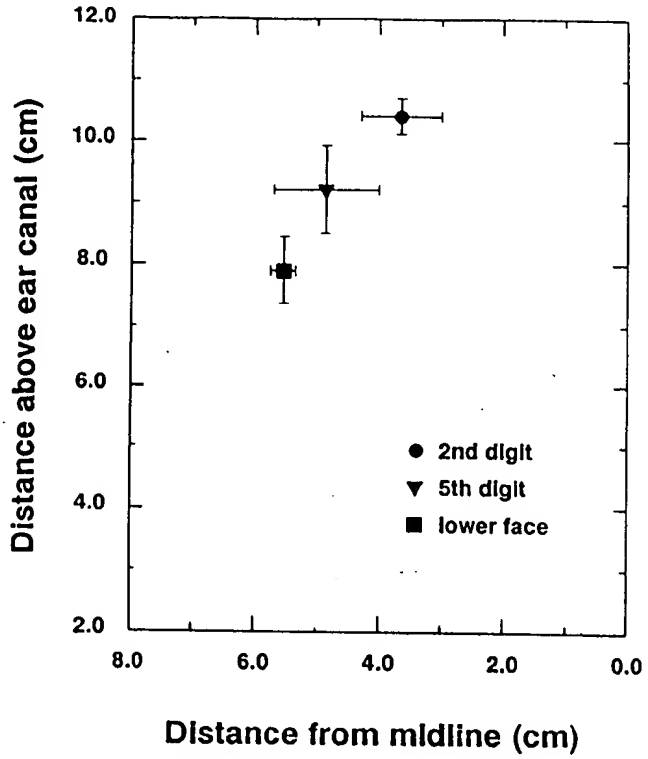

Fig. 2. Mean vertical-lateral position of dipole sources for movements of 2nd and 5th digits and of the lower face. The horizontal axis (right to left) represents distance from the sagittal midline toward the left ear canal and the vertical axis represents distance above the ear canal. Thin cross lines indicate 1 S.D.

between face and 5th digit source locations (mean = 2.14±0.83 cm, $P<0.01$) and between locations for the face and 2nd digit (mean = 3.65±0.68 cm, $P<0.001$). Dipole strength estimates varied across subjects but tended to be quite consistent within subjects.

Fig. 3A shows the locations of the fitted dipole sources in the head coordinate system of one subject who performed 7 different movements including: flexions of the right thumb, index finger, small finger and wrist, dorsiflexions of the right foot and protrusions of the tongue. The distribution of the source locations for all movements roughly follows the orientation of the central sulcus of the left hemisphere. Locations of the fitted dipole sources have also been projected onto a coronal magnetic resonance image (Fig. 3B) confirming these sources to be at the level of cortex within this region. The placement of the source for tongue protrusions was the only localization inconsistent with source activity at the level of cortex, although its greater depth may indicate the activation of a large area of cortex (due to wider dispersion of the field maxima [cf. 12]) which would be consistent with a reported larger area of representation of tongue movements in human motor cortex [14].

A notable exception in our findings was that the source location for 5th digit movements was more lateral to the location for 2nd digit movements — opposite to

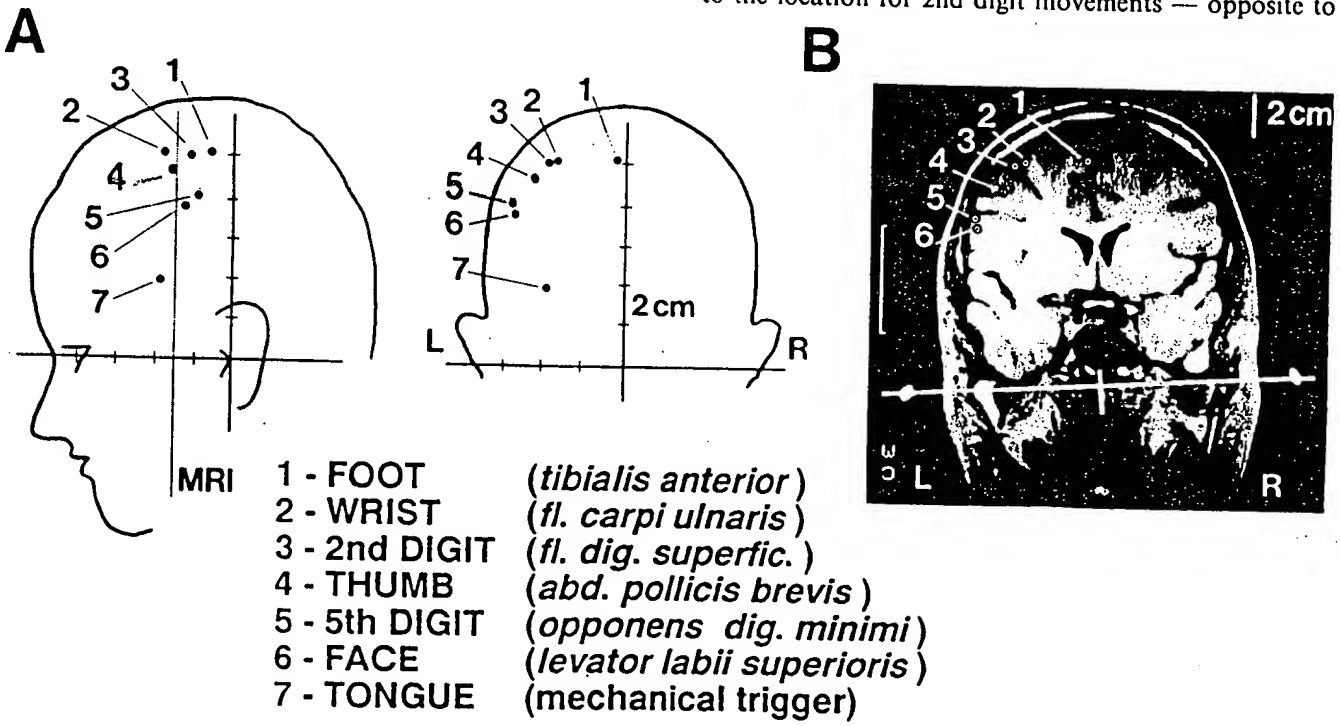

Fig. 3. A: three-dimensional dipole source locations for 7 different movement conditions projected onto lateral and posterior views of the subject's head. Head outlines are drawn from digitized points taken over the sagital and coronal midlines using the 3-D digitizing system also used to produce the head coordinate system. Dipole locations are indicated by filled circles and are numbered with respect to the movement performed, and the muscle from which the EMG trigger was recorded as indicated in the legend below. B: source locations projected onto a coronal magnetic resonance image (MRI) taken from the same subject. A thin tube filled with contrast agent was placed over the anatomical landmarks used to establish the head coordinate system in order to align the dipole coordinate system to that of the MR images. The MR plane shown here lies parallel to the vertical-lateral plane of the head coordinate system at the level indicated by the dotted line in the head diagram in A.

that indicated in the homunculus of Penfield [14]. However, in their original descriptions, Penfield and his colleagues reported the most common response to be movements of all of the fingers together [ref. 13, p. 411] and finger locations were often overlapping. Furthermore, hand movements were described as movements 'at the metacarpophalangeal joints' and *medially* represented with respect to the fingers. Since, in the present study, finger flexions also involved movements about this same joint and were performed in an individuated manner it is difficult to compare directly these previous results to those obtained here. Nevertheless, these observations suggest that methods measuring physiological activation of motor cortex may produce different results than those obtained with electrical stimulation.

Recent attempts to map the human motor cortex non-invasively by 'transcranial' electrical stimulation [3] have reported the ability to differentiate responses for movements of the upper arm and hand, but not for individual digits. However, artificial stimulation of the motor cortex may often evoke complex muscle synergies and may also indirectly stimulate *input* to pyramidal tract neurons as well as the output pathways themselves, thus making maps constructed from such techniques difficult to interpret [10]. Neuromagnetic recordings, on the other hand, offer the unique opportunity to study the activity of functional units of cortex during voluntarily produced motor behaviour in normal subjects. The fitted dipole locations based on the MEG data are consistent with activation of different regions of cortex along the length of the precentral gyrus, producing a somatotopic map for motor output, however, initial results suggest that this map may differ in certain respects to the 'classic' homunculus based on electrical stimulation of the cortex. This approach may thus provide new and useful information regarding the functional organization of the human motor cortex and its role in voluntary movement.

Supported by an NSERC of Canada Postdoctoral Fellowship to the first author and an IBRO/UNESCO Research Fellowship to the second author. Development of the MEG system was supported in part by grants from the FWF (Fonds zur Förderung der wissenschaftlichen Forschung) of Austria, the Austrian National Bank and the Ministry of Science and Research of Austria.

The authors wish to express their thanks to G. Lindinger, Dipl. Eng. for technical assistance and to Dr. Ch. Baumgartner for comments on the manuscript. Preliminary results from this study were presented at the 7th International Conference on Biomagnetism, New York, August, 1989.

1 Boschert, J. and Deecke, L., Cerebral potentials preceding voluntary toe, knee and hip movements and their vectors human precentral gyrus, Brain Res., 376 (1986) 175–179.
2 Cheyne, D. and Weinberg, H., Neuromagnetic fields associated with unilateral finger flexions: pre-movement and movement-evoked fields, Exp. Brain Res., 78 (1989) 604–612.
3 Cohen, L.G. and Hallet, M., Methodology for non-invasive mapping of human motor cortex with electrical stimulation, Electroencephalogr. Clin. Neurophysiol., 69 (1988) 403–411.
4 Deecke, L., Weinberg, H. and Brickett, P., Magnetic fields of the human brain accompanying voluntary movements: Bereitschaftsmagnetfeld, Exp. Brain Res., 48 (1982) 144–148.
5 Deecke, L., Scheid, P. and Kornhuber, H.H., Distribution of readiness potential, pre-motion positivity and motor potential of the human cerebral cortex preceding voluntary finger movements, Exp. Brain Res., 7 (1969) 158–168.
6 Hari, R. and Lounasmaa, O.V., Recording and interpretation of cerebral magnetic fields, Science, 244 (1989) 432–436.
7 Hari, R., Joutsiniemi, S.L. and Sarvas, J., Spatial resolution of neuromagnetic records: theoretical calculations in a spherical model, Electroencephalogr. Clin. Neurophysiol., 71 (1988) 64–72.
8 Homan, R.W., Herman, J. and Purdy, P., Cerebral location of international 10-20 system electrode placement, Electroencephalogr. Clin. Neurophysiol., 66 (1987) 376–382.
9 Kwan, H.C., MacKay, W.A., Murphy, J.T. and Wong, W.C., Spatial organization of precentral cortex in awake primates. II. Motor outputs, J. Neurophysiol., 41 (1978) 1120–1131.
10 Lemon, R.N., The output map of the primate motor cortex, Trends Neurosci., 11 (1988) 501–506.
11 Leyton, A.S.F. and Sherrington, C.S., Observations on the excitable cortex of the chimpanzee, orang-utan and gorilla, Q. J. Exp. Physiol., 11 (1917) 135–222.
12 Okada, Y., Discrimination of localized and distributed current dipole sources and localized single and multiple sources. In H. Weinberg, G. Stroink and T. Katila (Eds.), Biomagnetism: Application and Theory, Pergamon Press, New York, 1985, pp. 266-272.
13 Penfield, W. and Boldry, E., Somatic motor and sensory representation in the cerebral cortex of man as studied by electrical stimulation, Brain, 60 (1937) 389–443.
14 Penfield, W. and Rasmussen, T., The Cerebral Cortex of Man, Hafner, London, 1968 (facsimile of 1950 edition).
15 Rose, D.E., Smith, P.D. and Sato, S., Magnetoencephalography and epilepsy research, Science, 238 (1987) 329–335.
16 Strick, P.L. and Preston, J.B., Two representations of the hand in area 4 of a primate. I. Motor output organization, J. Neurophysiol., 48 (1982) 139–149.

Exp Brain Res (1989) 78:604-612

Experimental Brain Research

Neuromagnetic fields accompanying unilateral finger movements: pre-movement and movement-evoked fields

D. Cheyne and H. Weinberg
Brain Behaviour Laboratory, Simon Fraser University, Burnaby, B.C., Canada

Summary. Neuromagnetic fields accompanying voluntary flexions of the right index finger were studied in five subjects. In all subjects, slow magnetic fields were observed over the central scalp beginning about 1 second prior to movement onset. These fields displayed a similar time course to the electrically recorded "readiness potential", but with reversals of field direction over regions of the rolandic fissure over both hemispheres. Least-squares fitting of two current dipole sources for the pre-movement fields resulted in a consistent localization of one source in the region of the rolandic fissure contralateral to the side of movement in four subjects. Ipsilateral dipole sources fitted inconsistently at deeper locations or outside the head indicating the inability of a single dipole source to account for the ipsilateral fields. A large field reversal was also observed over the contralateral (left) hemisphere, 90–130 ms after onset of EMG activity in the active muscles. In some subjects, single dipole sources could be fitted to this "movement-evoked" field at locations slightly deeper and posterior to the pre-movement source locations in the contralateral hemisphere, possibly indicating unilateral activation of somatosensory cortex related to sensory feedback during the onset of this movement. Subtraction of pre-movement field activity from post-movement fields improved the ability to fit a single contralateral rolandic source for all subjects suggesting that pre-movement sources continue to be active during movement onset. These findings confirm previous reports that voluntary finger movements are preceded by slow magnetic fields. However, the present data indicate that the spatial distribution of these fields is complex and that bilaterally distributed field reversals are observed which suggests ipsilateral, as well as contralateral, hemispheric activity prior to and during voluntary unilateral movements.

Key words: Magnetoencephalography – Motor cortex – Voluntary movement – Source localization – Sensory feedback

Offprint requests to: D. Cheyne, Neurological University Clinic, Lazarettgasse 14, A-1090 Vienna, Austria

Introduction

It is known that self-paced voluntary movements in humans are preceded by a slow electrical shift recordable at the scalp, termed the readiness potential or Bereitschaftspotential (Kornhuber and Deecke 1965). It is thought that such electrical changes may stem from underlying sources in cortical motor areas associated with the planning, preparation and execution of movement (for a recent review, see Deecke 1987). Although it has been speculated that multiple cortical (as well as sub-cortical) areas may be active prior to voluntary movements and may thus contribute to the observed widespread distribution of the electrically recorded readiness potential, the exact nature of these sources is not yet known.

It has been previously reported that slow magnetic field changes at the scalp surface can also be detected prior to self-paced movements, and that these neuromagnetic fields follow a similar time course to readiness potentials (Deecke et al. 1982; Deecke et al. 1983; Hari et al. 1983). Furthermore, these fields demonstrate field direction changes in a manner similar to fields recorded during evoked brain activity (ie., averaged responses to sensory stimuli). Such field direction reversals can be used to estimate the location and number of possible underlying "equivalent sources" in cortex which behave as current dipoles. More recent developments in the use of neuromagnetic recording techniques have

improved the ability to localize dipole sources associated with event-related magnetic fields (for review, see Romani and Rossini 1988). There has been a great deal of success in localizing equivalent dipole sources within somatosensory cortex associated with fields evoked by peripheral nerve stimulation (Hari and Kaukoranta 1985) since sources located in the rolandic fissure where the intracellular current flow is primarily tangential to the scalp are of optimal depth and orientation for neuromagnetic measurements (Williamson and Kaufman 1981).

It is known that multiple cortical areas may be active during the preparation and execution of voluntary movements, in particular sources active in sensorimotor cortex in the region of the rolandic fissure. Furthermore, it is likely that it is the combined activity of these different areas which accounts for the systematic changes in amplitude and distribution of movement-related potentials observed at the scalp surface under different conditions, such as lateralization of the movement (Kristeva and Deecke 1980) or amount of applied force or effort (Kutas and Donchin 1974; Becker and Kristeva 1980). Thus, a better understanding of the number and distribution of cortical sources that may be active during movement preparation and performance would be useful in the further interpretation of these observed differences. In the present study, the topographical distribution of magnetic flux over the scalp was recorded in normal subjects during self-paced, unilateral finger movements in an attempt to identify cortical sources associated with the performance of simple voluntary movements.

Methods

Procedure

Magnetic fields accompanying self-paced finger flexions were recorded in five right-handed adult volunteers using a single channel, third-order SQUID biogradiometer system (Vrba et al. 1982). Subjects sat in a non-magnetic chair and performed voluntary, biphasic (flexion–extension) movements of the right index finger at their own pace while fixating on a target. Field activity was recorded sequentially from 28 to 32 positions over the scalp with the aid of a computer-guided gantry system which recorded the gradiometer location and orientation with respect to the head position. A digitized head model was made for each subject prior to recording which aided in the accurate placement of the recording coil at pre-selected sites over the scalp.

The amplified signals (bandpass 0.03–15 Hz) were digitized at a rate of 128 samples/sec and stored on magnetic tape. Markers were placed on the tape indicating the onset of the rectified EMG signal recorded bipolarly from the surface of the forearm overlying the superficial flexor muscles of the digits (bandpass 0.3–150 Hz). In addition, a single electrode placed at Cz (International 10–20 system, referenced to an electrode over the left mastoid) was monitored during the recordings in order to ensure consistency of the movement-related potentials over repetitions of the task. Electro-oculogram was recorded from medial supra-orbital and lateral infra-orbital electrodes. 40 artifact-free trials were collected for each recording position and stored for averaging off-line.

Extensive care was taken to eliminate head and eye movement artifacts by training subjects to fixate their gaze and hold their breath 1–2 s prior to and during the movement. Head movements were further minimized by the use of a wooden head rest and vacuum-cast pillow arrangement. A strain-gauge attached to the subject's forehead was also used to detect excessive head movements during the movement task. In some subjects, magnetic recordings were repeated for selected positions in order to examine the consistency of the responses over the duration of the recording sessions.

Data analysis

Averages were produced for each recording location for the period 1.5 s prior to 0.5 s following movement onset as defined by the EMG onset. Iso-contour maps of field intensity for selected time intervals were produced using a 2-dimensional quintic spline interpolation (Preusser 1984). These spatial maps were used to identify dipolar field patterns and to determine the time periods used for source localization analysis.

Sources were modelled as "equivalent" (ie., vector sum) current dipoles and their strength and location determined as the best fit to the observed data using an iterative least-squares fitting algorithm based on the Simplex method, described elsewhere (Weinberg et al. 1986). A modified version of the program described by Harrop et al. (1987) was used to fit multiple current dipoles using corrections for both the gradiometer geometry and sensing coil area. The deviation of the gradiometer axis from the radial direction (with respect to the head model origin) was also taken into account using information provided by the computer-controlled positioning system. The extent to which the fitted dipoles provided an adequate model was expressed as the degree to which the calculated fields could account for the observed data, referred to here as the 'goodness of fit' (g), where, $g = 1 - (\text{sum of squared differences/sum of squared observed values}) \times 100\%$ (cf., Kaukoranta et al. 1986).

Results

Spatial distribution of movement-related magnetic fields

In all subjects, slow magnetic field shifts were observed over the central scalp which displayed a similar time course to the subjects' electrically recorded readiness potential, with reversal of field direction (eg., outgoing laterally and ingoing medially) over the region of the rolandic fissure over both hemispheres. Figure 1 shows averaged waveforms for selected positions over the left and right central scalp in two subjects. The fields at these locations were characterized by a slow steady increase in amplitude beginning approximately 1 second prior to onset of EMG activity in the flexor muscles of the forearms (indicated as time 0 in all figures). This was followed by a large field reversal beginning at about

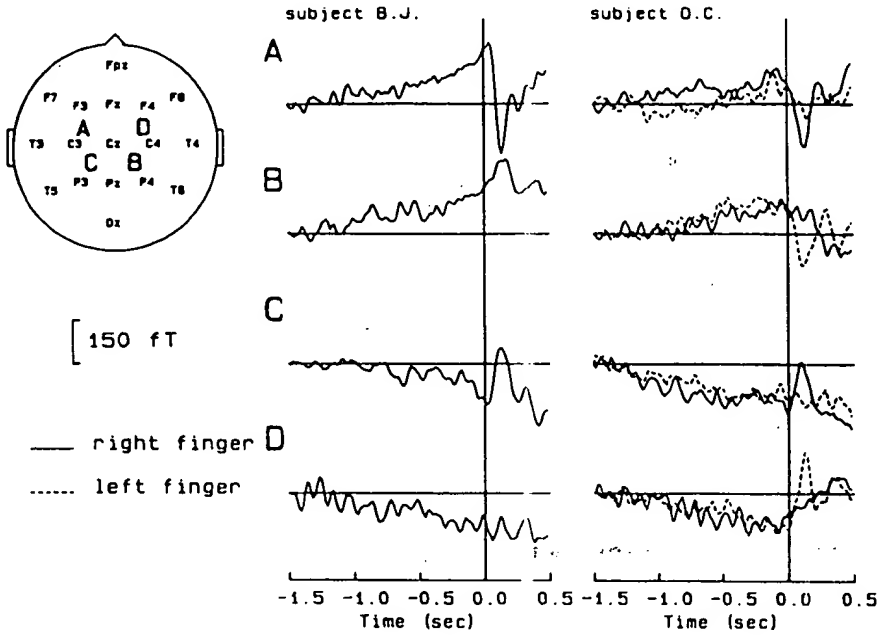

Fig. 1. Magnetic fields accompanying voluntary movements of the right index finger (solid traces) in 2 subjects recorded from homologous locations over either hemisphere as indicated by the letters **A** to **D** in the head outline shown to the left. International 10–20 system electrode placements are shown for comparison. Fields for left finger flexions (dotted traces) are also shown for subject D.C. Note similarity of large response following EMG onset restricted to opposite hemispheres. EMG onset occurs at 0 ms. Upward deflections indicate magnetic flux out of the head

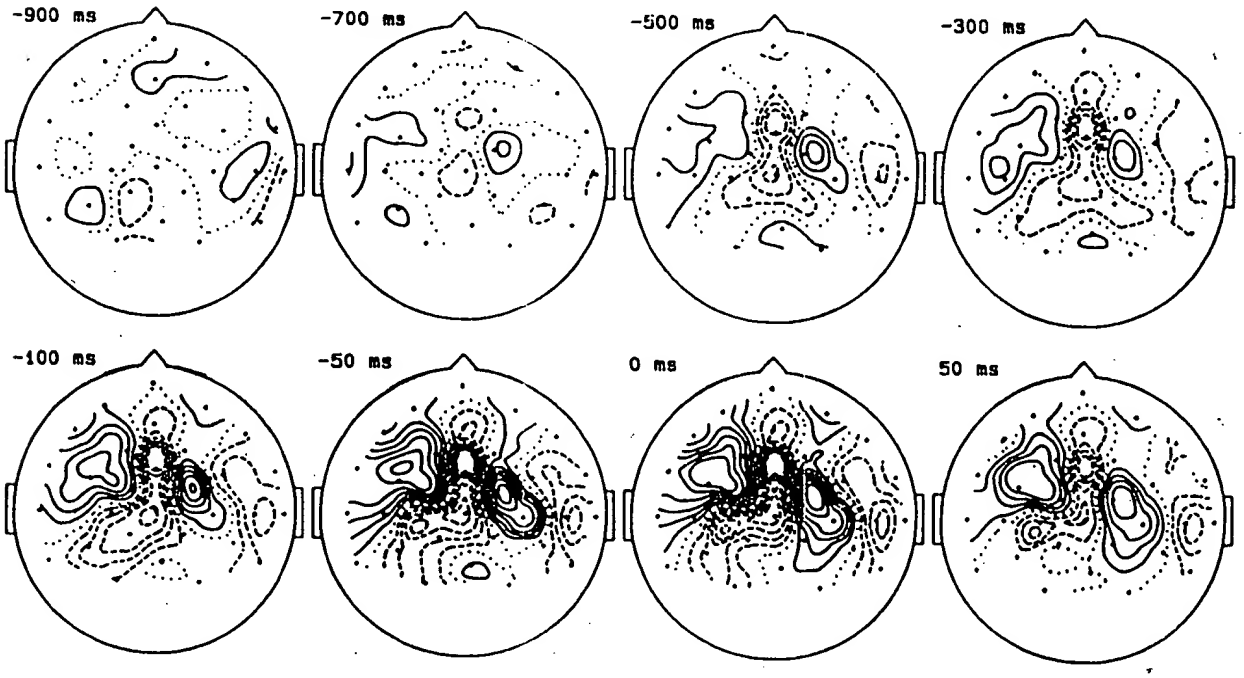

Fig. 2. Iso-contour maps of magnetic flux over the scalp for selected time intervals prior to and following EMG onset (0 ms) in one subject (B.J.). Time periods averaged over 40 ms with the mean time given in ms above each map. Contour steps are 30 fT. The maps represent equidistant polar projections of the head (nose upwards) with the map center lying 2–3 cm posterior to electrode placement Cz and outer border extending to approximately 10 cm above the ear canal. Solid lines represent flux out of the head. Small dots indicate projections of the recording positions onto the map

90 ms after EMG onset over the contralateral hemisphere. In recordings over the ipsilateral hemisphere, the pre-movement shifts increased slowly and continued during movement onset at some locations or returned to baseline.

In one subject (D.C.), activity was also measured for left index finger movements. The fields accompanying both left and right voluntary movements were remarkably similar, except for reversals following EMG onset which were primarily confined to

the hemisphere opposite to the side of movement (see Fig. 1). EMG recordings from the forearms did not show any consistent activity of the forearm flexor muscles in the ipsilateral limb (ie., movement of the fingers opposite to the instructed side of movement).

Figure 2 shows iso-contour map projections of field intensity for selected time periods before and during movement onset in one subject. In both subjects, ingoing and outgoing flux can be observed over either hemisphere (indicated by dotted and solid lines, respectively) producing dipolar patterns with maxima centered over the region of the rolandic fissure on either side. These patterns become clearly dipolar around 400 to 500 ms prior to the movement, and reach maximum amplitude at, or just prior to, the onset of EMG activity in the forearm. Following EMG onset, the pattern over the contralateral hemisphere is replaced by a reversal of opposite orientation and slightly posterior to the pre-movement pattern, reaching peak amplitude between 90 and 130 ms after EMG onset.

Dipole source estimation

Dipole source estimates were computed for time periods preceding and during movement chosen on the basis of the topographical maps of field activity. Since bilateral reversals were present in all subjects prior to EMG onset, a two dipole model was chosen for the pre-movement period assuming equivalent current dipole sources located in either hemisphere (Table 1). Figure 3a shows the theoretical (calculated) field map (right) based on two dipoles fitted to the observed data map (left) in one subject, taking the mean amplitudes for the pre-movement period of 70 to 30 ms prior to EMG onset.

Figure 3b shows the 3-dimensional locations of the fitted dipoles which accounted for more than 60% of the variance in the observed data for this time period. The dipoles are shown as projections in a right-handed head coordinate system, in which the horizontal (x–y) plane passes through the nasion and pre-auricular points with the positive z-axis passing through the skull at a point 2–3 cm posterior to Cz (International 10–20 system). In four subjects, fits between 61% and 82% were achieved using a two dipole model with one equivalent source being localized to the region of the rolandic cortex contralateral to the side of movement. The pre-movement dipole estimates had an average magnitude of 9.5 ± 2.6 nanoampere-meters (nA-m) and were localized to relatively superficial sites with a average radius of 10.1 ± 0.9 cm. Orientation of the dipoles varied from horizontal, directed anteriorly, to a more vertical orientation. Estimates of ipsilateral equivalent sources were inconsistent across subjects with locations either deep below the rolandic fissure or with an unreasonably large radius, ie., one that would place the dipole outside of the head (Fig. 3b).

A single equivalent dipole model was chosen for the early movement-evoked field (90–130 ms after EMG onset) based on the large contralateral reversals observed at this time interval in three subjects (Table 2a). Dipoles sources could be fitted for all three subjects and these were located at slightly greater depths (radius $= 8.8 \pm 0.7$ cm) than the pre-

Table 1. Parameters for least-squares fitted dipoles for the pre-movement field −70 to −30 ms prior to EMG onset. Contralateral (C) and ipsilateral (I) dipoles were fitted simultaneously. Moment: dipole moment in nanoAmpere meters. Position coordinates refer to a right-handed coordinate system with the positive y-axis passing through the left pre-auricular point, the positive x-axis passing through the nasion, and the positive z-axis passing through the skull 2–3 cm posterior to electrode placement Cz. The orientation of each dipole is given as a unit vector in the same coordinate system. Goodness of fit refers to amount of variance accounted for by the fit given as percentage

Subject	Dip	Moment (nA-m)	Position (cm) X	Y	Z	Orientation x	y	z	Radius (cm)	Goodness of fit
T.R.	C	6.5	1.01	3.98	10.77	0.16	0.39	0.91	11.5	81%
	I	1.7	−0.08	−3.19	6.30	0.97	0.26	0.03	7.1	
B.J.	C	20.3	−0.97	3.57	9.38	0.54	0.12	0.83	10.1	63%
	I	5.7	2.00	−7.22	11.74	0.97	0.24	0.03	13.9	
R.G.	C	7.1	2.03	2.31	9.17	0.96	0.20	−0.17	9.7	82%
	I	8.8	3.44	−2.56	4.77	0.87	0.48	0.08	6.4	
D.C.	C	10.7	2.21	1.93	9.31	0.95	−0.06	0.29	9.8	61%
	I	3.8	0.61	−5.92	9.28	0.86	0.09	0.51	11.0	
H.W.	C	3.1	4.12	3.29	7.60	0.99	−0.01	0.14	9.2	52%
	I	2.9	2.81	−3.42	8.22	0.99	0.00	0.05	9.3	
Mean	C	9.5 (±2.6)							10.1 (±0.9)	
	I	4.6 (±1.7)							9.5 (±1.7)	

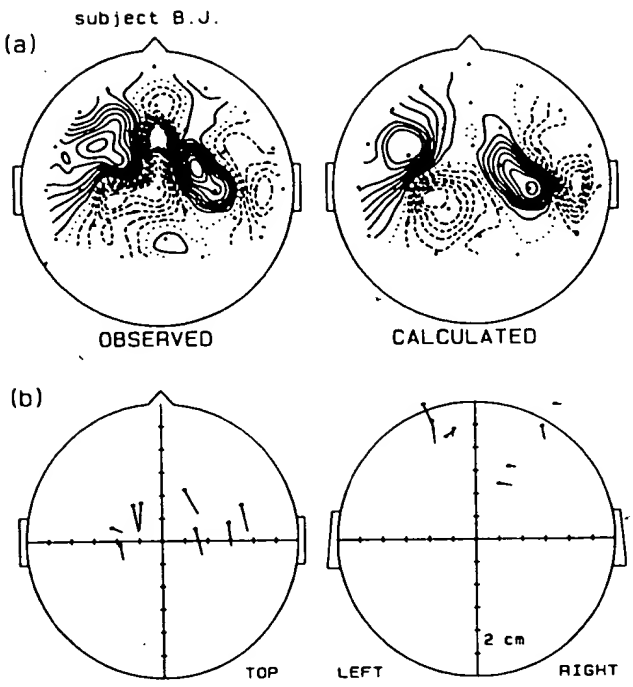

Fig. 3. a Iso-contour maps showing the field patterns for the observed pre-movement field (−70 to −30 ms) (left) and the calculated field (right) for the fitted dipole (map details as described in Figure 2). Contour steps are 22 fT. **b** Locations of the fitted dipoles for the pre-movement period shown above for 4 subjects shown as projections in head coordinate system described in Table 1. Actual location is the midpoint of each dipole. Square arrow head indicates negative pole. Left: head viewed from above (x–y projection). Right: head viewed from behind (z–y projection). Scale is 2 cm per division. A 12 cm circular head outline is shown to provide perspective only

movement sources. These dipoles were greater in strength than those of the pre-movement sources and were directed in the posterior-lateral direction oriented tangential to the scalp surface (Fig. 5a). The goodness of fit values were relatively low, most likely due to the additional flux over the ipsilateral hemisphere.

Field subtraction

From examination of the MEG waveforms and contour maps it was noted that the dipolar patterns observed prior to movement onset appeared to continue during movement onset over the hemisphere ipsilateral to the side of movement, whereas the pattern changed significantly on the contralateral side. In order to assess the extent to which the pre-movement fields could account for the pattern after EMG onset, a field subtraction procedure was employed in which the pre-movement field (−70 to −30 ms) was subtracted from the post-EMG onset period where the maximum reversal was observed (90–130 ms). For subjects showing clear post-movement reversals, these "difference fields" did not differ greatly from the original data. However, for the subjects who did not have clearly interpretable patterns, the field subtraction resulted in the emergence of very clear dipolar patterns over the contralateral rolandic region; an example of this effect is shown in Fig. 4. Single dipole fits computed for the difference fields resulted in locations of equivalent dipoles that were similar to those com-

Table 2. Parameters for least-squares fitted dipoles for the movement-evoked field **a** and difference fields **b** for the same time period in each subject. For description of dipole parameters see Table 1

a "Movement-evoked field"

Subject	Moment (nA-m)	Position (cm) X	Y	Z	Orientation x	y	z	Radius (cm)	Goodness of fit
T.R.	20.7	0.67	2.18	8.64	−0.17	0.84	0.51	8.9	74%
B.J	—	—	—	—	—	—	—	—	<50%
R.G.	27.1	−0.46	1.26	8.10	−0.50	0.00	−0.87	8.2	68%
D.C.	—	—	—	—	—	—	—	—	<50%
H.W.	15.0	0.71	2.13	8.92	−0.75	0.51	0.41	9.2	60%
Mean	20.9 (±2.5)							8.8 (±0.7)	

b "Difference field"

Subject	Moment (nA-m)	Position (cm) X	Y	Z	Orientation x	y	z	Radius (cm)	Goodness of fit
T.R.	21.8	0.27	1.83	8.96	−0.26	0.92	0.29	9.2	88%
B.J.	37.5	−0.65	3.04	9.26	−0.51	−0.18	−0.84	9.8	90%
R.G.	31.6	−0.93	1.84	8.35	−0.49	−0.23	−0.84	8.6	86%
D.C.	25.7	0.60	0.85	8.12	−0.92	0.11	0.38	8.2	65%
H.W.	11.4	−0.21	2.50	9.37	−0.92	0.39	0.04	9.7	65%
Mean	25.6 (±3.2)							9.1 (±0.8)	

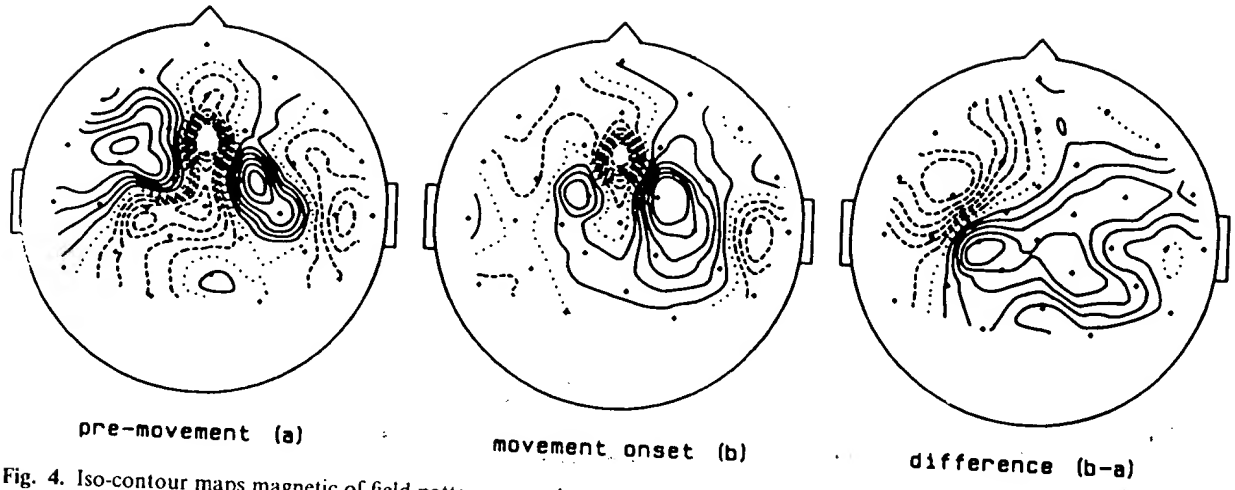

Fig. 4. Iso-contour maps magnetic of field patterns over the scalp in one subject (B.J.) showing effect of field subtraction procedure (map details as described in Fig. 2). Left: pre-movement field −70 to −30 ms as shown in Fig. 2. Middle: movement onset period 90–130 ms after EMG onset. Right: "difference" field as result of subtracting pre-movement field (**a**) from movement-onset field (**b**). Contour steps are 30 fT

puted without field subtraction but accounted for much more of the variance (see Table 2b). Figure 5 shows the comparison of dipoles fitted to the same time interval with and without field subtraction.

Discussion

Magnetic fields accompanying voluntary movements

The slow magnetic field shifts observed prior to voluntary, unilateral flexions of the index finger, in all subjects tested, resembled the previously reported slow fields preceding movements of the digits (Deecke et al. 1982; Hari et al. 1983). As in these previous studies, the slow pre-movement or "readiness fields" observed in this study demonstrated reversals over the region of the rolandic fissure contralateral to the side of movement indicating sources located in sensorimotor cortex. However, field reversals were also present over the ipsilateral hemisphere suggesting that additional sources in ipsilateral cortex also contribute to slow magnetic field shifts prior to movement. Dipole source estimates for the period immediately preceding movement onset (approximately 50 ms prior to EMG onset) indicate that contralateral field reversals can be explained by an equivalent current dipole source located in the region of the rolandic fissure directed anteriorly. This observation is consistent with the hypothesis that dipolar sources arise from localized current flow in the region of the hand area of the primary motor cortex (MI) with anteriorly directed current flow away from the cortical surface, al-

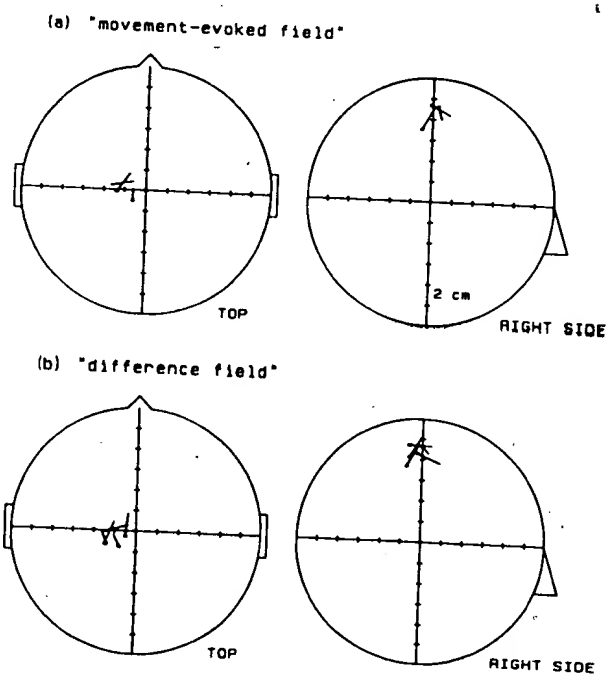

Fig. 5a, b. Comparison of 3-dimensional locations of dipole source fitted to movement-evoked fields **a** and "difference fields" **b** as given in Table 2. Left: head viewed from above (x–y projection). Right: head viewed from right side (z–x projection). Dipoles are projections in head coordinate system described in Table 1

though, in some subjects, these dipoles showed a tendency towards a vertical orientation. The algorithm used placed the second equivalent dipole in the ipsilateral hemisphere, but not in a consistent location across all subjects, indicating that a single

dipole may not adequately describe the ipsilateral activity.

These observations agree with recent evidence regarding slow negative potential shifts in both contralateral and ipsilateral sensorimotor cortex preceding unilateral finger movements obtained from subdural recordings in humans (Neshige et al. 1988). The bilateral activity reported was followed by increased contralateral negativity beginning 250 to 400 ms prior to EMG onset, which also corresponds to the time interval in which magnetic fields reversals over the contralateral rolandic area became discernible in the present study. Furthermore, in the study of Neshige et al. the generators of these potentials were estimated to be vertically oriented, surface negative, dipolar sources, or in some subjects, posteriorly directed dipoles oriented horizontally in the rolandic fissure. The assumption that MEG fields are primarily due to *intracellular* current flow, as opposed to extracellular volume currents (Williamson and Kaufman, 1981) would account for the opposite orientation of the anteriorly directed dipoles predicted from the neuromagnetic measurements.

The topography of readiness fields recorded in the present study did not suggest sources within the supplementary motor area (SMA), although this area is likely involved in the preparation for voluntary movements, as a variety of evidence indicates (Deecke 1987; Goldberg 1985). Accordingly, the SMA should be bilaterally active prior to movement onset and therefore contribute to the overall pattern of flux over the central scalp. However, it can also be speculated that bilaterally active SMA sources would, in general, produce relatively weak fields at the surface (due to their depth and opposing orientations) and are consequently obscured by the larger fields arising from more superficial sources in primary motor cortex. Evidence of SMA sources of magnetic field activity preceding movement has been previously reported (Deecke et al. 1983) although this was with respect to a small number of recordings concentrated over the frontal midline. Furthermore, these authors used a more complex finger tapping task which may have elicited more activation of the SMA. Thus, it is not yet clear to what extent SMA activity may contribute to premovement fields recorded at the scalp surface and to what extent this may vary with the type of movements being performed.

Ipsilateral readiness fields

Although the presence of slow shifts over the ipsilateral hemisphere was noted in previous studies of movement-related magnetic fields (cf., Deecke et al. 1982), the topographical distribution of these fields has not been extensively examined. The distribution of ipsilateral shifts observed in the present study constituted separate field reversals over the ipsilateral hemisphere and did not appear to be related to reversals over the contralateral hemisphere. Recordings of EMG activity in both forearms indicated that these shifts cannot be directly attributed to 'mirrored' movements of the ipsilateral fingers, suggesting that sources in both cerebral hemispheres were activated during the preparation for unilateral movements. Neshige et al. (1988) also observed ipsilateral slow potentials in sensorimotor cortex in their subdural recordings. Their subdural potentials constituted a slowly increasing negativity which persisted throughout the movement period peaking after EMG onset and they bear a strong resembalance to the slow ipsilateral magnetic fields observed in the present study.

The origin of ipsilateral field reversals observed in the MEG data is still unclear although they are most likely related to preparatory processes in ipsilateral motor systems which are active, even when the subjects are instructed to perform unilateral movements. Although the ipsilateral fields observed could not be attributed to a simple dipolar source in the rolandic fissure, the possible activation of ipsilateral motor cortex can not be ruled out since this activation may be widespread or inhibitory (and possibly non-dipolar) in nature.

Movement-evoked fields and sensory feedback

Fields observed immediately following EMG onset were restricted to the contralateral hemisphere and also reversed in direction over the rolandic fissure. The onset of these fields in the present study occurred at about 90 msec following onset of EMG activity and may be related to the beginning of physical movement of the finger. Thus, the term "movement-evoked field" (MEF) is used here to describe those changes occurring after onset of electromyographic activity.

The results of the field subtraction procedure employed here were particularly instructive. The lack of the presence of a MEF in two subjects was initially assumed to reflect movement-induced artifact. However, subtraction of pre-movement activity produced clearly dipolar fields over the contralateral post-rolandic area in subjects who showed complex (non-dipolar) post-EMG onset fields. Interestingly, subjects who had such non-dipolar fields also had the most pronounced pre-movement fields, indicating that individual differences in cortical

morphology (eg., different orientations of cortical dipoles) may account for the observed differences since these fields would summate at the scalp differently in different subjects. One possible interpretations of the results of the subtraction procedure on the MEF is that there is a temporal overlapping of the pre-movement "motor fields" with other sources arising in the same region at the time of movement onset. This interpretation is consistent with the further observations of Neshige et al., in which they noted that the subdurally recorded pre-movement 'motor potential' appeared to continue up to 130 ms following EMG onset and overlapped in time with other potentials which became active during movement onset.

It was possible to achieve significant dipole fits for the "difference field" MEFs with consistent locations across subjects. The subtraction of pre-movement fields changed only slightly, the dipole locations and magnitudes for those fields to which a dipole could be previously fitted, and produced very similar source locations in subjects whose original data showed very non-dipolar patterns during the same time interval. Equivalent dipole sources were fitted to the contralateral rolandic area, posterior to, and approximately 1 cm greater in depth than the fitted pre-movement sources. Given their depth and horizontal orientation, these sources may reflect activity in somatosensory cortex located in the posterior bank of the rolandic fissure (areas 3a and 3b) which receives both muscle and cutaneous afferents (Kass 1984) and may be related to sensory feedback from the periphery during movement onset. Although the latency of the MEF suggests that it originates from peripheral input during movement onset, it is not yet clear as to whether such responses are related to sensory feedback alone or whether they could also be attributed to the activity of post-rolandic neurons involved in voluntary movement onset itself (Fromm and Evarts 1982). Additionally, the indication of a persistence of pre-rolandic activity during movement onset may be explained in terms of peripheral or central feedback to motor cortex (Wiesendanger and Miles 1982).

The present study indicates that neuromagnetic recordings can provide useful information regarding cortical sources associated with voluntary movement and the possible role of both contralateral and ipsilateral generators in scalp-recorded movement-related potentials. Cortical sources related to magnetic field changes accompanying movement onset (movement-evoked fields) can also be identified, although such sources may be of a complex nature and probably represent simultaneous activity in both pre- and post-central cortex associated with the control and sensory-feedback of the actual movement.

References

Becker W, Kristeva R (1980) Cerebral potentials prior to various force deployments. Prog Brain Res 54: 189–195

Deecke L (1987) Bereitschaftspotential as an indicator of movement preparation in supplementary motor area and motor cortex. In: Porter R (ed) Motor areas of the cerebral cortex. Ciba Foundation symposium 132. Wiley, Chichester, pp 231–250

Deecke L, Boschert J, Brickett, P, Weinberg H (1983) Magnetoencephalographic evidence for possible supplementary motor area participation in human voluntary movement. In: Weinberg H, Stroink, G, Katila T (eds) Biomagnetism: applications and theory. Pergamon Press, New York, pp 369–372

Deecke L, Boschert J. Weinberg H, Brickett P (1983) Magnetic fields of the human brain (Bereitschaftsmagnetfeld) preceding voluntary foot and toe movements. Exp Brain Res 52: 81–86

Deecke L, Weinberg H, Brickett P (1982) Magnetic fields of the human brain accompanying voluntary movements: Bereitschaftsmagnetfeld. Exp Brain Res 48: 144–148

Fromm C, Evarts EV (1982) Pyramidal tract neurons in somatosensory cortex: central peripheral inputs during voluntary movement. Brain Res 238: 186–191

Goldberg G (1985) Supplementary motor area structure and function: review and hypothesis. Behav Brain Sci 8: 567–616

Hari R, Kaukoranta, E (1985) Neuromagnetic studies of somatosensory system: principles and examples. Progr Neurobiol 24: 233–256

Hari R, Antervo A, Katila T, Poutanen T, Seppänen M, Tuomisto T, Varpula T (1983) Cerebral magnetic fields associated with voluntary limb movements. Nuova Cimento 2D: 484–494

Harrop R, Weinberg H, Brickett P, Dykstra C, Robertson A, Cheyne D, Baff M, Crisp D (1987) The biomagnetic inverse problem: some theoretical and practical considerations. Phys Med Biol 32; 1545–1557

Kaas JH (1984) The organization of somatosensory cortex in primates and other mammals. In: Euler C von, Franzen O, Lindblom O, Ottoson D (eds) Somatosensory mechanisms. Macmillan Press, London, pp 51–59

Kaukoranta E, Hämäläinen M. Sarvas J, Hari R (1986) Mixed and sensory nerve stimulation activate different cytoarchitectonic areas in the human somatosensory cortex SI. Exp Brain Res 63: 60–66

Kornhuber HH, Deecke L (1965) Hirnpotentialänderungen bei Willkürbewegungen und passiven Bewegungen des Menschen: Bereitschaftspotential und reafferente Potentiale. Pflügers Arch 284: 1–17

Kristeva R, Deecke L (1980) Cerebral potentials preceding right and left unilateral and bilateral finger movements in sinistrals. Prog Brain Res: 54 748–754

Kutas M, Donchin E (1974) The effect of handedness, the responding hand, and response force on the contralateral dominance of the readiness potential Science 186: 545–548

Neshige R, Lüders H, Shibasaki H (1988) Recording of movement-related potentials from scalp and cortex in man. Brain 111: 719–736

Preusser A (1984) Computing contours by successive solution of quintic polynomial equations. ACM Trans Math Software 10: 463–472

Romani GL, Rossini P (1988) Neuromagnetic functional localization: principles, state of the art, and perspectives. Brain Topog 1: 5–21

Vrba J, Fife A, Burbank M, Weinberg H, Brickett P (1982) Spatial discrimination in SQUID gradiometers and 3rd order gradiometer performance. Can J. Phys 60: 1060–1073

Weinberg H, Brickett P, Coolsma F, Baff M (1986) Magnetic localization of intracranial dipoles: simulation with a physical model. Electroenceph Clin Neurophysiol 64: 159–170

Wiesendanger M, Miles TS (1982) Ascending pathway of low-threshold muscle afferents to the cerebral cortex and its possible role in motor control. Physiol Rev 62: 1234–1270

Williamson SJ, Kaufman L (1981) Magnetic fields of the cerebral cortex. In: Erne SN, Hahlbohm HD, Lübbing H (eds) Biomagnetism. Walter De Gruyter, Berlin New York, pp 353–402

Received April 11, 1989 / Accepted June 30, 1989

Electroencephalography and clinical Neurophysiology, 91 (1994) 286–294

EEG 93624

A spatio-temporal dipole model of the readiness potential in humans. II. Foot movement

Koen B.E. Böcker [a,b,*], Cornelis H.M. Brunia [b] and Pierre J.M. Cluitmans [c]

[a] *Co-operation Centre Tilburg and Eindhoven Universities, Tilburg (The Netherlands),* [b] *Physiological Psychology Section, Tilburg University, P.O. Box 90153, 5000 LE Tilburg (The Netherlands), and* [c] *Division of Medical Electrical Engineering, Eindhoven University of Technology, Eindhoven (The Netherlands)*

(Accepted for publication: 18 May 1994)

Summary Readiness potentials (RP) have been recorded in 9 subjects who performed voluntary unilateral plantar flexions with the right or left foot. These show a paradoxical ipsilateral dominance. Spatio-temporal dipole models were obtained for these data, by iterative parameter estimation. The non-uniqueness of the inverse problem leads to several models which describe the data almost equally well, and which all pass orthogonality tests for the individual residuals and source waves. In these dipole models the ipsilateral preponderance is attributed to generators in the contralateral hemisphere, which agrees with results from MEG recording. According to these models the main generators of the RP are in the primary motor cortex, one bilaterally in its posterior wall and the other in the contralateral crown. This agrees with earlier results for finger RPs. However, for foot RPs, it was difficult to distinguish individual sub-components in both the observed scalp potentials and the estimated temporal activation patterns of the dipoles. Some of the presented models include a fronto-central dipole which possibly represents activity of the supplementary motor area. It is concluded that this finding is at best suggestive and needs further investigation.

Key words: Readiness potential; Paradoxical lateralization; Equivalent dipole sources

The execution of self-paced movements is preceded by a slow negative scalp potential, the readiness potential (RP; Kornhuber and Deecke 1965; Deecke and Kornhuber 1977). A robust finding in topographical studies comparing RPs preceding finger and foot movements is that the former show the expected contralateral preponderance, whereas the latter show a paradoxical ipsilateral dominance or no lateralization at all (Brunia and Vingerhoets 1981; Shibasaki et al. 1981; Deecke et al. 1983; Hari et al. 1983a,b; Brunia and Van den Bosch 1984; Brunia et al. 1985).

The hypothesis that this is due to the somatotopic organisation of the primary motor cortex (MI) has been generally accepted. The alternatives, a larger contribution of the uncrossed part of the pyramidal tract to foot than to finger movements or the implication of the ipsilateral cortex in stabilizing movements are quite improbable, given the existing evidence. Hari et al. (1983b) realized that MEG recording might be very useful in discriminating these hypotheses. The readiness magnetic field (RF), the magnetic counterpart of the RP, preceding foot movements showed a pattern which was consistent with a generator in the contralateral mesial cortex and not with a generator in the lateral motor cortex ipsilateral to the movement. However, the negative pole of the activated motor foot area is directed towards the ipsilateral hemisphere. This constitutes the base of the paradoxical lateralization. More recently the homuncular somatotopy of the generators of the RF has been confirmed (Cheyne et al. 1991).

The reasoning of Hari et al. (1983b) could be considered as a precursor of more formal algorithms which use either potential or magnetic field distributions, or both, to infer the underlying generators. These algorithms start with a forward model, which describes the expected potential distribution at the scalp given a specific set of generators (e.g., Helmholtz 1853; Wilson and Bayley 1950). The inverse problem is solved by an iterative search for the localization and orientation parameters of equivalent (or vector-sum) dipoles which best describe the observed potentials (e.g., Scherg and Picton 1991). These parameters together with the time-course of the dipole moments, the so-called source waves, form a spatio-temporal dipole model which best describes the observed data.

Below we shall present spatio-temporal dipole models of the RP preceding foot movements. One objective

* Corresponding author. Tel.: +31 13 662492; Fax: +31 13 662370; E-mail: K.B.E.Bocker@KUB.NL.

SSDI 0013-4694(94)00153-C

is to test the above interpretation of the ipsilateral dominance of the RP from electrical recordings directly. A possible ipsilaterally located and radially oriented source which contributes to the paradoxical lateralization might have gone unnoticed so far, because MEG is insensitive to radially oriented dipoles (i.e., dipoles perpendicular to the surface, for example in the crown of a gyrus). In contrast, the EEG is sensitive to radial as well as tangential sources.

A second goal is to test whether the spatio-temporal dipole model previously proposed for finger RPs can also be used to describe RPs preceding foot movements. This model (Böcker et al. 1994) consists of a bilateral source in the posterior wall of the precentral gyrus and two contralateral sources in its crown. The former generate the bilaterally symmetrical part of the RP (BP_{sym}) and the latter the contralaterally dominant part or negative slope (NS') and the peak of the RP, i.e., the motor potential (MP), respectively. This model agrees with some earlier findings (Neshige et al. 1988; Kristeva et al. 1991; Bötzel et al. 1993) but not with others. For example, arguments have been put forward for a role of both the supplementary motor area (SMA; e.g., Lang et al. 1991a; Ikeda et al. 1992) and the pre-motor area (PM; e.g., Sasaki and Gemba 1991) in generating the BP_{sym}. Because the amplitude of RPs is generally larger preceding foot movements than preceding finger movements, and the signal-to-noise ratio (S/N ratio) better, it might be possible to obtain better fits, especially for the BP_{sym}, which is rather small preceding finger movements.

Finally, we test the hypothesis that the post-movement reafferent potential (RAP) is generated by the primary somatosensory cortex (SI), as shown by Kristeva et al. (1991) for MEG and Bötzel et al. (1993) for EEG. In our previous study (Böcker et al. 1994) we were unable to model the RAP.

Methods

A more detailed account of the methods is given in the accompanying paper (Böcker et al. 1994).

Subjects, procedure, recording, data analysis and mapping

Nine paid, right handed volunteers participated in the experiment. They produced 125 unilateral plantar flexions with each foot. These were produced in 10 blocks of 25 trials each. Data on 10 blocks of finger contractions were also recorded (Böcker et al. 1994). From these 20 blocks a pseudo-random sequence was constructed.

The feet rested on two separate foot-plates, elevated 30° from the horizontal. The force needed to depress the plates until closure of the switch was adjusted by a spring to be subjectively equal on both sides. Averages were time-locked on switch closure.

The EEG was measured from 23 electrode locations centred around Cz' (1 cm anterior to Cz). Filter settings were at 0.005 Hz (high-pass) and 35 Hz (low-pass) respectively. The EEG and the right vertical EOG (0.005–35 Hz) were A/D converted off-line from −2500 to +2500 sec at 128 Hz. The paper-chart output was scanned for artifacts. All artifact-free trials were averaged for each limb separately. Those averages were divided in 100 msec bins (from −2000 to +1000 msec), which served as input for an ANOVA with Electrode (in antero-posterior and lateral directions), Hemisphere (left, right) and Response side (left, right) as repeated measure factors. Maps of surface potentials (SP) have been computed at selected latencies by spline interpolation (Perrin et al. 1989, 1990), to explore the spatial domain.

Spatio-temporal dipole modelling

BESA software (Versions 1.8 and 1.9; Scherg 1989) was used to obtain spatio-temporal dipole models for the grand-average wave forms. Such a model consists of estimated localization and orientation parameters of stagnant current dipoles and their moment over time which describe the observed scalp potentials as well as possible (Scherg and Picton 1991). Primarily the BESA algorithm is aimed at decreasing the residual variance

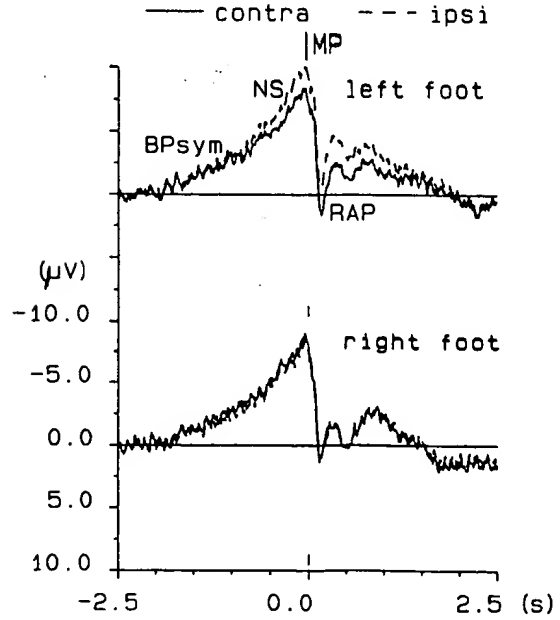

Fig. 1. Time series representation of the grand-average readiness potential (RP; n = 9) preceding plantar flexions of the left (upper graph) and right foot (lower graph) over the C1' and C2', which are either contralateral (solid line) or ipsilateral (broken line), depending on the movement side. Note the paradoxical ipsilateral dominance with left foot movements. BP_{sym}: symmetrical part of the RP; NS': negative slope; MP: motor potential; RAP: reafferent potential.

(RV), an index of the difference between observed and predicted scalp potentials. This cost function was extended with an extra term to penalize solutions with large dipole moments in order to avoid solutions with close-by dipoles which interfere with each other (a so-called energy constraint; Scherg and Berg 1991).

In modelling foot RPs the same 2 initial steps as with finger movements (Böcker et al. 1994) were employed:

(1) Fit two symmetrical regional sources in either hemisphere, on both left and right foot RPs together. A regional source is a system of 3 orthogonal dipoles, which describe the local current flow in each direction (Scherg and Picton 1991).

(2) As 1, but fit both regional sources independently.

The second step resulted in two regional sources at midline positions. Both lateral pointing dipoles nullified each other's activity at the scalp completely and the other pair of tangential dipoles (with an anteroposterior orientation) also partly cancelled out. Therefore, the next step was to:

(3) Remove both laterally oriented and the least active of the sagittally oriented dipoles and fit the 3 remaining dipoles independently.

To test the reliability of this model the next step was to:

(4) Fit the resulting model on left and right foot data separately. This resulted in models with 2 radial and 1 tangential (sagittally oriented) or intermediate dipole. To test whether a more parsimonious 2-dipole model could also account for the data the final step was to:

(5) Remove either radial dipole and fit the 2 remaining dipoles.

This strategy has been complemented by two alternative ones. First MI activity was deliberately modelled by two opposing, laterally oriented dipoles around the midline, with or without a radial, fronto-central dipole, in conformity with the models resulting from steps 4 and 5. This was motivated by anatomical knowledge about the position of the foot motor area (in the mesial part of the precentral gyrus) and the results of a preliminary moving dipole fit constrained to bilateral symmetry. The latter provided the initial positions and orientations for the dipole pair. Second, the models were compared with those which resulted from modelling foot RPs starting from models describing the finger RPs (Böcker et al. 1994).

All models were subjected to residual orthogonality tests (ROT) on the summed cross-products of all pairs of residuals and to source wave orthogonality tests (SOT) on the time series of the dipole moments (Achim et al. 1988, 1991). The ROT evaluates the null hypoth-

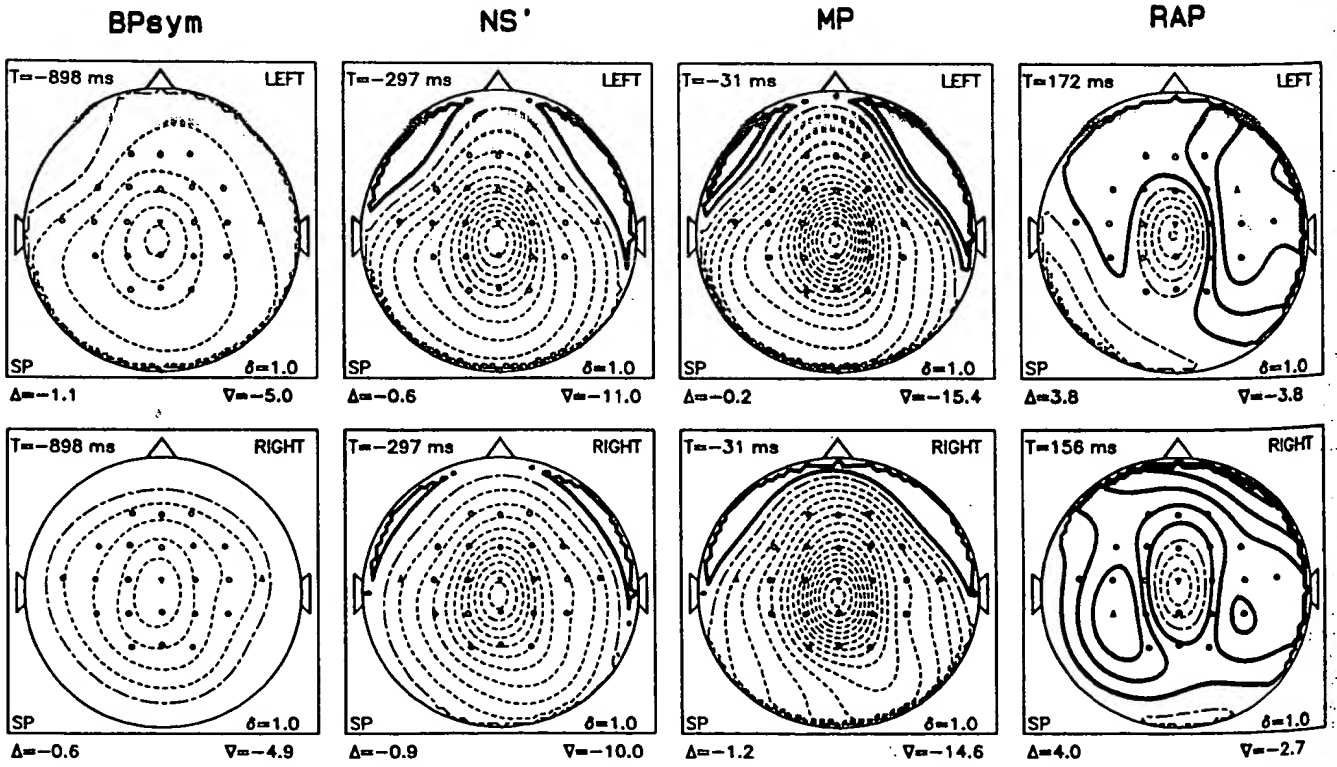

Fig. 2. Radially projected surface potential (SP) maps for each of the RP components preceding left (upper) and right (lower) foot movements. Latency is shown at the top left (in msec). Solid lines indicate positive potentials, broken lines negativity. Electrode positions are shown as dots, except for the ones which show the minimum (▽) and maximum (△) values. The latter values (in μV) are indicated below the map. Spacing between isopotential lines is 1 μV (δ).

sis that all signal and nothing but the signal has been ccounted for, both in space and time. The SOT indiates whether a certain equivalent dipole represents gnificant activity or not. By calculating SOTs at each individual sample it can be investigated during which interval a given source is significantly active. Both orthogonality tests and F values from the ANOVA were evaluated at the 5% level.

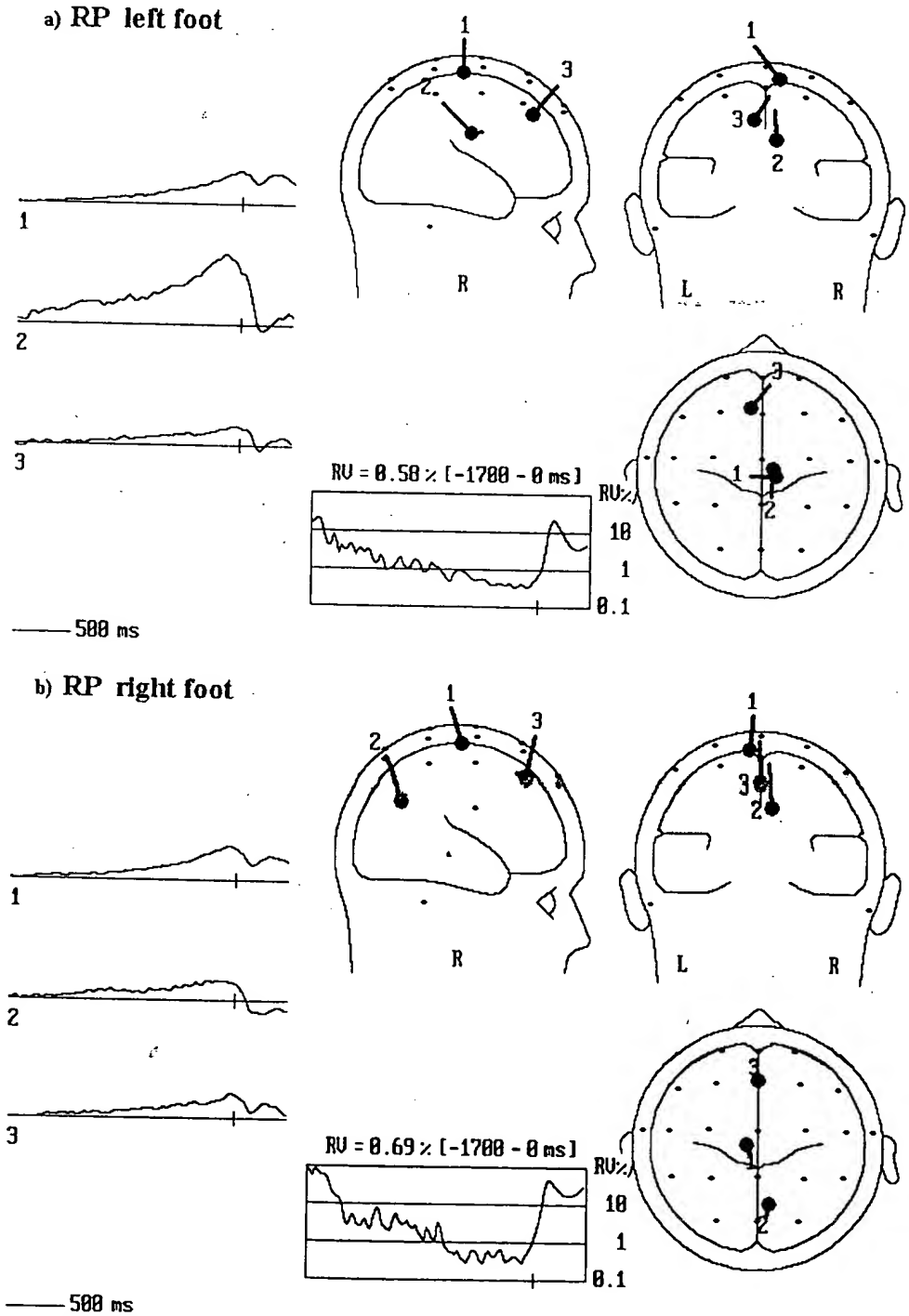

Fig. 3. Spatio-temporal dipole models for left (a) and right (b) foot RPs resulting from step 4 (see text). The fronto-central dipole (dipole 3) is suggestive of SMA activity. Left column: temporal activation pattern of each dipole source in arbitrary units, the so-called source wave. Negativity in the direction of the dipole arrow is plotted upwards. The vertical bar on the time axis (extending from −2000 msec until +500 msec) indicates switch closure (0 msec). The head diagrams represent perpendicular projections of the location and orientations of the corresponding dipole sources, smaller dots indicate electrode positions. The lower part of the middle column shows both the average residual variance (RV) over the whole fit interval (−1700 to 0 msec) and its evolution over time on a logarithmic scale. The RV shows a steep increase at the end of the fit interval.

Results

Time series and topographical maps

The individual averages for left and right foot RPs contained 103 ± 40 and 99 ± 53 trials respectively. The grand averages of these RPs (Fig. 1) show a smooth increase preceding the movement. The ANOVA indicates that the average potential over all channels becomes significantly different from zero at −1700 msec. This effect lasts until 100 msec after switch closure ($6.81 < F\ (1,\ 8) < 50.58$ during this interval). Differences between electrodes are significant from −1900 until +100 msec ($5.88 < F < 21.82$, with Greenhouse-Geisser ϵ equals 0.24 and 0.16 respectively, and nominal degrees of freedom (df) equal to 8, 64). The NS' can only be identified in comparing left and right foot

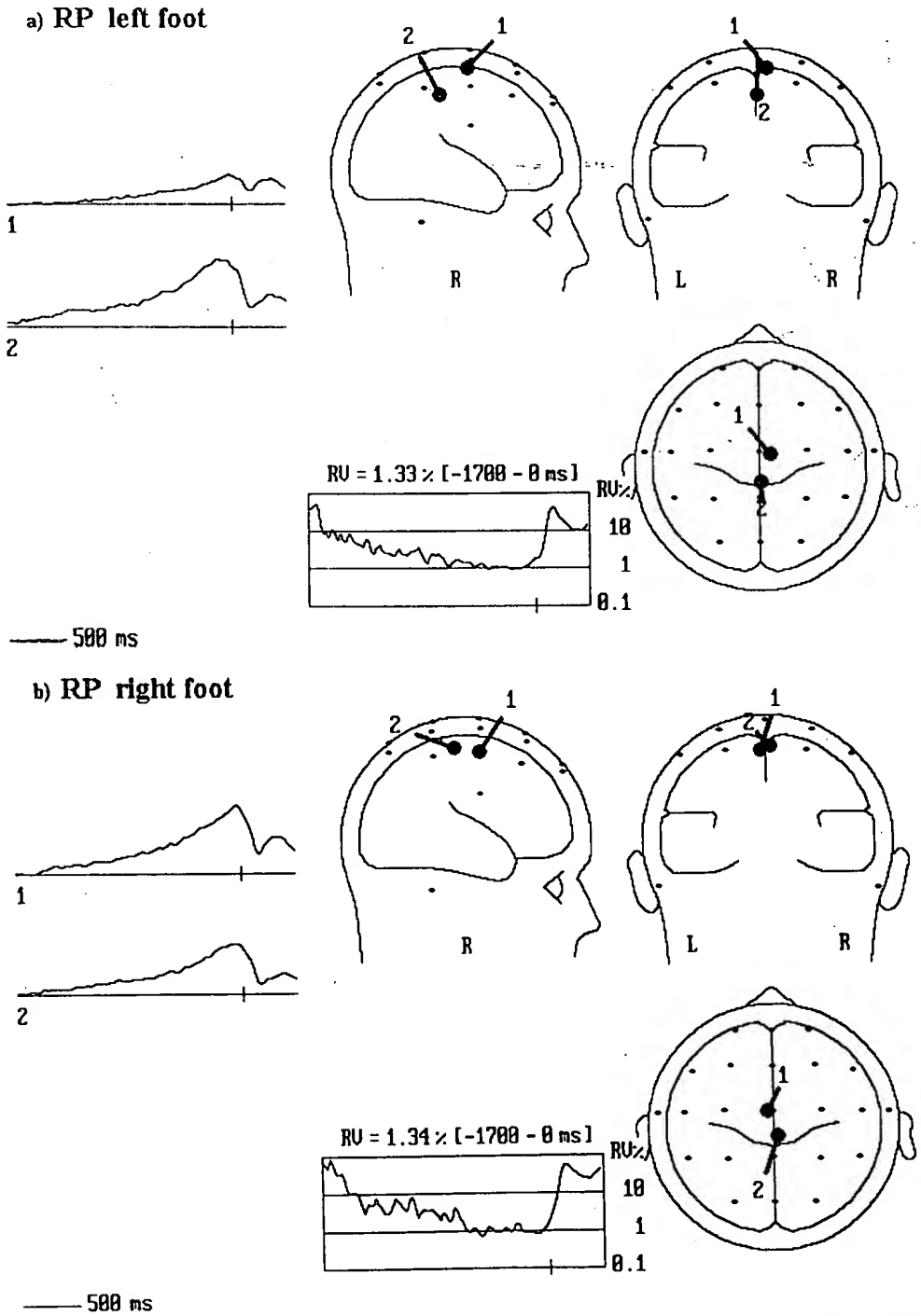

Fig. 4. Spatio-temporal dipole models for left (a) and right (b) foot RPs after deletion of dipole 3 (step 5, see text). The contralateral dipole 1 produces ipsilateral dominant scalp potentials. See Fig. 3 for further legends.

responses over both hemispheres. This comparison shows the expected paradoxical ipsilateral dominance for left foot movements only. In the ANOVA this is expressed as Response side × Hemisphere interaction (−400 msec, +1000 msec; $13.15 < F\ (1, 8) < 91.70$) and the 3-way Response side × Hemisphere × Electrode interaction (−400 msec, 0 msec, $2.90 < F < 4.03$, $\epsilon = 0.39$ and 0.35 respectively and nominal $df = 8, 64$). Based on this analysis we conclude that the BP_{sym} interval extends from −1700 to −400 msec, which is the start of the NS'. The NS' itself terminates at the onset of the MP, i.e., at about −100 msec. A last significant effect prior to switch closure is the Response side × Electrode interaction from −300 to −100 msec ($F = 3.54$ and 3.75, $\epsilon = 0.28$ and 0.30 respectively, and nominal $df = 8, 64$). This interaction is produced by a slightly larger NS' for left compared to right foot movement at precentral, postcentral and parietal electrodes (Fig. 2). After +200 msec the grand average amplitude, the main effect of Response side and the 3-way interaction are significant during different intervals.

It can be seen from the grand averages (Fig. 1) that the MP peaks at −31 msec for both responses and the RAP at +172 msec and +156 msec for left and right foot responses, respectively. A paired t test on the individual RAP latencies indicates that the left-right difference is not statistically significant ($t\ (8) = 0.49$, NS). The small positive-going peak, reminiscent of a PMP, which precedes the MP at latencies of −94 msec and −125 msec respectively, could not be identified reliably in single subjects.

The SP maps show a nearly perfect bilaterally symmetrical distribution at all pre-movement latencies (Fig. 2). Only the RAP is characterized by a different pattern.

Spatio-temporal dipole modelling of the RP preceding plantar flexion of the foot

Figs. 3 and 4 show the models which result after step 4 and step 5 (after deletion of dipole 3) respectively. The models in Fig. 4 essentially do not differ from those obtained starting out from Fig. 3 and deleting dipole 1. Probably due to larger amplitudes for foot RPs compared to finger RPs, and consequently better S/N ratios, these models account for over 90% of the data from as early as −1700 msec onwards, i.e., from the onset of BP_{sym}. Therefore all models have been fitted to account for the data from −1700 until 0 msec. The models with 3 dipoles (Fig. 3) perform slightly better (with regard to RV) than models with only 2 dipoles (Fig. 4). After reinsertion of the deleted frontal dipole (dipole 3) in the models of Fig. 4 it does not describe any variance nor interfere with the other dipoles (1 and 2). However, after all parameters are optimized once again the models of Fig. 3 reappear. When the SMA test dipole proposed by Bötzel et al. (1993) is inserted in Fig. 4 it also fails to describe any activity, even after optimizing its orientation. SOTs for this dipole never reach significance.

ROTs (Table I) show that there is some signal left at Fz' in left foot residuals of the 2-dipole model (Fig. 4a). SOTs on dipole moments show them to be significant during the entire test interval for nearly all dipoles in Figs. 3 and 4 (none fails to achieve an overall significant t value). Inspection of the individual source waves for the 2-dipole model presented in Fig. 5 leads to the same conclusion.

Starting out from the 4-dipole solutions reached for finger data presented in our previous paper (Böcker et al. 1994, Fig. 6) and deleting dipoles which interfere too much, or show essentially zero moments, one arrives at solutions comparable to those presented in Fig.

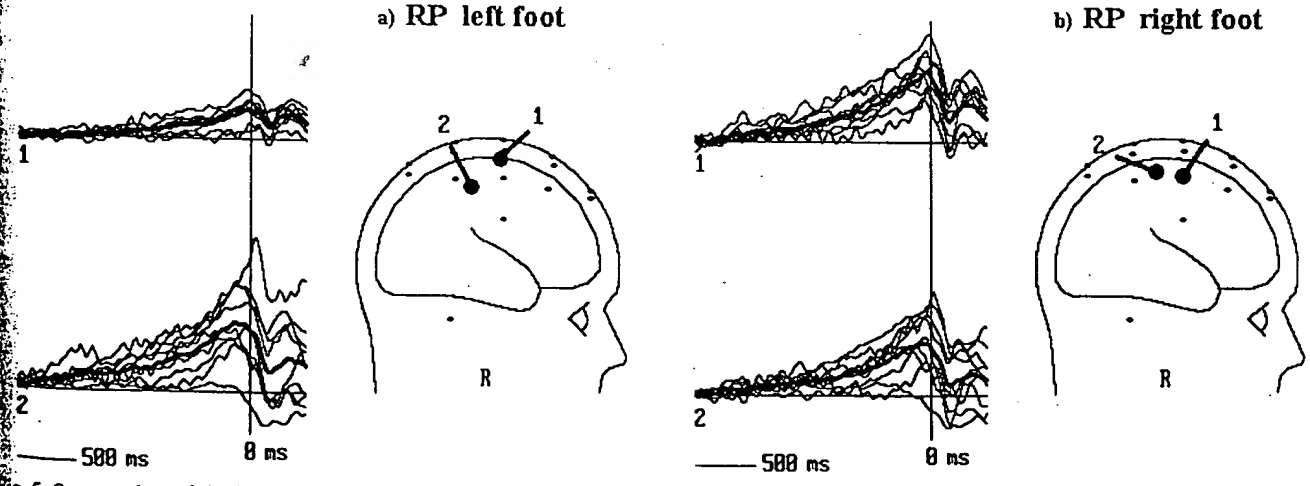

Fig. 5. Scatter plots of the individual (thin lines) and grand average (thick line) source waves for the 2-dipole models (Fig. 4) for left (a) and right (b) foot RPs. For most subjects both dipoles are active during the whole interval of fit (−1700 to 0 msec).

TABLE I
Residual variances (RV) for the interval of fit (−1700 to 0 msec) and results of orthogonality tests on residuals (ROT; third column) and source waves (right column). The first column gives the number of the figure which graphically represents the corresponding model. The second column gives the RV not explained by the model in percentage of the power of the observed potentials. For ROTs channels with significant residual signal are listed, indicating failure of the model to describe all systematic variance. For SOTs the sources which fail to reach significance overall are given. This indicates that the individual dipole moments do not show systematic time courses.

Figure no. of corresponding model	RV (%)	ROT	SOT
3a (left foot)	0.58	–	–
3b (right foot)	0.69	–	–
4a (left)	1.33	Fz'	–
4b (right)	1.34	–	–

4. Ergo, the models presented in Figs. 3 and 4 are sufficiently reliable in that they can be reached from different starting positions and can be mutually transformed into each other by adding or removing dipole 3, respectively.

The efforts to model MI activity by two opposing sources in the mesial part of area 4 failed, because those dipoles largely interfered and cancelled each other's activity. Correlations over time between potentials predicted at the scalp ranged from −0.54 to −0.66 for those dipoles. Furthermore they did not pass the ROT.

As indicated by the steep increase in RV after switch closure (Figs. 3 and 4) the models presented so far are clearly deficient in describing the RAP. Attempts to extend those models with extra dipoles to describe the RAP either failed or resulted in physiologically irrelevant models (too deep and too lateral dipoles for example), which did not pass the ROT or SOT.

Discussion

This study was aimed at constructing a spatio-temporal dipole model for the RP preceding foot movements. The two main objectives were to test and extend the previous model for finger RPs (Böcker et al. accompanying paper) and to evaluate the interpretation which is generally given to account for the ipsilateral dominance of the RP preceding foot movements.

To start with the latter issue, all models include a radial dipole (dipole 1) which is located in the contralateral hemisphere, but is directed to the ipsilateral one. This is even true for right foot RPs (Figs. 3b and 4b) which did not show a clear lateralization at the scalp. So, the conclusion of Hari et al. (1983b) based on MEG recording is confirmed by our models based on EEG. The paradoxical ipsilateral dominance of the foot RP is due to the location of the foot motor area in the mesial cortex.

With regard to the RP models in general we first note that with foot movements the interval in which the models are able to account for over 90% of the variance (−1700 to 0 msec) starts at the onset of BP_{sym}. However, as with finger movements (Böcker et al. 1994), we fail to model the RAP.

The choice between the models of Figs. 3 and 4 comes down to choosing for the presence or absence of dipole 3 and its interpretation. The most reasonable interpretations of this dipole are activation of the SMA (Lang et al. 1991a) or PM bilaterally (Sasaki and Gemba 1991). The fact that it was found with foot, but not with finger movement, can be explained by the difference in S/N ratio. However, from a modelling point of view both possibilities are improbable. Activation of the SMA bilaterally would lead to almost perfect cancellation at the scalp (Lang et al. 1991a). A rough simulation, without added noise, indicated that a single dipole could account for only 40% of the resulting negativity around FCz'. It is also very improbable that a bilateral activation of PM would be lumped onto a single dipole. In the case of finger movements, recorded with the same electrode array in the same experiment, we were able to separate ipsilateral and contralateral contributions from the lateral motor cortices (Böcker et al. 1994), although the foot representation within PM would be closer to the midline (Hashimoto et al. 1981). However, the Fig. 3 model does account for all the signal, whereas the Fig. 4a model leaves some variance at Fz' during the last 200 msec preceding the response. Considering the location, at the border of the electrode set-up, and timing, during NS' and MP which we presume to stem from MI (Böcker et al. 1994), of this small residual signal we do not consider it as very important for the present argument. On the other hand, models for left and right foot RP differ considerably with the presence of dipole 3 and are almost equal in its absence. In this sense the Fig. 4 model is more reliable. Furthermore, if dipole 3 is merely inserted into Fig. 4, its source wave is almost flat, i.e., it does not account for the signal which is not explained by dipoles 1 and 2. In conclusion, we consider the more parsimonious 2-dipole model (Fig. 4) as our best model in describing the RP preceding foot movements, although we cannot totally exclude a possible contribution of either the SMA or PM.

The interpretation of our final model (Fig. 4) is quite straightforward and converges with the one for finger RPs (Böcker et al. 1994). First of all, as with finger movements, all generators are supposed to be inside the primary motor cortex (Neshige et al. 1988; Bötzel et al. 1993). Dipole 1 represents the crown of the precentral gyrus at the edge of the lateral and

mesial cortex (see Scherg and Picton 1991). By its orientation, this source produces the ipsilaterally dominant scalp potentials. Dipole 2, which is at the midline, represents the bilateral activation of the posterior wall of the precentral gyrus. A similar dipole was described by Cheyne et al. (1991) to account for the magnetic counterpart of the RP preceding foot movements. Both dipoles 1 and 2 show a forward torque with respect to truly radial and tangential orientations. This agrees with a comparable torque of the central sulcus near the midline on MRI scans (Steinmetz et al. 1989).

The model is not clearly defined in the time domain. Both source waves are significant during almost the entire fit interval for both left and right RPs (Fig. 5). Based on our former study (Böcker et al. 1994) we would expect both the NS' and the MP to show up on separate radial dipoles. However, the NS' shows up on the tangential dipole 2 instead. Furthermore, for left foot responses the MP is characterized by a positive shift in dipole 2, as opposed to a discrete peak at dipole 1. From our spatio-temporal models the timing of cortical activation therefore seems to be different for foot as compared to finger movements, or at least more variable from trial to trial. This is in agreement with the fact that the scalp potentials themselves are also less defined in the time domain. For instance the PMP, the epiphenomenon of the transition between NS' and MP (Neshige et al. 1988; Böcker et al. 1994), is not present in our individual average foot RPs.

The lack of temporal specification of the data, and the fact that the generators are closely together in space (the mesial foot motor areas), may have produced a mislocation of variance among the dipoles which are part of the models. The details of the present model might be improved by research in for instance Parkinson patients (Dick et al. 1989) or under different experimental conditions (Lang et al. 1991b), which selectively affect some RP components and not others. A combined investigation of the RP preceding finger and foot movements, like the research presented here, benefits from the temporal resolution of the former and the increased S/N ratio of the latter. With this type of research the RP might be shown to involve different loops (Dick et al. 1989) from both the cerebellum and the SMA, via the thalamus to multiple functional motor areas in MI (e.g., in its wall and crown). Spatio-temporal dipole modelling guided by a priori knowledge and combined with a statistical test like the ROT (Achim et al. 1988, 1991) will be capable of disentangling both loops.

References

Achim, A., Richer, F., Alain, C. and Saint-Hilaire, J.-M. A test of model adequacy applied to the dimensionality of multi-channel average auditory evoked potentials. In: F. Samson-Dollfus et al. (Eds.), Statistics and Topography in Quantitative EEG. Elsevier, Paris, 1988: 161–171.

Achim, A., Richer, F. and Saint-Hilaire, J.-M. Methodological considerations for the evaluation of spatio-temporal source models. Electroenceph. clin. Neurophysiol., 1991, 79: 227–240.

Böcker, K.B.E., Brunia, C.H.M. and Cluitmans, P.J.M. A spatio-temporal dipole model of the readiness potential in humans. I. Finger movement. Electroenceph. clin. Neurophysiol., 1994, 91: 275–285.

Bötzel, K., Plendl, H., Paulus, W. and Scherg, M. Bereitschaftspotential: is there a contribution of the supplementary motor area? Electroenceph. clin. Neurophysiol., 1993, 89: 187–196.

Brunia, C.H.M. and Van den Bosch, W.E.J. Movement-related slow potentials. I. A contrast between finger and foot movements in right-handed subjects. Electroenceph. clin. Neurophysiol., 1984, 57: 512–527.

Brunia, C.H.M. and Vingerhoets, A.J.J.M. Opposite hemisphere differences in movement related potentials preceding foot and finger flexions. Biol. Psychol., 1981, 13: 261–269.

Brunia, C.H.M., Voorn, F.J. and Berger, M.P.F. Movement-related slow potentials. II. A contrast between finger and foot movements in left-handed subjects. Electroenceph. clin. Neurophysiol., 1985, 60: 135–145.

Cheyne, D., Kristeva, R. and Deecke, L. Homuncular organization of human motor cortex as indicated by neuromagnetic recordings. Neurosci. Lett., 1991, 122: 17–20.

Deecke, L. and Kornhuber, H.H. Cerebral potentials and the initiation of voluntary movement. In: J.E. Desmedt (Ed.), Attention, Voluntary Contraction and Event-Related Cerebral Potentials. Prog. Clin. Neurophysiol., Vol. 1. Karger, Basel, 1977: 132–150.

Deecke, L., Boschert, J., Weinberg, H. and Brickett, P. Magnetic fields of the human brain (Bereitschaftsmagnetfield) preceding voluntary foot and toe movements. Exp. Brain Res., 1983, 52: 81–86.

Dick, J.P.R., Rothwell, J.C., Day, B.L., Catello, R., Buruma, O., Gioux, M., Benecke, R., Berardelli, A., Thompson, P.D. and Marsden, C.D. The Bereitschaftspotential is abnormal in Parkinson's patients. Brain, 1989, 122: 233–244.

Hari, R., Antervo, A. and Salmi, T. Slow EEG potentials preceding self-paced plantar flexion of hand and foot. Acta Physiol. Scand., 1983a, 119: 55–59.

Hari, R., Antervo, A., Katila, T., Poutanen, T., Seppäläinen, M., Tuomisto, T. and Varpula, T. Cerebral magnetic fields associated with voluntary limb movements in man. Nuovo Cimento, 1983b, 2D: 484–494.

Hashimoto, S., Gemba, H. and Sasaki, K. Distribution of slow cortical potentials preceding self-paced hand and hindlimb movements in the premotor and motor areas of monkeys. Brain Res., 1981, 224: 247–259.

Helmholtz, H. Ueber einige Gesetze der Vertheilung elektrischer Ströme in körperlichen Leitern mit Anwendung auf die thierisch-elektrischen Versuche. Ann. Phys. Chem., 1853, 89: 211–233.

Ikeda, A., Lüders, H.O., Burgess, R.C. and Shibasaki, H. Movement-related potentials recorded from supplementary motor area and primary motor area. Role of supplementary motor area in voluntary movements. Brain, 1992, 115: 1017–1043.

Kornhuber, H.H. and Deecke, L. Hirnpotentialänderungen bei Willkürbewegungen und passiven Bewegungen des Menschen: Bereitschaftspotential und reafferente Potentiale. Pflügers Arch., 1965, 284: 1–17.

Kristeva, R., Cheyne, D. and Deecke, L. Neuromagnetic fields accompanying unilateral and bilateral voluntary movements: topography and analysis of cortical sources. Electroenceph. clin. Neurophysiol., 1991, 81: 284–298.

Lang, W., Cheyne, D., Kristeva, R., Beistainer, R., Lindinger, G. and

Deecke, L. Three-dimensional localization of SMA activity preceding voluntary movement. A study of electric and magnetic fields in a patient with infarction of the right supplementary motor area. Exp. Brain Res., 1991a, 87: 688–695.

Lang, W., Cheyne, D., Kristeva, R., Lindinger, G. and Deecke, L. Functional localization of motor processes in the human cortex. In: C.H.M. Brunia, G. Mulder and M.N. Verbaten (Eds.), Event-Related Brain Research. Electroenceph. clin. Neurophysiol. (Suppl. 42). Elsevier, Amsterdam, 1991b: 97–115.

Neshige, R., Lüders, H. and Shibasaki, H. Recording of movement-related potentials from scalp and cortex in man. Brain, 1988, 111: 719–736.

Perrin, F., Pernier, J., Bertrand, O. and Echallier, J.F. Spherical splines for scalp potential and scalp current density mapping. Electroenceph. clin. Neurophysiol., 1989, 72: 184–187.

Perrin, F., Pernier, J., Bertrand, O. and Echallier, J.F. Corrigendum. Electroenceph. clin. Neurophysiol., 1990, 76: 565.

Sasaki, K. and Gemba, H. Cortical potentials associated with voluntary movements in monkey. In: C.H.M. Brunia, G. Mulder and M.N. Verbaten (Eds.), Event-Related Brain Research. Electroenceph. clin. Neurophysiol. (Suppl. 42). Elsevier, Amsterdam, 199: 80–96.

Scherg, M. Brain Electrical Source Analysis. Versions 1.8 and 1.9 1989–1992.

Scherg, M. and Berg, P. Use of prior knowledge in brain electromagnetic source analysis. Brain Topogr., 1991, 4: 143–150.

Scherg, M. and Picton, T.W. Separation and identification of event-related potential components by brain electric source analysis. In: C.H.M. Brunia, G. Mulder and M.N. Verbaten (Eds.), Event-Related Brain Research. Electroenceph. clin. Neurophysiol. (Suppl. 42). Elsevier, Amsterdam, 1991: 24–37.

Shibasaki, H., Barrett, G., Halliday, E. and Halliday, A.M. Cortical potentials associated with voluntary foot movements in man. Electroenceph. clin. Neurophysiol., 1981, 52: 507–516.

Steinmetz, H., Fürst, G. and Meyer, B.-U. Craniocerebral topography within the international 10–20 system. Electroenceph. clin. Neurophysiol., 1989, 72: 499–506.

Wilson, F.N. and Bayley, R.H. The electric field of an eccentric dipole in a homogenous spherical conducting medium. Circulation, 1950, 1: 84–92.

Electroencephalography and clinical Neurophysiology, 91 (1994) 275–285

EEG 93623

A spatio-temporal dipole model of the readiness potential in humans. I. Finger movement

Koen B.E. Böcker [a,b,*], Cornelis H.M. Brunia [b] and Pierre J.M. Cluitmans [c]

[a] *Co-operation Centre Tilburg and Eindhoven Universities, Tilburg (The Netherlands),* [b] *Physiological Psychology Section, Tilburg University, P.O. Box 90153, NL-5000 LE Tilburg (The Netherlands), and* [c] *Division of Medical Electrical Engineering, Eindhoven University of Technology, Eindhoven (The Netherlands)*

(Accepted for publication: 18 May 1994)

Summary Preceding unilateral finger movements readiness potentials (RPs) were recorded in 9 right-handed subjects. The data are presented as time series, potential maps and spatio-temporal dipole models. The latter are interpreted with respect to the underlying generators of the RP. Explicit hypotheses about the unilateral or bilateral activation of particular sensorimotor areas preceding unilateral movements are addressed. The choice for the best spatio-temporal dipole model was guided by a test on the orthogonality of the individual residuals and by a priori neurophysiological evidence. From the final model it is concluded that the initial bilateral symmetrical part of the RP is generated in the posterior walls of the precentral gyrus bilaterally, whereas the later lateralized components originate from the crown of that same gyrus contralaterally. This confirms and extends data from subdural recording, magnetoencephalography (MEG) and EEG.

Key words: Readiness potential; Motor asymmetries; Lateral sensorimotor cortices; Equivalent dipole sources; Residual orthogonality test

In 1965 Kornhuber and Deecke were the first to observe that a simple self-paced finger movement is preceded by a slow negative potential starting 1500 msec before movement onset. This potential has become known as the *Bereitschaftspotential* (BP) or readiness potential (RP).

Different components are distinguished in the RP complex (Fig. 1a). It starts with a bilaterally symmetrical part (BP_{sym}). From about −500 msec (i.e., 500 msec before movement onset) the negative slope of the potentials contralateral to the movement side increases, constituting the negative slope (NS'; Shibasaki et al. 1980). Next, at about −100 msec, follows a positive deflection, the pre-motion positivity (PMP), which was reported to be either bilaterally symmetrical (Deecke and Kornhuber 1977) or to show an ipsilateral [1] dominance (Shibasaki and Kato 1975; Shibasaki et al. 1980). The maximum negativity, or motor potential (MP) is generally observed at about movement onset over the contralateral scalp. The MP is interpreted as the cortical activation of the final common pathway, the pyramidal tract. Direct physiological evidence for this interpretation comes from combined recordings of slow potentials and multiple unit activity in the monkey (Arezzo et al. 1977). The post-movement potentials are generally dominated by 2 positive peaks, the reafferent potentials (RAPs). In the remainder of the paper we shall reserve the acronym RP to denote the whole complex of potentials which precedes self-paced movements.

The interpretation of the results from RP recording under different experimental conditions (e.g., Lang et al. 1990) and in patients with, for example, Parkinson's disease (Dick et al. 1989) or large brain resections (Singh and Knight 1990) would profit from knowledge about the generators of the RP. Arguments for different functional interpretations of the RP recorded from different parts of the scalp are reviewed elsewhere (Brunia 1987, 1988). Yet, the physics of volume conduction imply that there is no one-to-one relationship between the potential at a certain scalp position and the cortex directly underneath. In principle knowledge about the generators could be gained from solving the inverse problem by dipole source modelling (e.g., Scherg and Picton 1991). The location and orientation parameters of the dipoles within the model, together with the time-course of the dipole moments provide a

* Corresponding author. Tel.: +31 13 662492; Fax: +31 13 662370; E-mail: K.B.E.Bocker@KUB.NL.

[1] The expressions ipsi- and contralateral are used with respect to the movement side.

SSDI 0013-4694(94)00152-B

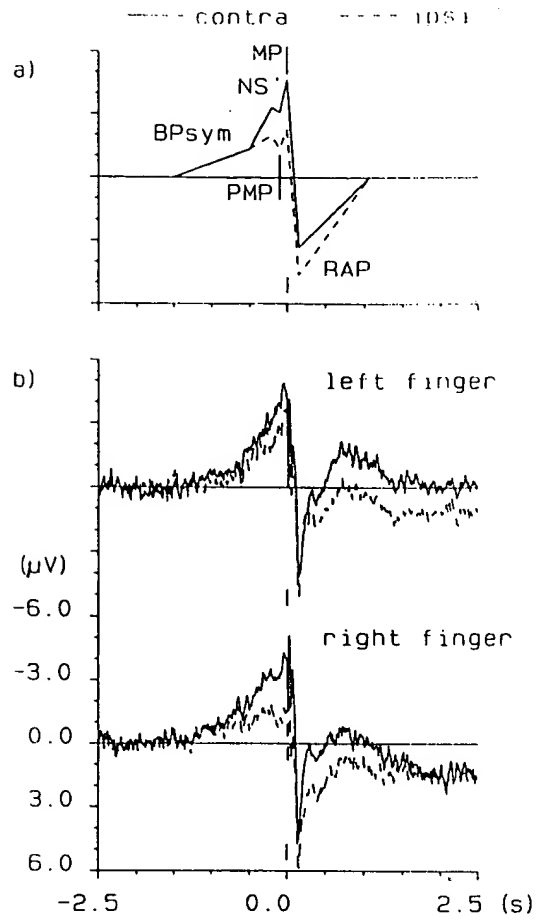

Fig. 1. a: schematic representation of the readiness potential (RP) over the contralateral (solid line) and ipsilateral (broken line) hemispheres; b: grand-average RPs (n = 9) recorded preceding left (upper graph) and right (lower graph) finger flexions over C3′ and C4′, which are either contralateral (solid line) or ipsilateral (broken line) depending on the movement side. Note the contralateral dominance. BP_{sym}: symmetrical part of the RP; NS′: negative slope; PMP: premotion positivity; MP: motor potential; RAP: reafferent potential.

spatio-temporal model of the observed potentials. The present study is aimed at constructing such a model of the RP preceding finger flexions.

However, the solution of the inverse problem is not unique and a priori knowledge is necessary to guide the modelling strategy and to evaluate the validity of the obtained solutions. For RPs this knowledge might be gained from invasive measurements during the execution of voluntary self-paced movements. Unfortunately the outcome of these studies differs according to the species under investigation and the dependent measure. At the one extreme are the studies of Sasaki and Gemba (1991, for an overview) who recorded transcortical potentials in macaque monkeys and concluded that the pre-motor cortex (PM), the primary motor cortex (MI) and the somatosensory cortex (SI) are activated in succession prior to movement onset. In their experiments all 3 areas are active bilaterally, but MI and SI show a clear contralateral preponderance. On the other side, Neshige et al. (1988) concluded from epicortical recording in man that the RP is generated by MI exclusively, BP_{sym} by bilateral activation and NS′ and MP by contralateral activation. Blood flow changes were also restricted to MI, at least with simple repetitive movements (Roland et al. 1980; Walter et al. 1992). A possible role of the supplementary motor area (SMA) is much debated. Epicortical recording (Ikeda et al. 1992, 1993) in man and magnetoencephalography (MEG) in a patient with a unilateral SMA lesion (Lang et al. 1991) indicate that the SMA is active at least during the early part of the RP (BP_{sym}).

EEG dipole modelling studies gave inconsistent results. Bötzel et al. (1993) noted the absence of SMA activity and Toro et al. (1993) its presence. Apart from methodological differences this might be due to the fact that the volume currents produced by bilateral activation of the SMA largely cancel each other (Lang et al. 1991). The size of this (partial) cancellation effect depends on the exact spatial distribution of activity within the SMA and its effect on dipole modelling has not yet been accounted for in sufficient detail. Furthermore, neither study presented statistical evidence to indicate whether or not the contribution of the presumed SMA dipole was statistically significant.

Apart from the role of the SMA, Bötzel et al. (1993) and Toro et al. (1993) agree on the modelling of the BP_{sym}/NS′ by a bilateral pair of dipoles and the MP by a contralateral one. All dipoles presumably represent activation of MI. However, both studies report somewhat different orientations for corresponding dipoles. The antero-posterior component of the tangential BP_{sym} dipoles reported in those studies coincides with that of the bilateral symmetrical pair of dipoles described by Kristeva et al. (1991) for the magnetic counterpart of the RP. The latter authors interpreted these dipoles to lie in the posterior wall of the precentral gyrus, which is part of MI.

In modelling the RP we shall test the hypotheses put forward by Brunia (1987, 1988). The first hypothesis is that the BP_{sym} is generated by bilateral activity from the SMA and/or PM. Furthermore, we propose that the NS′ is mainly generated by MI, with a contralateral preponderance (see also Neshige et al. 1988). The MP is hypothesized to stem from a very small area of the contralateral pre-central gyrus, i.e., MI (Arezzo and Vaughan 1975). And finally the RAP would be mainly generated by SI. However, some of the most direct evidence (Neshige et al. 1988; Bötzel et al. 1993) points to the possibility that MI may be the sole generator of all pre-movement potentials (BP_{sym}, NS′, MP) in the RP complex. With respect to the generators of the PMP we lack a precise hypothesis, but we doubt whether it constitutes an independent neurophysiological event (Neshige et al. 1988).

We shall test these hypotheses by developing spatio-temporal dipole models for the RP preceding self-paced finger flexions, recorded in healthy human subjects. In humans the fingers are represented at rather lateral positions within all sensorimotor areas except the SMA. Scalp potentials which are generated by the synchronous activity of 2 homologous lateral areas, like the finger motor areas, cannot be described accurately by a 1-dipole model. So, by spatio-temporal dipole modelling it is possible to discriminate unilateral from bilateral generators of the RP preceding finger flexions, which will be represented by either 1 dipole or a symmetrical pair of dipoles, respectively.

The spatio-temporal form of dipole source analysis is a powerful tool to disentangle the activity of sources which overlap in time (Achim et al. 1988a). This is useful because the BP_{sym}, NS' and MP seem to ride on top of each other. More specifically we shall evaluate our models by their ability to separate the MP from the other components and impose penalties on temporal overlap to ensure such separation (see below). Finally, we shall statistically test whether a given model describes all signal and nothing but the signal and whether all dipoles in that model are significantly active or not (Achim et al. 1988b, 1991). Up to now, such conclusions have been drawn on the base of subjective criteria only.

Methods

Subjects

Nine right-handed subjects, 6 women and 3 men, age range 19–30 years, participated in the experiment. They were paid volunteers and received Dfl. 75.-- (about US $45.--) for their participation in the experiment.

Procedure

Subjects were seated comfortably in a slightly reclining chair, placed in a sound attenuating, electrically shielded room. They were instructed to produce unilateral self-paced finger or foot movements at a slow pace. Responses which followed the preceding one by less than 6 sec were discarded from later analyses. A complete registration consisted of 500 trials (4 limbs × 5 blocks × 25 trials). The target limb was varied pseudo-randomly between blocks. Only finger movements will be discussed here. Data on foot movements are presented in the accompanying paper (Böcker et al. 1994).

The arms of the subject rested on the adjustable arms of the chair. The subject held a small cylinder (length 5.5 cm), mounted on top of the chair's arm, between thumb and index finger (pincer-grasp). Flexion of thumb and index finger produced the closure of a switch, which delivered the trigger pulse for all subsequent averaging.

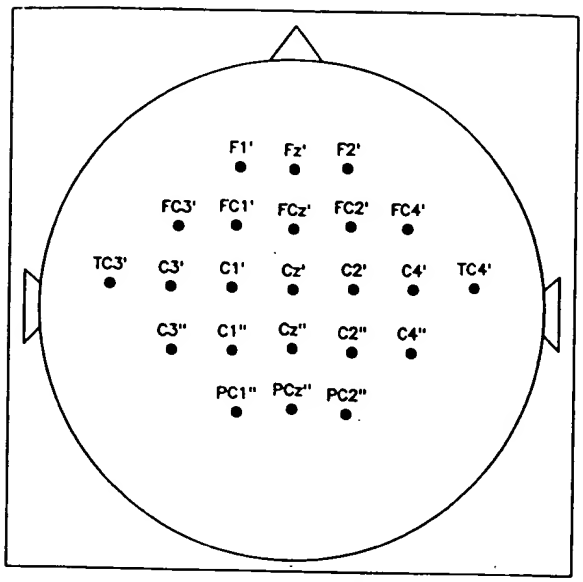

Fig. 2. The electrode set-up used in this study. Nomenclature is derived from the international 10–20 system. Primes (') denote positions 1 cm anterior and double primes (") positions 2 cm posterior to the standard coordinates. The inter-electrode distances measure 10% of the nasion-inion distance. Reference electrode: software-linked mastoids.

Subjects were instructed to fixate their gaze on a point on the wall 2 m in front (to preclude eye movements and blinks) and to prevent all kinds of movement, like gross body movements, sneezing and swallowing, from about 3 sec before until 3 sec after the movement.

Electrophysiological recording

The EEG was recorded from 23 electrodes at scalp positions which were defined with respect to the international 10–20 system (Fig. 2). The electrode array was centred around Cz and consequently covered the scalp above the areas which are hypothesized to generate the RP. All recordings were referenced to software-linked mastoids. The signals were amplified by two 14-channel Nihon Kohden 4314F EEG machines with a modified 30 sec time constant, which shared the reference and ground electrodes. Low-pass filtering was at 35 Hz (−6 dB/octave). After storage on 2 TEAC SR58 analog tape recorders, the data were A/D converted off-line on a VAXLAB equipped with an ADQ32 ADC, at 128 Hz in burst mode.

The vertical EOG of the right eye was recorded with the same filter settings as the EEG for monitoring of ocular artifacts. Additionally, the horizontal and left vertical EOGs were available on paper-chart.

Data analysis

Trials free of artifacts for a 5 sec interval centred around the trigger pulse (i.e., switch closure) were

selected, based on the paper-chart output. These trials were baseline corrected over the first 500 msec.

For each subject 4 average RPs were obtained, one for each limb. The average finger RPs were divided into 100 msec bins from −2000 to +1000 msec. The average amplitudes within each bin for each of the 18 non-midline electrodes were subjected to an analysis of variance (ANOVA) with Electrode (in antero-posterior and lateral direction), Hemisphere (left, right) and Response side (left, right) as repeated measure factors. The main purpose of the ANOVA was to indicate the transition between BP_{sym} and NS', which should be characterized by a significant Hemisphere × Response side and/or 3-way interaction. Greenhouse-Geisser corrected degrees of freedom were used for factors comprising more than 2 levels (Vasey and Thayer 1987). The F statistics were evaluated at the 5% level.

The spatial dimension of the grand average RPs was investigated by calculating surface potential (SP) maps after Perrin et al. (1989, 1990) at selected latencies. These are presented because the potential distribution is used to estimate the location and orientation of the dipoles in equivalent dipole models.

Spatio-temporal dipole modelling

Spatio-temporal dipole modelling uses time-variant, spatially stagnant, equivalent current dipoles to model electrically active brain areas (Scherg and Picton 1991). An overview of the possibilities and limitations of the method (Lopes da Silva and Spekreijse 1991; Mitzdorf 1991; Scherg and Picton 1991) can be summarized by stating that spatio-temporal dipole modelling is quite capable of describing the physiological basis of macroscopic scalp potentials, like the RP. In the present study, spatio-temporal dipole modelling was carried out using BESA software, versions 1.8 and 1.9 (Scherg 1989). Using BESA required to convert the data to average reference and to reduce to 40 Hz sample rate, after 10 Hz (−24 dB/octave) digital low-pass filtering to prevent aliasing. The models were fitted on the grand average, to obtain models which describe the most reliable characteristics of the spatio-temporal data matrix. Besides, the signal-to-noise ratio of the grand average is better than that of the individual traces.

The general non-uniqueness of the inverse problem is dealt with in BESA by providing the researcher with tools to incorporate a priori knowledge about the generators (i.e., to impose restrictions) interactively. For example, the cost-function (the residual variance, RV) was extended to include a penalty for large moments in general, to avoid solutions comprising close-by, interfering dipoles. Within BESA this is called an energy constraint (Scherg and Berg 1991). The following strategy was used in obtaining the final results for RPs preceding unilateral finger flexions:

(1) Fit two symmetrical regional sources, one in each hemisphere. A regional source is a system of 3 orthogonal dipoles. Such a system describes the local current flow in all directions (Scherg and Picton 1991).

(2) As step 1 but fit both regional sources independently, i.e., they are allowed to assume asymmetrical locations.

(3) Remove the laterally pointing dipoles because of interference and fit the remaining 4 dipoles independently.

All the above steps were executed on left and right hand data together. By doing so a symmetrical solution was reached, because each hemisphere serves as both ipsilateral and contralateral hemisphere at once. In this model, the time series of the moment of a given dipole which are associated with ipsilateral and contralateral movements respectively, already indicate whether the brain area represented by that dipole is unilaterally or bilaterally activated. This already answers our main research question, which is to gain insight into the bilateral or unilateral activation of the lateral cortical sensorimotor areas preceding voluntary movement, provided the model is correct. If it is correct indeed, then the model should also describe the data of each movement separately. Therefore, subsequent steps involved:

(4) Fit the model to the RP of one hand at a time and incorporate converging evidence (see above) that the MP is generated by a circumscribed cell assembly within MI. This was done by extending the cost-function of BESA with a so-called variance constraint (Scherg and Berg 1991) which penalizes variance (i.e., dipole moments) outside a certain time interval for a given source.

(5) Transpose the dipoles to homologous positions in the opposite hemisphere, i.e., mirror them with respect to the mid-sagittal plane. Subsequently this mirror image was fitted to the RP preceding flexions of the opposite finger.

The last two steps were executed twice, once starting with the left and once again with the right hand RP as input.

The reliability of the inverse solution was assessed by applying residual orthogonality tests (ROT; Achim et al. 1988b, 1991) to evaluate multiple solutions which explain nearly equal amounts of variance. The ROT is based on a Student's t test on the sum of cross-products of the residuals over space and time, and it tests for the presence of systematic spatio-temporal patterns in these residuals over all possible pairs of sub-ensemble averages. A significant positive t value indicates undermodelling, i.e., a failure to describe all systematic variance. On the contrary, a significant negative t value indicates overmodelling, i.e., a partial fit on the noise. All t statistics were evaluated for significance at the 5% level. We used the individual averages as sub-ensemble averages. To decrease the large error variance

associated with between-subject ROTs, we did not calculate the residuals with respect to the grand average model. Instead, we calculated the residuals after a least-squares fit of the individual time-variant dipole moments. The time series of the dipole moments can also be subjected to an orthogonality test (Achim et al. 1991), which we will call source wave orthogonality test (SOT). Similar to the residuals in the ROT, the sum of cross-products of the source waves is tested for significance over all possible pairs of sub-averages. A significant positive t value indicates that a proposed source contributes significantly and systematically to potentials recorded at the scalp. A more detailed insight into the temporal dynamics of the source waves was obtained by calculating SOTs at each point in time separately. So, the reliability of the spatial dimension of the models is evaluated by the ROT, because the time-variant dipole moments were individually adjusted, whereas the inter-individual stability of their temporal dynamics is tested by the SOT.

Results

Time series and topographical maps

The individual averages for left and right finger RP contained 101 ± 48 and 102 ± 44 trials, respectively. The grand averages of these RPs (Fig. 1b) show the expected time pattern. According to the ANOVA results the average potential over all electrodes is significantly different from zero between -1000 and $+200$ msec (F (1, 8) ranges from 6.15 to 30.94 in this interval). The Response side × Hemisphere interaction is significant from -600 until $+1000$ msec ($8.19 \leq F$ (1, 8) ≤ 49.90) and the 3-way interaction of the latter effect with Electrode from -800 to $+1000$ msec ($3.26 \leq F \leq 22.36$, with Greenhouse-Geisser ϵ equal to 0.38 and 0.32 respectively and nominal degrees of freedom (df) equal to 8 and 64 for numerator and denominator, respectively). The only further effect which extends over a period of more than 100 msec is that of Electrode from -600 to $+100$ msec ($4.48 \leq F \leq 12.08$, $\epsilon =$ 0.25 and 0.18 respectively, nominal $df = 8, 64$). From these results and the time series themselves (Fig. 1b) we conclude that the BP_{sym} starts at -1000 msec and lasts until -600 msec, which marks the start of NS'. The grand average PMP shows onset latencies of -117 msec and -148 msec and peaks at -78 and -109 msec for left and right finger RPs, respectively. Furthermore, it has an ipsilateral preponderance. The next component, the MP, peaks just before switch closure, i.e., at -31 msec and -16 msec for left and right finger flexions and is contralaterally dominant. The largest peak of the RAPs has a latency of $+164$ msec and $+156$ msec, respectively. Paired t tests indicate that none of the differences in latencies between response sides is statistically significant.

Fig. 3 shows the surface potential maps at latencies corresponding to the components which are distinguished in the time domain. All maps up to 0 msec

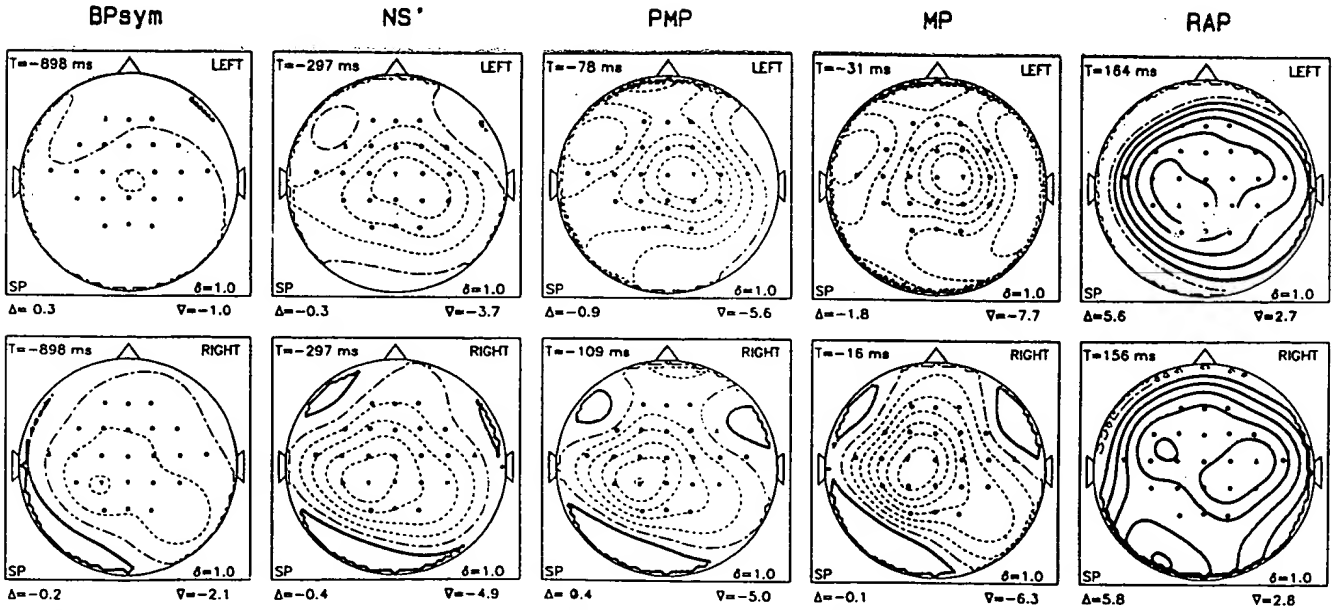

Fig. 3. Radially projected surface potential (SP) maps for each of the RP components preceding left (upper) and right (lower) finger movements. Latency is shown at the top left (in msec). Solid lines indicate positive potentials, broken lines negativity. Electrode positions are shown as dots, except for the ones showing the minimum (∇) and maximum (Δ) values. The latter values (in μV) are indicated below the map. Spacing between isopotential lines is 1 μV (δ).

show a widespread negativity with a contralateral dominance. The RAPs are characterized by a widespread positivity.

Spatio-temporal dipole modelling of the RP preceding finger flexion

The first choice in spatio-temporal dipole modelling is that of the interval of fit. Preliminary fits showed that models including 2 or 3 regional sources described more than 90% of the variance in the data during the interval from about −600 to 0 msec. Therefore, the models presented here (Figs. 4–7) were fitted to the data inside this interval. All attempts to fit a spatio-temporal dipole model for the RAP failed.

Fig. 4 shows the final stage for fits on both left and right RPs together (steps 1–3). Although symmetry constraints no longer apply to this solution, the final dipole locations and orientations remain fairly symmetrical. The model consists of a radial pair (1 and 2) and a tangential pair of dipoles (3 and 4). The tangential dipoles have an antero-posterior orientation. From the time-course of the dipole moments, the source waves (Fig. 4, left column), it can be concluded that from the

TABLE I

Residual variances (RV) for the interval of fit (−600 to 0 msec) and results of orthogonality tests on residuals (ROT, third column) and source waves (SOT, right column). The first column gives the number of the figure which graphically represents the corresponding model. The second column gives the RV not explained by the model in percentage of the variance of the observed potentials. For ROTs channels with significant residual signal are listed, indicating failure of the model to describe all systematic variance on that channel. For SOTs the sources which fail to reach significance over the whole interval of fit are presented. This indicates that the individual dipole moments do not show systematic time courses. The subscript m denotes the mirror image of the original model, which describes RPs preceding movements of the opposite hand and the mirror image of the individual dipoles in the latter model.

Figure no. of corresponding model	RV (%)	ROT	SOT
4 (left finger)	2.29	TC3′	2
(right finger)	4.04	F2′, FC4′, PC1″, C1′	1, 3
5 (left)	1.46	–	–
5_m (right)	2.24	–	–
6_m (left)	1.38	–	$2a_m$, 3_m
6 (right)	1.24	–	3
7_m (left)	1.50	TC3′	2_m
7 (right)	2.24	–	3

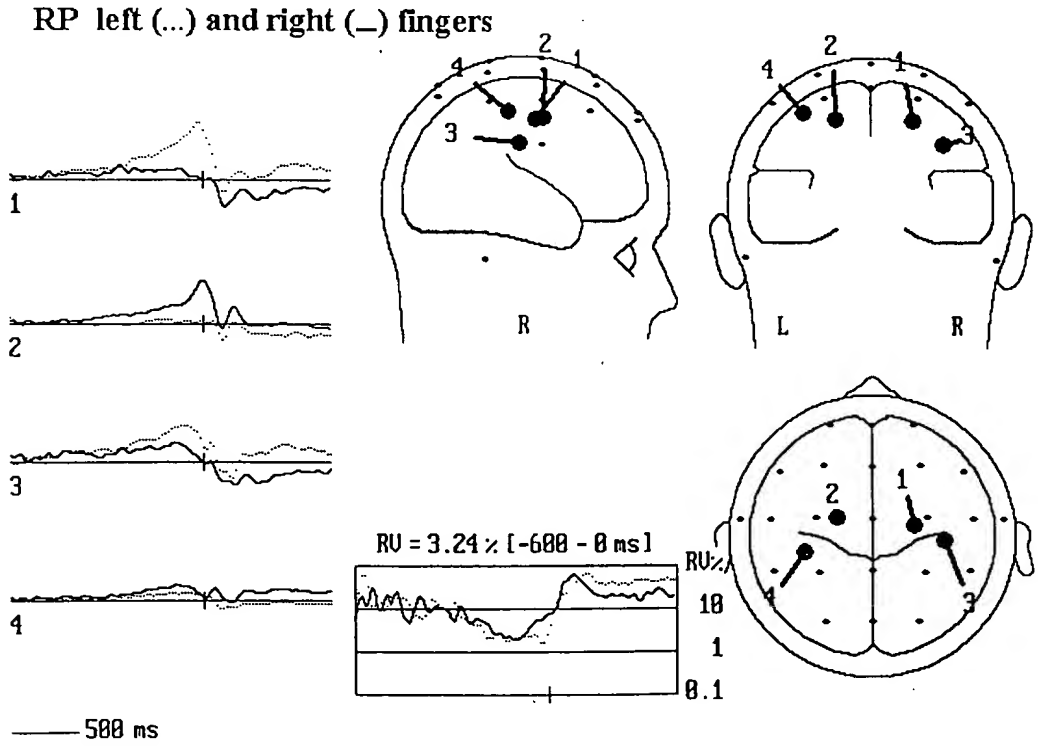

Fig. 4. Spatio-temporal dipole model accounting for both right and left finger RPs (after step 3, see text). Left column: temporal activation pattern of each dipole source in arbitrary units, the so-called source waves. Negativity in the direction of the dipole arrow is plotted upwards. The vertical bar on the time axis (extending from −1500 to +1000 msec) indicates switch closure (0 msec). Note that sources 1 and 2 are only active with left (dotted line) and right (solid line) hand movements, respectively. The head diagrams represent perpendicular projections of the location and orientations of the corresponding dipole sources, smaller dots indicate electrode positions. The lower part of the middle column shows both the average residual variance (RV) over the fit interval (−600 to 0 msec) and its evolution over time on a logarithmic scale.

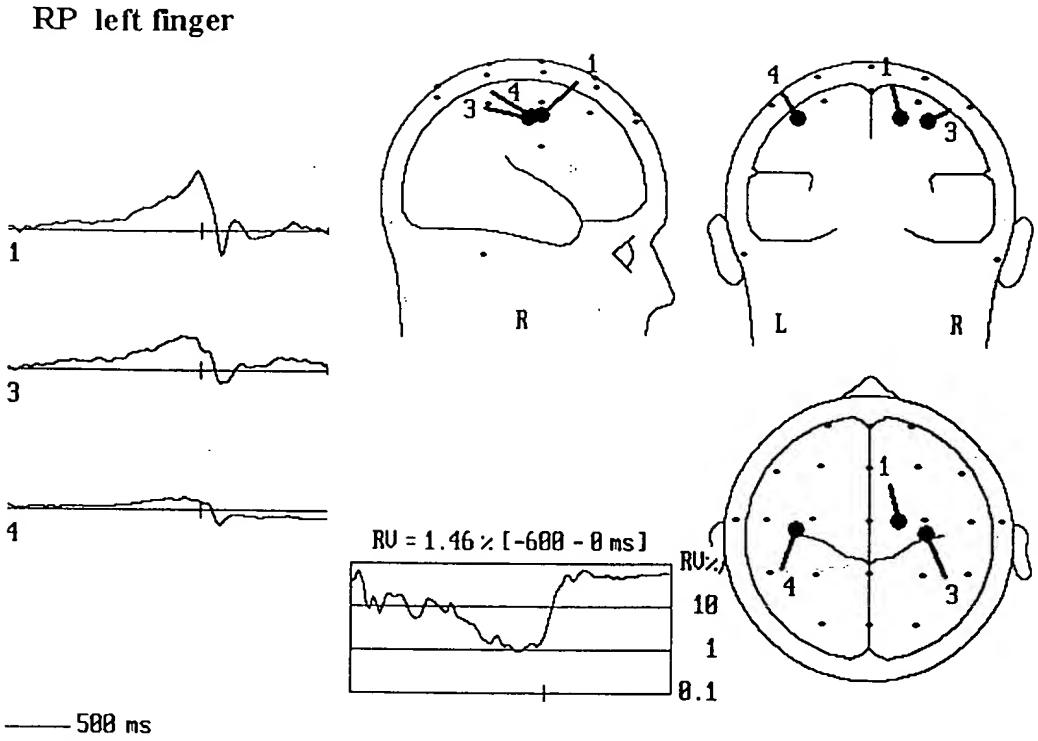

Fig. 5. Spatio-temporal dipole model obtained after fitting the model of Fig. 4 to the left finger RP separately (step 4, see text). The ipsilateral radial dipole (dipole 2) was removed because it did not describe substantial scalp potentials. Note that the RV slowly decreases before and shows a steep increase after the fit interval. See Fig. 4 for further legends.

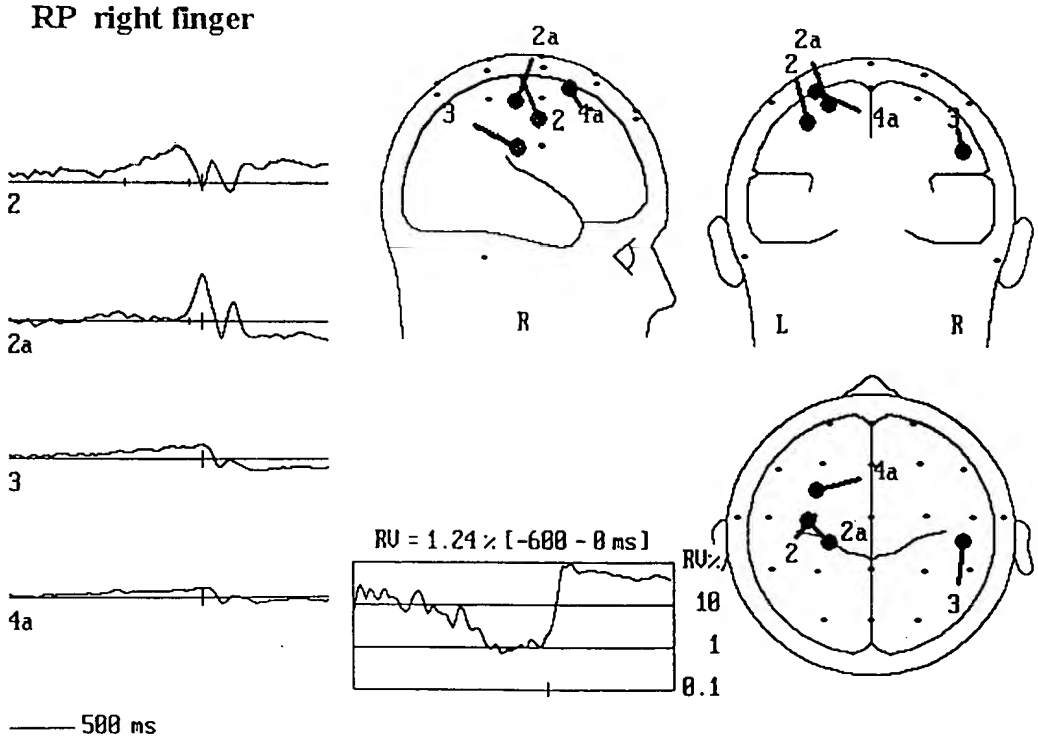

Fig. 6. Spatio-temporal dipole model obtained after fitting the model of Fig. 4 to the right finger RP (step 4, see text). Note the similar activation patterns of sources 3 and 4a, and the activation of sources 2 and 2a during NS' and MP intervals respectively, which was emphasized by variance constraints on dipoles 2 and 2a, for the intervals which are shown by the smaller bars on the time axis. See Fig. 4 for further legends.

radial dipoles only the one contralateral to the moving finger is active. This is confirmed by the SOT (Table I). The tangential pair shows larger moments with contralateral movements than with ipsilateral ones. The ROT shows that the model does not explain all variance at all channels with either response side (Table I).

Fitting the Fig. 4 model on the left finger RP (step 4) leads to minor adjustments only (Fig. 5). The ipsilateral radial dipole (dipole 2) remained at its place, without accounting for much variance and therefore was deleted from the model. The resulting model describes 98.5% of the data. The next step involved transposing all dipoles to the opposite hemisphere. This mirror image describes 97.8% of the right finger RP after optimization (Table I). Both the Fig. 5 model and its mirror image pass the orthogonality tests. So, the individual residuals are orthogonal and all the signal has been accounted for. Furthermore all dipoles are significantly active over the whole interval tested (−600 to 0 msec), with the exception of the ipsilateral dipole for left hand data (dipole 4), which is only significant from −450 to −25 msec. In fact the moments of the contralateral dipoles already are significant before the onset of the fit interval.

Fitting the Fig. 4 solution to right finger RPs (step 4, second time) leads to a model with again only 1 ipsilateral dipole, but in this case 3 contralateral ones (Fig. 6). From the starting position (Fig. 4) dipole 1 assumed a location near dipole 2, indicated as dipole 2a. These 2 dipoles, 2 and 2a, which are closely together in space, showed a tendency to be active in separate time intervals. These intervals roughly correspond to that of NS' and MP respectively. This separation was emphasized by applying variance constraints to force the variance during the NS' (−600, −100 msec) and MP intervals (−100, 0 msec) on sources 2 and 2a, respectively. Finally, dipole 4 is located more anteriorly and is oriented laterally instead of sagittally. It is therefore marked as 4a, to indicate that its parameters have changed considerably in comparison with dipole 4. The final model describes 98.8% of the variance. The mirror image of this model (step 5) again needs only minor adjustments to capture 98.6% of the variance in the left finger data (Table I). However, the mirrors of dipoles 2 and 2a almost coincide in this latter model, and the mirror of 2a is not significantly active according to the SOT (Table I). The model of Fig. 6 and its mirror image pass the ROT (Table I), but the SOT shows the ipsilateral tangential dipole (dipole 3 and its mirror image) to be insignificant for both right and left RPs.

Evaluating Fig. 6 with respect to the hypotheses put forward in the introduction suggested 2 further tests. The first one involved invoking spatial constraints on

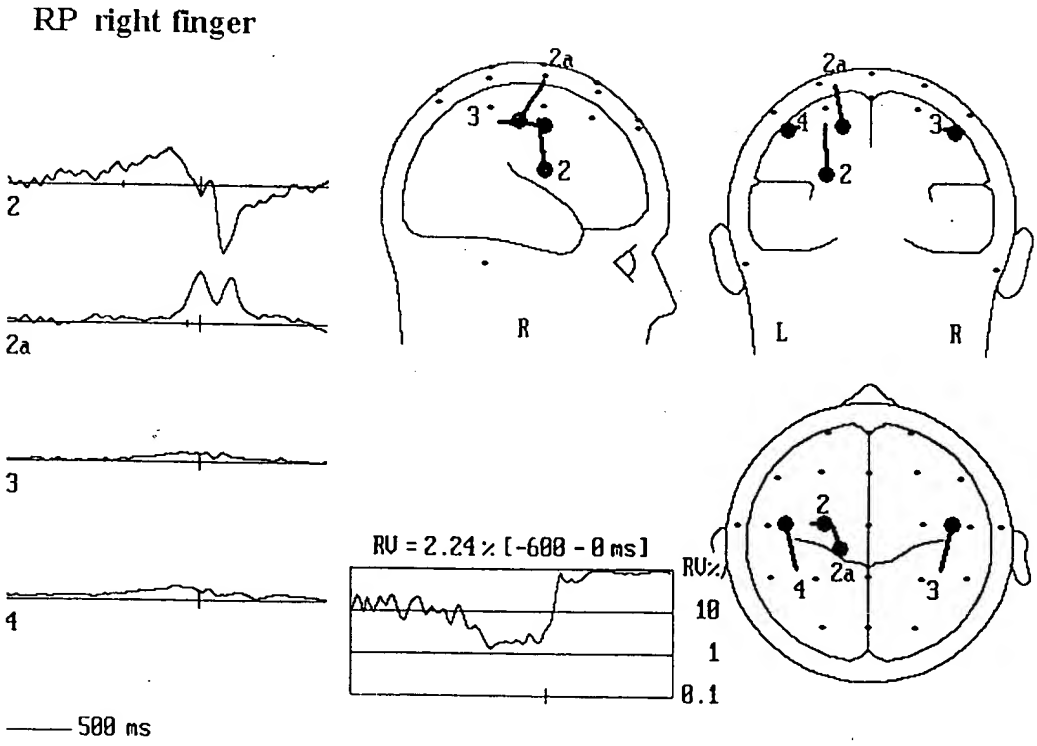

Fig. 7. The model of Fig. 6 after imposition of a mirror constraint on dipoles 3 and 4. This (final) model incorporates the most important aspects of the former ones, i.e., the symmetry of dipoles 3 and 4 and the separation of NS' and MP on dipoles 2 and 2a, respectively. See Fig. 4 for further legends.

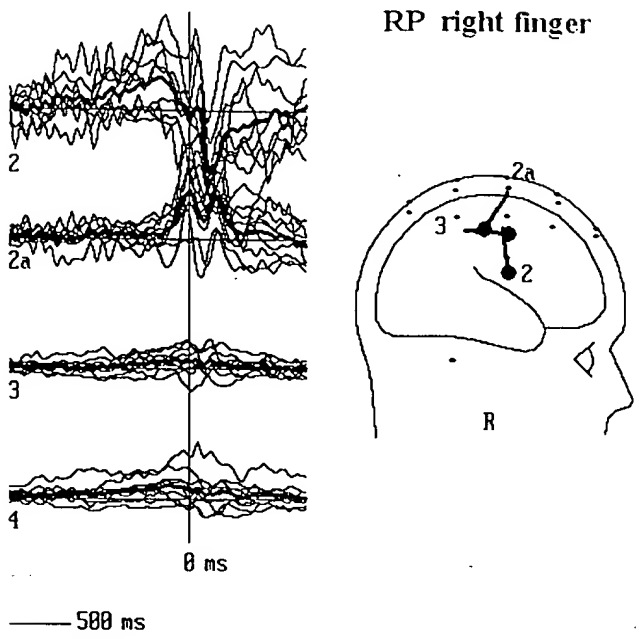

Fig. 8. Scatter plot of the individual (thin lines) and grand average (thick line) source waves for the final dipole model (Fig. 7). The inter-individual consistency of these source waves is demonstrated by significant SOTs (Table I) except for the early activity of dipole 3.

dipoles 3 and 4a to verify whether they could be interpreted as being symmetrical, as they are in Fig. 4. Starting optimization from Fig. 6 with a symmetrical pair at the location of dipole 4a with the orientation of dipole 3 resulted in the model presented in Fig. 7. For left finger data the same strategy resulted in a similar model. From Table I it can be seen that the RV increases only slightly. Only TC3', at the corner of the electrode array, does not pass the ROT with left finger movements. The individual source waves which are tested by the SOT are shown in Fig. 8, to permit a visual assessment of their consistency (compare Bötzel et al. (1993), their Fig. 5). The SOT shows that with right finger flexions dipole 3 is only significant from −250 to −100 msec. Notwithstanding the fact that dipole 2 does not pass the SOT overall with left finger flexions (Table I), it is significant from −350 to −125 msec, i.e., during the latter part of NS'.

Secondly, we addressed the issue whether or not the SMA participates in generating the RP in general and its early bilaterally symmetrical part (BP_{sym}) in particular. We assumed the same SMA coordinates as Bötzel et al. (1993), i.e., 11 mm anterior to Cz and 39 mm below the scalp. A test dipole within the SMA showed a zero moment, after being inserted in the Fig. 6 and 7 models, both when vertically oriented and after optimization of its direction. SOTs on the source waves of the test dipoles did not reach significance at any single time-point.

Discussion

The main objective of the present paper was to construct a spatio-temporal dipole model for the RP to gain more insight in its neurophysiological base, which would increase its usefulness in ERP research and clinical settings. We hypothesized that the RP preceding finger flexions is especially suited to investigate the possible unilateral or bilateral contributions of PM, MI and SI, which should be clearly lateralized because of the somatotopic organization of these cortical areas. Our final model (Fig. 7) indeed shows a mix of unilateral sources, which are only activated by contralateral movements (dipoles 2 and 2a), and bilaterally symmetrical generators (dipoles 3 and 4). Furthermore, we expected spatio-temporal dipole modelling to be capable of separating overlapping source activities. The final model clearly separates BP_{sym} (dipoles 3 and 4), NS' (dipole 2) and MP (dipole 2a) in space and time, both for the grand average and in most of the individual subjects (Figs. 7 and 8).

The Fig. 7 model integrates the most important characteristics of the earlier models. From Figs. 4 and 5 it incorporates the bilateral tangential pair of dipoles (3 and 4), with an early onset of activation. Such a pair has repeatedly been presented as part of equivalent dipole models based on MEG (Cheyne and Weinberg 1989; Kristeva et al. 1991) and EEG recordings (Bötzel et al. 1993; Toro et al. 1993). These dipoles have been shown to be located in the posterior wall of the pre-central gyrus by a combination of MRI and MEG techniques (Cheyne et al. 1991; Walter et al. 1992; Thatcher et al. 1993). The estimated direction of the intracellular current flow (anteriorly), in combination with the assumption that it is caused by EPSPs at the apical dendrites, leads to the same conclusion.

Likewise, Fig. 7 incorporates the separation of NS' and MP on 2 separate dipoles, 2 and 2a respectively, which was also present in Fig. 6. Such separation is supported by evidence from research on voluntary movements in animals (Arezzo et al. 1977; Sasaki and Gemba 1991) and man (Neshige et al. 1988). This evidence indicates that the MP comes from a very small portion of MI. Dipole 2a can indeed be interpreted as representing activation of a smaller area than dipole 2, because dipole 2a is more superficial than dipole 2. If we assume dipoles 3 and 4 to stem from the posterior wall of the pre-central gyrus, then dipoles 1, 2 and 2a would be interpreted to stem from the crown of that same gyrus. This supports the conclusion drawn by Neshige et al. (1988), which was based on direct subdural recording, that MI is the main generator of the RP.

The present study differs in one important finding from earlier ones (Kristeva et al. 1991; Bötzel et al. 1993; Toro et al. 1993): we could not model the RAP. This could be due to limitations of the method. Fitting

3 or 4 dipoles may be as much as we can do based on 23 recording sites. Note that the number of degrees of freedom in spatio-temporal dipole modelling is equal to the number of electrodes × the number of independent wave forms. Based on a principal component analysis the latter was estimated to be 2 for the present data (Böcker and Van den Berg-Lenssen 1994). Fitting the RAP is even more difficult if we assume SI to be active after the movement, as indicated by the other studies, because SI is in the close vicinity of other active areas. A second indication that we reached the limit of the resolution power of the method, given the present experimental parameters, is that the Fig. 7 model was seriously distorted without a symmetry constraint on dipoles 3 and 4 (compare dipoles 3 and 4a in Fig. 6).

The main difference between the studies of Toro et al. (1993) and Bötzel et al. (1993) is the presence or absence of an SMA dipole, respectively. Our results confirm those of Bötzel et al. (1993). A test source in the SMA does not describe any signal, which statement was qualified by a negative SOT result in our study. In fact the orientation of the SMA dipole of Toro et al. (1993) is at variance with that of Lang et al. (1991), and it was absent in 4 out of 10 subjects and in 3 out of 4 in a later study (Thatcher et al. 1993).

Overall our results confirm those of Bötzel et al. (1993). The main differences are in the orientations of the dipoles and in application of a formal test on the inter-subject reliability of the model (ROT) and the significance of the source waves (SOT). Given that radial sources do not generate measurable magnetic fields, our model complies somewhat better with models of the magnetic readiness field (Cheyne et al. 1991, 1992; Kristeva et al. 1991) than theirs. A last difference is that we were able to separate BP_{sym} and NS' on sources 3/4 and 2, respectively.

The first hypothesis put forward in the introduction, i.e., that the BP_{sym} stems from either the SMA or from bilateral activity in PM, is not supported by the present evidence. Using a test dipole (after Bötzel et al. 1993) no SMA activity could be shown preceding finger flexions. Given the rather deep position of dipole 2 in Fig. 6 and especially Fig. 7, we cannot totally exclude a small unilateral contribution of PM to the NS', but not to the BP_{sym}. However, both the source waves and some of the SOTs for the models in Figs. 4–7 indicate an early (i.e., prior to −600 msec) activation of dipoles 3 and 4. Therefore, the present models suggest bilateral activation of the posterior wall of MI as the source of the BP_{sym}. The BP_{sym} will be discussed more extensively in relation to models for foot RPs (Böcker et al. 1994), which describe this component better than the present models, which are not sufficient during the BP_{sym} interval (−1000 to −600 msec).

The hypotheses that the NS' and the MP are mainly generated by contralateral MI activation are clearly confirmed. Both probably stem from the crown of the precentral gyrus and the NS' comprises a wider area than the MP.

With respect to the PMP, the small positive deflection preceding the MP, we did not formulate an exact hypothesis. Its topography has been controversial (Shibasaki and Kato 1975 versus Deecke and Kornhuber 1977). Neshige et al. (1988) remark that they were never able to record the PMP from subdural electrodes, and they propose that the PMP is an epiphenomenon of the transition between NS' and MP. The models presented here (Figs. 5–7) support this hypothesis. Although the time series of the moments do not show a PMP, the predicted scalp potentials do. As noted before, we were not able to model the post-movement RAP, so it is probably generated outside MI.

In evaluating the final model (Fig. 7) as a whole we already mentioned that it incorporates evidence on the origin of the MP from invasive techniques (Arezzo et al. 1977; Neshige et al. 1988) and confirms the main results of Kristeva et al. (1991) and Bötzel et al. (1993). The model shows a large asymmetry, whereas the RP as recorded from the scalp appears widespread, with a relatively small contralateral preponderance. This apparent discrepancy can be explained by volume conduction. By application of spatio-temporal dipole modelling, we were able to separate the activity of multiple functional areas within the posterior wall and the crown of MI in time and space. These areas generate the BP_{sym}, NS' and MP as recorded at the scalp, respectively. This confirms and extends evidence from direct cortical recording (Neshige et al. 1988).

The authors want to thank M. Van den Berg-Lenssen, G. Van Boxtel, E. Damen, J. Beneken and P. Praamstra for their useful comments on earlier drafts of this paper. Furthermore we are indebted to A. Achim for discussing variations on his residual orthogonality test and for correcting our software implementation of this test. Finally, we want to thank J. Van Avermaete and J. Van den Broek for developing the software for spherical spline interpolation of scalp potentials and designing the graphical output of the topographical maps.

References

Achim, A., Richer, F. and Saint-Hilaire, J.-M. Methods for separating temporally overlapping sources of neuroelectric data. Brain Topogr., 1988a, 1: 22–28.

Achim, A., Richer, F., Alain, C. and Saint-Hilaire, J.-M. A test of model adequacy applied to the dimensionality of multi-channel average auditory evoked potentials. In: F. Samson-Dollfus et al. (Eds.), Statistics and Topography in Quantitative EEG. Elsevier, Paris, 1988b: 161–171.

Achim, A., Richer, F. and Saint-Hilaire, J.-M. Methodological considerations for the evaluation of spatio-temporal source models. Electroenceph. clin. Neurophysiol., 1991, 79: 227–240.

Arezzo, J. and Vaughan, Jr., H.G. Cortical potentials associated with voluntary movements in the monkey. Brain Res., 1975, 88: 99–104.

Arezzo, J., Vaughan, Jr., H.G. and Koss, B. Relationship of neuronal activity to gross movement-related potentials in monkey pre- and postcentral cortex. Brain Res., 1977, 132: 362–369.

Böcker, K.B.E. and Van den Berg-Lenssen, M.M.C. Temporal, spatial and spatiotemporal data-representations of the readiness potential. In: F.J. Maarse et al. (Eds.), Computers in Psychology V. Swets-Zeitlinger, Amsterdam, 1994: in press.

Böcker, K.B.E., Brunia, C.H.M. and Cluitmans, P.J.M. A spatio-temporal dipole model of the readiness potential in humans. II. Foot movement. Electroenceph. clin. Neurophysiol., 1994, 91: 286–294.

Bötzel, K., Plendl, H., Paulus, W. and Scherg, M. Bereitschaftspotential: is there a contribution of the supplementary motor area? Electroenceph. clin. Neurophysiol., 1993, 89: 187–196.

Brunia, C.H.M. Brain potentials related to preparation and action. In: H. Heuer and A.F. Sanders (Eds.), Perspectives on Preparation and Action. Lawrence Erlbaum, Hillsdale, NJ, 1987: 105–130.

Brunia, C.H.M. Movement and stimulus preceding negativity. Biol. Psychol., 1988, 26: 165–178.

Cheyne, D. and Weinberg, H. Neuromagnetic fields accompanying unilateral finger movements: pre-movement and movement-evoked fields. Exp. Brain Res., 1989, 78: 604–612.

Cheyne, D., Kristeva, R. and Deecke, L. Homuncular organization of human motor cortex as indicated by neuromagnetic recordings. Neurosci. Lett., 1991, 122: 17–20.

Cheyne, D., Kristeva, R., Deecke, L. and Weinberg, H. Spatiotemporal source modelling of sensorimotor cortex activation accompanying human voluntary movement. In: M. Hoke, S.N. Erné, Y.C. Okada and G.L. Romani (Eds.), Biomagnetism: Clinical Aspects. Elsevier, Amsterdam, 1992: 717–721.

Deecke, L. and Kornhuber, H.H. Cerebral potentials and the initiation of voluntary movement. In: J.E. Desmedt (Ed.), Attention, Voluntary Contraction and Event-related Cerebral Potentials. Prog. Clin. Neurophysiol., Vol. 1. Karger, Basel, 1977: 132–150.

Dick, J.P.R., Rothwell, J.C., Day, B.L., Catello, R., Buruma, O., Gioux, M., Benecke, R., Berardelli, A., Thompson, P.D. and Marsden, C.D. The Bereitschaftspotential is abnormal in Parkinson's patients. Brain, 1989, 122: 233–244.

Ikeda, A., Lüders, H.O., Burgess, R.C. and Shibasaki, H. Movement-related potentials recorded from supplementary motor area and primary motor area. Role of supplementary motor area in voluntary movements. Brain, 1992, 115: 1017–1043.

Ikeda, A., Lüders, H.O., Burgess, R.C. and Shibasaki, H. Movement-related potentials associated with single and repetitive movements recorded from human supplementary motor area. Electroenceph. clin. Neurophysiol., 1993, 89: 269–277.

Kornhuber, H.H. and Deecke, L. Hirnpotentialänderungen bei Willkürbewegungen und passiven Bewegungen des Menschen: Bereitschaftspotential und reafferente Potentiale. Pflügers Arch., 1965, 284: 1–17.

Kristeva, R., Cheyne, D. and Deecke, L. Neuromagnetic fields accompanying unilateral and bilateral voluntary movements: topography and analysis of cortical sources. Electroenceph. clin. Neurophysiol., 1991, 81: 284–298.

Lang, W., Obrig, H., Lindinger, G., Cheyne, D. and Deecke, L. Supplementary motor area activation while tapping bimanually different rhythms in musicians. Exp. Brain Res., 1990, 79: 504–514.

Lang, W., Cheyne, D., Kristeva, R., Beistainer, R., Lindinger, G. and Deecke, L. Three-dimensional localization of SMA activity preceding voluntary movement. A study of electric and magnetic fields in a patient with infarction of the right supplementary motor area. Exp. Brain Res., 1991, 87: 688–695.

Lopes da Silva, F. and Spekreijse, H. Localization of visually evoked responses: using simple and multiple dipoles. An overview of different approaches. In: C.H.M. Brunia, G. Mulder and M.N. Verbaten (Eds.), Event-Related Brain Research. Electroenceph. clin. Neurophysiol. (Suppl. 42). Elsevier, Amsterdam, 1991: 38–46.

Mitzdorf, U. Physiological sources of evoked potentials. In: C.H.M. Brunia, G. Mulder and M.N. Verbaten (Eds.), Event-Related Brain Research. Electroenceph. clin. Neurophysiol. (Suppl. 42). Elsevier, Amsterdam, 1991: 47–57.

Neshige, R., Lüders, H. and Shibasaki, H. Recording of movement-related potentials from scalp and cortex in man. Brain, 1988, 111: 719–736.

Perrin, F., Pernier, J., Bertrand, O. and Echallier, J.F. Spherical splines for scalp potential and scalp current density mapping. Electroenceph. clin. Neurophysiol., 1989, 72: 184–187.

Perrin, F., Pernier, J., Bertrand, O. and Echallier, J.F. Corrigendum. Electroenceph. clin. Neurophysiol., 1990, 76: 565.

Roland, P.E., Larsen, B., Larsen, N.A. and Skinhøj, E. Supplementary motor area and other cortical areas in the organization of voluntary movements in man. J. Neurophysiol., 1980, 43: 118–136.

Sasaki, K. and Gemba, H. Cortical potentials associated with voluntary movements in monkey. In: C.H.M. Brunia, G. Mulder and M.N. Verbaten (Eds.), Event-Related Brain Research. Electroenceph. clin. Neurophysiol. (Suppl. 42). Elsevier, Amsterdam, 1991: 80–96.

Scherg, M. Brain Electrical Source Analysis. Version 1.8 and 1.9. 1989–1992.

Scherg, M. and Berg, P. Use of prior knowledge in brain electromagnetic source analysis. Brain Topogr., 1991, 4: 143–150.

Scherg, M. and Picton, T.W. Separation and identification of event-related potential components by brain electric source analysis. In: C.H.M. Brunia, G. Mulder and M.N. Verbaten (Eds.), Event-Related Brain Research. Electroenceph. clin. Neurophysiol. (Suppl. 42). Elsevier, Amsterdam, 1991: 24–37.

Shibasaki, H. and Kato, M. Movement-associated cortical potentials with unilateral and bilateral simultaneous hand movement. J. Neurol., 1975, 208: 191–199.

Shibasaki, H., Barrett, G., Halliday, E. and Halliday, A.M. Components of movement-related cortical potentials and their scalp topography. Electroenceph. clin. Neurophysiol., 1980, 49: 213–226.

Singh, J. and Knight, R.T. Frontal lobe contribution to voluntary movements in humans. Brain Res., 1990, 531: 45–54.

Thatcher, R.W., Toro, C., Pflieger, M. and Hallett, M. Human neural network dynamics using multimodal registration of EEG, PET and MRI. In: Proc. Soc. Magnetic Resonance in Functional MRI of the Brain, Arlington, VA, 1993.

Toro, C., Matsumoto, J., Deuschl, G., Bradley, J.R. and Hallett, M. Source analysis of scalp-recorded movement-related electrical potentials. Electroenceph. clin. Neurophysiol., 1993, 86: 167–175.

Vasey, W.M. and Thayer, J.F. The continuing problem of false positives in repeated measurements ANOVA in psychophysiology: a multivariate solution. Psychophysiology, 1987, 24: 474–486.

Walter, H., Kristeva, R., Knorr, U., Schlaug, G., Huang, Y., Steinmetz, H., Nebeling, B., Herzog, H. and Seitz, R.J. Individual somatotopy of primary sensorimotor cortex revealed by intermodal matching of MEG, PET and MRI. Brain Topogr., 1992, 5: 183–187.

Ed Mock
234-1534

F. Bloom (Editor)
Progress in Brain Research, Vol. 100

CHAPTER 21

Human cortical functions revealed by magnetoencephalography

Riitta Hari

Low Temperature Laboratory, Helsinki University of Technology, 02150 Espoo, Finland

Introduction

Magnetoencephalography, MEG, complements the traditional microlevel and macrolevel approaches to unravelling the functions of the human brain. MEG recordings are based on non-invasive detection of weak magnetic fields produced by cerebral electric currents. Signals from various cortical regions can be differentiated with good temporal and spatial resolution. MEG studies have so far focused on functional mapping of the healthy human cerebral cortex but some clinical applications are also emerging. For details of the MEG method, see previous reviews (Hari and Lounasmaa, 1989; Sato, 1990; Hämäläinen et al., 1993).

MEG is closely related to EEG, the recording of electric potential differences on the scalp. MEG patterns caused by multiple simultaneous sources are often more straightforward to interpret than the corresponding EEG distributions. One reason for this is that concentric electric inhomogeneities do not affect the magnetic field. A combination of MEG and EEG is necessary for identifying all active brain areas and all orientations of the source currents (cf. Wikswo et al., 1993).

Measurements

Electric currents flowing in the brain generate weak magnetic signals, typically 100–1000 fT (fT = femto-Tesla = 10^{-15} T), i.e. only one part in 10^9 or 10^8 of the Earth's geomagnetic field. The signals are first picked up by superconducting flux transformers (Fig. 1*A*) and then detected by SQUIDs (Superconducting QUantum Interference Devices), which are extremely sensitive to magnetic fields. The configuration of the flux transformer (a magnetometer, axial gradiometer, or a planar gradiometer; Fig. 1*B*) affects the instrument's sensitivity to various brain versus noise sources.

To localize the underlying neural activity, the field pattern outside the head must be determined in detail. Instead of earlier time-consuming sequential mapping with (1–37)-channel instruments, it is now possible to record signals simultaneously over the entire cortex. The first whole-head helmet-type magnetometers were constructed recently by Neuromag Ltd (Espoo, Finland; 122 channels, Fig. 1*C*) and by CTF Systems Inc. (Vancouver, Canada; 64 channels).

Origin and interpretation of MEG signals

An inherent limitation of the MEG (and EEG) method is the non-uniqueness of the inverse problem. This means that, in principle, several current distributions may produce identical signal patterns outside the brain. Therefore, source models are used for data interpretation. The most common model of a local source is a tangential current dipole within a sphere. The orientation, strength and three-dimensional location of the equivalent current dipole (ECD), which best explains the measured field pattern, are determined by means of a least-squares fit to the data. The

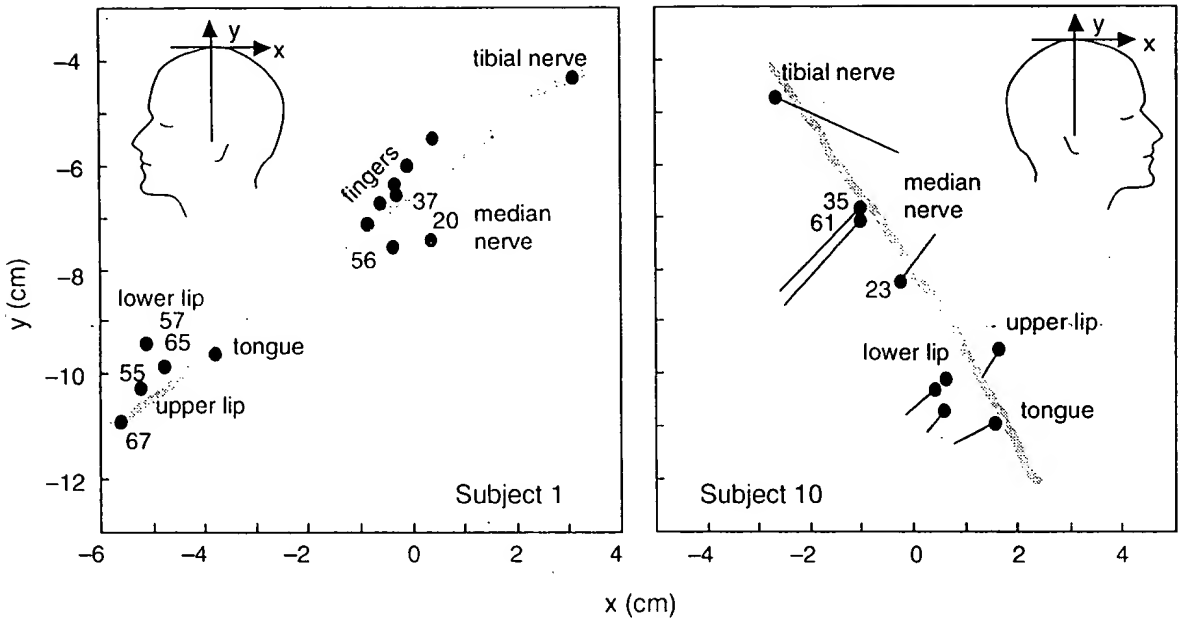

Fig. 3. ECD locations for stimulation of different parts of the body in two subjects. The numbers indicate response latencies in ms. For Subject 10, dipole orientations are also shown. The thick grey line illustrates the approximate course of the Rolandic fissure, determined on the basis of ECD locations and orientations. Adapted from Hari et al. (1993b).

Such recordings suggest that the auditory sensory memory lasts about 10 s (Sams et al., 1993).

Somatosensory responses and somatotopy

Recordings of somatosensory evoked fields (SEFs) can be employed to study functional organization of the somatosensory cortices. In the contralateral primary somatosensory cortex SI, a clear somatotopical order is evident, with different body parts represented at different locations (Fig. 3). The non-invasively identified Rolandic fissure is an important functional landmark in studies of epileptic foci and in preoperative planning of epilepsy surgery.

SEF recordings also indicate activation of other cortical areas. At 100–140 ms, signals peak in the secondary somatosensory cortices SII of both hemispheres, with slightly longer latencies for the ipsi- than the contralateral stimuli (Hari et al., 1993b). A novel source area was recently found in the posterior parietal cortex, medial and posterior to the SI hand area (Forss et al., 1994); this source was most active 70–110 ms after the stimulus.

Signals following voluntary blinking

The eye acts as a strong electric dipole and eye movements and blinks are serious sources of artefacts in EEG and MEG recordings. EEG responses have been observed in the posterior parts of the brain about 200 ms after blink artefacts; the signals were interpreted as visual evoked responses caused by luminance changes (Heuser-Link et al., 1992).

Figure 4 (left) shows magnetic field patterns associated with voluntary blinking (Hari et al., 1994); the magnetic signals were averaged using the vertical electro-oculogram as the trigger. Strong signals occur close to both orbits during a blink. About 200 ms later, another signal with a dipolar field pattern emerges in the posterior head areas. Superposition of its ECD on the brain surface (Fig. 4, right; white circles) indicates activation of the parieto-occipital midline. The signals

disappeared when blinking occurred in complete darkness. However, since the source location was clearly distinct from that of early visually evoked fields (Fig. 4, right; black circle), the blink-related posterior response does not seem to be an ordinary visual evoked response but rather a sign of activation of the posterior parietal cortex (PPC).

The PPC is known to be strongly associated with the control of eye movements and fixation. In monkey, eye-movement-related neurons in this area react preferentially to large, salient stimuli which "signal the presence of an important stimulus in the visual environment" (Goldberg and Robinson, 1977). Interestingly, the PPC is strongly connected to prefrontal cortical areas underlying spatial working memory (Wilson et al., 1993). The observed response in the human PPC might thus be related to updating of the spatial working memory, necessary for maintaining a continuous image of the environment, despite interruption of the visual input for a tenth of a second during each blink.

Clinical perspectives and conclusions

During preoperative evaluation of epileptic patients, irritative foci have been located in relation to functional landmarks at cortical projection areas, determined on the basis of magnetic evoked responses. A good agreement has been reported in several patients between MEG foci and intraoperative corticographic findings. Determining the temporal relationships between several foci may also be clinically important. For example, in some patients, it is possible to find the callosal conduction time between foci in homologous

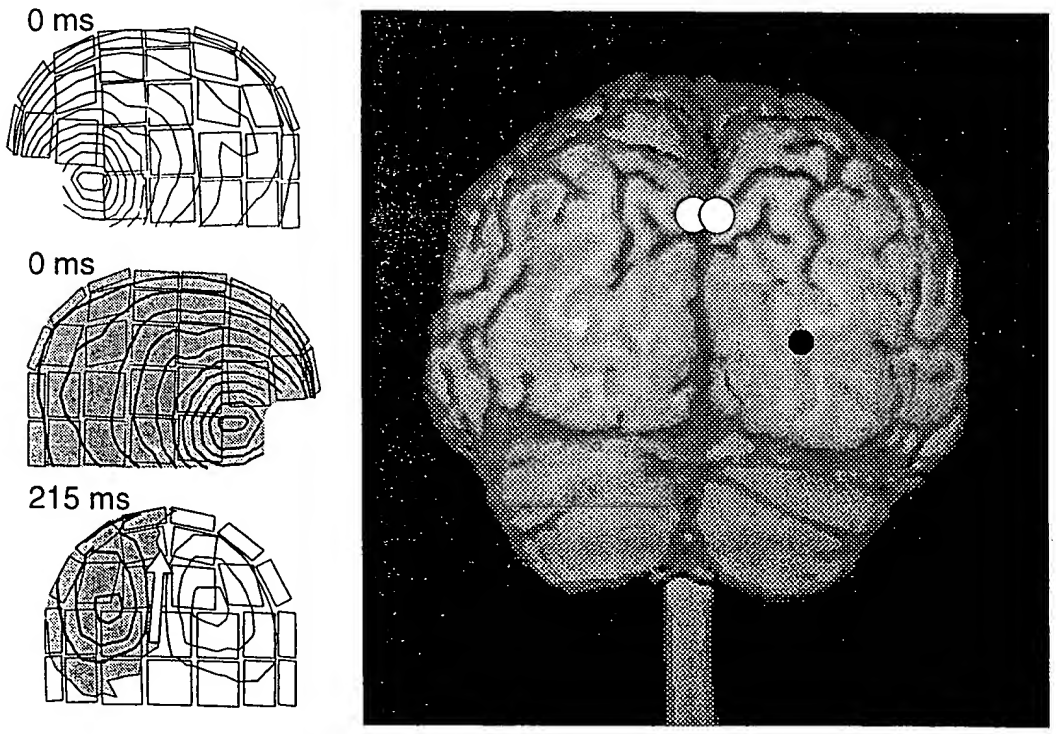

Fig. 4. *Left*: Field patterns over the left and right hemispheres during the maximum blink signal (0 ms) and over the back of the head during the peak of the posterior response (215 ms). The isocontours are separated by 200 fT (upper two patterns) and by 100 fT (the lowest pattern). *Right*: ECDs superimposed on a MRI surface reconstruction of the brain, viewed from the back. The white circles indicate ECDs for the blink-associated signals, determined from two measurements; the dipole orientations are perpendicular to the course of the parieto-occipital sulcus. The black circle shows the ECD for visual evoked field. Modified from Hari et al. (1994).

areas of the two hemispheres (Hari et al., 1993a). Other clinical applications aim at a better understanding of the pathophysiology of different neurological diseases (Hari, 1993). More extensive clinical applications necessitate installation of high-quality multichannel instruments into hospital environments.

MEG complements information obtained from other brain imaging methods in studying human cortical functions. The MEG approach lacks the accuracy of single-cell recordings but is non-invasive and gives information on an analysis level that is relevant for an understanding of the macroscopic functional organization of the cerebral cortex.

Whole-head MEG recordings allow comparison of hemispheric differences in the processing of complex stimuli, such as speech sounds. This is of paramount importance for research into the neural basis of cognitive activity in humans, such as studies of brain dynamics and related disorders during complex problem solving. One recent whole-head MEG study revealed the activation sequence of several cortical areas associated with overt and covert picture naming (Salmelin et al., 1994). In addition to evoked response recordings, the whole-head neuromagnetometers provide a global picture of ongoing spontaneous activity, which is of great interest for both basic neuroscience and for clinical applications.

Acknowledgments

This study has been financially supported by the Academy of Finland and by the Sigrid Jusélius Foundation. The MRIs were obtained at the Department of Radiology, Helsinki University Central Hospital. I thank Olli V. Lounasmaa, Linda McEvoy and Riitta Salmelin for comments on the manuscript.

References

Forss, N., Hari, R., Salmelin, R., Ahonen, A., Hämäläinen, M., Kajola, M., Knuutila, J. and Simola, J. (1994) Activation of the human parietal cortex by median nerve stimulation. *Exp. Brain Res.*, in press.

Goldberg, M. and Robinson, D. (1977) Visual mechanisms underlying gaze: function of the cerebral cortex. In: R. Baker and A. Berthoz (Eds.), *Control of Gaze by Brain Stem Neurons. Developments in Neuroscience*, Vol. 1, Elsevier, pp. 469–476.

Hämäläinen, M., Hari, R., Ilmoniemi, R., Knuutila, J. and Lounasmaa, O.V. (1993) Magnetoencephalography – theory, instrumentation, and applications to noninvasive studies of the working human brain. *Rev. Modern Phys.*, 41: 413–497.

Hari, R. (1993) Magnetoencephalography as a tool of clinical neurophysiology. In: E. Niedermeyer and F. Lopes da Silva (Eds.), *Electroencephalography. Basic Principles, Clinical Applications and Related Fields*, 3rd edition, Williams & Wilkins, Baltimore, pp. 1035–1061.

Hari, R. and Lounasmaa, O.V. (1989) Recording and interpretation of cerebral magnetic fields. *Science*, 244: 432–436.

Hari, R., Ahonen, A., Forss, N., Granström, M.-L., Hämäläinen, M., Kajola, M., Knuutila, J., Mäkelä, J.P., Paetau, R., Salmelin, R. and Simola, J. (1993a) Parietal epileptic mirror focus detected with a whole-head neuromagnetometer. *NeuroReport*, 5: 45–48.

Hari, R., Karhu, J., Hämäläinen, M., Knuutila, J., Salonen, O., Sams, M. and Vilkman, V. (1993b) Functional organization of the human first and second somatosensory cortices: a neuromagnetic study. *Eur. J. Neurosci.*, 5: 724–734.

Hari, R., Salmelin, R., Tissari, S., Kajola, M. and Virsu, V. (1994) Visual stability during eyeblinks. *Nature*, 367: 121–122.

Heuser-Link, M., Dirlich, G., Berg, P., Vogl, L. and Scherg, M. (1992) Eyeblinks evoke potentials in the occipital brain region. *Neurosci. Lett.*, 143: 31–34.

Mäkelä, J., Ahonen, A., Hämäläinen, M., Hari, R., Ilmoniemi, R., Kajola, M., Knuutila, J., Lounasmaa, O.V., McEvoy, L., Salmelin, R., Sams, M., Simola, J., Tesche, C. and Vasama, J.-P. (1993) Functional differences between auditory cortices of the two hemispheres revealed by whole-head neuromagnetic recordings. *Human Brain Mapping*, 1: 48–56.

Salmelin, R., Hari, R., Lounasmaa, O.V. and Sams, M. (1994) Dynamics of brain activation during picture naming. *Nature*, in press.

Sams, M., Hari, R., Rif, J. and Knuutila, J. (1993) The human auditory sensory memory trace persists about 10 s: neuromagnetic evidence. *J. Cogn. Neurosci.*, 5: 363–370.

Sato, S. (Ed.) (1990) *Magnetoencephalography. Advances in Neurology*, Vol. 54, Raven Press, New York.

Tissari, S., Hämäläinen, M., Hari, R. and Mäkelä, J. (1993) Sources of auditory evoked fields superimposed on 3D-reconstruction of temporal lobes. In: *9th Int. Conf. Biomagnetism*, Vienna, 1993, Volume of Abstracts, pp. 138–139.

Wikswo, J.J., Gevins, A. and Williamson, S. (1993) The future of EEG and MEG. *Electroencephalogr. Clin. Neurophysiol.*, 87: 1–9.

Wilson, F.A.W., Ó Schalaidhe, S.P. and Goldman-Rakic, P.S. (1993) Dissociation of object and spatial processing domains in primate prefrontal cortex. *Science*, 260: 1955–1958.

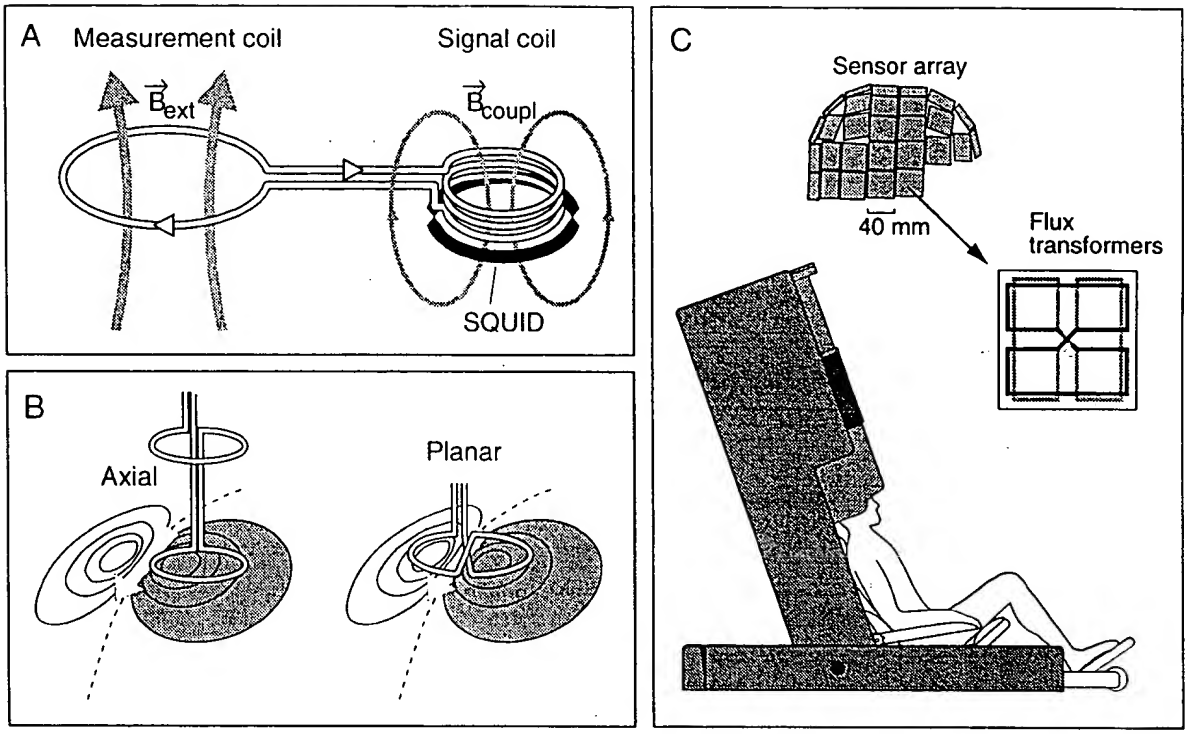

Fig. 1. *A*, Principle of MEG signal detection. The external magnetic field induces into the superconducting flux transformer a current that couples the magnetic field from the signal coil to the SQUID. *B*, Two flux transformer configurations above a schematic magnetic field pattern produced by a current dipole. The axial gradiometer picks the maximum signal at both field extrema whereas the planar figure-of-eight transformer senses the strongest signal (gradient) just above the dipole. *C*, Schematic illustration of a whole-head neuromagnetometer. The subject's head is inside the dewar, which contains the SQUID sensors immersed in liquid helium. With this 122-channel device (Neuromag-122^{TM}), the gradient of the magnetic field is picked up outside the head simultaneously at 61 locations of the helmet-shaped sensor array (upper insert); at each location, two orthogonal field gradients are measured with planar flux transformers of figure-of-eight configuration (lower insert). The experiments are carried out inside a magnetically shielded room.

MEG signals are caused mainly by intracellular synaptic currents in the fissural cortex (cf. Hämäläinen et al., 1993). Physiologically, the ECD reflects the centre of gravity of an active cortical layer smaller than 2 cm in diameter. Multiple simultaneous sources can be modelled with time-varying multidipole models.

The solutions can be improved considerably by incorporating the anatomical constraints obtained, for example, from magnetic resonance images (MRIs). Such a combination of structural (MRI) and functional (MEG) information is especially useful for clinical purposes. Future developments will also include integration of MEG and positron emission tomography (PET) data.

Examples

Auditory responses and sensory memory

Figure 2*A* shows auditory evoked magnetic fields elicited by short tones. The most prominent deflection, N100m, peaks about 100 ms after sound onset and has dipolar field patterns over both temporal lobes (Fig. 2*B*). The signals are slightly larger and earlier in the left (contralateral) than the right hemisphere. A two-dipole model, one ECD in each supratemporal cortex, explained the signal distribution satisfactorily. Superposition of the ECDs on the 3D-MRI reconstruction (Fig. 2*C*) implies that N100m may receive a contribu-

tion from Heschl's gyrus (cf. Tissari et al., 1993), although its main source is probably in the cortex of planum temporale.

Sensory memory in its simple form can be studied by determining recovery cycles of different MEG responses. The N100m amplitude increases with the interstimulus interval (ISI) and reaches a plateau at ISIs of about 8 s. As shown in Fig. 2*D*, the ISI dependence is similar in the left and right hemispheres, implying that tones leave traces of similar duration into auditory cortices of both hemispheres. The storage of auditory information for a few seconds can also be demonstrated by presenting infrequent deviant sounds among a series of monotonously repeated standard sounds.

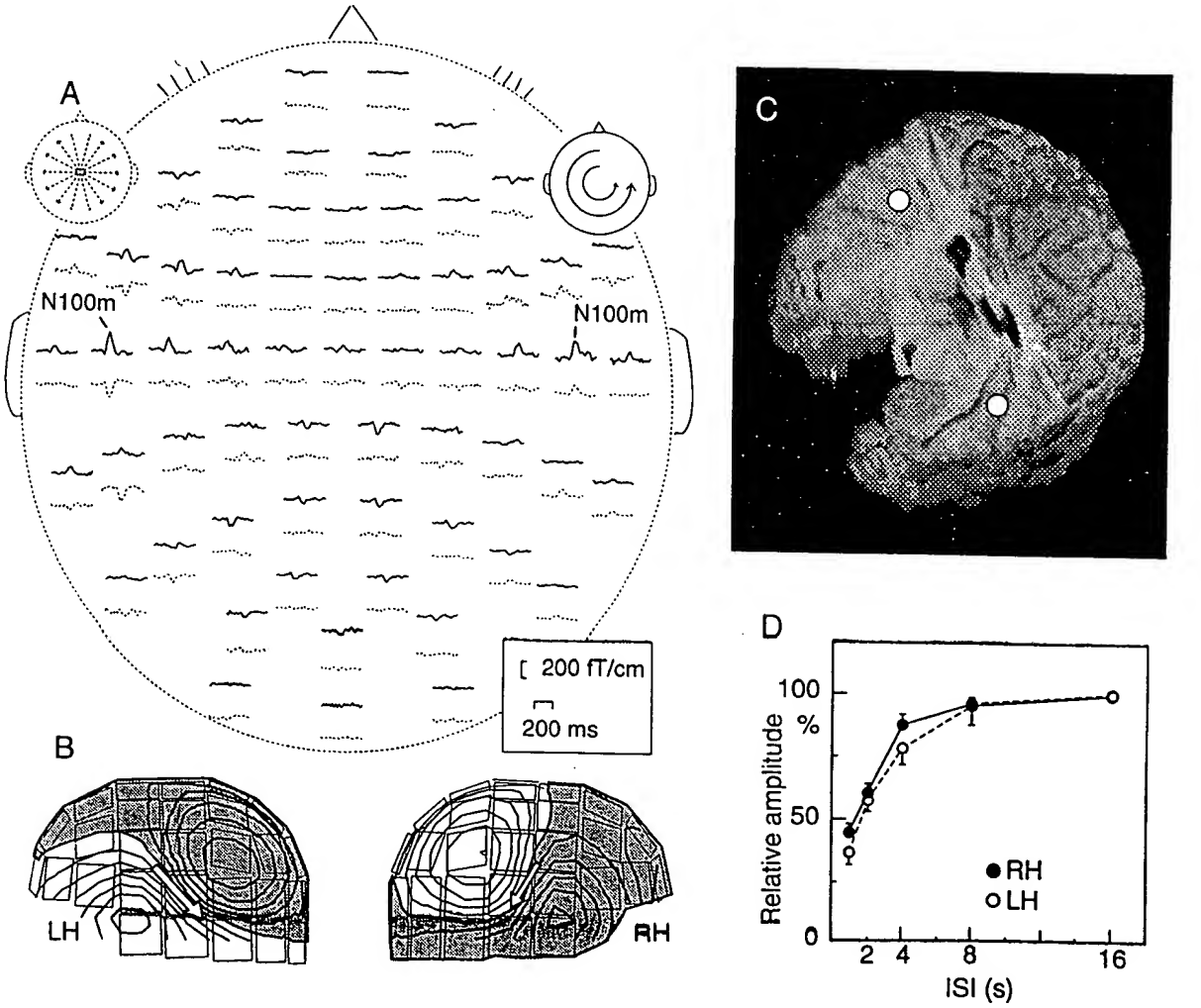

Fig. 2. *A*, AEFs to 50-ms tones presented to the right ear once every 4 s. In each response pair, the upper (solid) curves indicate the azimuthal and the lower (dotted) ones the polar derivatives (illustrated in the right- and left-sided insert heads, respectively); the relative amplitudes of the two traces indicate the direction of the source current at each location. The head is viewed from above, with the nose pointing to the top of the figure. The traces start 50 ms before the tone onset. Passband is 0.03–40 Hz. *B*, Field patterns during N100m over the left (LH) and right (RH) hemispheres. The maps have been drawn over the helmet-shaped sensor array. The shadowed areas indicate magnetic flux out of the skull. The arrows show the sites and orientations of the equivalent current dipoles best explaining the signal patterns. The isocontours are separated by 100 fT. *C*, 3-D MRI reconstruction of the subject's brain. The frontal lobes have been removed to expose the surfaces of the temporal lobes. The white circles indicate the sources of N100m. Adapted from Tissari et al. (1993). *D*, Mean (± SEM; 9 subjects) relative amplitudes of N100m over the left and right hemispheres to contralateral stimulation. Adapted from Mäkelä et al. (1993).

Siegfried Schneider, PhD • Eckhardt Hoenig, PhD • Helmut Reichenberger, PhD • Klaus Abraham-Fuchs, MS • Werner Moshage, MD • Arnulf Oppelt, PhD • Hermann Stefan, MD • Andreas Weikl, MD • Axel Wirth, MS

Multichannel Biomagnetic System for Study of Electrical Activity in the Brain and Heart[1]

The authors designed a multichannel system for noninvasive measurement of the extremely weak magnetic fields generated by the brain and the heart. It uses a flat array of 37 superconducting magnetic field-sensing coils connected to sophisticated superconducting quantum interference devices. To prevent interference from external electromagnetic fields, the system is operated inside a shielded room. Complete sets of coherent data, even from spontaneous events, can be recorded. System performance was evaluated with phantom measurements and evoked-response studies. A spatial resolution of a few millimeters and a temporal resolution of a millisecond were obtained. First results in patients with partial epilepsy and investigations of the cardiac conductive pathway indicate that biomagnetism is now ready for a systematic clinical evaluation. Interpretation of measurements was facilitated by highlighting biomagnetically localized electrical activity in three-dimensional digital magnetic resonance images.

Index terms: Biomagnetism • Brain, abnormalities, 134.89 • Epilepsy • Heart, diseases, 51.899 • Heart, experimental studies, 51.1299 • Heart, function, 51.899

Radiology 1990; 176:825–830

MEDICAL imaging has now reached a high level of quality in displaying anatomical and morphologic details. Of further interest is information on organ function. Chemical function can be investigated with nuclear medicine and magnetic resonance (MR) spectroscopic studies. Electrical function of the heart and the brain is studied by measuring electrical potentials with the electrocardiogram (ECG) and the electroencephalogram (EEG).

To localize bioelectric current sources, invasive measurements of potentials have to be performed with the use of catheters or depth electrodes. Usually only information on the time course of the source strength can be gained from measurements of electrical surface potentials, since tissue conductivity and boundaries are unknown.

A promising approach is the measurement and evaluation of magnetic fields, which are generated simultaneously with the electrical potentials. These are influenced by tissue conductivity much less than electric potentials are (1,2), therefore rendering possible the localization of intracorporeal current sources by means of noninvasive measurements.

SUBJECTS AND METHODS

Biomagnetic fields at the surface of the body are weaker than the earth's magnetic field by six to nine orders of magnitude and range from about 50 pT (10^{-12} T) for the R wave of the magnetocardiogram (MCG) down to a few femtoteslas (10^{-15} T) for fields resulting from evoked responses of the cortex. They are measured with superconducting pickup coils connected to superconducting quantum interference devices (SQUIDs), which are magnetic flux sensors of extreme sensitivity (3) (Fig 1).

During the past decade, investigations in biomagnetism could be performed only with systems with a single channel (4–6) or with a few channels (7–9). Although work with these systems suggested possible applications of biomagnetism, they were not suitable for systematic clinical research. To localize sources with reasonable accuracy, field values for identical electrical events have to be recorded at a minimum of 15 positions (10). To measure the field distribution sequentially, investigations could last from several hours to several days. Field distributions from spontaneous events could not be measured at all. Therefore, there was a need for a multichannel system with the capability of obtaining true coherent measurements in a reasonable time.

Biomagnetic Multichannel System

The Krenikon (from the Greek *krene* [source or spring] and *ikon* [image]) biomagnetic multichannel system (Siemens, Erlangen, Federal Republic of Germany) was developed to allow measurements in a normal urban environment (11) (Fig 2). It can be operated by trained clinical personnel. The system has been designed as a general-purpose instrument suited for investigation of the brain and the heart.

To prevent interference from external electromagnetic fields, the system is operated inside a shielded room, which is made of two layers of soft magnetic material (Mumetal; Vacuumschmelze) with one layer of aluminum in between. Mechanical vibrations, which could induce intolerable interfering signals, are avoided by mounting the shielded room and the support of the measurement system on a specially designed concrete foundation. The field sensors are located in a cryostat filled with liquid helium, which can be adjusted vertically and tilted in two directions for access to any part of the patient. The patient is examined in a relaxed, reclining position on an adjustable couch (Fig 3). Because of the large (19-cm-diameter) sensitive area, only one recording has to be obtained. Electrical signals (EEG with surface or depth electrodes, ECG), other physiologic signals (eg, respiration), and trigger signals can

[1] From the Medical Engineering Group (S.S., H.R., K.A.F., A.O., A.Wirth) and the Central Research Laboratories (E.H.), Siemens, Henkestrasse 127, 8520 Erlangen, Federal Republic of Germany, and Medical Clinic II Cardiology and Policlinic (W.M., A.Weikl) and Neurological Clinic (H.S.), Universität Erlangen-Nürnberg, Erlangen, Federal Republic of Germany. From the 1989 RSNA scientific assembly. Received November 30, 1989; revision requested January 29, 1990; revision received March 26; accepted April 27. Address reprint requests to S.S.

Abbreviations: ECG = electrocardiogram, EEG = electroencephalogram, MCG = magnetocardiogram, MEG = magnetoencephalogram, S/N = signal-to-noise ratio, SQUID = superconducting quantum interference device, WPW = Wolff-Parkinson-White.

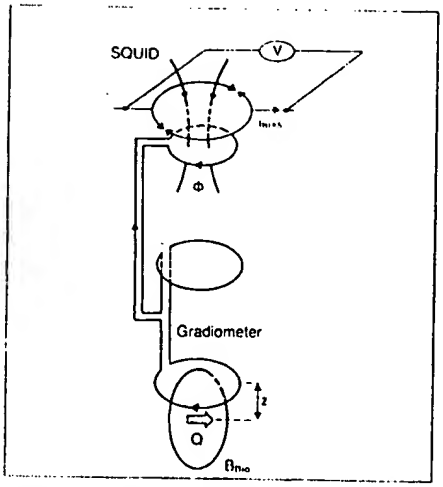

Figure 1. Diagram of system for the measurement of biomagnetic fields (flux density B_{BIO}). The pickup coil is positioned at distance z from the intracorporeal current source, *Q*. To compensate for interfering fields from distant external sources, the pickup coil is combined with a counterwound coil (so-called gradiometer). The magnetic flux recorded with the gradiometer is transferred to a coil, which couples the flux ϕ to the SQUID (i_{BIAS} = current to adjust the operating point of a SQUID). There the flux signal is transformed into a voltage signal *v*.

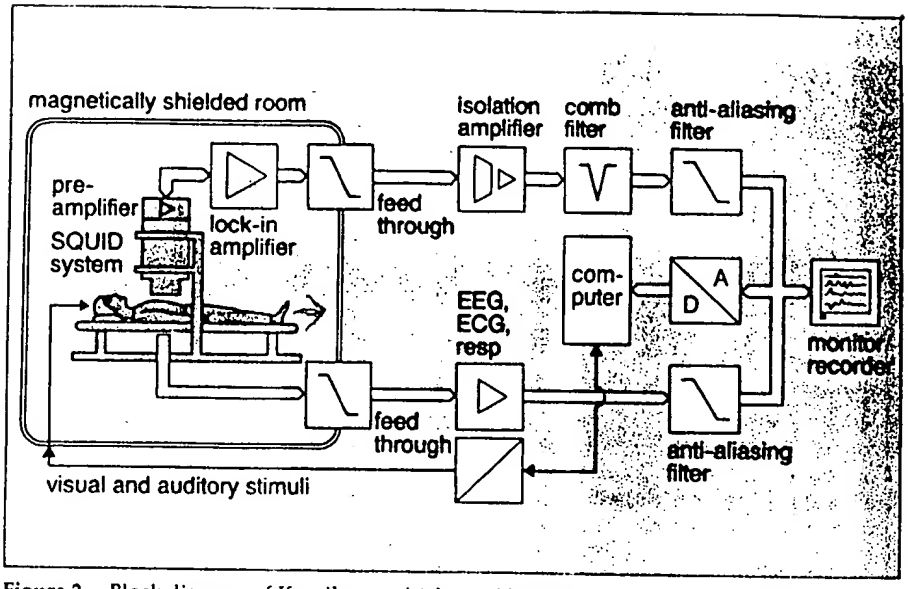

Figure 2. Block diagram of Krenikon multichannel biomagnetic system. The entire measurement system is located inside a shielded room (Vacuumschmelze, Hanau, Federal Republic of Germany). The cryostat, filled with liquid helium, contains the gradiometer array and the SQUIDs. It is made of fiberglas epoxy and is mounted on a stable dual-column support. Magnetic signals (MEG, MCG) are amplified in the shielded room to a level insensitive to external interferences and are led outside by special feedthroughs. Interferences from power lines can be removed with comb filters. Subsequent to antialiasing filtering, digitization is performed with a 64-channel multiplexer and a 12-bit analog-to-digital converter (*A/D*). Maximum sampling rate is 4 kHz per channel. Parallel to the magnetic signals, additional channels (EEG, ECG, respiration) can be digitized. Magnetic and electrical analog signals can be recorded in parallel by monitors and chart recorders. The signals are processed on a computer workstation, which also controls stimulus generation for auditory and visual evoked field studies.

be recorded in parallel with the magnetic fields. Special nonmagnetic electrodes and sensors are used. Further means are provided to transmit auditory and visual stimuli.

The multichannel sensor consists of an arrangement of 37 superconducting pickup coils combined with counterwound compensating coils distributed over a flat, circular disk 19 cm in diameter (Fig 4). This sufficiently large measurement area allows observations to be made at any part of the human body and makes it possible to examine magnetic field distributions from deep-lying sources without repositioning. The coil combinations, called gradiometers, further suppress interfering external fields. The electrical current induced in the gradiometers by the biomagnetic field is transferred to coupling coils, which direct magnetic flux into dedicated arrays of SQUIDs. Ten SQUIDs are combined on a single silicone chip.

The SQUID is the most sensitive sensor for measurement of magnetic flux. To provide an electrical signal proportional to the magnetic field at the pickup coil, the SQUID has to be operated in a feedback loop with a lock-in amplifier. Within the shielded room, a sensitivity of 10 $fT/\sqrt{Hz}$ at frequencies above 10 Hz is yielded (Fig 5).

The SQUID signals are further processed with notch filters to prevent interference from the line frequency and with high-pass and antialiasing filters to improve the signal-to-noise ratio (S/N). Data are digitized with 400–1,000 Hz (depending on the application) and evaluated with a computer system. Typically, 10-minute recordings are obtained.

S/N can be improved by averaging. Periodic signals (eg, from a regular cardiac cycle or from evoked potentials) are added together with respect to a trigger pulse. For sporadic events, signals are recorded during a time period in which several identical events are expected. One event is then identified by means of visual inspection of the recording. The corresponding pattern of all magnetic signals is used as a template, which is moved in time over the whole set of measured data. When the correlation coefficient exceeds a certain threshold, this is considered to represent the occurrence of an identical event (13).

Source Localization and Combination with Imaging

Because the mathematical problem is underdetermined, there exists no unique solution for reconstructing a current distribution from its magnetic field distribution. The physiologic current source is therefore most simply modeled as a current source and current sink, separated by an infinitesimal distance. The product current times length is referred to as an "equivalent current dipole." This equivalent current dipole sends volume currents into the body, which have to be taken into consideration in evaluating the generated magnetic field. For this, the human head is approximated as a homogeneous sphere and the human chest as a homogeneous infinite half space. In a nonlinear optimization procedure, the equivalent electrical dipole position and strength are found iteratively by minimizing the difference between measured and calculated magnetic field maps.

The diagnostic value of biomagnetically yielded locations can be improved significantly if they can be inspected with reference to human anatomy and morphology. Best suited is a combination of biomagnetic evaluation with MR imaging, because the latter modality provides three-dimensional images. To enable fusion of biomagnetic localizations with MR images, common reference coordinates have to be established. This is achieved during a magnetoencephalographic (MEG) investigation by fixing the patient's head to a support by means of a silicone rubber impression of the upper teeth. The support is mounted on the patient couch and is then removed and used during the MR examinations. The biomagnetic sensor coordinates are defined with respect to the support, and water-filled markers allow identification of reference points in the MR images.

For MCG measurements, the patient's position is determined either from reference points on the chest (eg, jugular notch of the sternum) or with use of a system of calibration coils fixed to the patient's body. During MR imaging these coils are replaced by contrast medium–filled markers. Coordinate transformation is done with the use of coils and markers as common reference points.

The iterative localization procedure is

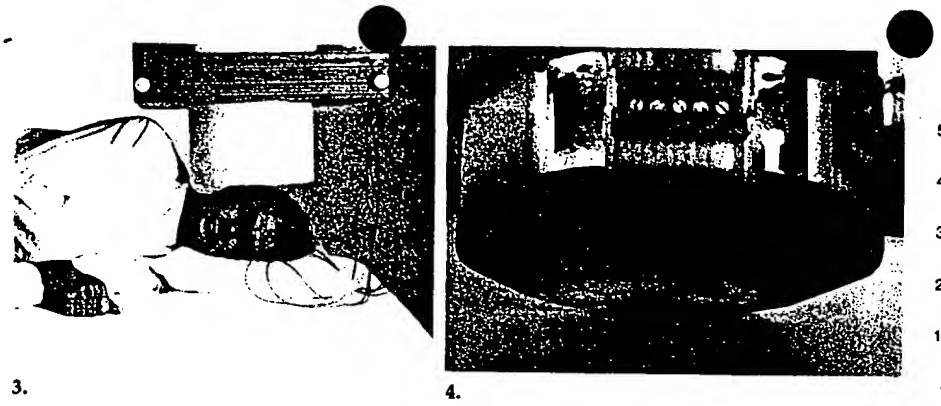

3. 4.

Figures 3, 4. (3) Arrangement for MEG measurement in the temporal region with simultaneous EEG recording. (4) Multichannel sensor consisting of 37 axial first-order gradiometers: 37 field-sensing coils are arranged on a plane with an overall diameter of 19 cm, and compensating coils are on a parallel plane 7.1 cm above. The hexagonal superconducting coils are manufactured from flexible printed circuit material; spacing is 2.7 cm. The gradiometers are coupled to dedicated silicone chips with integrated direct current SQUIDs (12) (not shown).

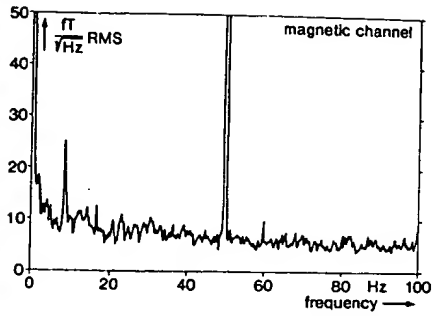

Figure 5. Typical noise spectrum of one SQUID channel during multichannel operation in the shielded room under urban noise conditions (spectral resolution = 0.24 Hz; Hanning window; *RMS* = root mean square).

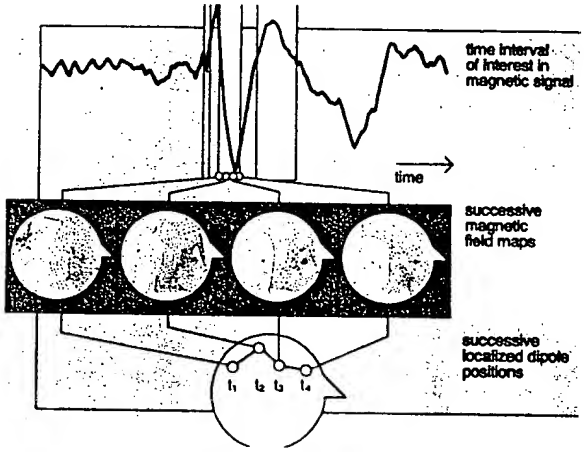

6.

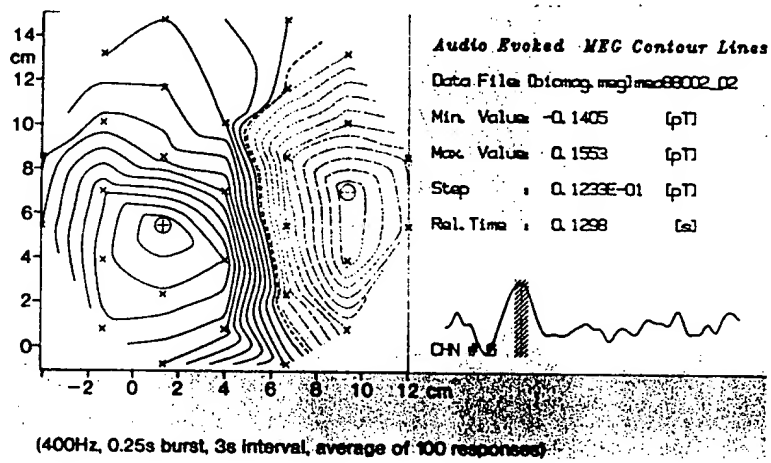

7.

Figures 6, 7. (6) Localization of propagating electrical activity. At each sampling interval, magnetic field distributions (maps) are measured. Time windows (shaded areas in the time curve), in which continuous equivalent current dipolar activity is localized, are marked. During a window period, successive dipole locations are plotted as a continuous curve. Since a true three-dimensional localization is obtained, such curves can be projected into arbitrary planes. (7) Auditory evoked MEG. Magnetic field contour lines at maximum of N100 (stimulation frequency = 400 Hz, interstimulus interval = 3 seconds, 100 stimuli, x = center of field coils).

performed automatically over a time interval of interest (Fig 6). At every sampled data point an equivalent current dipole is localized. The validity of the resulting localizations is automatically checked against four criteria that ensure physiologic and mathematical consistency: (*a*) The deviation between the measured and the calculated magnetic field maps must not exceed a threshold that is determined from the S/N. (*b*) The location must be within the part of the body under investigation (eg, the brain). (*c*) The maximum allowed distance between successive dipole positions is defined by the sampling interval and the maximum possible conductance velocity plus the maximum systematic error. (*d*) The dipole positions are stable within a time typical for the duration of action potentials of the type of nerves considered and within the limit of the conductance velocity.

This validation scheme automatically rejects unreliable dipole localizations and thus greatly reduces the possibility of misinterpreting erroneous localizations due to model errors and algorithmic faults. It results in a chain of localized electrical dipoles that represent the propagation of electrical activity within the body.

Investigations

System performance was tested with measurements on isolated magnetic dipoles (single coils in air and coil arrangements in air) and on current dipoles in water phantoms. The thorax was modeled by a basin, the skull by a glass sphere; both were filled with saline solution. Accuracy of localization was found to be on the order of 1 mm.

To test the performance of the system on spontaneous MEGs, auditory and visual evoked MEGs and MCGs were recorded in volunteers.

Clinical MEG investigations were performed on 13 patients with pharmacoresistant temporal lobe epilepsy. The MEG was recorded during withdrawal from antiepileptic drugs. Simultaneously with the MEG, the EEG was recorded (scalp, sphenoidal, and/or foramen ovale electrodes). Additional investigations included video EEG monitoring, interictal and ictal technetium-99m hexamethyl-propyleneamine oxime single photon emission computed tomography, positron emission tomography, and intraoperative electrocortigraphy.

For localization studies of accessory pathways in patients suffering from Wolff-Parkinson-White (WPW) syndrome, MCG recordings from 10 patients were evaluated. Five of these patients were also examined with catheter mapping and blood-pool scintigraphy for comparison.

Informed consent was obtained from the subjects after the nature of the bio-

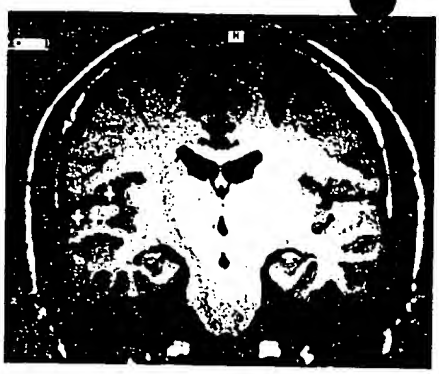

Figure 8. Localization from the auditory evoked MEG. MR image with equivalent current dipole positions for four different frequencies at the maximum of N100 (stimulation frequencies from basal to central = 400, 800, 1,600, and 3,200 Hz).

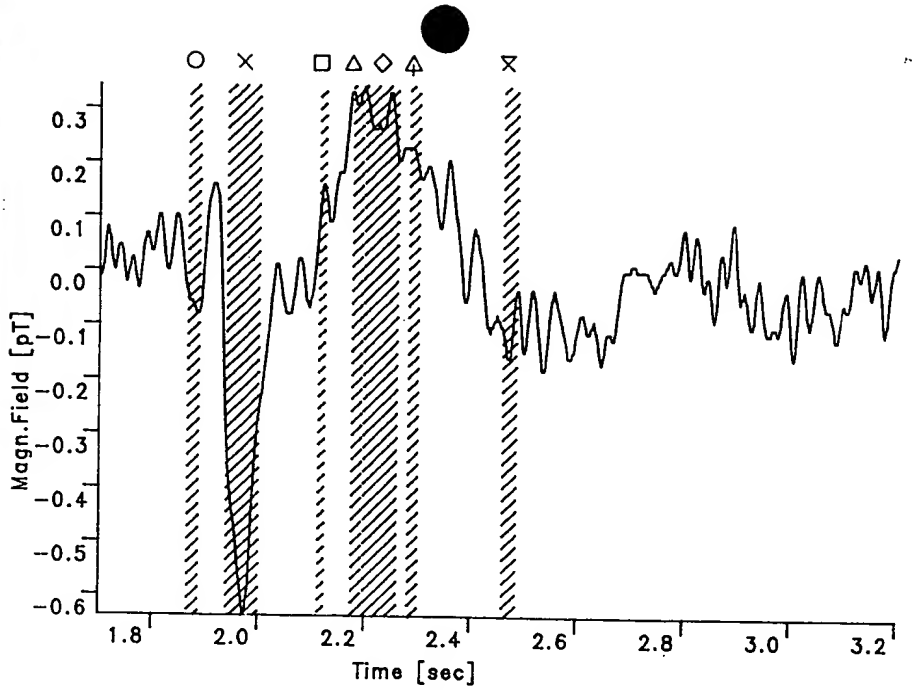

Figure 9. Activity in patient with temporal lobe epilepsy caused by an angioma. Graph shows signals recorded during a spike-wave event (MEG signals of 14 identical events found with automated spatiotemporal correlation were averaged). Hatched areas indicate time intervals during which valid equivalent current dipoles were localized. Time intervals are marked by various symbols at top.

magnetic measurement and the accompanying procedures had been explained.

RESULTS

The auditory evoked MEG was measured over the hemisphere contralateral to the stimulated ear. The total measurement time for one stimulation frequency was about 7 minutes, given by the number of signals to be averaged. The magnetic signals showed the peak of the cortical response about 100 msec after stimulus onset, which was already known from electrical potential measurements (so-called N100 [N stands for negative peak]). The corresponding field map at signal maximum shows a structure typical for a current dipole (Fig 7). For stimulation frequencies of 400–3,200 Hz, evaluation of the signal maximum yielded a sequence of dipole localizations, which shifted radially from the surface to the center of the brain with increasing frequency (Fig 8).

Figures 9 and 10 show results for a patient suffering from complex partial seizures of temporal lobe origin. Dipolar activity could be localized during a single interictal spike-wave event, as well as from averaging several identical spike-wave events identified with the temporal correlation procedure (Fig 9). The localization from the averaged spike-wave signal combined with MR images showed not only the primary focal activity, apparently caused by an angioma, but also responses in distant parts of the brain (Fig 10), which were in accordance with findings from intracortical electrode measurements and positron emission tomography.

In 11 patients with interictally recorded MEGs, the evaluation and comparison of the localization of the epileptic focus obtained with the other applied techniques showed lobar or even intralobar congruence of the results.

The accessory pathways of patients suffering from WPW syndrome could be localized from the magnetic field distribution of the delta wave of the MCG just before the onset of the R wave (6). Figure 11 shows the results in a patient with WPW syndrome who also underwent catheter mapping and blood-pool scintigraphy.

Valid equivalent dipoles were found within the total duration of the delta wave in most patients with WPW syndrome. The localization of the accessory pathway agreed with the findings obtained with the other diagnostic methods within 1–2 cm in five cases. In three cases, localizations derived from MCG data gave plausible results in relation to the heart anatomy, which have yet to be confirmed with catheter mapping. In two cases some doubt about the true location remained.

DISCUSSION

In vitro and in vivo studies performed with a prototype of the Krenikon system have shown the potential usefulness of multichannel measurements of biomagnetic fields. With the possibility of localizing electrical sources with a time resolution of milliseconds, biomagnetic evaluation has the potential to become a valuable tool in functional diagnosis, especially in combination with anatomic imaging.

Results from auditory field measurements are in agreement with those from earlier studies (5). In the three-dimensional MR images the current sources in the region along the auditory fissure are localized with a precision of a few millimeters.

The localization accuracy of studies in epilepsy is similar in magnitude. However, it must be considered that none of the conventionally applied techniques has a spatial and temporal resolution similar to that of MEG; thus, localizations from magnetic measurements in patients are difficult to verify with control methods.

The situation is similar with WPW syndrome: Whereas the biomagnetic evaluation localizes the ventricular end of the accessory bundle, catheter mappings are usually carried out in the reentry state, so that the atrial end of the accessory bundle is determined. Blood-pool scintigraphy gives time-resolved images of the blood turbulence due to the contraction of the myocardium. Within the limits of these methods, the results of all three determinations agreed well. This corresponds with the localization accuracy reported by other researchers (14).

a. b. c.

Figure 10. MR images of patient in Figure 9. Centers of electrical activity during four different phases of the spike-wave event are outlined. (a) Primary phase of excitation corresponds to the surrounding tissue of the angioma in the temporal neocortex. (b) Second and third phases of propagating activity are mesiotemporal, in the right and left hippocampal areas. (c) From the focal epileptic activity, the equivalent current dipole sources also spread to posterior midline regions and then back to the focus.

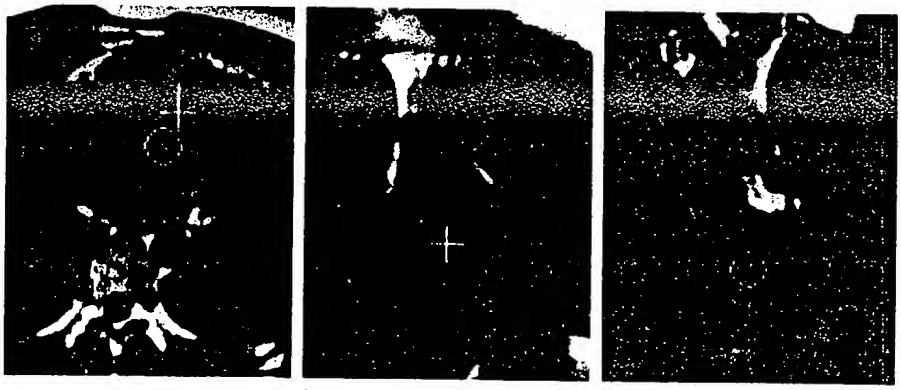

a. b. c.

Figure 11. Axial (a) and frontal (b, c) MR images of a patient with WPW syndrome. Localization results from MCG (+) and from catheter mapping (O) are depicted.

To quantify the spatial resolution of the biomagnetic localization method, the main sources of localization errors have to be defined: coordinate transfer into the MR image, system noise, "biologic" noise from electrical background activity of the human body (15), and modeling inaccuracies.

Influence of system noise was studied with phantoms, and an error of 1–2 mm was found. The reproducibility of the head position in the MEG device and the MR imaging system is typically 2 mm for a point in the temporal region and about 4 mm for a point in the occipital region. All other errors can be estimated only qualitatively with mathematical simulations (10,16–18).

Summarizing all our experiences, we estimate that the localization error for typical electrophysiologic sources in the brain is less than 0.5 cm for cortical sources, increasing to 1–2 cm for sources as deep as 2 cm from the center of the brain (center of the equivalent model sphere). Sources within an inner sphere with a 2-cm radius around the center of the brain could not be localized. The relative accuracy of sequences of localizations derived from data acquired without changing the patient's position is 0.2–1.0 cm, depending on the signal strength of the MEG. For the heart, the total localization accuracy is on the order of 1–2 cm.

The equivalent current dipole has proved to be a sufficient model in many applications. More sophisticated models, like minimum norm reconstruction (19) and statistical dipole models (15), are being considered for localizing distributed current densities (eg, during the QRS complex of the cardiac cycle). Realistic object models, instead of the simple sphere and half-space shapes, can further improve localization accuracy (20,21).

Applications of biomagnetic multichannel systems of interest today are in the brain and the heart. Brain function can be explored with use of auditory, visual, or somatosensory stimulated fields. Primary and secondary foci can be localized from interictal activity in patients with focal epilepsy. The potential of biomagnetism for the understanding and diagnosis of ischemic states (22) and as a tool for follow-up during treatment and prognosis has to be investigated. The application to diffuse disorders like Alzheimer disease and schizophrenia is also worthy of investigation.

The study of the cardiac conduction system allows noninvasive localization of the accessory bundle in WPW syndrome. Other excitation centers, like ventricular ectopic areas of activity causing extrasystoles, can be studied, too. Besides information about geometric locations, quantitative information about source strength can also be obtained. In patients with cardiac hypertrophy, the source strength derived from the MCG correlates significantly better with the wall thickness determined with ultrasound or MR imaging than with the corresponding factor from the MCG (23).

In conclusion, it appears that the Krenikon multichannel biomagnetic system will prove to be a clinically useful research tool. Neurologic and cardiologic studies, although in an early state, have already produced interesting results. Further research is necessary to explore the full potential of biomagnetism. ■

References

1. Cuffin BN. On the use of electric and magnetic data to determine electric sources in a volume conductor. Ann Biomed Eng 1978; 6:173–193.
2. Mondt JP. On the effects on source localization of volume currents in neuroelectric and neuromagnetic signals. Phys Med Biol 1989; 34:1073–1088.
3. Zimmerman JE. Cryogenics. In: Williamson SJ, Romani GL, Kaufman L, Modena I, eds. Biomagnetism: an interdisciplinary approach. New York: Plenum, 1982; 43–67.
4. Ricci GB, Leoni R, Romani GL, Campitelli F, Buonomo S, Modena I. 3-D neuromagnetic localization of sources of interictal activity in cases of focal epilepsy. In: Weinstock H, Stroink G, Katila T, eds. Biomagnetism. New York: Pergamon, 1984; 304–310.
5. Romani GL, Williamson SJ, Kaufman L, Brenner D. Characterization of the human auditory cortex by the neuromagnetic method. Exp Brain Res 1982; 47:381–393.
6. Katila T, Maniewski R, Maekijaervi M, Nenonen J, Siltanen P. On the accuracy of source localization in cardiac measurements. Phys Med Biol 1987; 32:125–131.

7. Kajola M, Ahlfors S, Ahonen A, et al. Low noise seven-channel DC-SQUID magnetometer for brain research. In: Atsumi K, Kotani M, Ueno S, et al, eds. Biomagnetism '87. Tokyo: Tokyo Denki University Press, 1987; 430–433.
8. Williamson SJ, Pelizzone M, Okada L, et al. Magnetoencephalography with an array of SQUID sensors. In: Colland H, Berglund P, Krusius M, eds. Proceedings of the 10th International Cryogenic Engineering Conference. Guildford, England: Butterworth, 1984; 339–348.
9. Romani GL, Leoni R, Salustri C. Multichannel instrumentation for biomagnetism. In: Hahlbohm HD, Lübbig H, eds. SQUID '85: superconducting quantum interference devices and their applications. Berlin: de Gruyter, 1985; 919–932.
10. Abraham-Fuchs K, Schneider S, Reichenberger H. MCG inverse solution: influence of coil size, grid size, number of coils, and SNR. IEEE Trans Biomed Eng 1988; 35:573–576.
11. Hoenig HE, Daalmans G, Folberth W, Reichenberger H, Schneider S, Seifert H. Biomagnetic multi-channel system with integrated SQUIDs and first order gradiometers operating in a shielded room. Cryogenics 1989; 29:809–813.
12. Clarke J, Goubau WM, Ketchen MW. Tunnel junction DC-SQUID: fabrication, operation, and performance. J Low Temperature Phys 1976; 28:99–145.
13. Abraham-Fuchs K, Härer W, Schneider S, Stefan H. Pattern recognition in biomagnetic signals by spatiotemporal correlation and application to the localization of propagating neuronal activity. Med Biol Eng Comput (in press).
14. Fenici RR, Melillo G, Maselli M, Capelli A. Magnetocardiographic three-dimensional localization of Kent bundles. In: Atsumi K, Kotani M, Ueno S, et al, eds. Biomagnetism '87. Tokyo: Tokyo Denki University Press, 1987; 140–141.
15. de Munck JC, Vijn PCM, Spekreijse H. Random dipoles as a model for EEG background activity. In: Williamson SJ, Hoke M, Kotani M, Stroink G, eds. Advances in biomagnetism. New York: Plenum (in press).
16. Cuffin BN. Effects of measurement errors and noise on MEG moving dipole inverse solutions. IEEE Trans Biomed Eng 1986; BME33:854–860.
17. Hari R, Joutsiniemi SL, Sarvas J. Spatial resolution of neuromagnetic records: theoretical calculations in a spherical model. EEG Clin Neurophys 1988; 71:64–72.
18. Meijs JWH, Peters MJ, Boom HBK, Lopes da Silva FH. Relative influence of model assumptions and measurement procedures in the analysis of the MEG. Med Biol Eng Comput 1988; 26:136–142.
19. Clarke CSJ, Janday BS. The solution of the biomagnetic inverse problem by maximum statistical entropy. Inverse Probl 1989; 5:483–485.
20. Peters MJ, Elias PJH. On the magnetic field and the electrical potential generated by bioelectric sources in an anisotropic volume conductor. Med Biol Eng Comput 1988; 11:617–623.
21. Purcell CJ, Stroink G, Horacek BM. Effect of torso boundaries on electric potential and magnetic field of a dipole. Trans Biomed Eng 1988; 35:671–678.
22. Vieth J, Sack G, Schüler P, Grummich P, Schneider S. Ischemic and epileptic lesions measured by AC- and DC-MEG. In: Williamson SJ, Hoke M, Kotani M, Stroink G, eds. Advances in biomagnetism. New York (in press).
23. Moshage W, Weikl A, Schneider S, Röhrlein G, Folbert W, Bachmann K. Magnetokardiographie (MKG): klinische anwendungen eines vielkanalsystems bei linkshypertrophie (abstr). Z Kardiol 1989; 78(suppl 1):106.